NASA/CP—2004-212963/VOL1

2003 NASA Seal/Secondary Air System Workshop

September 2004

The NASA STI Program Office . . . in Profile

Since its founding, NASA has been dedicated to the advancement of aeronautics and space science. The NASA Scientific and Technical Information (STI) Program Office plays a key part in helping NASA maintain this important role.

The NASA STI Program Office is operated by Langley Research Center, the Lead Center for NASA's scientific and technical information. The NASA STI Program Office provides access to the NASA STI Database, the largest collection of aeronautical and space science STI in the world. The Program Office is also NASA's institutional mechanism for disseminating the results of its research and development activities. These results are published by NASA in the NASA STI Report Series, which includes the following report types:

- TECHNICAL PUBLICATION. Reports of completed research or a major significant phase of research that present the results of NASA programs and include extensive data or theoretical analysis. Includes compilations of significant scientific and technical data and information deemed to be of continuing reference value. NASA's counterpart of peer-reviewed formal professional papers but has less stringent limitations on manuscript length and extent of graphic presentations.

- TECHNICAL MEMORANDUM. Scientific and technical findings that are preliminary or of specialized interest, e.g., quick release reports, working papers, and bibliographies that contain minimal annotation. Does not contain extensive analysis.

- CONTRACTOR REPORT. Scientific and technical findings by NASA-sponsored contractors and grantees.

- CONFERENCE PUBLICATION. Collected papers from scientific and technical conferences, symposia, seminars, or other meetings sponsored or cosponsored by NASA.

- SPECIAL PUBLICATION. Scientific, technical, or historical information from NASA programs, projects, and missions, often concerned with subjects having substantial public interest.

- TECHNICAL TRANSLATION. English-language translations of foreign scientific and technical material pertinent to NASA's mission.

Specialized services that complement the STI Program Office's diverse offerings include creating custom thesauri, building customized databases, organizing and publishing research results . . . even providing videos.

For more information about the NASA STI Program Office, see the following:

- Access the NASA STI Program Home Page at ***http://www.sti.nasa.gov***

- E-mail your question via the Internet to help@sti.nasa.gov

- Fax your question to the NASA Access Help Desk at 301–621–0134

- Telephone the NASA Access Help Desk at 301–621–0390

- Write to:
  NASA Access Help Desk
  NASA Center for AeroSpace Information
  7121 Standard Drive
  Hanover, MD 21076

NASA/CP—2004-212963/VOL1

2003 NASA Seal/Secondary Air System Workshop

Proceedings of a conference held at Ohio Aerospace Institute
sponsored by NASA Glenn Research Center
Cleveland, Ohio
November 5–6, 2003

National Aeronautics and
Space Administration

Glenn Research Center

September 2004

This work was sponsored by the Low Emissions Alternative Power Project of the Vehicle Systems Program at the NASA Glenn Research Center.

Available from

NASA Center for Aerospace Information
7121 Standard Drive
Hanover, MD 21076

National Technical Information Service
5285 Port Royal Road
Springfield, VA 22100

Available electronically at http://gltrs.grc.nasa.gov

TABLE OF CONTENTS
Volume 1

LOW EMISSIONS ALTERNATIVE POWER (LEAP)

Gary T. Seng
National Aeronautics and Space Administration
Glenn Research Center
Cleveland, Ohio

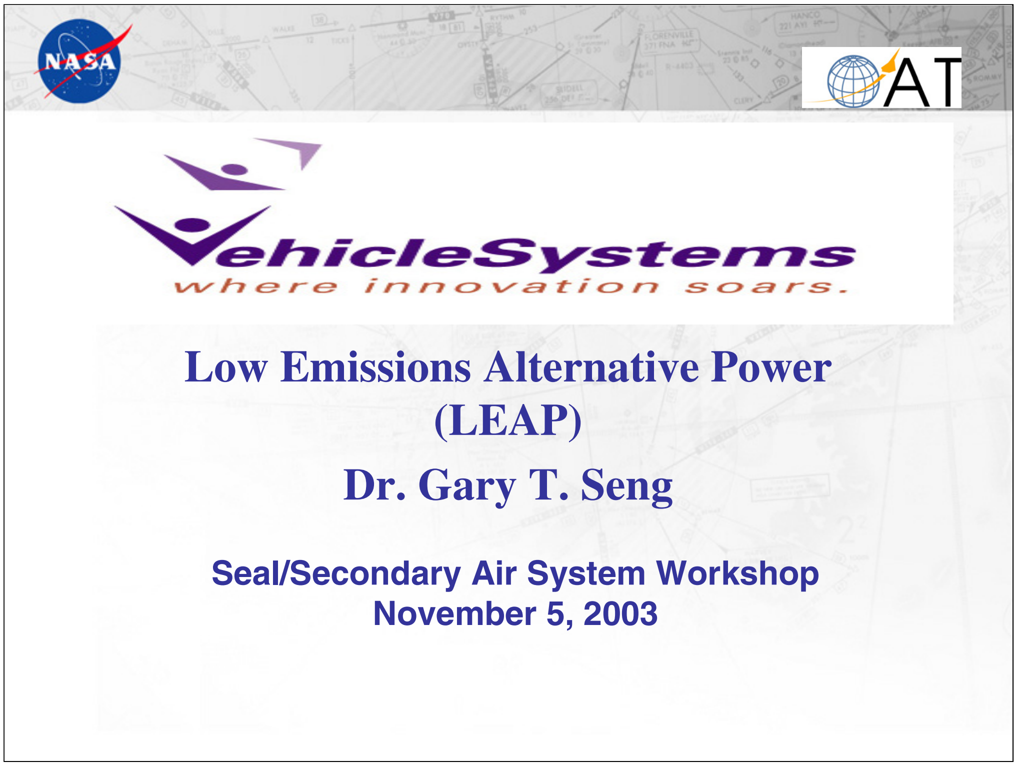

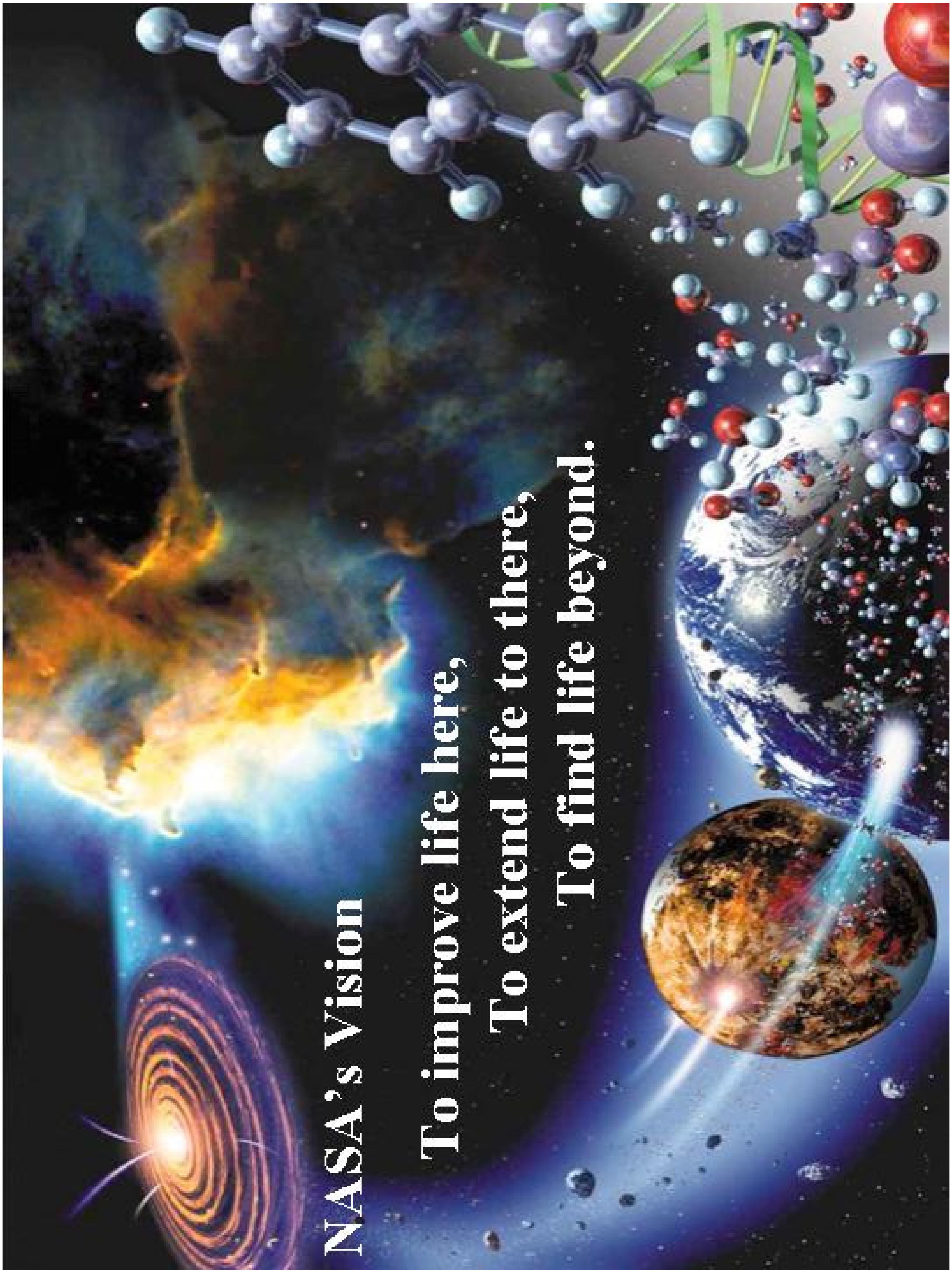
NASA's Vision
To improve life here,
To extend life to there,
To find life beyond.

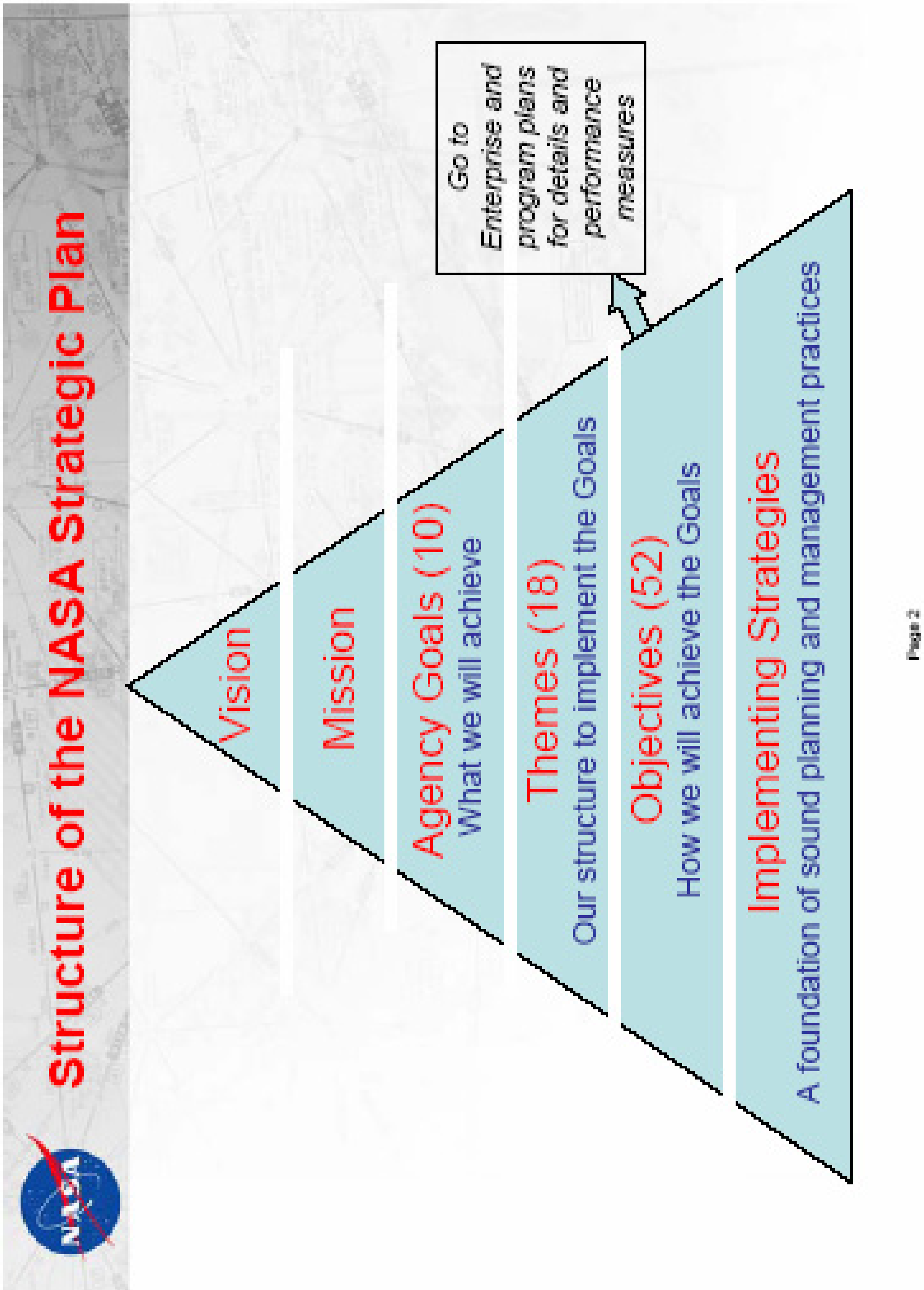
Structure of the NASA Strategic Plan
Vision
Mission
Agency Goals (10)
What we will achieve
Themes (18)
Our structure to implement the Goals
Objectives (52)
How we will achieve the Goals
Implementing Strategies
A foundation of sound planning and management practices
Go to Enterprise and program plans for details and performance measures
Page 2

NASA Strategic Structure -- From Strategic Plan to Programs (FY03)

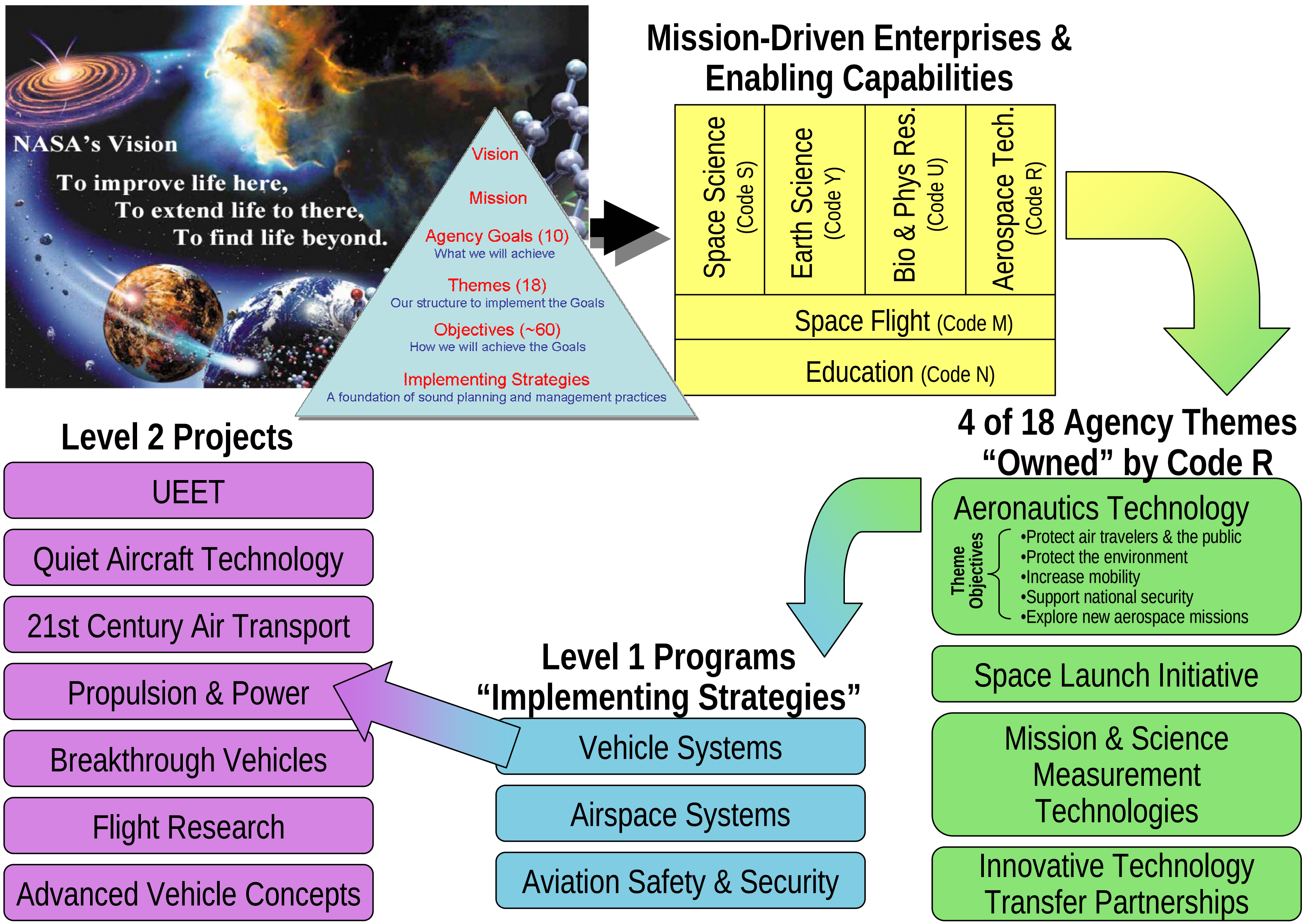

Aeronautics Technology – Three Integrated Programs

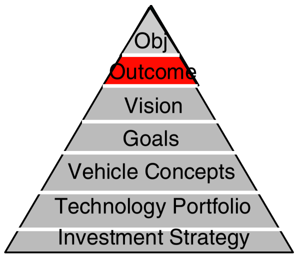

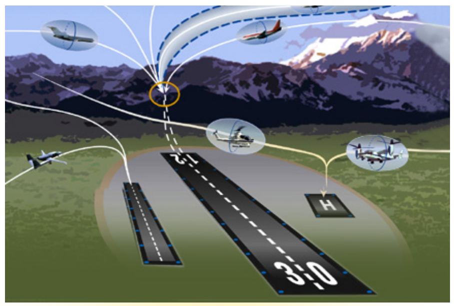

Airspace Systems

Aviation Safety & Security

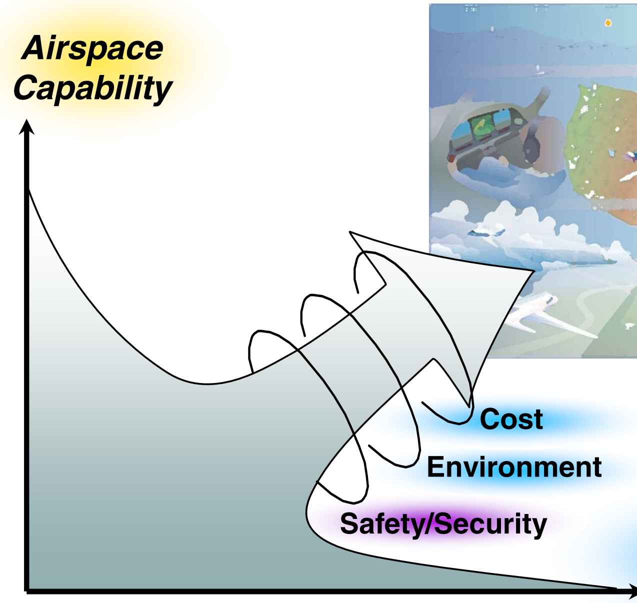

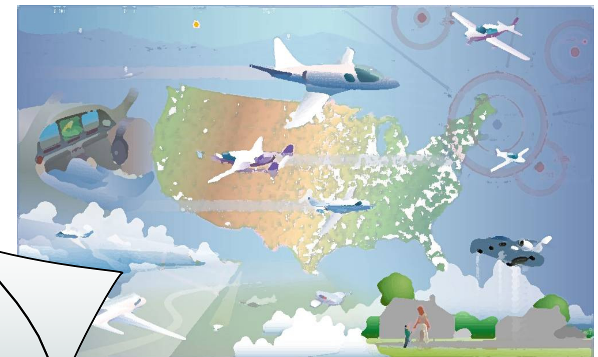

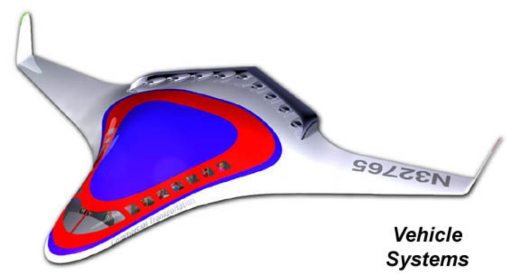

Vehicle Systems

Vehicle Systems Program (FY03)

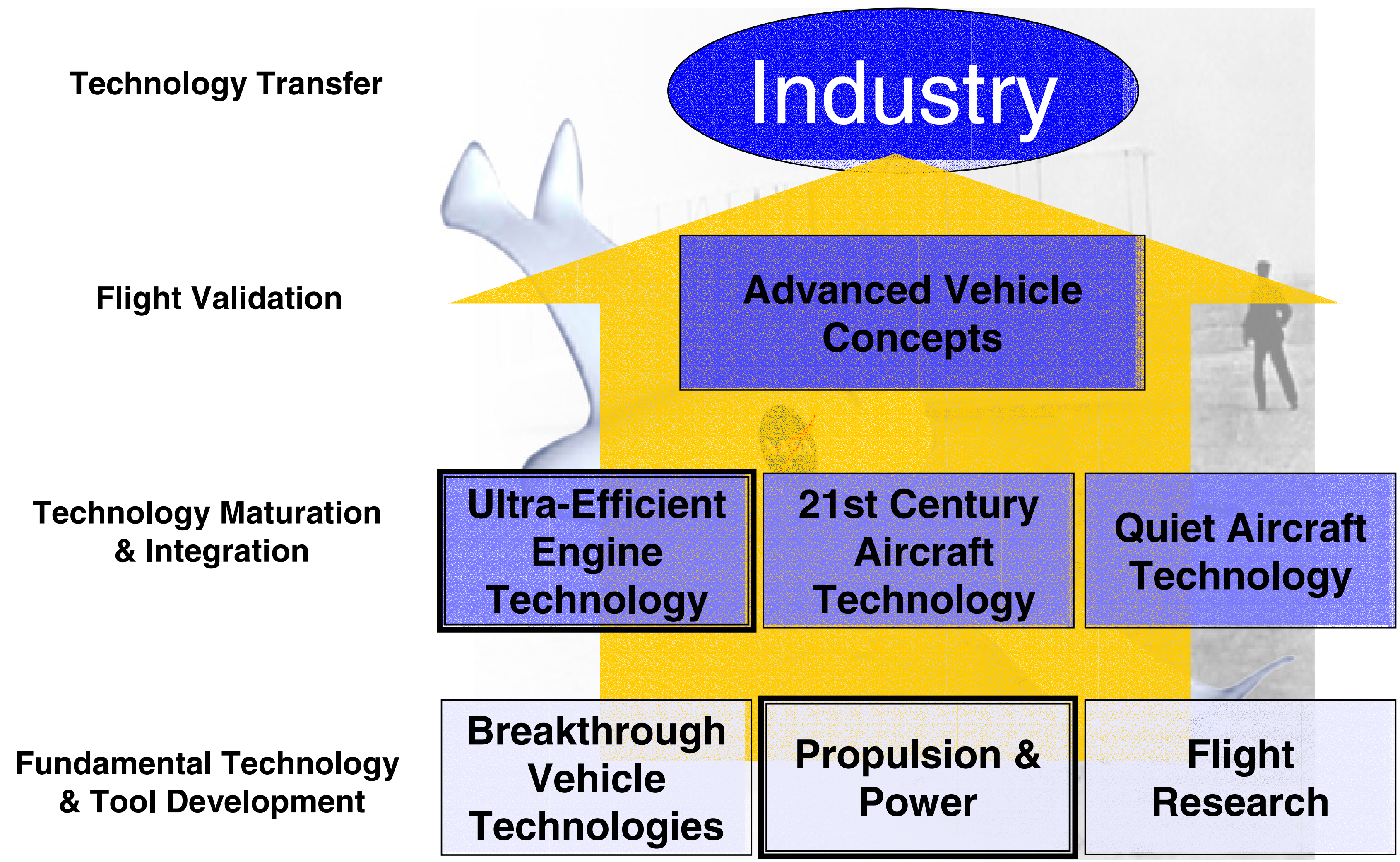

Strategic Technology Focus Areas

Six long-term technology focus areas

- Key long term investment areas
- Primary places where technology advances will occur
- Projects achieve finite steps within these areas

- *Environmentally Friendly, Clean Burning Engines*
  Focus: Develop innovative technologies to enable intelligent turbine engines that significantly reduce harmful emissions while maintaining high performance and increasing reliability

- *New Aircraft Energy Sources and Management*
  Focus: Discover new energy sources and intelligent management techniques directed towards zero emissions and enable new vehicle concepts for public mobility and new science missions

- *Quiet Aircraft for Community Friendly Service*
  Focus: Develop and integrate noise reduction technology to enable unrestricted air transportation service to all communities

Strategic Technology Focus Areas (contd)

- *Aerodynamic Performance for Fuel Efficiency*
  Focus: Improve aerodynamic efficiency, structures and materials technologies, and design tools and methodologies to reduce fuel burn and minimize environmental impact and enable new vehicle concepts and capabilities for public mobility and new science missions

- *Aircraft Weight Reduction and Community Access*
  Focus: Develop ultralight smart materials and structures, aerodynamic concepts, and lightweight subsystems to increase vehicle efficiency, leading to high altitude long endurance vehicles, planetary aircraft, advanced vertical and short takeoff and landing vehicles and beyond

- *Smart Aircraft and Autonomous Control*
  Focus: Enable aircraft to fly with reduced or no human intervention, to optimize flight over multiple regimes, and to provide maintenance on demand towards the goal of a feeling, seeing, sensing, sentient air vehicle

Vehicle Systems Strategic Focus Areas

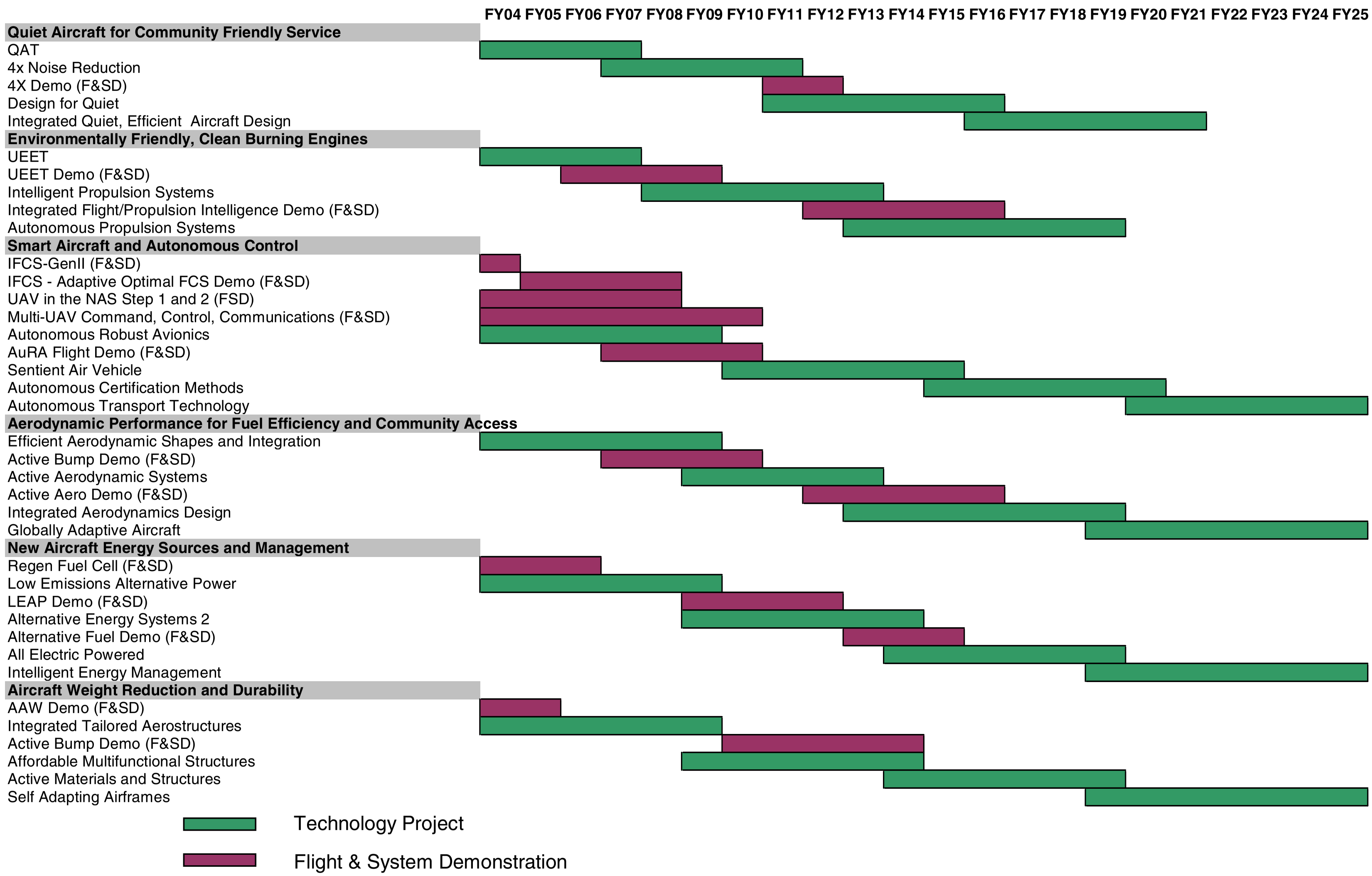

Vehicle Systems Program Structure (FY04+)

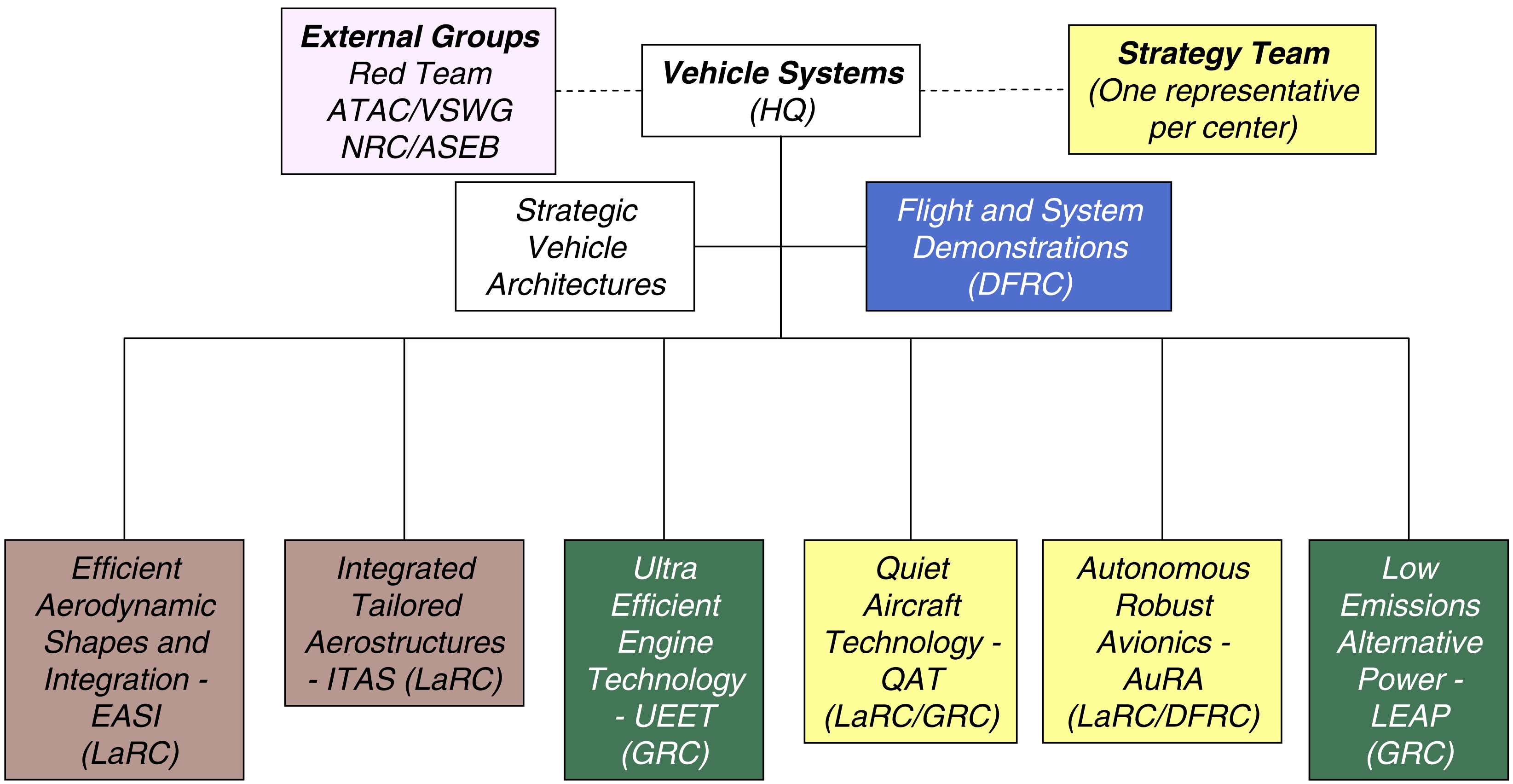

New Level II Projects

NASA's Technology Readiness Level (TRL) Scale

TRL	General NASA Definition
9	Actual system "flight proven" on operational flight
8	Actual system completed and "flight qualified" through test and demonstration
7	System prototype demonstrated in flight environment
6	System/subsystem model or prototype demonstrated/validated in a relevant environment
5	Component and/or breadboard verification in a relevant environment
4	Component and/or breadboard test in a laboratory environment
3	Analytical and experimental critical function, or characteristic proof-of-concept
2	Technology concept and/or application formulated (candidate selected)
1	Basic principles observed and reported

System Test & Operations (TRL 8–9)

System/Sub-sys Development (TRL 6–8)

Technology Demonstration (TRL 5–6)

Technology Development (TRL 3–5)

Research to Prove Feasibility (TRL 2–3)

Basic Technology Research (TRL 1–2)

LEAP Span (TRL 1–6)

New UEET Span (TRL 1–6)

Theme Objectives Addressed by Vehicle Systems

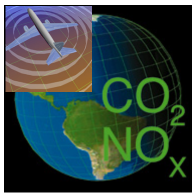

Protect the Environment
Protect local and global environmental quality by reducing aircraft noise and emissions.

Increase Mobility
Enable more people and goods to travel faster and farther, anywhere, anytime with fewer delays

Protect the Nation
Enhance the nation's security through aeronautical partnerships with DOD and other government agencies.

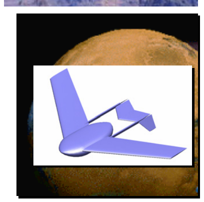

Explore Revolutionary Aeronautical Concepts
Pioneer novel aeronautical concepts to support earth and space science missions and new commercial markets.

Twelve Notional Vehicles of the Vehicle Systems Program

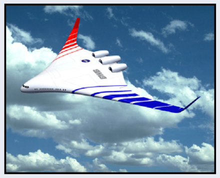

Minimum environmental impact, maximum efficiency

ST: Clean Transport

Strengthen national security through rapid deployment and global reach

SSA: Global Strike

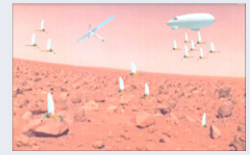

Conduct extended science and exploration missions

UAV: Planetary Flight Vehicles

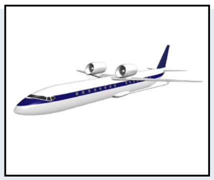

All hour access to any location without noise disturbance

ST: Santa Monica at Midnight

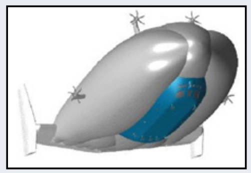

Global reach and on-demand delivery

ST: Global Reach Transport

Rural, regional, and intra-urban transportation

PAV: Personal Air Vehicle

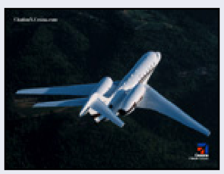

Rural and regional economic growth, time critical transport

ST: Heartland Express

Automated refueling capability, ultra-long endurance, wide speed range

ST: Tanker

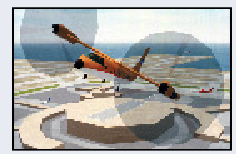

Enables city center access in all weather

RIA: V/STOL Commuter

Expands the use of existing airport infrastructure

RIA: Extreme STOL Transport

Reduce passenger flight time by at least a factor of 2

SSA: Supersonic Overland

High altitude observations for science, and defense

UAV: High Altitude Long Endurance

ST: Subsonic Transport, SSA: Supersonic Aircraft, PAV: Personal Air Vehicle, UAV: Uninhabited Air Vehicle, RIA:Runway Independent Aircraft

Vehicle Systems
Work Breakdown Structure

New Aircraft Energy Sources and Management *<Strategic Focus>*

Focus: Discover new energy sources and intelligent management techniques directed towards zero emissions and enable new vehicle concepts for public mobility and new science missions

- **Low Emissions Alternative Power - LEAP (GRC)** **<Project>**
  - GRC - Constant Volume Combustion Cycle Engine
  - GRC – Aircraft Fuel Cell Power System
  - GRC - Alternative Fuel Foundation Technologies <Subprojects>
  - GRC - Propulsion URETI
  - HQ - Advanced Aircraft

Environmentally Friendly, Clean Burning Engines *<Strategic Focus>*

Focus: Develop innovative technologies to enable intelligent turbine engines that significantly reduce harmful emissions while maintaining high performance and increasing reliability

- **Ultra Efficient Engine Technology - UEET (GRC)** **<Project>**
  <Subprojects>
  - GRC - 70% NOx Reduction Combustor (GRC)
  - GRC - Highly Loaded, Light Weight Compressor and Turbine
  - LaRC - Highly Integrated Inlet
  - GRC - UEET Integration and Demonstration
  - GRC - Intelligent Propulsion System Foundation Technologies

& Noise Reduction

Vehicle Systems Strategic Focus - Supporting Projects

New Aircraft Energy Sources and Management

Discover new energy sources and intelligent energy management techniques directed towards zero emissions and enable new vehicle concepts for public mobility and new science missions.

New Aircraft Energy Sources and Management

FY04 FY05 FY06 FY07 FY08 FY09 FY10 FY11 FY12 FY13 FY14

Regen Fuel Cell (FSD)

Flight demonstration of multiple day, unrefueled flight using a hydrogen/air fuel cell power system.

Low Emissions Alternative Power

LEAP

Demonstrate through integrated ground tests, a constant volume combustor in an engine system, and a UAV/small transport aircraft fuel cell-based power generation system.

LEAP Demo (FSD)

Flight demonstration of a UAV fuel cell-based power system providing extremely long duration flights.

Alternative Energy Systems

Perform a ground demonstration of an integrated alternative-fueled engine-power system for a small transport aircraft.

FSD = Full Scale Demonstration

LEAP Subprojects

Constant Volume Combustion Cycle Engine (CVCCE) - Develop hybrid constant volume combustion engine subsystem and system technology, and demonstrate feasibility through system analysis and ground demonstration testing.

Aircraft Fuel Cell Power System (AFCPS) - Develop and demonstrate a prototype fuel cell based power generation system for UAV/small transport aircraft in an integrated ground test.

Alternative Fuel Foundation Technologies (AFFT) - Discover new energy sources, unconventional propulsion systems and engines, and new power systems that have the potential to greatly reduce emissions, enable new vehicle concepts for public mobility, enhance national security or develop new scientific concepts (technology concept horizon 20-40 years).

University Research Engineering, Technology Institute (URETI) - Develop revolutionary aeropropulsion and power technologies and design methods in a systems-oriented integration environment.

LEAP Project Structure

Low Emissions Alternative Power

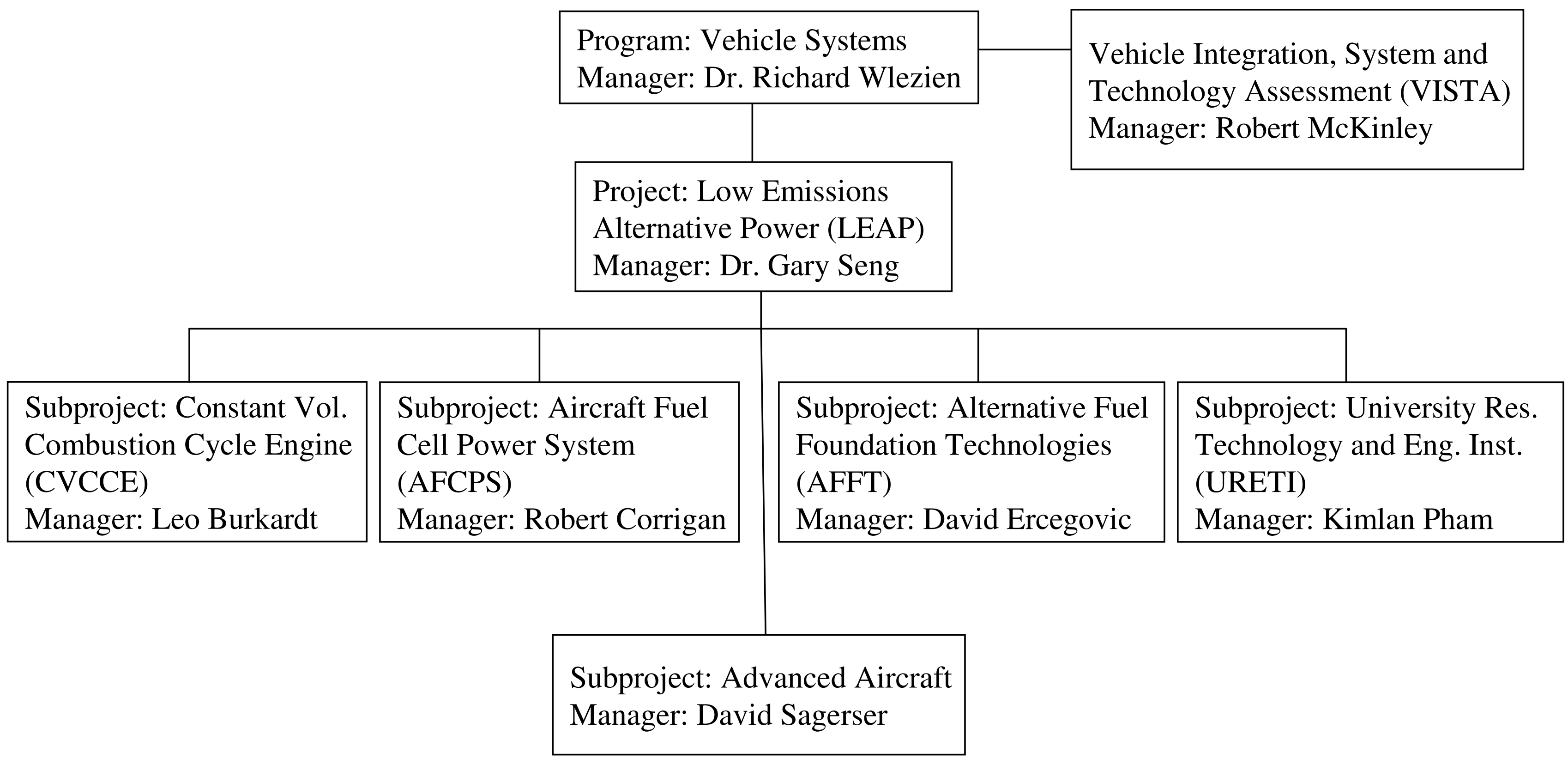

Aeropropulsion Vision

Advanced propulsion and power technologies and new concepts to enable Aeropropulsion Revolutions.

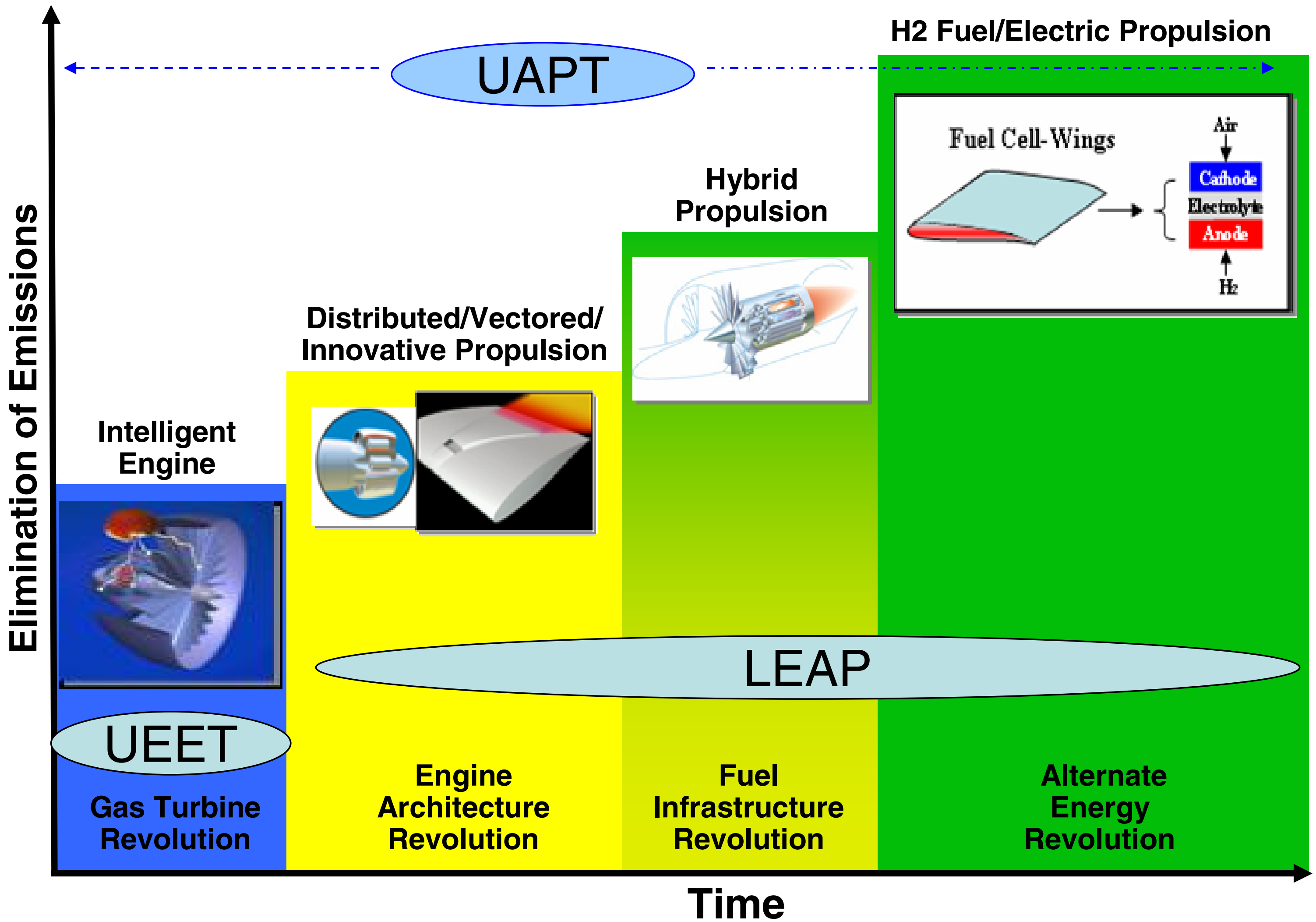

OVERVIEW OF NASA GLENN SEAL DEVELOPMENTS

Bruce M. Steinetz, Margaret P. Proctor, and Patrick H. Dunlap, Jr.
National Aeronautics and Space Administration
Glenn Research Center
Cleveland, Ohio

Irebert Delgado
U.S. Army Research Laboratory
Glenn Research Center
Cleveland, Ohio

Jeffrey J. DeMange
University of Toledo
Toledo, Ohio

Christopher C. Daniels and Scott B. Lattime
Ohio Aerospace Institute
Brook Park, Ohio

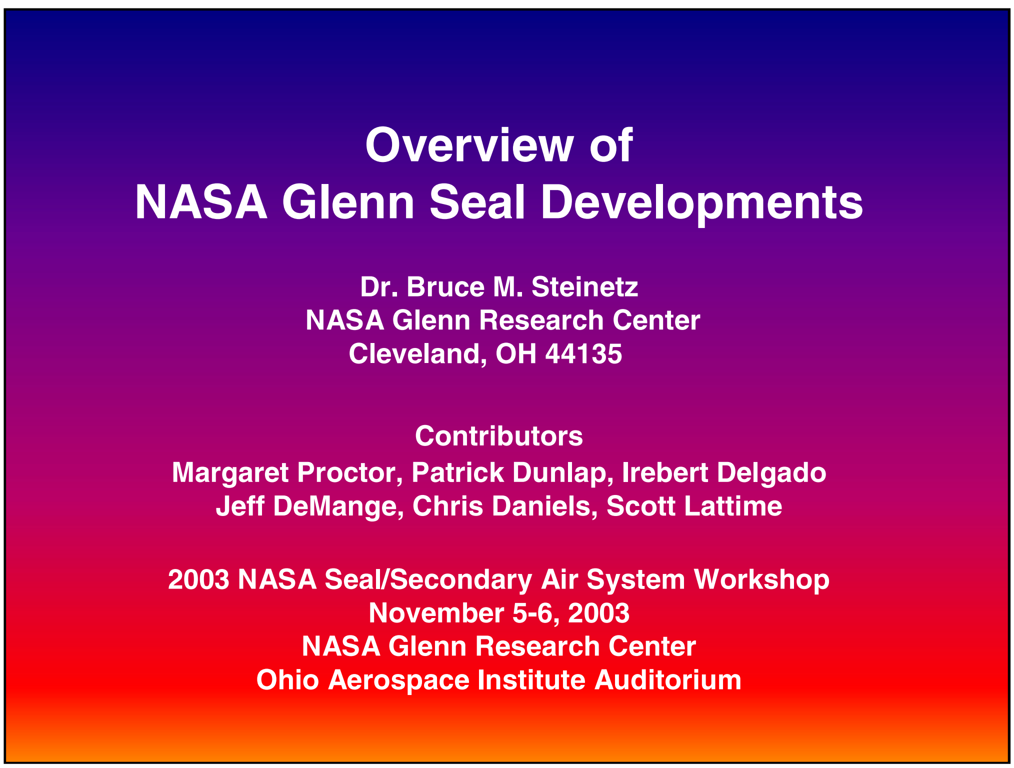

NASA Glenn hosted the Seals/Secondary Air System Workshop on November 5-6, 2003. At this workshop NASA and our industry and university partners shared their respective seal technology developments. We use these workshops as a technical forum to exchange recent advancements and "lessons-learned" in advancing seal technology and solving problems of common interest. As in the past we are publishing the presentations from this workshop in two volumes. Volume I will be publicly available and individual papers will be made available on-line through the web page address listed at the end of this chapter. Volume II will be restricted under International Traffic and Arms Regulations (I.T.A.R.).

Workshop Agenda

Wednesday, Nov. 5, Morning

Registration	**8:00 a.m.–8:30 a.m.**
Introductions	**8:30-9:30**
Introduction	Dr. Bruce Steinetz, R. Hendricks/NASA GRC
Welcome	Mr. Vern (Bill) Wessel, Director, Safety and Mission Assurance
Overview of NASA's Low Emissions Alternative Power Project	Dr. Gary Seng, Dir., Aeropropulsion/Power Research/GRC
Overview of NASA Glenn Seal Developments	Dr. Bruce Steinetz/NASA GRC
Program Overviews and Requirements	**9:30-10:30**
Overview of NASA's UEET Project	Ms. Catherine Peddie, Dr. Joe Shaw /NASA GRC
Overview of NASA's Access to Space Programs	Mr. Harry Cikanek/NASA GRC
Revolutionary Turbine Accelerator (RTA) Engine Dev. Overview	Dr. Paul Bartolotta, K. Suder, N. McNelis/NASA GRC
Break	**10:30 -10:45**
Turbine Seal Development Session I	**10:45-12:30**
GE90 Aspirating Seal Engine Demonstration Test Update	Ms. Marcia Boyle, B. Albers/GE Aircraft Engines
Overview of Industrial Seal Developments at GE-GRC	Dr. Ray Chupp/GE Global Research Center
Geared Fan High Misalignment Seal Test Status	Mr. Dennis Shaughnessy, L. Dobek/P&W E. Hartford
Overview of Turbine Seal Testing at GRC	Mr. Irebert Delgado/U.S. Army Lab, M. Proctor/ NASA
Compliant Foil Seal Investigations	Ms. Margaret Proctor/NASA GRC, I. Delgado/U.S. Army Research Laboratory
Lunch OAI Sun Room	**12:30-1:30**

NASA Glenn Research Center
Seal Team

The first day of presentations included overviews of NASA programs devoted to advancing the state-of-the-art in aircraft power and turbine engine technology. Dr. Gary Seng provided an overview of NASA's Low Emissions Alternative Power Project. Ms. Peddie presented an overview of the Ultra-Efficient-Engine Technology (UEET) program that is aimed at developing highly-loaded, ultra-efficient engines that also have low emissions (NOx, unburned hydrocarbons, etc.). Mr. Cikanek of NASA's Space Project office summarized NASA's Access to Space Programs citing areas where advanced seals are required.

Dr. Bartollotta provided an overview of the turbine-based-combined-cycle (TBCC)/Revolutionary Turbine Accelerator (RTA) project. The goal of this project is to develop turbine engine technology that would enable a turbine-engine based first stage launch system for future highly re-usable launch vehicles.

Dr. Steinetz presented an overview of NASA seal developments. Representatives from GE provided insight into their advanced seal developments for both aircraft engines and ground power. Mr. Shaughnessy presented an overview of the work P&W and Stein Seal are doing on the development of high misalignment carbon seals for a geared fan application. Mr. Delgado of NASA Glenn presented an overview of turbine testing at NASA GRC. Ms. Proctor provided results from compliant foil seals investigations performed at NASA GRC.

Workshop Agenda
Wednesday, Nov. 5, Afternoon

Turbine Seal Development Session II	**1:30-3:30**
Test Rig for Evaluating Active Turbine Blade Tip Clearance Control Concepts	Dr. Scott Lattime/OAI, B. Steinetz/NASA GRC
Controls Considerations for Turbine Active Clearance Control	Mr. Kevin Melcher/NASA GRC
Microwave Blade Tip Sensor Technology Overview	Mr. Jon Geisheimer, Radatech Inc.
Non-contacting Seal Developments	Mr. John Justak/Advanced Technologies Group
Non-Contacting Finger Seal Design Considerations	Dr. Jack Braun/U. Akron, H. Pierson/U. Akron et al
Effect of Flow-induced Radial Load on Brush Seal/Rotor Contact Mechanics	Haifang Zhao & Dr. Robert J. Stango; Marquette University
Break	**3:30-3:45**
Turbine Seal Development Session III	**3:45-5:00**
Seal Developments at FlowServe	Mr. Andrew Flaherty, Mr. L. Young, & Mr. W. Key, Flowserve
Investigations of High Pressure Acoustic Waves in Resonators With Seal-like Features	Dr. Chris Daniels, OAI, B. Steinetz, J. Finkbeiner/GRC X. Li, and G. Raman/Illinois Institute of Tech.
Numerical Investigations of High Pressure Acoustic Waves in Resonators	Dr. Mahesh Athavale, M. Pindera/CFD Research C. Daniels, B. Steinetz/NASA GRC
Abradable Seal Developments at Technetics	Mr. Doug Chappel/Technetics Co.
6:15-?	**Group Dinner Viva Barcelona, Westlake**

NASA Glenn Research Center
Seal Team

Turbine engine studies have shown that reducing high pressure turbine (HPT) blade tip clearances will reduce fuel burn, lower emissions, retain exhaust gas temperature margin and increase range. Dr. Lattime presented the design and development status of a new Active Clearance Control Test rig aimed at demonstrating advanced ACC approaches and sensors. Mr. Melcher presented controls considerations for turbine active clearance control. Mr. Geisheimer of Radatech presented an overview of their microwave blade tip sensor technology. Microwave tip sensors show promise of operation in the extreme gas temperatures present in the HPT location.

Mr. Justak presented an overview of non-contacting seal developments at Advanced Technologies Group. Dr. Braun presented investigations into a non-contacting finger seal under development by NASA GRC and University of Akron. Dr. Stango presented analytical assessments of the effects of flow-induced radial loads on brush seal behavior. Mr. Flaherty presented innovative seal and seal fabrication developments at FlowServ. Mr. Chappel presented abradable seal developments at Technetics.

Dr. Daniels presented an overview of NASA GRC's acoustic seal developments. NASA is investigating the ability to harness high amplitude acoustic waves, possible through a new field of acoustics called Resonant Macrosonic Synthesis, to effect a non-contacting, low leakage seal. Dr. Daniels presented early results showing the ability to restrict flow via acoustic pressures. Dr. Athavale presented numerical results simulating the flow blocking capability of a pre-prototype acoustic seal.

Workshop Agenda

Thursday, Nov. 6, Morning

Registration at OAI	**8:00-8:30**
Space Vehicle Development	**8:30-10:15**
Shuttle Columbia Leading Edge Impact Investigations	Mr. Matthew Melis, M. Pereira, D. Revilock, D. Hopkins/NASA GRC
Nuclear Rocket Propulsion for Future NASA Missions	Dr. Stan Borowski,/NASA GRC
Overview of Boeing Advanced Space Vehicles and Seal Needs	Ms. Leanne Lehman/T. Steyer/Boeing Co.
Overview of ISTAR Engine Development & Seal Needs	Mr. Ravi Nigam, R. Kreidler/Pratt & Whitney
Break	**10:15-10:30**
Structural Seal Development	**10:30-12:00**
Atlas V Solid Rocket Motor Carbon Fiber Rope Status Review -> ***Withdrawn***	Mr. Michael Sears, Dr. Gary Luke/Aerojet
High Temperature Propulsion System Structural Seals for Future Space Launch Vehicles	Mr. Pat Dunlap, B. Steinetz/ GRC, J. Demange/U. Toledo
Advanced Control Surface Seal Development for Future Space Vehicles	Mr. Jeff DeMange/U. Toledo, P. Dunlap, B. Steinetz/GRC
CFD Analyses of ISTAR Engine Seals: An Update	Mr. Alton Reich, M. Athavale/CFD-RC
Lunch OAI Sun Room	**12:00-1:00**

NASA Glenn Research Center
Seal Team

Mr. Melis presented an overview of NASA GRC's leading edge impact investigations performed to support both the Columbia failure investigation and Shuttle return to flight. Dr. Borowski presented plans for nuclear propulsion to support NASA's goal of traveling to the outer reaches of the solar system in much shorter times than that possible through conventional propulsion systems. Ms. Lehman of Boeing Space and Communications presented Boeing's plans for future space vehicles and seal needs.

NASA is investigating hybrid rocket/air-breathing systems to increase propulsion system specific impulse. Mr. Nigam presented an overview of the ISTAR (Integrated System Test of an Air-breathing Rocket) program and engine seal challenges. Mr. Dunlap presented propulsion seal development efforts underway at GRC for engine ramps of future hypersonic airbreathing engines. Mr. DeMange presented control surface (e.g. hinge-line) seal development efforts underway at GRC for future re-entry vehicles. Dr. Athavale presented CFD/thermal analyses results of the ISTAR engine ramp seals indicating the challenging ramp seal thermal environments that demand high temperature seal designs.

Workshop Agenda
Thursday, Nov. 6, Afternoon

High Temperature Materials and Related Developments	**1:00-2:00**
Development of High Temperature Seal Preloaders	Mr. Ted Paquette/Refractory Composites, J. Palko/CRT Technologies
High Temperature Metallic Seal Development for Aeropropulsion Applications	Mr. Greg More/Advanced Products A. Datta/Advanced Components & Material
BrazeFoil Honeycomb	Mr. Geosef (Joey) Straza, AeroVision International
Tour of NASA Seal Test Facilities	**2:30-4:00**
Adjourn	

NASA Glenn Research Center
Seal Team

Advanced structural seals and preloading elements require application of advanced high temperature materials. The closing session of the workshop presented seal concepts and materials being developed at several locations. Mr. Paquette presented high temperature seal preloader development work being performed by Refractory Composites, under contract to NASA GRC. Mr. Palko presented finite element analyses of these candidate preloader systems helping guide preloader design selection. Mr. More (Advanced Products) and Dr. Datta (Advanced Components and Materials) presented an overview of their high temperature metallic seal development.

Mr. Straza of Aerovision and Daniel Kay presented an innovative BrazeFoil honeycomb that combines braze alloy and honeycomb together to facilitate brazing to turbine static structures for aerospace applications.

NASA Glenn Seal Team

Seal Team Leader: Bruce Steinetz

Mechanical Components Branch/5950

Turbine Seal Development

Develop non-contacting, low-leakage turbine seals

Margaret Proctor: Principal Investigator/POC

Irebert Delgado, Dave Fleming

Dan Breen, Joe Flowers

Structural Seal Development

Develop resilient, long-life, high-temp. structural seals

Pat Dunlap: Principal Investigator/POC

Jeff DeMange, Josh Finkbeiner

Malcolm Robbie, Gus Baker

Clearance Management

Develop novel approaches for blade-tip clearance control.

Scott Lattime: Principal Investigator/POC

Jim Smialek, Kevin Melcher, Chris Daniels

Malcolm Robbie

Emerging Areas

Acoustic Seals, Fuel Cell Seals

Pulse Detonation/Constant Vol. Combustion Engine Seals

Chris Daniels: Principal Investigator/POC

Josh Finkbeiner

NASA Glenn Research Center
Seal Team

The Seal Team is divided into four primary areas. The principal investigators and supporting researchers for each of the areas are shown in the slide. These areas include turbine seal development, structural seal development, clearance management, and seals for emerging areas. The first area focuses on high temperature, high speed shaft seals for turbine engine secondary air system flow management. The structural seal area focuses on high temperature, resilient structural seals required to accommodate large structural distortions for both space- and aero-applications.

Our goal in the clearance management project is to develop advanced sealing approaches for minimizing blade-tip clearances and leakage. We are planning on applying either rub-avoidance or regeneration clearance control concepts (including smart structures and materials) to promote higher turbine engine efficiency and longer service lives.

We are also contributing seal expertise in a range of emerging areas. These include acoustic seals (a GRC innovation), fuel cell seals, and seals for pulse detonation/constant volume combustion engines. GRC has received strong support for the development of pulse detonation hybrid engines and fuel cells for on-board power generation. These applications would see significant efficiency gains through the improvement of their sealing systems.

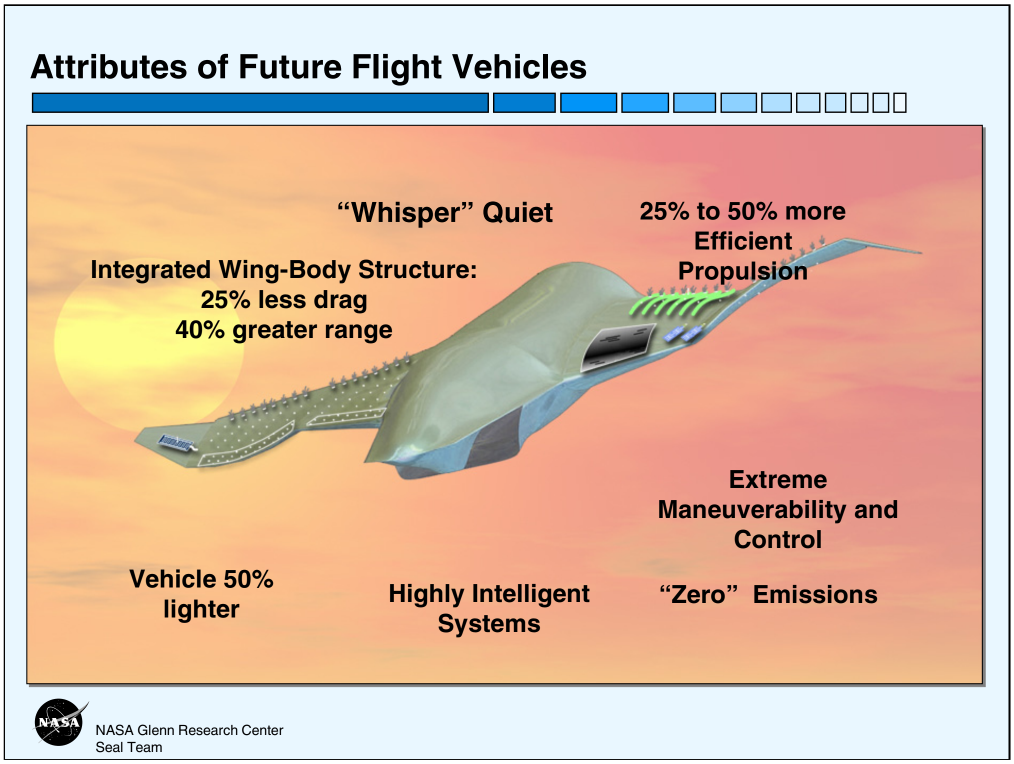

Attributes of future aircraft are illustrated here. Future vehicles will incorporate advanced materials to reduce weight and drag. Future aircraft will also use highly efficient quiet propulsion systems to reduce fuel burn, reduce emissions and reduce noise in and around airports.

One might ask: What role would advanced seals play in these future vehicles? Lower leakage engine seals reduce engine fuel burn and as a result reduce aircraft emissions. Cycle studies have shown the benefits of increasing engine pressure ratios and cycle temperatures to decrease engine weight and improve performance in next generation turbine engines (Steinetz and Hendricks, 1998). Advanced seals have been identified as critical in meeting engine goals for specific fuel consumption, thrust-to-weight, emissions, durability and operating costs. NASA and the industry are identifying and developing engine and sealing technologies that will result in dramatic improvements and address each of these goals for engines entering service in the 2005-2007 time frame.

Aspirating Seal Development: GE90 Demo Program

Funded UEET Seal Development Program

Goal:

Complete aspirating seal development by conducting full scale (36 in. diameter) aspirating seal demonstration tests in GE90 engine.

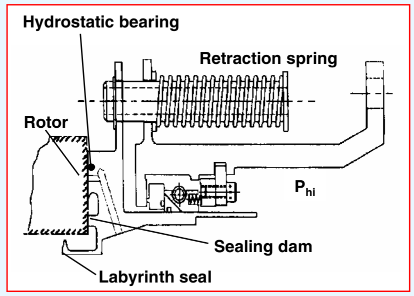

Payoffs:

- Leakage ~1/4th labyrinth seal
- Decrease SFC by 1.86% for three locations
- Operates without contact under severe conditions:
  - + 10 mil TIR
  - + 0.25°/0.8 sec tilt maneuver loads (0.08" deflection!)

General Electric GE90

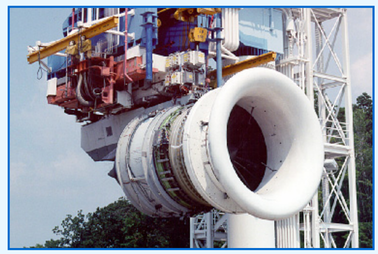

Schedule:

– Complete engine assembly 4Q CY03
– GE90 engine test: 1Q CY04

Partners:

GE/Stein Seal/CFDRC/NASA GRC

NASA Glenn Research Center
Seal Team

General Electric is developing a low leakage aspirating face seal for a number of locations within modern turbine applications. This seal shows promise both for compressor discharge and balance piston locations.

The seal consists of an axially translating mechanical face that seals the face of a high speed rotor. The face rides on a hydrostatic cushion of air supplied through ports on the seal face connected to the high pressure side of the seal. The small clearance (0.001-0.002 in.) between the seal and rotor results in low leakage (1/4th that of new labyrinth seals). Applying the seal to 3 balance piston locations in a GE90 engine can lead to >1.8% SFC reduction. GE Corporate Research and Development tested the seal under a number of conditions to demonstrate the seal's rotor tracking ability. The seal was able to follow a 0.010 in. rotor face total indicator run-out (TIR) and could dynamically follow a 0.25˚ tilt maneuver (simulating a hard maneuver load) all without face seal contact. The NASA GRC Ultra Efficient Engine Technology (UEET) Program is funding GE to demonstrate this seal in a ground-based GE-90 demonstrator engine in 2003. More details can be found in Boyle and Albers, 2004 in this Seal Workshop Proceedings and Turnquist, et al 1999.

NASA GRC Compliant Foil Seal Investigations

Objective:

Evaluate leakage and power loss performance of compliant foil seal

Approach:

- Evaluate leakage and lift performance using using new NASA GRC seal test rig (8.5" diameter).
- Measure seal tare torque and power loss using new torque meter.

Results:

- Measured performance data from 0-25 Krpm and 0-70 psid at 70 F.
- Tests identified seal design issues.
- Examining re-design options

Partners:

NASA GRC/ Mohawk MiTI (SBIR Ph 2)

Compliant Foil Seal (CFS) Schematic

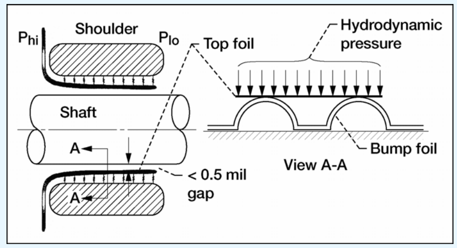

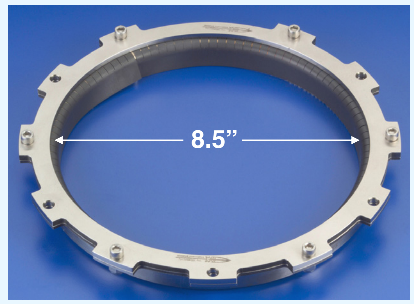

NASA Glenn Research Center
Seal Team

NASA GRC recently completed a series of tests to evaluate the performance of a compliant foil finger seal developed by Mohawk Innovative Technologies under a NASA SBIR Phase 2 contract.

Compliant foil seals incorporate features common to foil bearings including a top foil and underlying bump foils. A main difference is the addition of a closeout on the high pressure side to prevent leakage through the bump-foils. The seal is designed to operate without contact with small clearances - important parameters for long life and low leakage. In principal, clearance is maintained between the flexible foils and the rotor shaft through a hydrodynamic film that exists between the foil and the shaft.

The tests performed at GRC on an 8.5" diameter seal revealed some shortcomings of the current seal design and rotor coating. NASA and Mohawk are investigating what design changes could be incorporated to prevent seal-to-rotor contact in the future. For further details on the seal design and test results, please see Proctor et al, 2004, in this Seal Workshop Proceedings.

Non-Contacting Finger Seal Development
NASA GRC/University of Akron

Objective:

Develop non-contacting finger seal to overcome finger element wear and heat generation for future turbine engine systems

Approach:

- Solid modeling for stick and pad motion/stresses
- Fluid/solid interaction for leakage evaluation
- Experimental verification

Status:

- Developed a simplified spring-mass-damper model to assess seal's dynamic response.
- CFD-ACE+ (3-D Navier-Stokes code) utilized to analyze the thermofluid behavior and to obtain stiffness and damping parameters.
- Pressure patterns, mass flows and load carrying capabilities were assessed.

Program:

NASA/Univ. of Akron Coop. Agreement:
Dr. Braun (U. of Akron) M. Proctor, Monitor

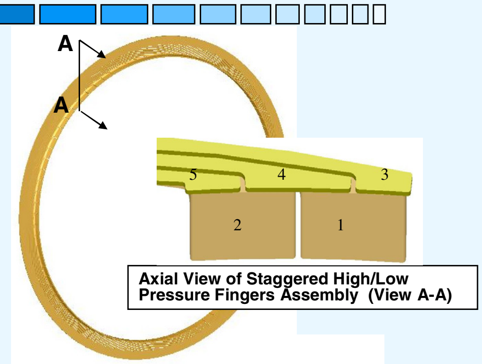

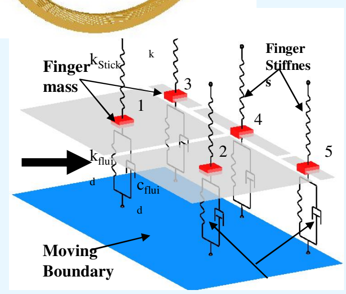

Spring-mass-damper model

NASA Glenn Research Center
Seal Team

Conventional finger seals like brush seals attain low leakage by operating in running contact with the rotor (Proctor, et al, 2002). The drawbacks of contacting seals include wear over time, heat generation, and power loss.

NASA Glenn has developed several concepts for a non-contacting finger seal. In one of these concepts the rear (low-pressure, downstream) fingers have lift pads (see pads 1 & 2 in inset figure) and the upstream (high pressure side) fingers are pad-less, and are designed to block the flow through the slots of the downstream fingers. The pressure-balance on the downstream-finger lift-pads cause them to lift. The front fingers are designed to ride slightly above the rotor preventing wear. Pressure acts to hold the upstream fingers against the downstream fingers. It is anticipated that the upstream/downstream fingers will move radially as a system in response to shaft transients. Though a small pin-hole leakage path exists between the inner diameter of the upstream fingers, the rotor, and the downstream fingers, this small pin-hole doesn't cause a large flow penalty especially considering the anticipated non-contacting benefits of the overall approach.

Dr. J. Braun of University of Akron is performing analyses and tests of this GRC concept through a cooperative agreement (Braun et al, 2003). University researchers developed an equivalent spring-mass-damper system to assess lift characteristics under dynamic excitation. Fluid stiffness and damping properties were obtained utilizing CFD-ACE+ (3-D Navier-Stokes code) and a perturbation approach. These stiffness and damping properties were input into the dynamic model expediting the solution for design purposes. More details can be found in Braun et al, 2004 in this Seal Workshop Proceedings. After feasibility tests are complete at the University, seals will be tested under high speed and high temperature conditions at NASA GRC.

Rotating Machinery Clearance Management

Develop and demonstrate clearance management technologies to improve turbine engine performance, reduce emissions, and increase service life through

- Rub-Avoidance
- Regeneration

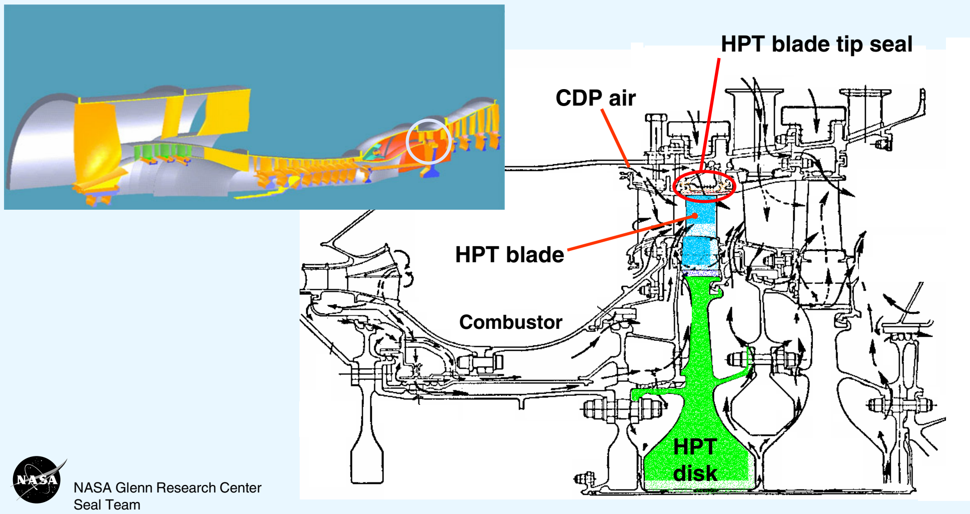

NASA Glenn Research Center
Seal Team

System studies have shown the benefits of reducing blade tip clearances in modern turbine engines. Minimizing blade tip clearances throughout the engine will contribute materially to meeting NASA's Ultra-Efficient Engine Technology (UEET) and Revolutionary Turbine Accelerator (RTA) turbine engine project goals. NASA GRC is examining two candidate approaches including rub-avoidance and regeneration which are explained in subsequent slides.

Benefits of Blade Tip Clearance Control

- Fuel Savings/ Reduced Emissions (HPT)
  - 0.010-in tip clearance is worth ~1% SFC
  - Emissions Reduction (Landing/Takeoff – Ref. GE Propulsion 21 Study)
    - » NOx
    - » CO
- Increased Cycle Life (Reduced Maintenance Costs)
  - Deterioration of exhaust gas temperature (EGT) margin is the primary reason for aircraft engine removal from service
  - 0.010-in tip clearance is worth ~10 ºC EGT
  - Allows turbine to run at lower temperatures, increasing cycle life of hot section components and engine time-on-wing (~1000 cycles)
- Increased Efficiency/Operability
  - Increased payload and mission range capabilities
  - Increased high pressure compressor (HPC) stall margin

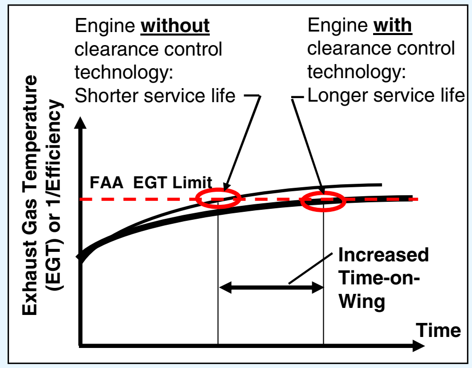

Clearance Control Technology Promotes High Efficiency and Long Life

NASA Glenn Research Center
Seal Team

Blade tip clearance opening is a primary reason for turbine engines reaching their FAA certified exhaust gas temperature (EGT) limit and subsequent required refurbishment. As depicted in the chart on the right, when the EGT reaches the FAA certified limit, the engine must be removed and refurbished. By implementing advanced clearance control measures, the EGT rises slower (due to smaller clearances) increasing the time-on-wing.

In summary, benefits of clearance control in the turbine section include lower specific fuel consumption (SFC), lower emissions (NOx, CO), retained exhaust gas temperature (EGT) margins, higher efficiencies, longer range (because of lower fuel-burn). Benefits of clearance control in the compressor include better compressor stability (e.g. resisting stall/surge), higher stage efficiency, and higher stage loading. All of these features are key for future NASA and military engine programs.

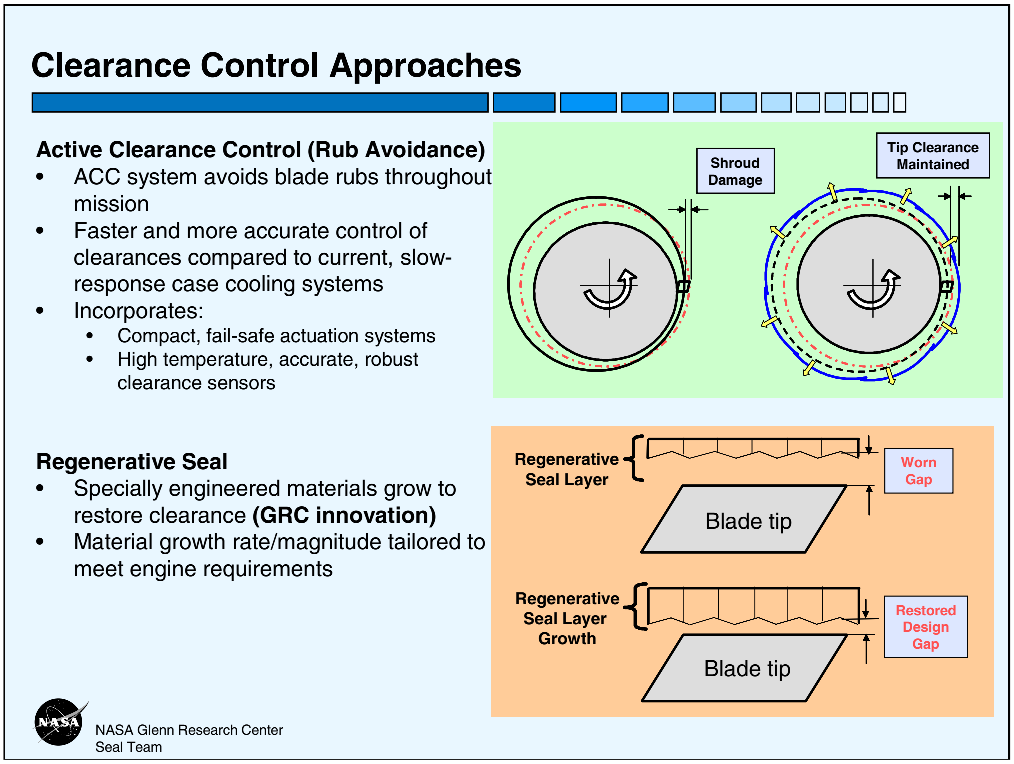

NASA Glenn is pursuing two approaches to controlling clearances. The first is rub-avoidance in which an active clearance control system would actively move the seal or shroud segments out of the way during the transient event to avoid blade rubs. The second is regeneration in which clearance openings are mitigated using specially-engineered materials that re-grow. Materials are being investigated that would grow at a rate comparable to the average rate of wear anticipated. More details regarding this program can be found in Lattime and Steinetz 2004 in this Seal Workshop Proceedings, and Lattime and Steinetz, 2002.

Regenerative Material Feasibility Testing

Observations:

- **Significant growth occurred at HPT temperatures (~2000 °F)**
- **Material remained structurally stable even after 15% growth**
- **Materials suitable for use in HPT environment**

100 hr Test

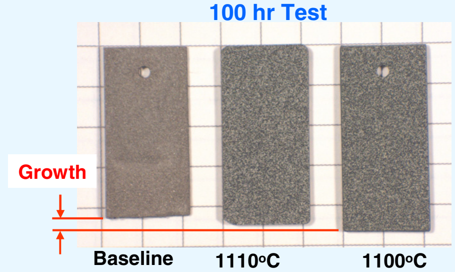

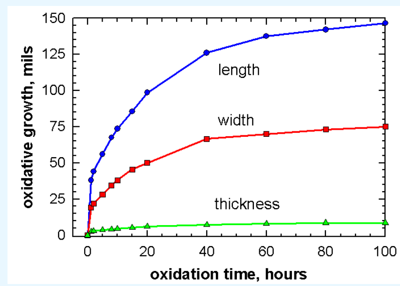

Research Areas Currently Being Pursued:

- **Material system composition effects on growth rate and magnitude**
  - **Collaborative effort with GRC Materials Division**
- **Structural design effects on reducing spallation potential**

NASA Glenn Research Center
Seal Team

GRC is investigating novel materials that exhibit self-adaptive behavior within their environment. Under the regenerative seal material project, GRC is developing and assessing whether materials can change volume and grow at an appropriate rate to mitigate clearance openings between the high pressure turbine blades and shrouds. In one recent trial, specially engineered materials were subjected to simulated HPT engine temperatures (2000+F) to determine the nature of their growth characteristics. Shown in the top figure are three specimens: a baseline as-sprayed sample, and two samples subjected to 100 hrs of 2000+F temperatures. One can see from the significant length change in both the photograph and measured dimensional data, that the specimens grew up to 15% of their original dimensions (length, width, and thickness). Also the material remained structurally stable after expansion.

Having demonstrated this initial growth feasibility, we are now pursuing additional research areas. These include identifying material system composition effect on growth rates and magnitudes and examining structural design effects on reducing material spallation potential.

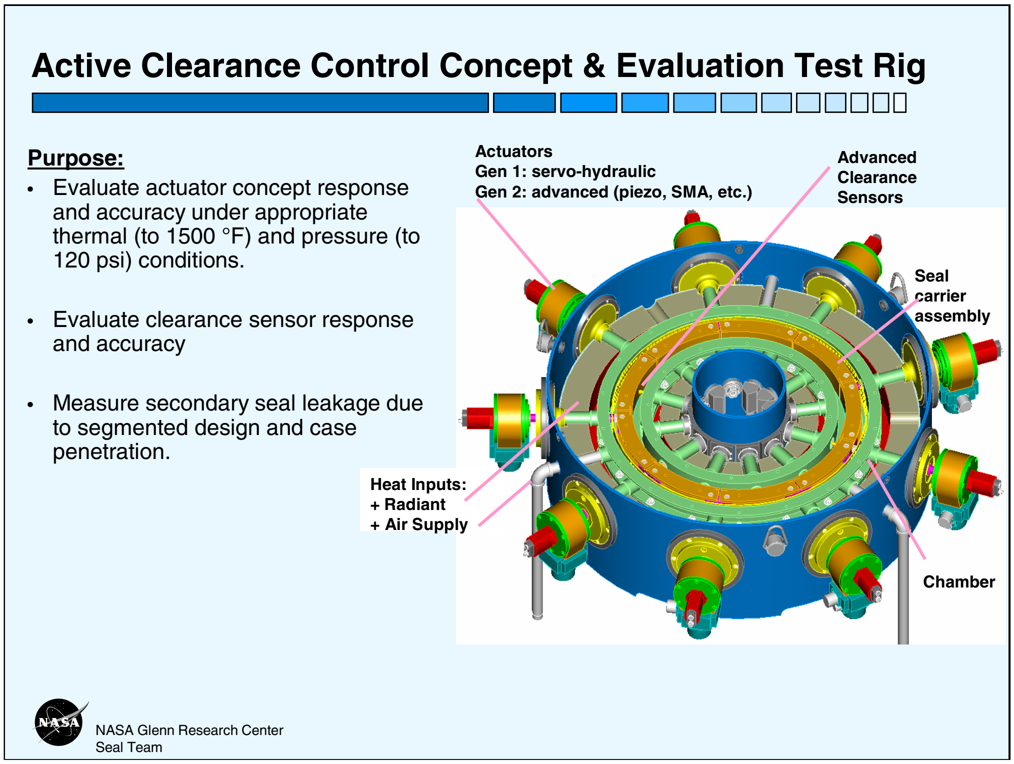

NASA GRC is developing a unique Active Clearance Control (ACC) concept and evaluation test rig. The primary purpose of the test rig is to evaluate actuator concept response and accuracy under appropriate thermal (up to 1500F) and pressure (up to 120 psig) conditions. Other factors that will be investigated include:

- Actuator stroke, rate, accuracy, and repeatability
- System concentricity and synchronicity
- Component wear
- Secondary seal leakage
- Clearance sensor response and accuracy

The results of this testing will be used to further develop/refine the current actuator design as well as other advanced actuator concepts. More details regarding this test rig can be found in Lattime and Steinetz 2004 in this Seal Workshop Proceedings, and Lattime et al, 2003.

Acoustic Seal Development

Goal: Develop a non-contacting, long-life seal using high amplitude acoustic pressures

How Does It Work?

Specially shaped acoustic resonator is driven at resonance generating acoustic pressures that prevent flow between high- and low-pressure cavities effecting a seal

Significance?

Acoustic-based, virtually zero-leakage, non-contacting seals would overcome two fundamental problems of conventional seals:

- Leakage
- Wear

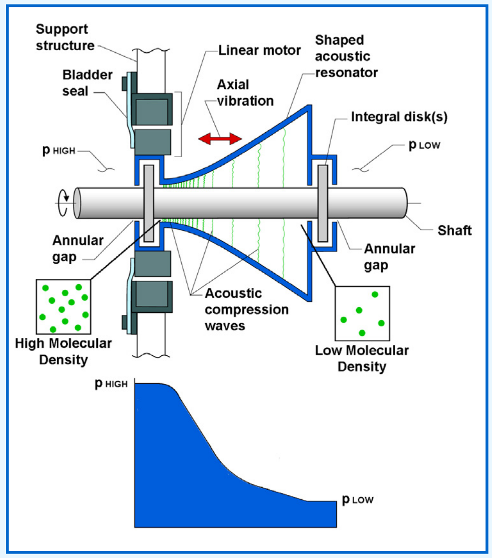

NASA Glenn Research Center
Seal Team

Our goal in the acoustic seal project is to develop non-contacting, low leakage seals exploiting the principles of advanced acoustics. We are currently investigating a new acoustic field known as Resonant Macrosonic Synthesis (RMS) to determine if one can harness the large acoustic standing pressure waves to form an effective air-barrier/seal. This project builds on Lucas' work in "Resonant Macrosonic Synthesis" (Lucas, 1996). Exploiting shock-free pressure waves and specially shaped resonating cavities, Macrosonics can produces peak acoustic pressures exceeding 200 psi - many thousands of times normal acoustic pressure levels.

In an acoustic seal, large acoustic standing waves would acoustically pressurize the gas in an acoustic resonator. The acoustic compression waves would result in a high pressure boundary condition adjacent to the high pressure side of the seal apparatus (left side in figure). This high pressure boundary condition would impede the flow of pressurized gas thru annular openings around the shaft thereby leading to an effective seal. Disks could be introduced to cause a line-of-sight blockage further minimizing seal leakage. More details regarding this program can be found in Daniels and Steinetz 2004 in this Seal Workshop Proceedings and Daniels et al, 2004.

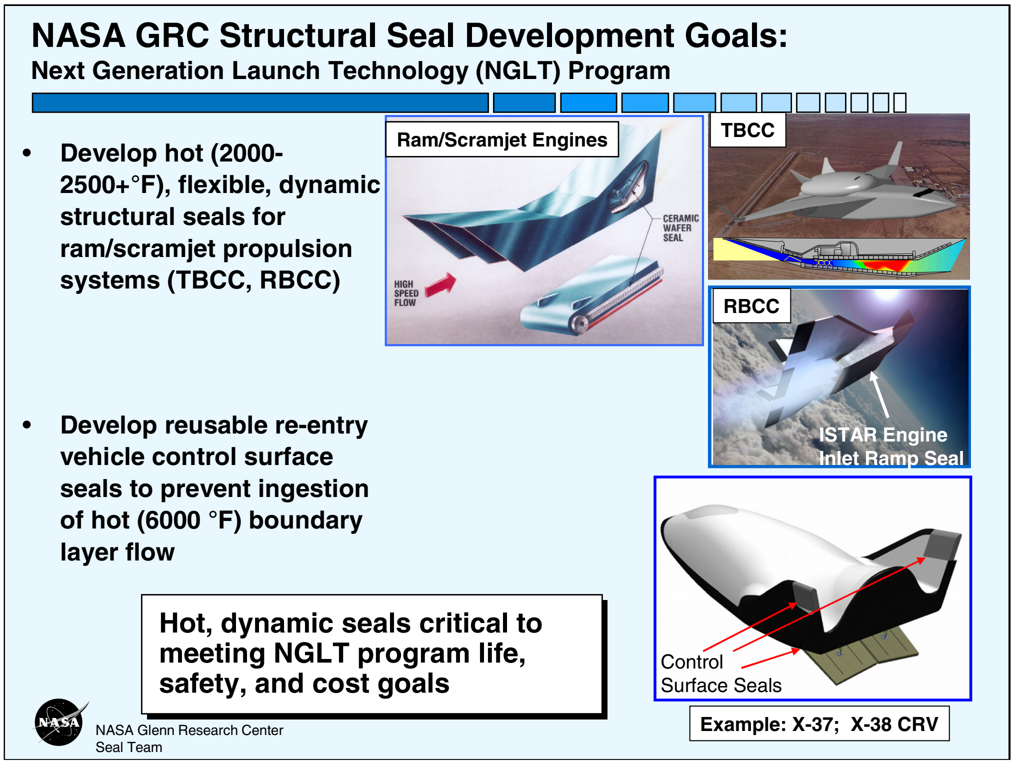

NASA is currently funding research on advanced technologies that could greatly increase the reusability, safety, and performance of future Reusable Launch Vehicles (RLV). Research work is being performed under NASA's Next Generation Launch Technology (NGLT) program on both high specific-impulse ram/scramjet engines and advanced re-entry vehicles.

NASA GRC is developing advanced structural seals for both propulsion and vehicle needs by applying advanced design concepts made from emerging high temperature ceramic materials and testing them in advanced test rigs that are under development. See Dunlap 2004, et al, and DeMange 2004, et al in this Seal Workshop Proceedings and Dunlap 2003, et al and DeMange 2003, et al for further details.

Example Structural Seals Being Investigated

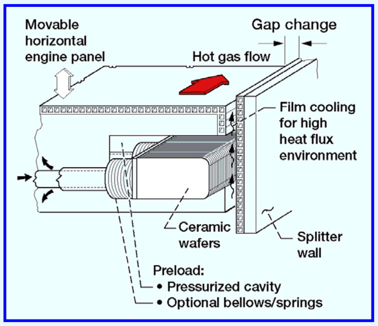

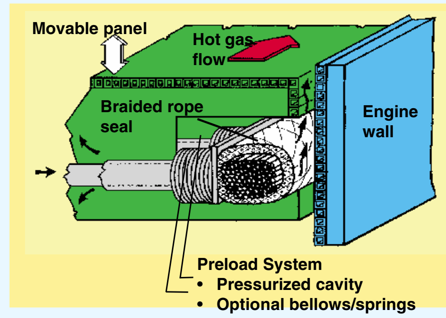

Ceramic Wafer Seal

- High temperature operation:up to 2500˚F
- Low Leakage
- Flexibility: Relative sliding of adjacent wafers conforms to wall distortions
- Ceramic material lighter weight than metal system
- Tandem seals permit central cavity purge (cooling)

Braided Rope Seal

- High temperature operation: 1500-2200+ °F (500-1200 °F hotter than graphite seals)
- Flexible: seals & conforms to complex geometries
- Hybrid design (ceramic core/superalloy wire sheath) resists abrasion
- Tandem seals permit central cavity purge (cooling)

NASA Glenn Research Center
Seal Team

NASA GRC's work on high temperature structural seal development began in the late 1980's during the National Aero-Space Plane (NASP) project. GRC led the in-house propulsion system seal development program and oversaw industry efforts for propulsion system and airframe seal development for this vehicle.

Two promising concepts identified during that program included the ceramic wafer seal (Steinetz, 1991) and the braided rope seal (Steinetz and Adams, 1998) shown here. By design, both of these seals are flexible, lightweight, and can operate to very high temperatures (2200+˚F). These seal concepts are starting points for the extensive seal concept development and testing planned under NASA's 3rd Generation high temperature seal development tasks.

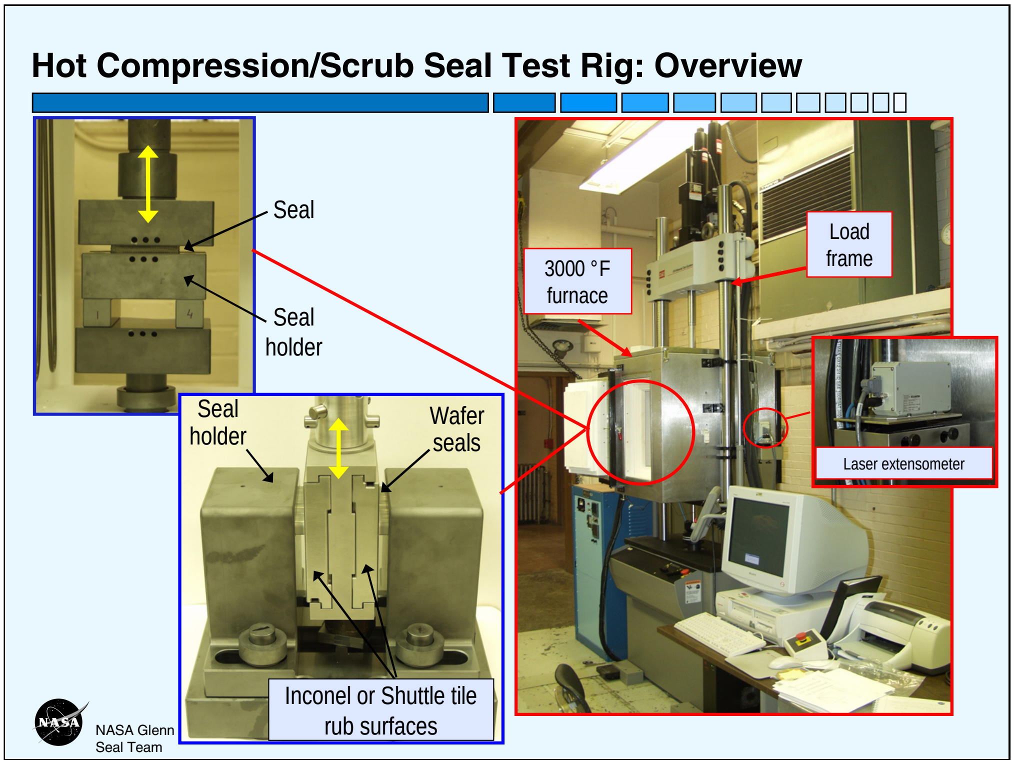

NASA GRC has installed state-of-the-art test capabilities for evaluating seal performance at temperatures up to 3000 °F (1650 °C). This one-of-a-kind equipment will be used to evaluate existing and new seal designs by simulating the temperatures, loads, and scrubbing conditions that the seals will have to endure during service. The compression test rig (upper left photo) is being used to assess seal load vs. linear compression, preload, & stiffness at temperature. The scrub test rig (middle photo) is being used to assess seal wear rates and frictional loads for various test conditions at temperature. Both sets of fixtures are made of silicon carbide permitting high temperature operation in air.

The test rig includes: an MTS servo-hydraulic load frame, an ATS high temperature air furnace, and a Beta LaserMike non-contact laser extensometer, and the special purpose seal holder hardware. Unique features of the load frame include dual load cells (with multi-ranging capabilities) for accurate measurement of load application, dual servo-valves to permit precise testing at multiple stroke rates (up to 8 in./s.), and a non-contact laser extensometer system to accurately measure displacements.

Development of Thermal Barriers for Shuttle RSRM’s

- **Shuttle RSRM’s have had periodic hot gas effects in nozzle joints, leading to extensive reviews before flight**
- **Thiokol re-designed joints with GRC carbon fiber rope (CFR) thermal barrier to prevent hot (5500˚F) gas from affecting downstream O-rings**

Status

- **Flight certification, static-motor tests have been completed for Joints 2, 5, and 6 (nozzle to case joint).**
- **Assembly of solid motors with thermal barriers commencing during 2003.**
- **Flight expected 2005 (depending on return- to-flight schedule)**

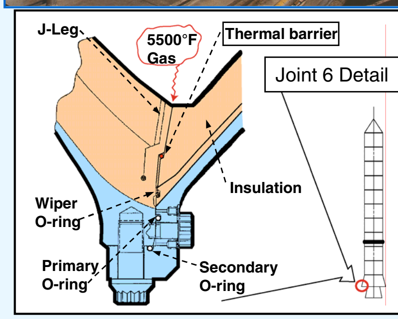

NASA Glenn Research Center
Seal Team

Periodically several of the Shuttle’s solid rocket motor nozzle joints experience hot gas effects. Over the past several years, engineers from NASA Glenn, Marshall Space Flight Center, Thiokol, and Albany-Techniweave have been investigating the feasibility of applying the NASA GRC developed carbon fiber thermal barrier to overcome this issue. (More details of this program can be found in Steinetz and Dunlap, 2001, and Steinetz and Dunlap Patent No. 6,446,979 B1). The thermal barrier reduces the temperature of the 5500°F rocket combustion gas and permits only relatively cool (<200 °F) gas to reach the O-rings. This important new technology improves on already high Shuttle safety margins and enables solid rocket motor joint assembly in significantly less time (approximately one-sixth the time) as compared to the previous joint fill compound approach with much higher degrees of reproducibility. Full-scale solid rocket motor test results showed that the thermal barrier protected the downstream O-rings even when intentional flaws were cut into the barrier.

In January, 2003, Thiokol completed flight certification tests on Joints 2, 5, 6. Assembly of the joints with the GRC thermal barriers is commencing this year. The first shuttle flight is expected in 2005 depending on Shuttle’s return to flight schedule.

Application of GRC Thermal Barrier in Atlas V SRM's

Final qualification test of Aerojet solid rocket motor with thermal barriers installed (Dec. 2002)

Atlas V boosted by two Aerojet SRM's incorporating GRC thermal barriers (July 17, 2003)

- **Aerojet experienced motor failure in spring 2002 qualification test of solid rocket motors for Atlas V**
- **Based on success in Shuttle RSRM's ground tests, Aerojet installed three thermal barriers in nozzle-to-case joint to protect O-rings from hot (5500+˚F), high pressure combustion gases. Certified for flight Dec. 2002.**
- **Lockheed-Martin/Aerojet Atlas V incorporated GRC thermal barriers. Successfully launched July 17, 2003!**

NASA Glenn Research Center
Seal Team

Based on the success of the carbon fiber rope thermal barriers in the shuttle solid rocket motors, Aerojet decided to implement the GRC thermal barriers into the nozzle-to-case joints in the SRMs for the Atlas V. A redesign of this critical joint was required after a March 2002 test resulted in a major motor failure.

Since implementing the GRC thermal barrier plus several other joint features, Aerojet has had 3 successful ground test firings and on July 17, 2003 successfully boosted the Lockheed-Martin Atlas V Enhanced Expendable Launch Vehicle carrying a Cablevision satellite into a successful transfer orbit. Aerojet's two boosters provided thrust in excess of 250,000 lbs. each. The boosters were ignited at liftoff, burned for more than 90 seconds and then were jettisoned. The mission was valued at $250M.

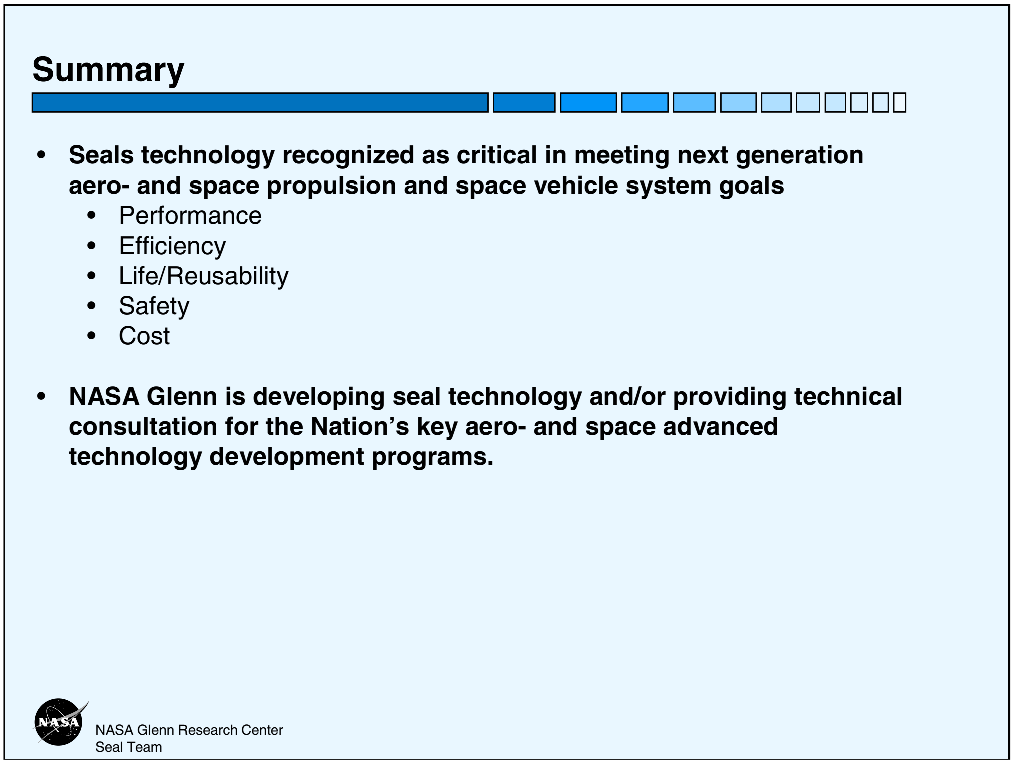

NASA Glenn is currently performing seal research supporting both advanced turbine engine development and advanced space vehicle/propulsion system development. Studies have shown that decreasing parasitic leakage through applying advanced seals will increase turbine engine performance and decrease operating costs.

Studies have also shown that higher temperature, long life seals are critical in meeting next generation space vehicle and propulsion system goals in the areas of performance, reusability, safety, and cost.

NASA Glenn is developing seal technology and providing technical consultation for the Agency's key aero- and space technology development programs.

NASA Seals Web Sites

- **Turbine Seal Development**
  - **http:/www.grc.nasa.gov/WWW/TurbineSeal/TurbineSeal.html**
    - » NASA Technical Papers
    - » Workshop Proceedings
- **Structural Seal Development**
  - **http://www/grc.nasa.gov/WWW/structuralseal/**
    - » NASA Technical Papers
    - » Discussion
    - » Seal Patents
  - **http://www/lerc.nasa.gov/WWW/TU/InventYr/1996Inv_Yr.htm**

NASA Glenn Research Center
Seal Team

The Seal Team maintains three web pages to disseminate publicly available information in the areas of turbine engine and structural seal development. Please visit these web sites to obtain past workshop proceedings and copies of NASA technical papers and patents.

References

- Braun, M.J., Choy, F.K., Pierson, H.M., 2003, "Structural and Dynamic Considerations Towards the Design of Padded Finger Seals", AIAA-2003-4698 presented at the AIAA/ASME/SAE/ASEE conference, July, Huntsville, AL.
- Daniels, C., Finkbeiner, J, Steinetz, B.M., Li, Xiaofan, Raman, G, 2004, "Non-linear Oscillations and Flow of Gas Within Closed and Open Conical Resonators," AIAA-2004-0677. To be presented at the 82nd AIAA Aerosciences Meeting, Reno, NV, January.
- DeMange, J.J., Dunlap, P.H., Steinetz, B.M., 2003, "Advanced Control Surface Seal Development for Future Space Vehicles," Presentation and Paper at 2003 JANNAF Conference, Dec. 1-5, Colorado Springs, CO, NASA/TM-2004-212898.
- Dunlap, P.H., Steinetz, B.M., DeMange, J.J., 2003, "High Temperature Propulsion System Structural Seals for Future Space Launch Vehicles," Presentation and Paper at 2003 JANNAF Conference, Dec. 1-5, Colorado Springs, CO. NASA/TM-2004-212907.
- Lattime, S.B., Steinetz, Bruce M., Robbie, M., 2003, "Test Rig for Evaluating Active Turbine Blade Tip Clearance Control Concepts," NASA TM-2003-212533, also AIAA-2003-4700, presented at the AIAA/ASME/SAE/ASEE conference, July, Huntsville, AL.
- Lattime, S.B., Steinetz, B.M. 2002 "Turbine Engine Clearance Control Systems: Current Practices and Future Directions, " NASA TM-2002-211794, AIAA 2002-3790.
- Lucas,T.S., 1996, "Acoustic Resonator Having Mode-Alignment-Cancelled Harmonics," US Patent 5,579,399.
- Proctor, M.P; Kumar, A.; Delgado, I.R.; 2002, "High-Speed, High Temperature, Finger Seal Test Results," NASA TM-2002-211589, AIAA-2002-3793.
- Steinetz, Bruce M., Dunlap, Patrick H., 2002, "Rocket Motor Joint Construction Including Thermal Barrier," U.S. Patent No. 6,446,979 B1, Issue Date: September 10.
- Steinetz, Bruce M.; Dunlap, Patrick H.: 2001, "Development of Thermal Barriers for Solid Rocket Motor Nozzle Joints" Journal of Propulsion and Power, Vol. 17 No. 5, pp. 1023-1034, September/October, also NASA-TM-1999-209191, June 1999.
- Steinetz, B.M., Hendricks, R.C., and Munson, J.H., 1998 "Advanced Seal Technology Role in Meeting Next Generation Turbine Engine Goals," NASA TM-1998-206961.
- Steinetz, Bruce M.; Adams, Michael L.: 1998, "Effects of Compression, Staging and Braid Angle on Braided Rope Seal Performance", J. of Propulsion and Power, Vol. 14, No. 6, also AIAA-97-2872, 1997 AIAA Joint Propulsion Conference, Seattle, Washington, July 7-9, 1997, NASA TM-107504, July 1997.
- Steinetz, B.M.: 1991, "High Temperature Performance Evaluation of a Hypersonic Engine Ceramic Wafer Seal," NASA TM-103737
- Turnquist, N.A.; Bagepalli, B; Lawen, J; Tseng, T., McNickle, A.D., Kirkes; Steinetz, B.M., 1999, "Full Scale Testing of an Aspirating Face Seal", AIAA-99-2682.

NASA Glenn Research Center
Seal Team

NASA ULTRA EFFICIENT ENGINE TECHNOLOGY PROJECT OVERVIEW

Catherine L. Peddie and Robert J. Shaw
National Aeronautics and Space Administration
Glenn Research Center
Cleveland, Ohio

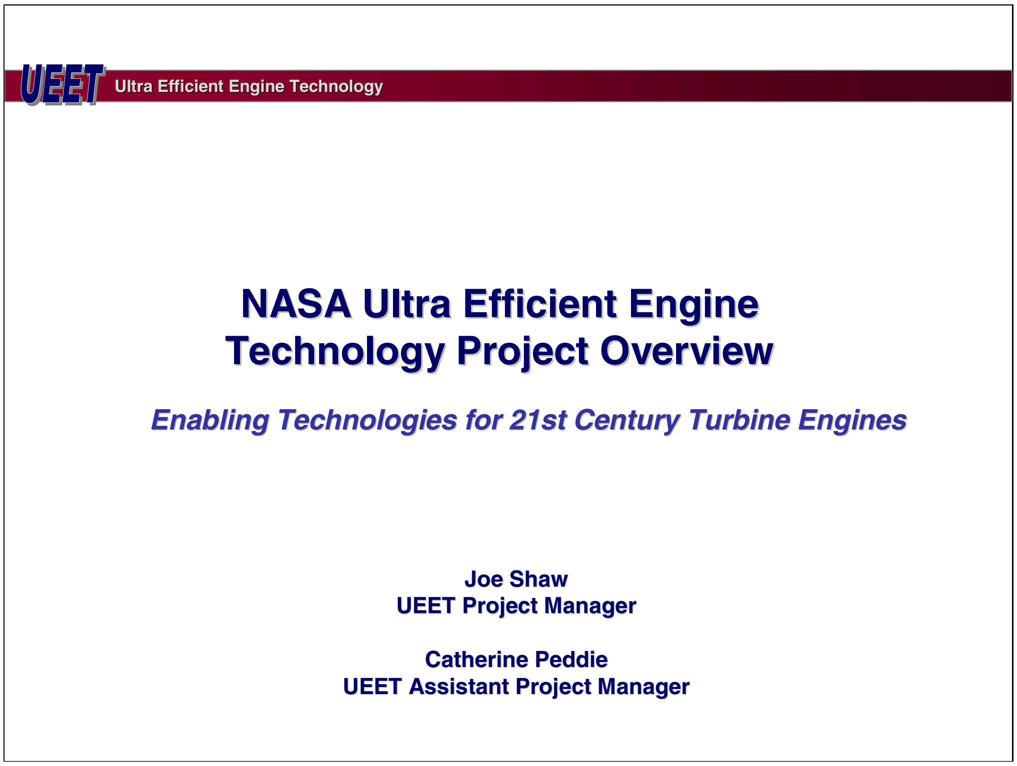

Outline

- Overview of current UEET Project
- Re invention of UEET as part of the Vehicle Systems Program

Current UEET Project

The NASA Mission

To understand and protect our home planet

To explore the Universe and search for life

To inspire the next generation of explorers

… as only NASA can.

Commercial Turbine
Engine Technology
Leadership for the
21st Century

NASA Glenn Research Center

UEET

Ultra-Efficient Engine Technology Program

The UEET Program will develop and transfer to the U. S. industry critical gas turbine engine technologies which will contribute to "enabling a safe, secure, and <u>environmentally friendly air transportation system"</u>.

Environmentally Friendly Aircraft

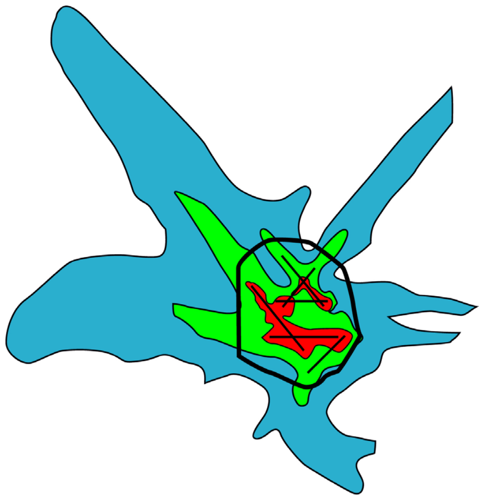

Noise within airport boundaries

Constrain objectionable noise to within airport boundaries

Smog-free

Minimize the contribution of air vehicles to the production of smog

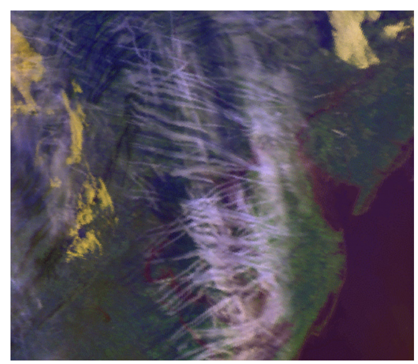

No impact on global climate

Minimize the impact of air vehicles on global climate

Revolutionize Aviation Goal Emissions Objective

UEET Ultra Efficient Engine Technology

Reduce emissions of future aircraft by a factor of three within 10 years (2007), and by a factor of five within 20 years.

NASA Three Pillars for Success-1997

Reduce NOx emissions of future aircraft by 70 percent within 10 years, and by 80 percent within 25 years (using the 1996 ICAO Standard for NO_x as the baseline. Reduce CO_2 emissions of future aircraft by 25 percent and by 50 percent In the same timeframes (using 1997 subsonic aircraft technology as the baseline).

NASA Aerospace Technology Enterprise Strategic Plan-2000

UEET will be the responsible propulsion program for delivering on this objective!

Vision: *Develop and hand off revolutionary turbine engine propulsion technologies that will enable future generation vehicles over a wide range of flight speeds.*

Goals:

Propulsion technologies to enable increases in system efficiency and, therefore, fuel burn reductions of up to 15 % (equivalent reductions in CO_2)

Combustor technologies (configuration and materials) which will enable reductions in LTO NO_x of 70% relative to 1996 ICAO standards.*

** LTO - Landing/Take-off*

Vision

UEET Ultra Efficient Engine Technology

Develop and hand off revolutionary propulsion turbine engine technologies that will enable future generation vehicles over a wide range of flight speeds.

We support the vision and are committed to the success of NASA's Ultra Efficient Engine Technology (UEET) Project.

William Koop, Air Force Research Laboratory

Gerald Brines, Allison-Rolls Royce

Mahmood Naimi, Boeing Commercial Airplane Company

Fred Krause, General Electric Aircraft Engines

Dimitri Mavris, Georgia Tech

Tim Conners, Gulfstream

Vinod Nangia, Honeywell

Tom Hartmann, Lockheed-Martin

Robert J. Shaw, NASA Glenn Research Center

Robert D. Southwick, Pratt & Whitney

Scott Cruzen, Williams International

Last Update-April 2003

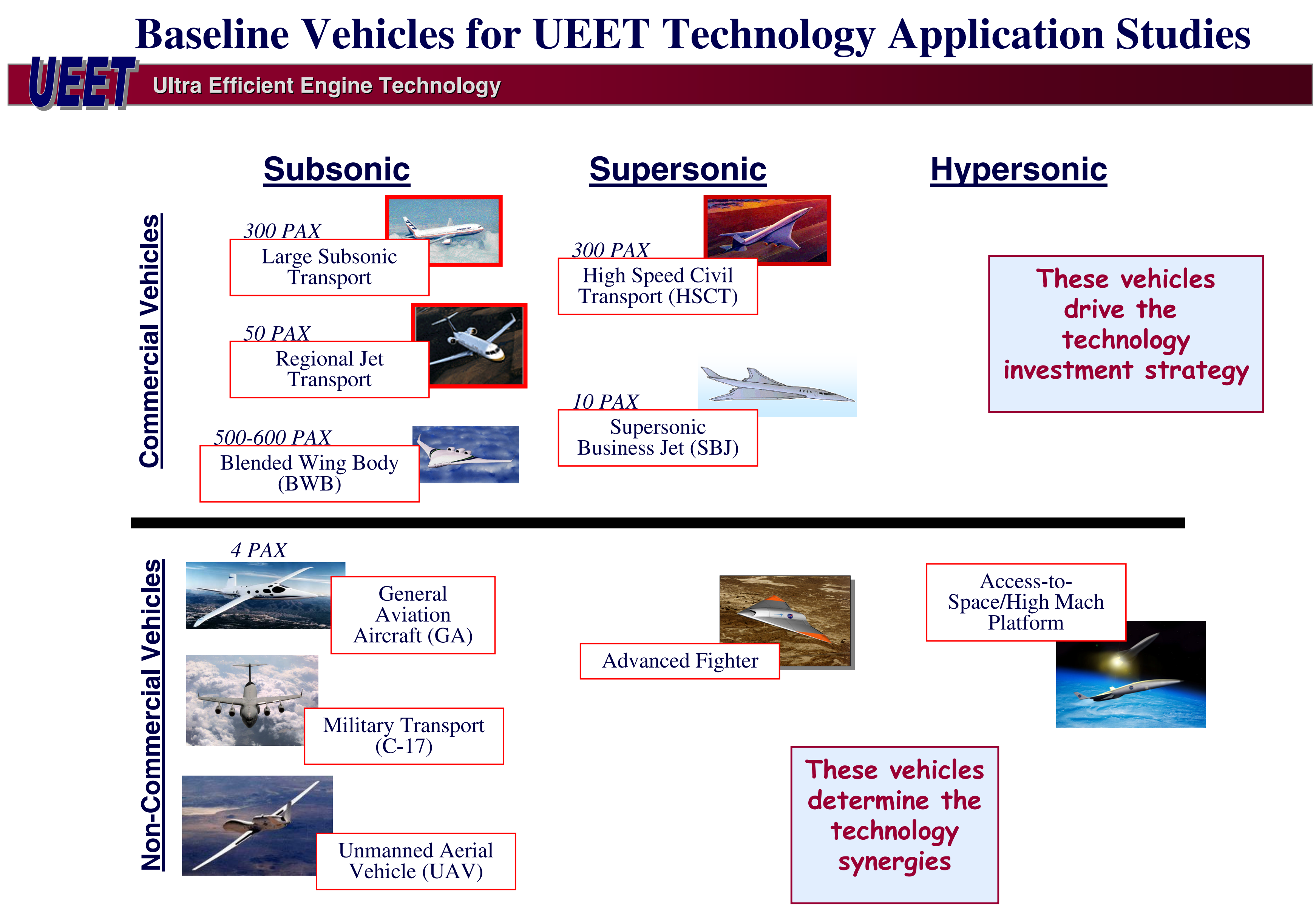

Baseline Vehicles for UEET Technology Application Studies
UEET
Ultra Efficient Engine Technology
Subsonic
Supersonic
Hypersonic
Commercial Vehicles
300 PAX
Large Subsonic Transport
50 PAX
Regional Jet Transport
500-600 PAX
Blended Wing Body (BWB)
300 PAX
High Speed Civil Transport (HSCT)
10 PAX
Supersonic Business Jet (SBJ)
These vehicles drive the technology investment strategy
Non-Commercial Vehicles
4 PAX
General Aviation Aircraft (GA)
Military Transport (C-17)
Unmanned Aerial Vehicle (UAV)
Advanced Fighter
Access-to-Space/High Mach Platform
These vehicles determine the technology synergies

Program Technical Objectives

UEET Ultra Efficient Engine Technology

	Goal	Minimum Success Criteria
CO_2 Goal	15% fuel burn reduction for large subsonic aircraft	12% fuel burn reduction for large subsonic aircraft
	8% fuel burn reduction for small subsonic, small / large supersonic	4% fuel burn reduction for small subsonic, small / large supersonic
NO_x Goal	70% N0x reduction (below ICAO 96) for subsonic (large/ regional) combustors over the LTO cycle	65% N0x reduction (below ICAO 96) for subsonic (large/ regional) combustors over the LTO cycle

NASA's Technology Readiness Level (TRL) Scale

UEET Ultra Efficient Engine Technology

TRL	General NASA Definition
9	Actual system "flight proven" on operational flight
8	Actual system completed and "flight qualified" through test and demonstration
7	System prototype demonstrated in flight environment
6	System/subsystem model or prototype demonstrated/validated in a relevant environment
5	Component and/or breadboard verification in a relevant environment
4	Component and/or breadboard test in a laboratory environment
3	Analytical and experimental critical function, or characteristic proof-of-concept
2	Technology concept and/or application formulated (candidate selected)
1	Basic principles observed and reported

System Test and Operations

System/Subsystem Development

Technology Demonstration

Technology Development

Research to Prove Feasibility

Basic Technology Research

Industry Role

Government Role

In partnership with DOD, industry

UEET

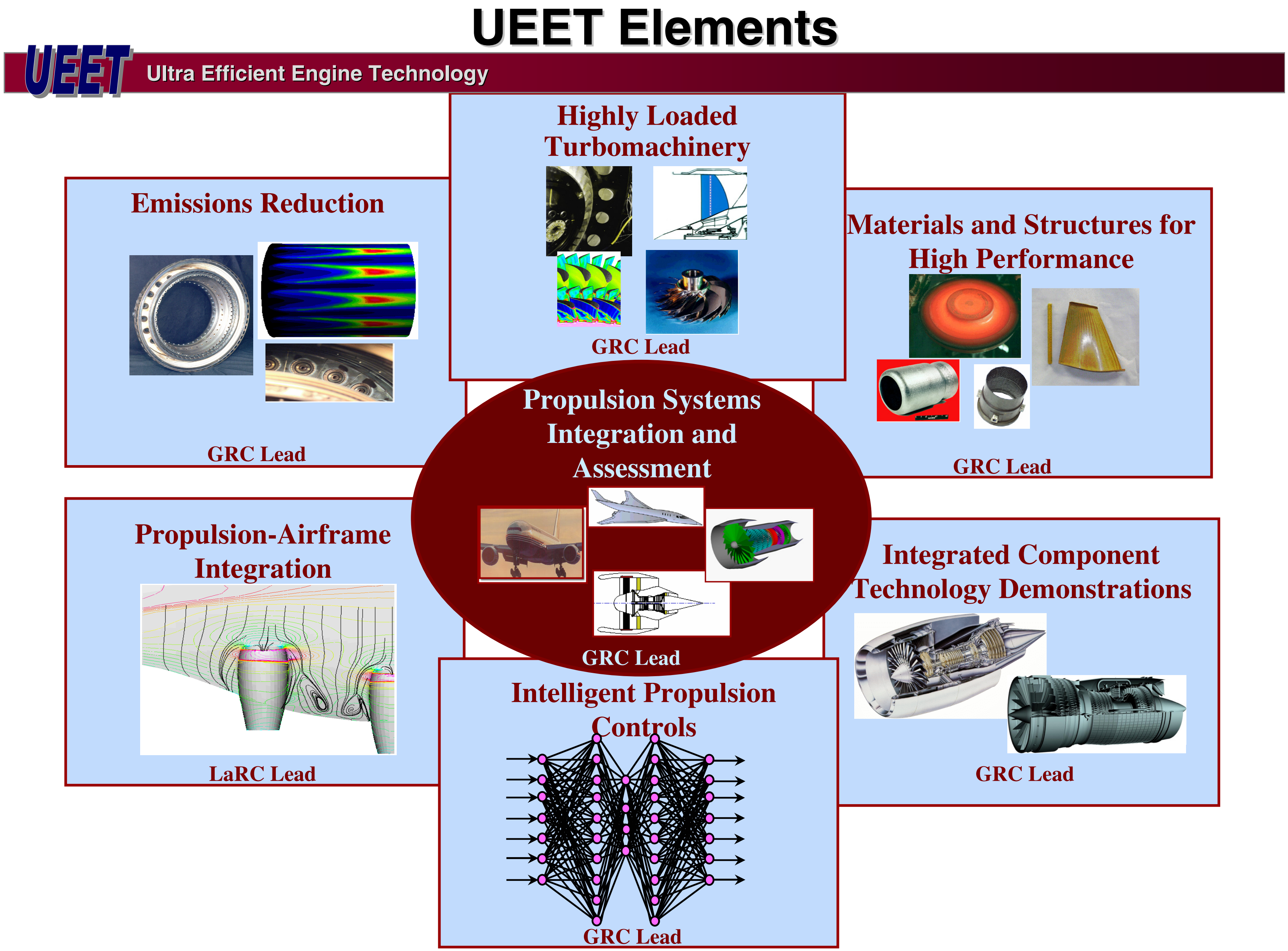
UEET Elements
UEET
Ultra Efficient Engine Technology
Emissions Reduction
GRC Lead
Highly Loaded Turbomachinery
GRC Lead
Materials and Structures for High Performance
GRC Lead
Propulsion Systems Integration and Assessment
GRC Lead
Propulsion-Airframe Integration
LaRC Lead
Integrated Component Technology Demonstrations
GRC Lead
Intelligent Propulsion Controls
GRC Lead

Selected Technical Highlights

UEET Ultra Efficient Engine Technology

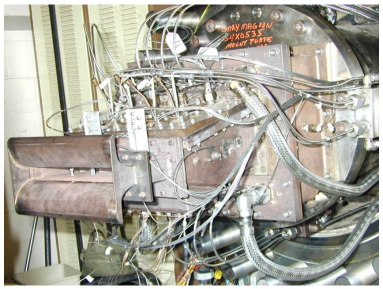

70% LTO NO_x
combustor sector tests

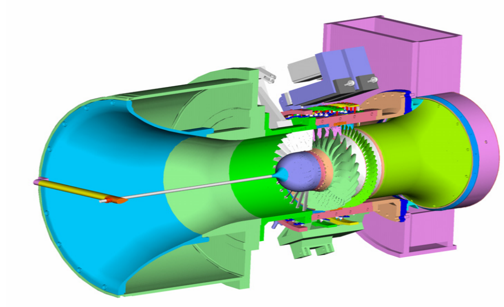

2 stage POC compressor rig design

Turbomachinery disk material
temperature limit

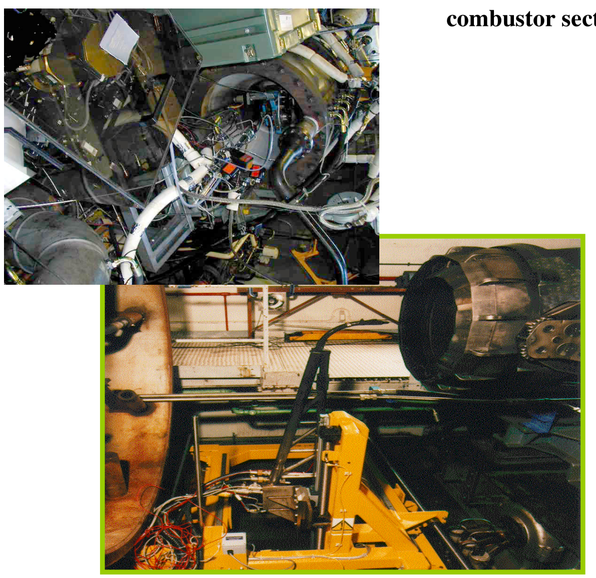

Rig/engine tests to measure
particulates, aerosol emissions

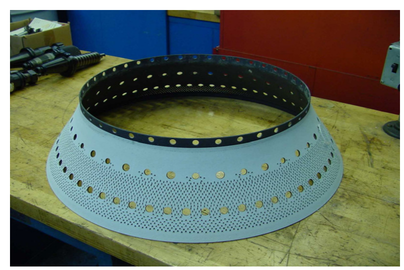

CMC combustor liner
for engine test

Active flow control
to reduce inlet distortion

The UEET "Roadmap"

UEET Ultra Efficient Engine Technology

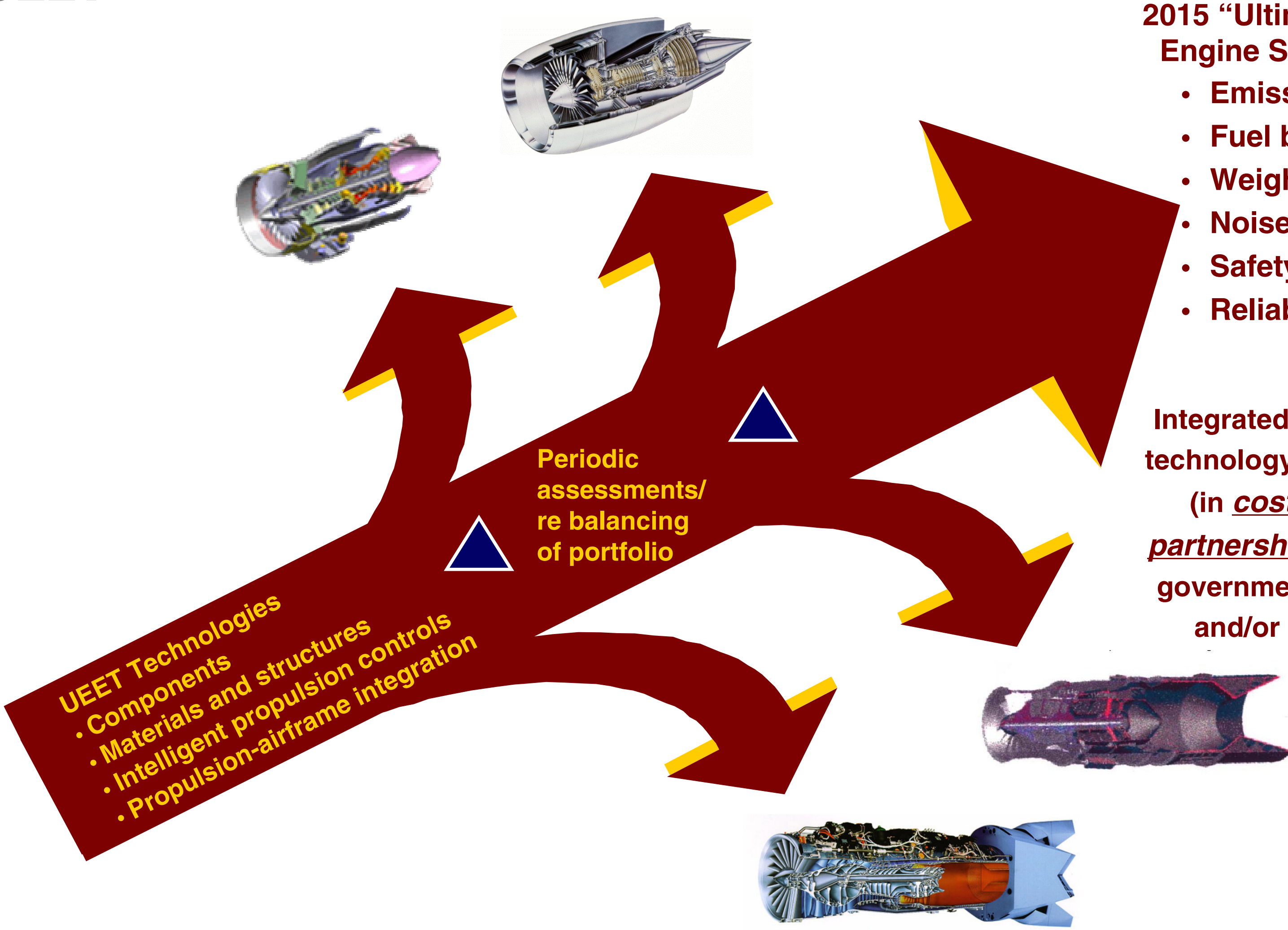

2015 "Ultimate" Turbine Engine Systems
- Emissions
- Fuel burn
- Weight
- Noise
- Safety
- Reliability

Integrated component technology validations (in *cost-sharing partnership* with other government agencies and/or industry)

The Path to Re Invention of the UEET Project

VehicleSystems

where innovation soars.

Aeronautics Technology – Three Integrated Programs

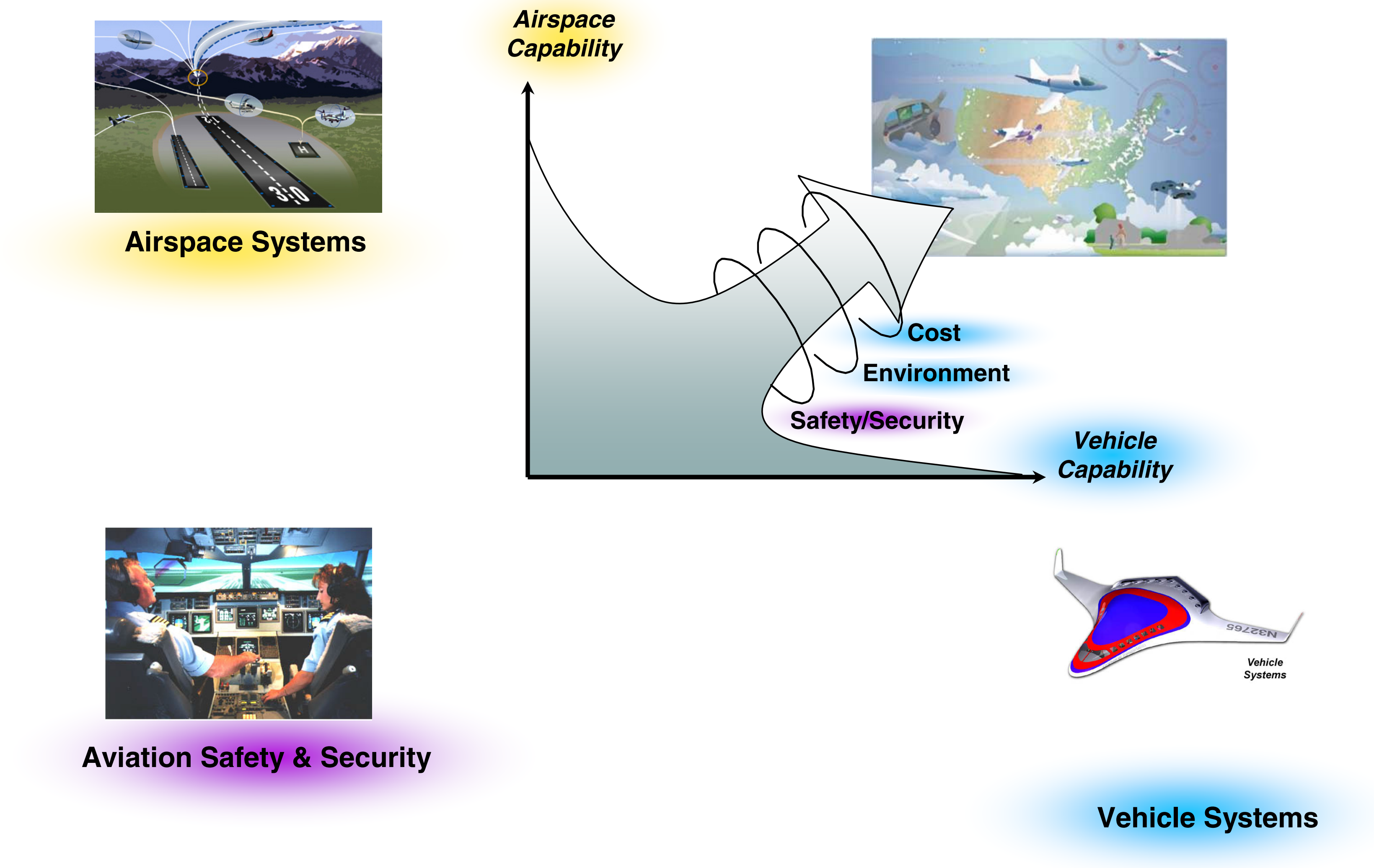

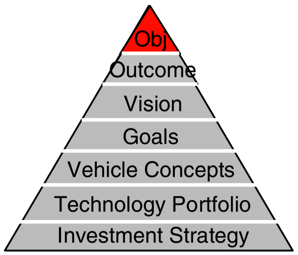

Aeronautics Theme Objectives for the Public Good

Protect the Environment

Protect local environmental quality and the global climate by reducing aircraft noise and emissions.

Increase Mobility

Enable more people and goods to travel faster and farther, anywhere, anytime with fewer delays

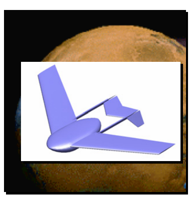

Explore New Aerospace Missions

Pioneer novel aerospace concepts to support earth and space science missions

Support National Security

Leverage NASA aeronautics technology investments in partnership with DOD to support their role of protecting the Nation

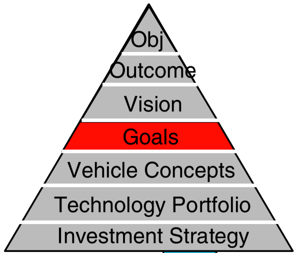

Environmentally Friendly Aircraft

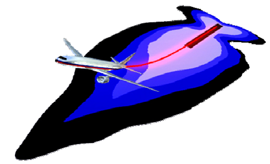

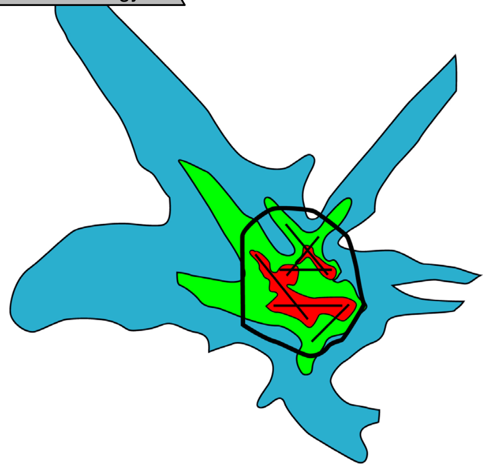

Noise within airport boundaries

Constrain objectionable noise to within airport boundaries

Smog-free

Minimize the contribution of air vehicles to the production of smog

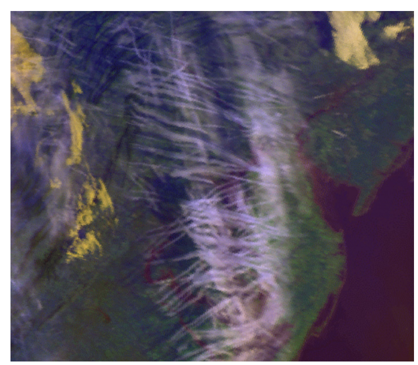

No impact on global climate

Minimize the impact of air vehicles on global climate

Aircraft for Public Mobility

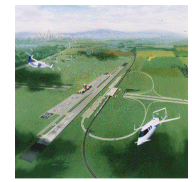

More Convenient

Expand access to aviation to more locations and make it available on-demand

More Affordable

Make air travel available to the entire population

Faster

Increase the speed of air travel

…without compromising safety

Innovative Vehicle Concepts to Identify Key Technology Requirements

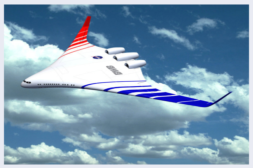

Minimum environmental impact, maximum efficiency

Clean Transport

Strengthen national security through rapid deployment and global reach

Global Strike

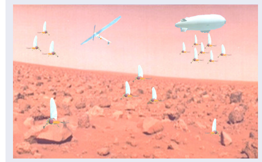

Conduct extended science and exploration missions

Planetary Flight Vehicles

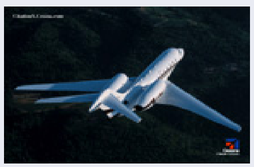

All hour access to any location without noise disturbance

Santa Monica at Midnight

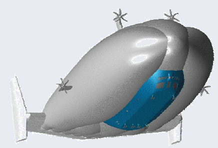

Global reach and on-demand delivery

Global Reach Transport

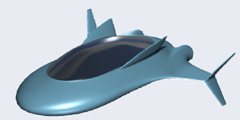

Rural, regional, and intra-urban transportation

Personal Air Vehicle

Rural and regional economic growth, time critical transport

Heartland Express

Automated refueling capability, ultra-long endurance, wide speed range

Tanker

Enables city center access in all weather

V/STOL Commuter

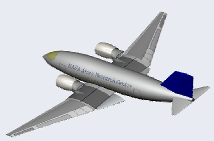

Expands the use of existing airport infrastructure

Extreme STOL Transport

Reduce passenger flight time by at least a factor of 2

Supersonic Overland

High altitude observations for science and defense

High Altitude Long Endurance

Project Evolution within Replanned Vehicle Systems Strategic Focus Areas

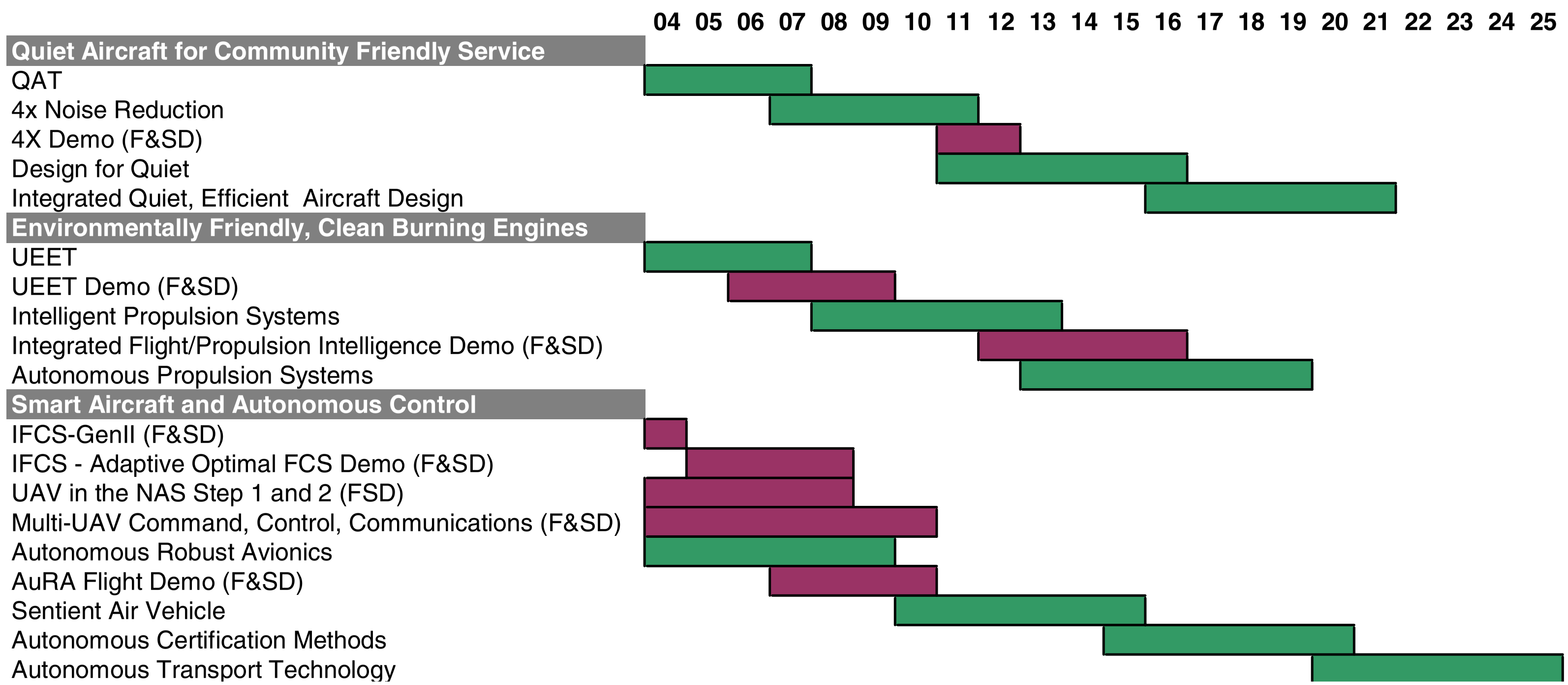

Factors Driving Change

• Administration/OMB drivers that are not going away
-Be more competitive (outhouse and in house) to get "best product"
-Right size the NASA institution (people and facilities)
-Proper role of government programs in aerospace R&D food chain

• Increasing stress on Federal budget
-Growing Federal deficits for foreseeable future
-Administration priorities (Homeland security and anti terrorism)
-Aerospace priorities (National and Agency)

Opportunities

UEET Ultra Efficient Engine Technology

Opportunity to:

-significantly strengthen UEET in the eyes of our customers/partners/stakeholders

--increase the support of key decision makers for UEET

-make major technology impacts on next generation gas turbine engine propulsion systems

- carry our relationship with DoD (IHPTET/VAATE) to the next level

-forge a partnership with NAI, NGLT

-be a leader in developing an new NASA/other government agencies/industry/university partnership model for aerospace R&T

How do we do it?

Vehicle Systems Program Structure

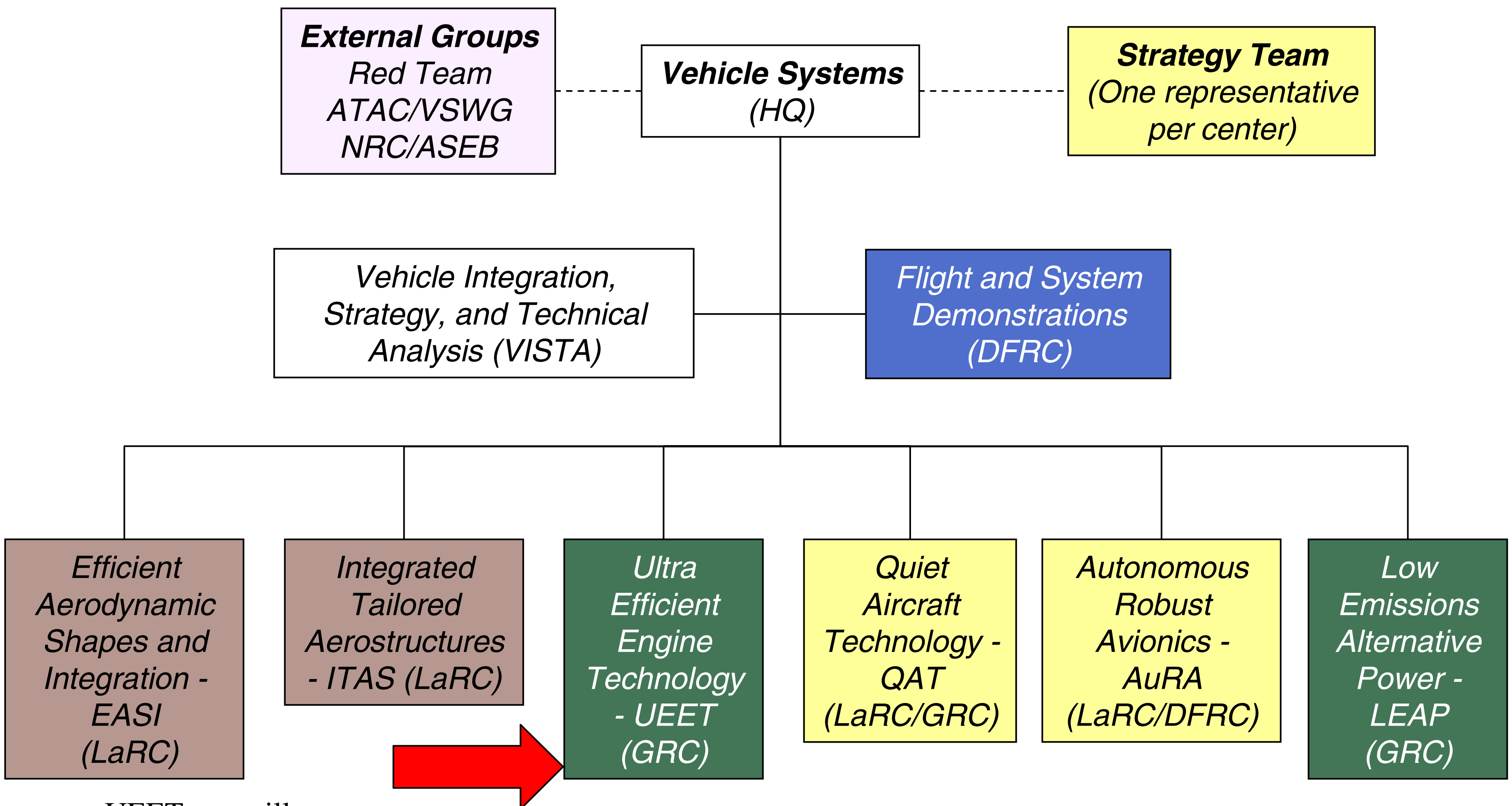

UEETnew will:
- Be a TRL 1-6 project.
- The **only** project in the Vehicle Systems Program **focused entirely on turbine engine propulsion systems.**
- Invest approximately 20% of resources into developing a technology foundation for the follow on project.

The FY04 Challenge

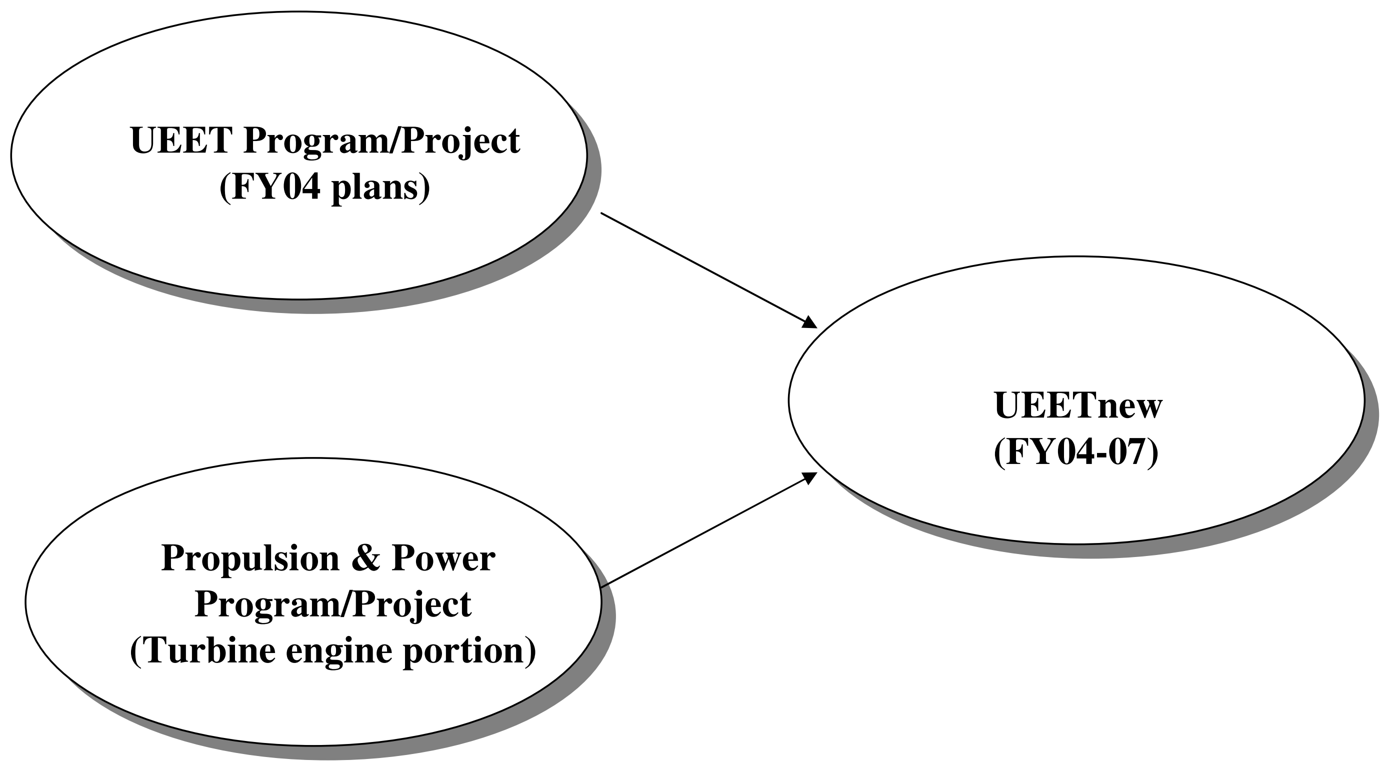

Vision: ***Develop and hand off revolutionary turbine engine propulsion technologies that will enable future generation vehicles over a wide range of flight speeds.***

Goals:

Propulsion technologies to enable increases in system efficiency and, therefore, fuel burn reductions of up to 15 % (equivalent reductions in CO_2)

Combustor technologies (configuration and materials) which will enable reductions in LTO* NO_x of 70% relative to 1996 ICAO standards.

** LTO - Landing/Take-off*

These will remain the same!

UEETnew "Characteristics"

UEET Ultra Efficient Engine Technology

- UEETnew will focus on technologies for subsonic and supersonic commercial systems.
  - The subsonic systems will be regional jets though large wide bodies
  - The supersonic systems will be SSBJ through commercial transports (10 -100 PAX)
- UEETnew will do selected rotorcraft technologies that are dual use technologies which benefit our prime customer base.
- UEETnew will continue to emphasize partnership efforts with DoD that emphasize collaborative efforts to develop dual use technologies.
- UEETnew will use systems studies results as a prime factor in prioritizing and selecting technology efforts. Expert opinion will be employed wherever appropriate (e.g. areas where systems studies cannot currently model technology impacts).

Critical aspects of UEET Re invention

Lower TRL efforts
-Lay foundation for follow on project-Intelligent Propulsion Systems
-All efforts openly competed and selected
-Partnerships encouraged

Higher TRL efforts
-Contribution to achievement of UEET goals
-Appropriate for NASA investment
-Possible dual use technology with partnering with DoD
-<u>Up front</u> commitments by <u>cost sharing</u> partner
- **Cost sharing amount and type**
- **Technology transition/insertion plan**
- **Approach to utilizing NASA personnel, facilities**

UEETnew Sub Project Structure

UEET Ultra Efficient Engine Technology

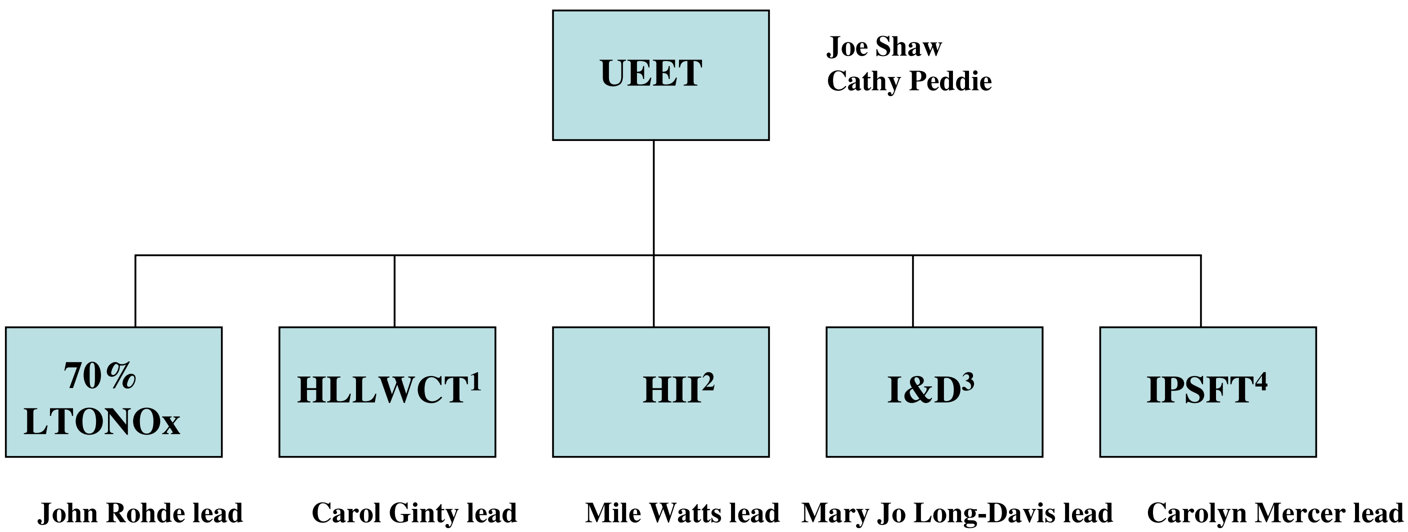

[1]HLLWCT-Highly Loaded, Low Weight Compressor and Turbine
[2]Highly Integrated Inlet
[3]Integration and Demonstration
[4]Intelligent propulsion System Foundation Technologies

Approach to Re inventing UEET

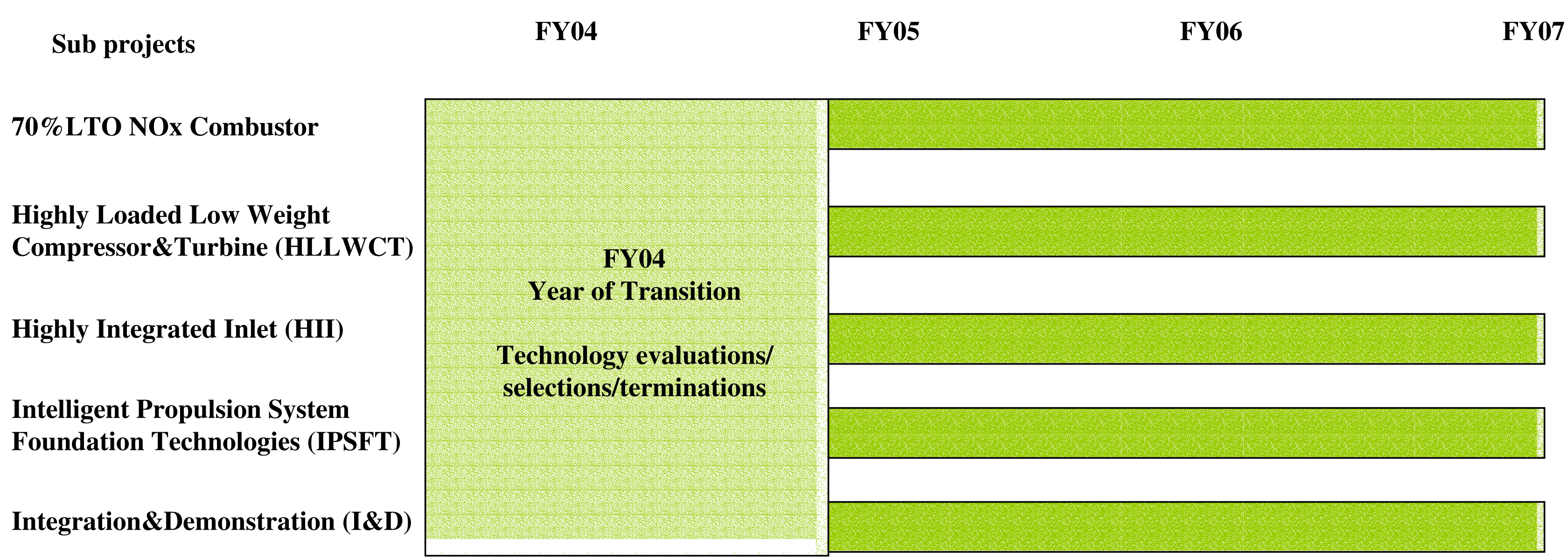

Approach to Re inventing UEET-Lower TRL

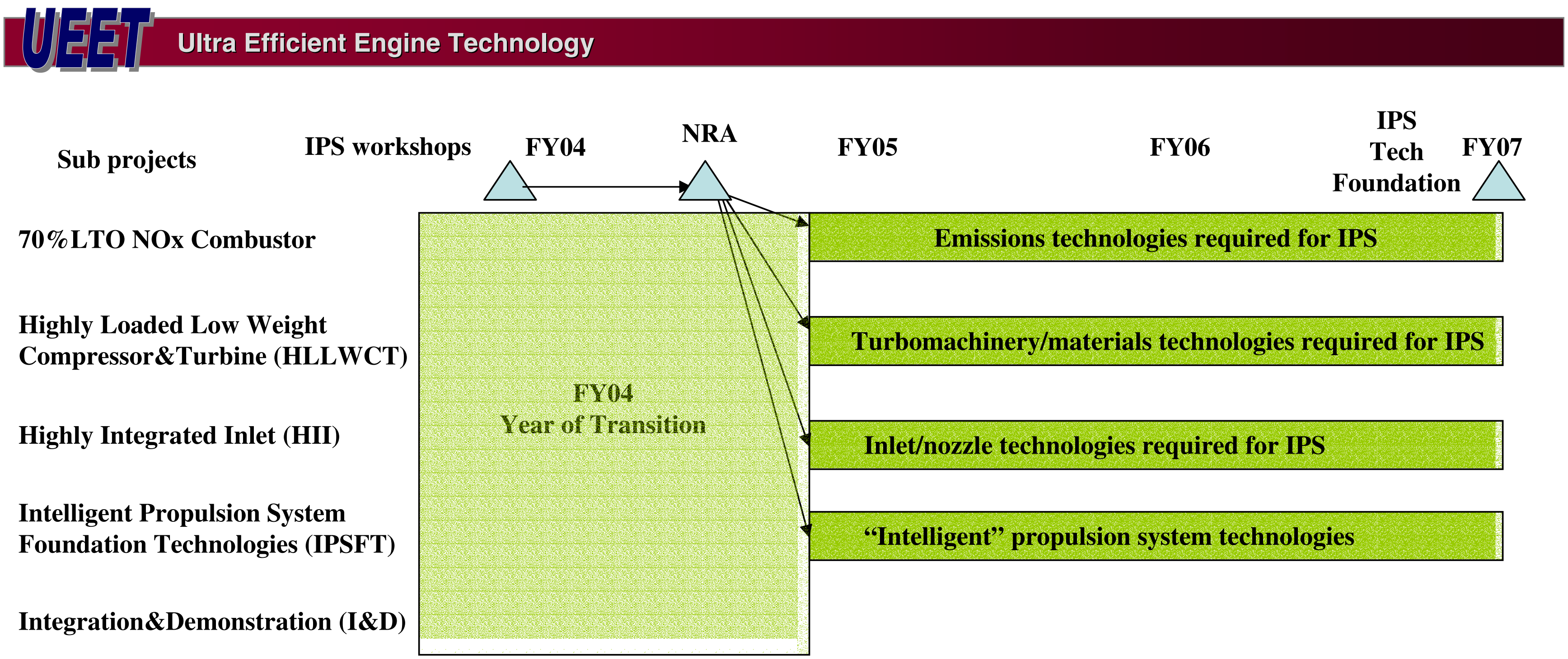

Approach to Re inventing UEET-Lower TRL

UEET Ultra Efficient Engine Technology

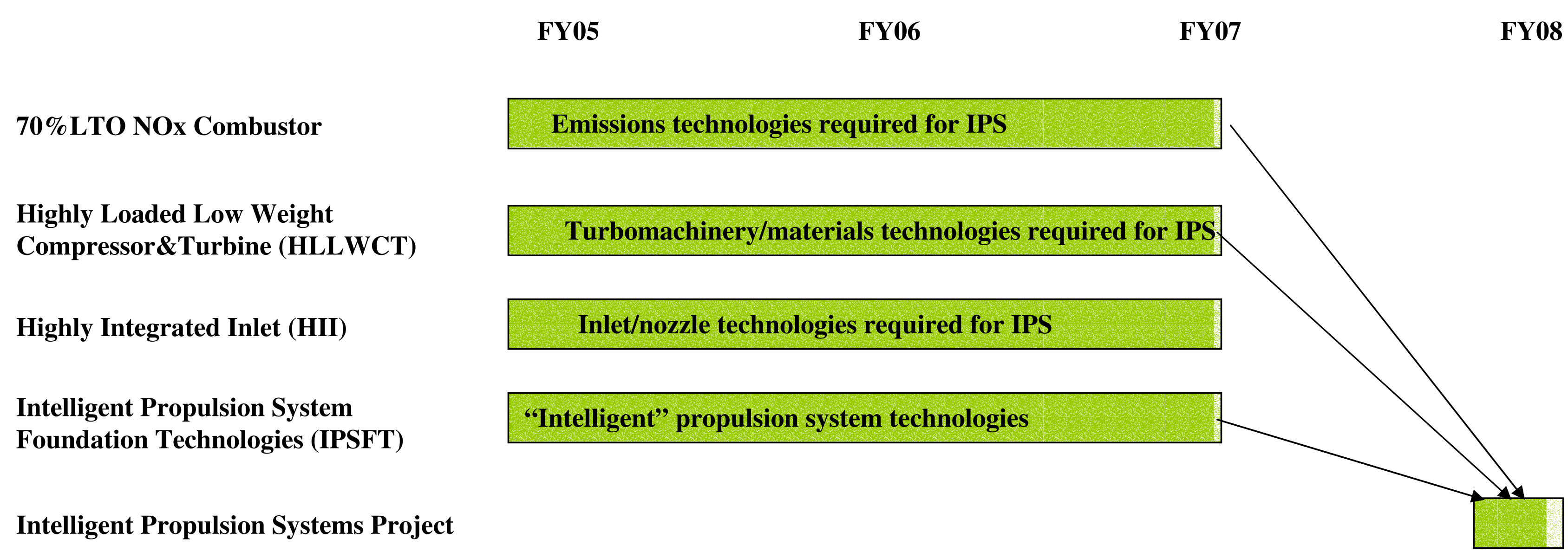

Developing Higher TRL Technology Partnerships/Transitions

UEET Ultra Efficient Engine Technology

A key part of the new UEET Project will be the selection and transition of UEET technologies with industry/ DoD partners to a sufficiently high level so that our partners can use them in future "product designs' after further technology efforts that go beyond NASA's charter (i.e. TRL6).

The success of this effort will be one measure as to how UEET will be graded both by the government (e.g. NASA HQ, OMB, Congress) and our partners.

But we must address "corporate welfare" concerns and doing DoD's job.

Approach to Re inventing UEET-Higher TRL’s

UEET Ultra Efficient Engine Technology

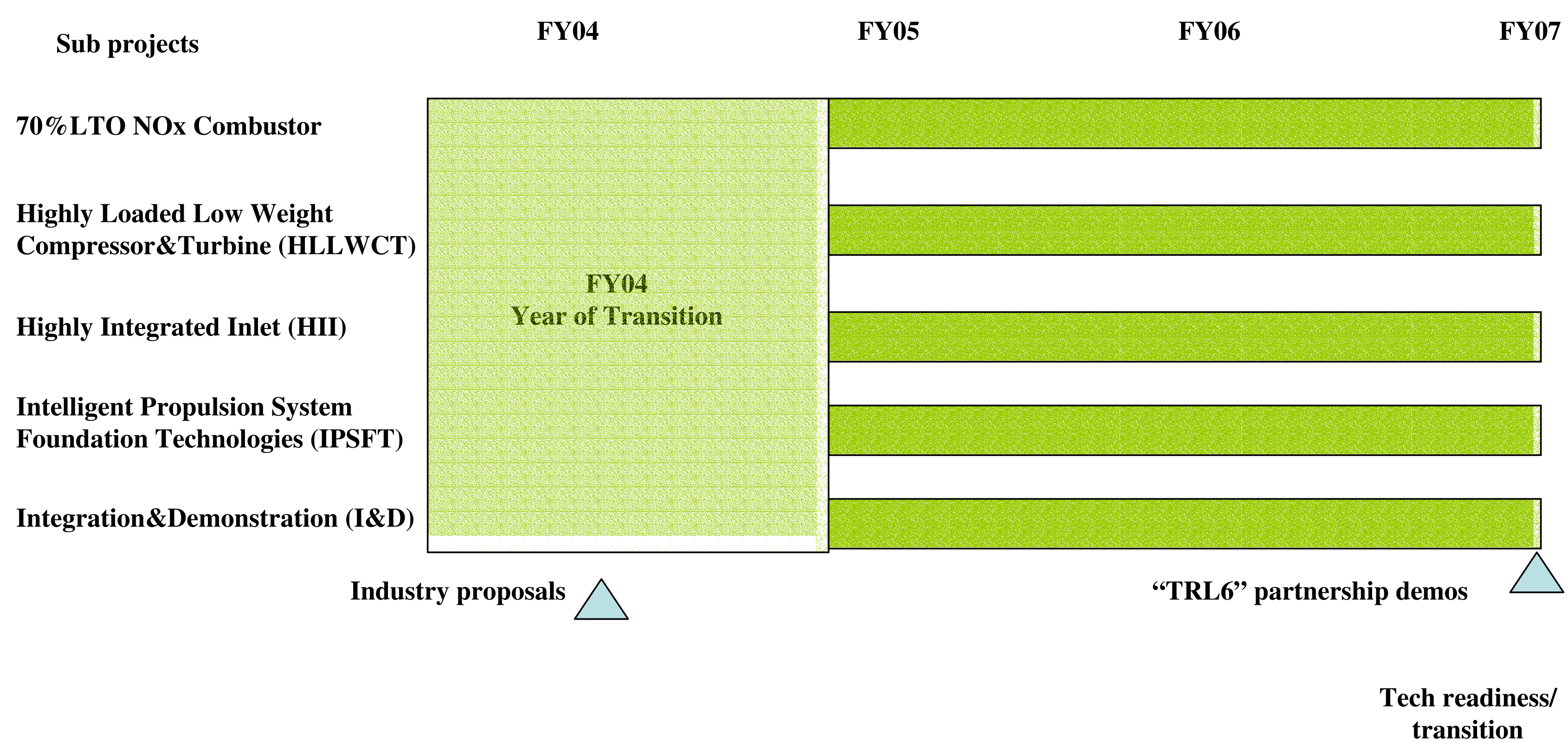

Approach to Re inventing UEET-Higher TRL’s

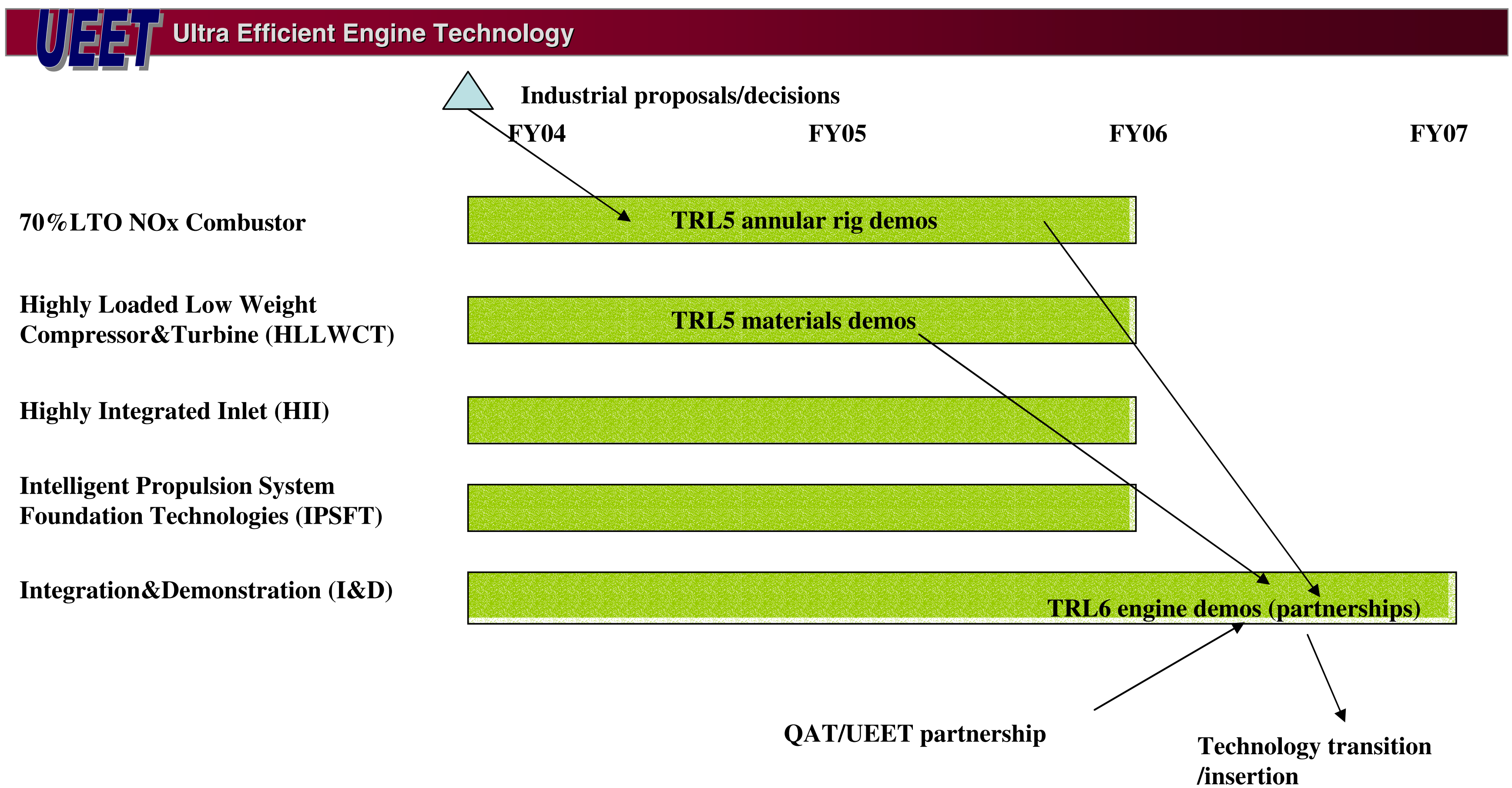

Approach to Re inventing UEET-Higher TRL’s

Ultra Efficient Engine Technology

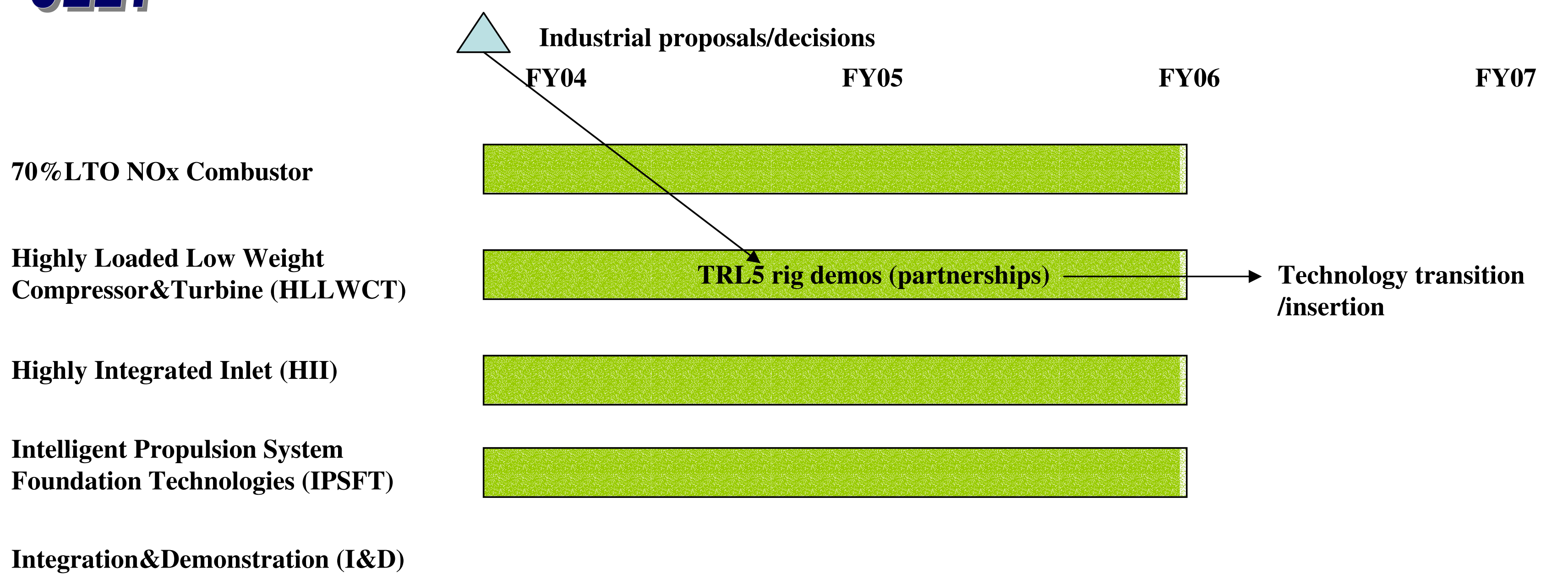

Some technologies will not require engine tests to successfully transition.

Approach to Re inventing UEET-Higher TRL's

UEET Ultra Efficient Engine Technology

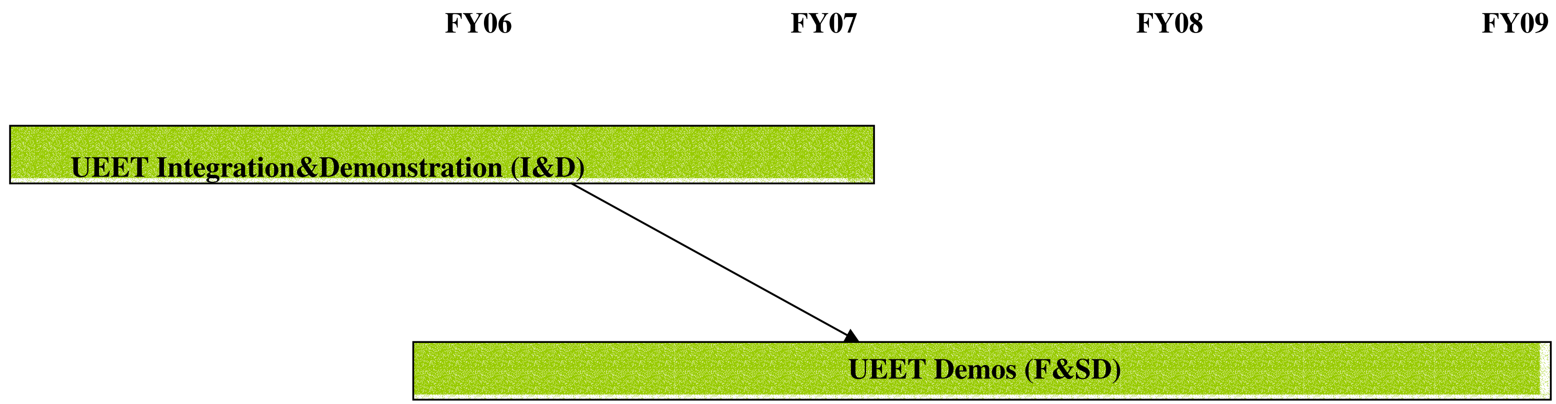

UEET and F&SD projects will TOGETHER proactively work with the customers to define and conduct the required flight demonstrations!

Some things won’t change!

Baseline Vehicles for UEET Technology Application Studies

UEET Ultra Efficient Engine Technology

Commercial Vehicles

Subsonic

300 PAX
Large Subsonic Transport

50 PAX
Regional Jet Transport

500-600 PAX
Blended Wing Body (BWB)

Supersonic

300 PAX
High Speed Civil Transport (HSCT)

10 PAX
Supersonic Business Jet (SBJ)

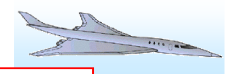

Hypersonic

These vehicles drive the technology investment strategy

Non-Commercial Vehicles

4 PAX
General Aviation Aircraft (GA)

Military Transport (C-17)

Unmanned Aerial Vehicle (UAV)

Advanced Fighter

Access-to-Space/High Mach Platform

These vehicles determine the technology synergies

Vision

UEET Ultra Efficient Engine Technology

Develop and hand off revolutionary propulsion turbine engine technologies that will enable future generation vehicles over a wide range of flight speeds.

We support the vision and are committed to the success of NASA's Ultra Efficient Engine Technology (UEET) Project.

William Koop, Air Force Research Laboratory

Gerald Brines, Allison-Rolls Royce

Mahmood Naimi, Boeing Commercial Airplane Company

Fred Krause, General Electric Aircraft Engines

Dimitri Mavris, Georgia Tech

Tim Conners, Gulfstream

Vinod Nangia, Honeywell

Tom Hartmann, Lockheed-Martin

Robert J. Shaw, NASA Glenn Research Center

Robert D. Southwick, Pratt & Whitney

Scott Cruzen, Williams International

Last Update-April 2003

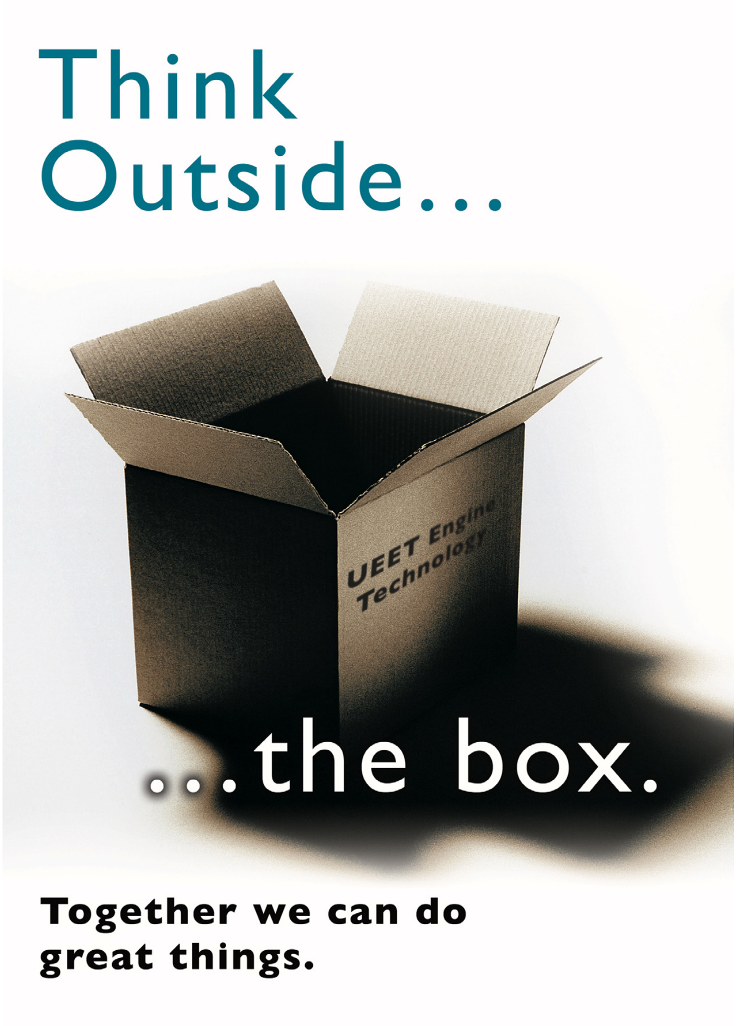

We are committed to working together in partnership to actively seek out opportunities for the transfer of appropriate technologies both into and out of UEET.

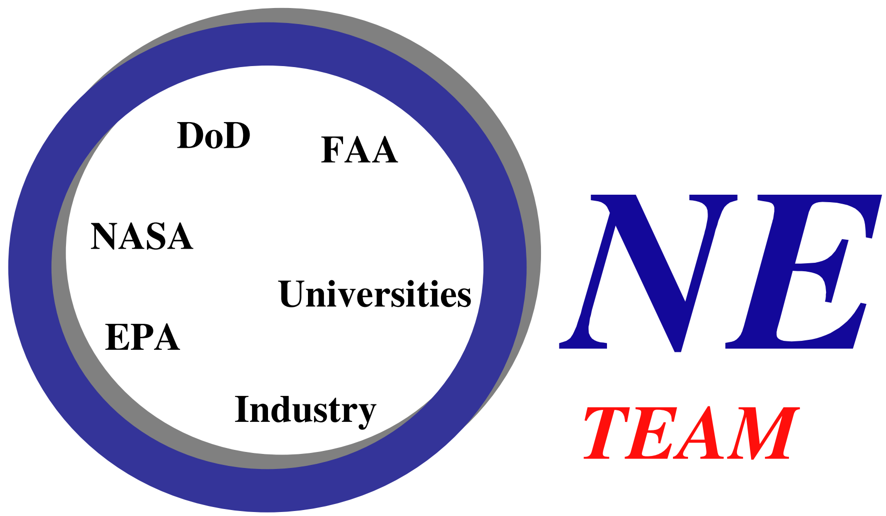

Addressing the key national agenda areas that will contribute to 21st Century U. S. aerospace leadership

Back-up

Program Status

Ultra Efficient Engine Technology

October 2003

Goal	Status	Remarks
15% fuel burn reduction for large subsonic	21% projected for 300 PAX 25% projected for BWB	Systems studies projections of combined impacts of UEET technologies using available (limited) test data in TRL2-3+ range. Initial probabilistic assessment results indicate 94% probability of meeting UEET goal for 300 PAX Benefit projections less than previous years' projections due to technology portfolio changes and refined technology projections.
8% fuel burn reduction for small subsonic, small / large supersonic	21% for 50 PAX 18% for 10 PAX SSBJ	
70% N0x reduction (below ICAO 96) for subsonic (large regional) combustors over the LTO cycle	NASA/industry partnership tests of sector configurations (TRL4) give confidence that target objective will be reached. 79% reduction projected for 300PAX 83% reduction projected for 50 PAX	Sector tests completed in 4Q of FY03

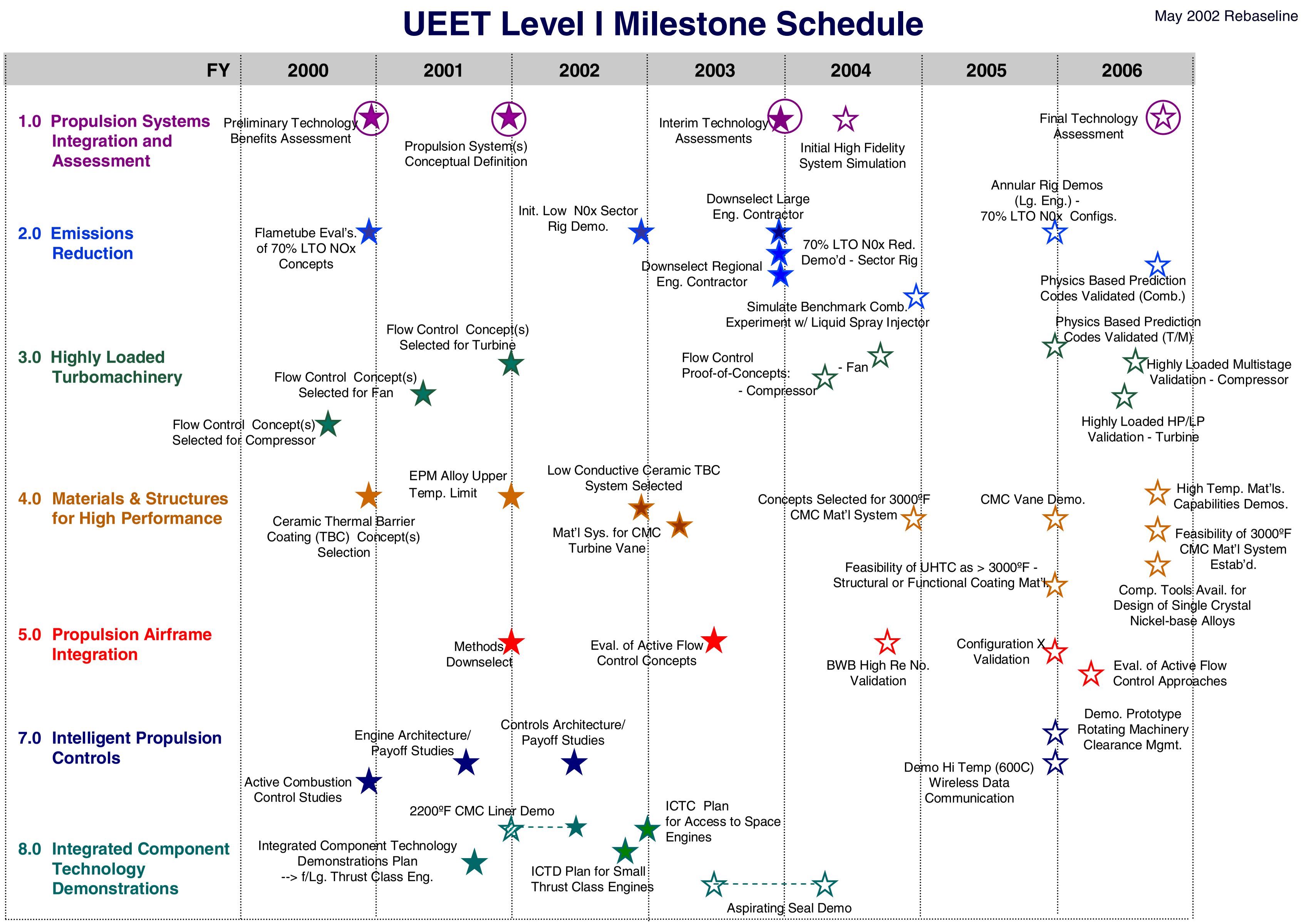

Notes: 1) PCA milestones are denoted by

2) WBS 6.0 reserved for Program Mgmt. functions

DEVELOPMENT OF HIGHER TEMPERATURE ABRADABLE SEALS
FOR INDUSTRIAL GAS TURBINES

Raymond E. Chupp
General Electric Global Research Center
Niskayuna, New York

Improved sealing in GE industrial turbine applications has been under development for several years. The work summarized in this presentation is being carried out at GE's Global Research Center in partnership with GE Power Systems. A team of over a dozen engineers at GE-GRC focus on developing advanced seals for several gas and steam turbine and other turbomachinery applications.

The focus of this presentation is abradable blade tip sealing for higher application temperatures in E-Class industrial gas turbines. The presentation includes: description of how abradable seals work; where abradables are located in gas turbines; types of abradable materials employed; development of a higher temperature, metallic abradables; and validation results.

Abradable Seals:

- Used in aviation gas turbines since late 1960's / early 1970's
- Gaining popularity in power generation turbomachinery
- Relatively simple, low cost approach:
  - Larger clearances are needed without abradable seals to prevent (1) rubbing due to tolerances, (2) out-of-round casings, and (3) rotor offset
  - Abradable is sacrificial; worn away without damaging rotating blade tips
  - Applied to casings and shrouds:
    abradable seals reduce clearances → reduced gas leakage

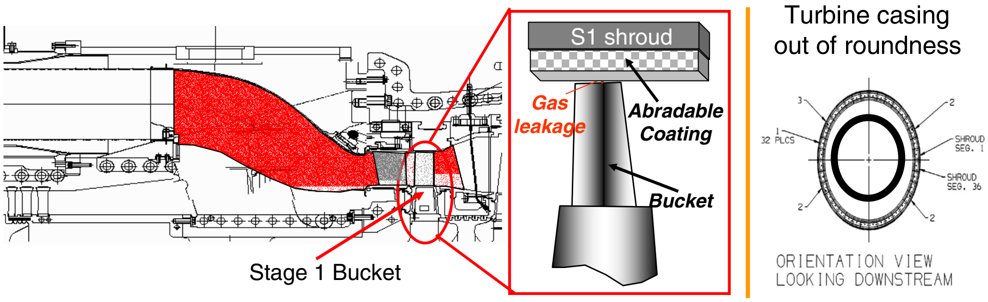

Benefit: Clearance reduction → performance gain

2003 NASA Seal/Secondary Air System Workshop, Nov. 5-6, 2003, Ohio Aerospace Institute, Cleveland, OH

GE Global Research

Abradable seals offer significant performance gains for turbines by decreasing the operating clearances of compressor and turbine blade tips. Abradable seal materials are applied to the casings of gas and steam turbines. These seals are worn-in by the rotating blade during service with little wear of the blade tips. The seals can reduce operating clearances by allowing tighter cold-build clearances without fear of damaging blade tips during tip/shroud closures during turbine both in transients and at steady state.

Abradable seals not only allow tighter radial clearances, but they also reduce the effect of casing out-of-roundness and rotor misalignment on increasing the tip clearance.

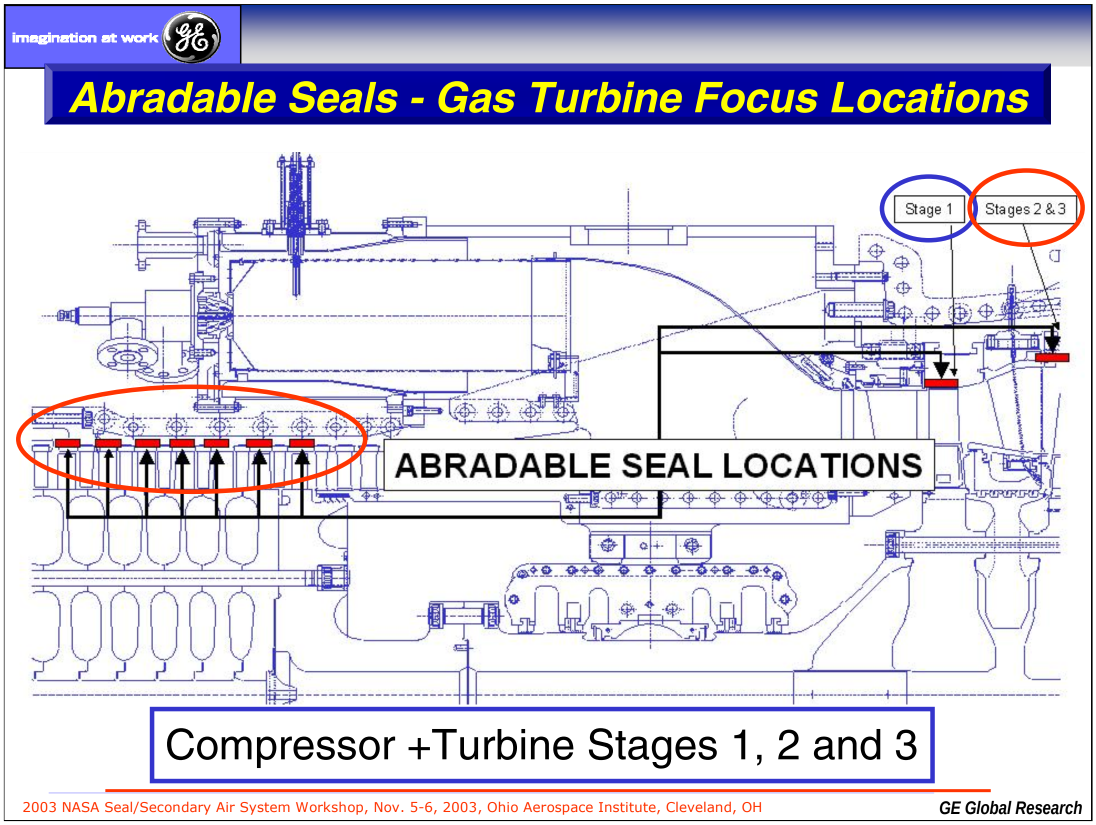

This chart shows representative abradable sealing areas being addressed in reducing tip clearances in industrial gas turbines. Locations include outer casing outside compressor blade tips and stationary shrouds outside the unshrouded first stage turbine blades and shrouded second and third stage turbine blades for an E-Class industrial gas turbines. The focus of this presentation will be on abradables for the stage 1 of the E-Class turbines where the temperatures are the highest for this type of turbine.

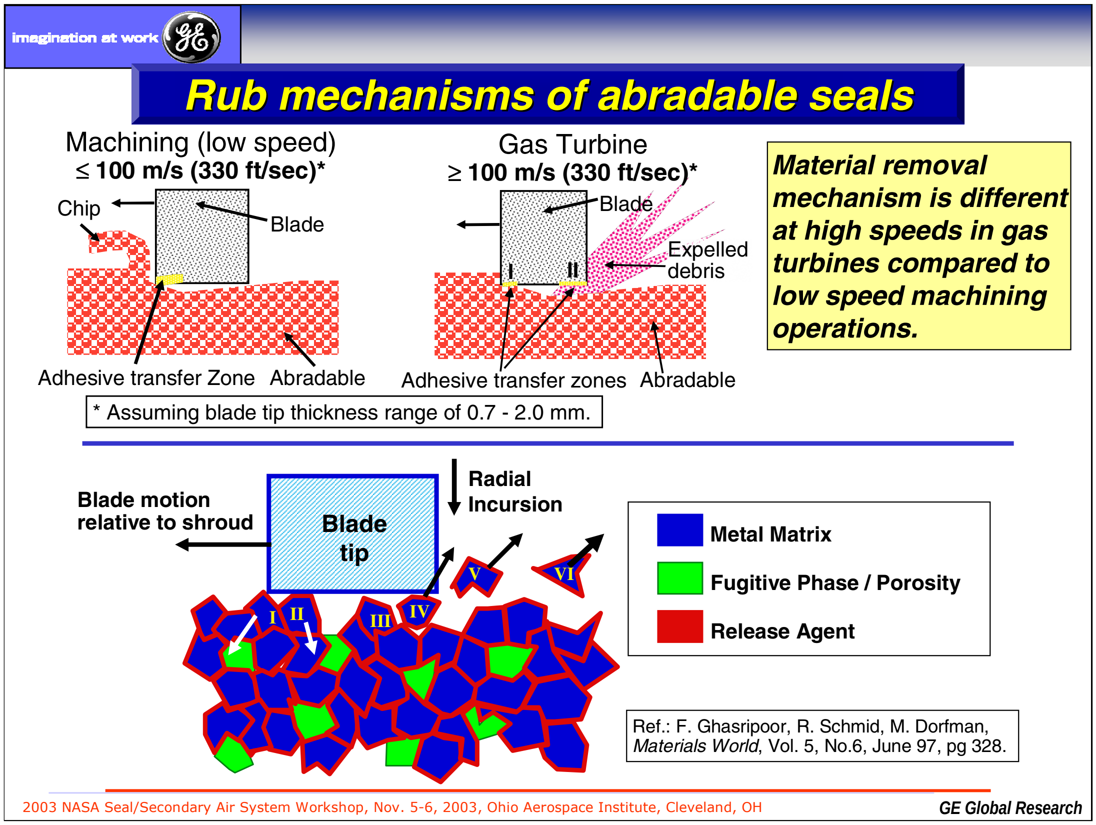

This chart shows the mechanisms by which abradable material is removed during a rub event. At low rotational speeds indicative of machining operations, the material is pushed out in front of the rotating part, such as a tool bit. At higher speeds typical of turbine blade tip applications, the material exits behind the cutting blade tip. The abradable material is structured so particles break loose and are thrown behind the blade tip without wearing the tip. This partially sets the criteria for material design and blade tip thicknesses especially when the tips are greater than 1 mm.

imagination at work

Design Considerations for Abradable Seals

Abradables have:

- Conflicting requirements:
  - Low strength → Susceptible to gas and particle erosion
  - Inherent porosity → Prone to oxidation at higher temperatures
- To be treated as a complete tribological system:
  - Relative motions and depth of cut - blade tip speed and incursion rate
  - Environment - temperature, fluid medium and contaminants
  - Cutting element geometry and material - blade tip thickness, shrouded or unshrouded blades
  - Counter element - abradable seal material and structure

Seals must be designed to suit the particular application based on the Tribo-System

2003 NASA Seal/Secondary Air System Workshop, Nov. 5-6, 2003, Ohio Aerospace Institute, Cleveland, OH — *GE Global Research*

This chart lists the various design considerations for abradable sealing applications that make the system unique. Thus, the seal must be designed to fit the particular application. There are many off-the-shelf abradable seal materials, but these materials usually have to be modified or redesigned to fit the particular set of design constraints.

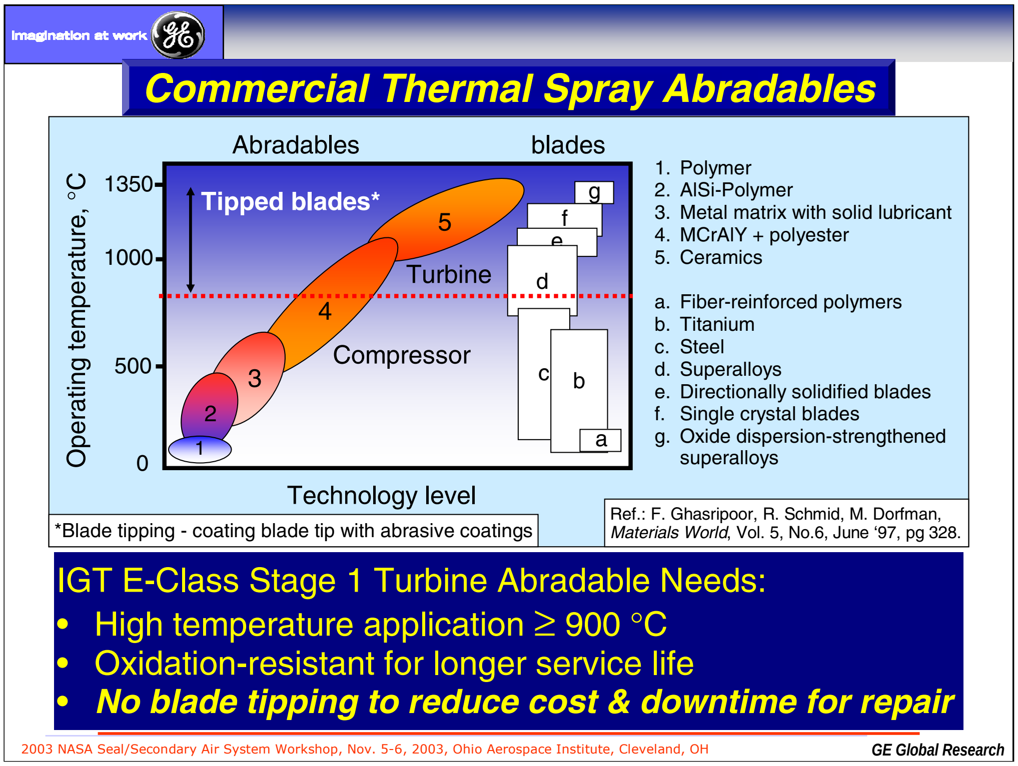

This chart shows the type of commercially available abradable materials. The use temperature varies from compressor applications (up to 550 C, 1020 F) to turbine temperatures (up to 1350 C, 2460 F). Sulzer Metco 2043 is an example of a Type 4, MCrAlY abradable primarily developed for compressor and other lower temperature turbomachinery applications. This material can be used for turbine applications up to 850 C (1560 F) while maintaining a reasonable oxidation life with the inherit porosity. For higher temperatures, ceramic materials are used for abradables with abrasive material needed on the blade tips. The focus of the current effort is to develop a higher temperature, metallic abradable material that can operate up to 900 C (1650 F) with an acceptable oxidation life. This material was to be abradable without the need for an abrasive blade tip treatment.

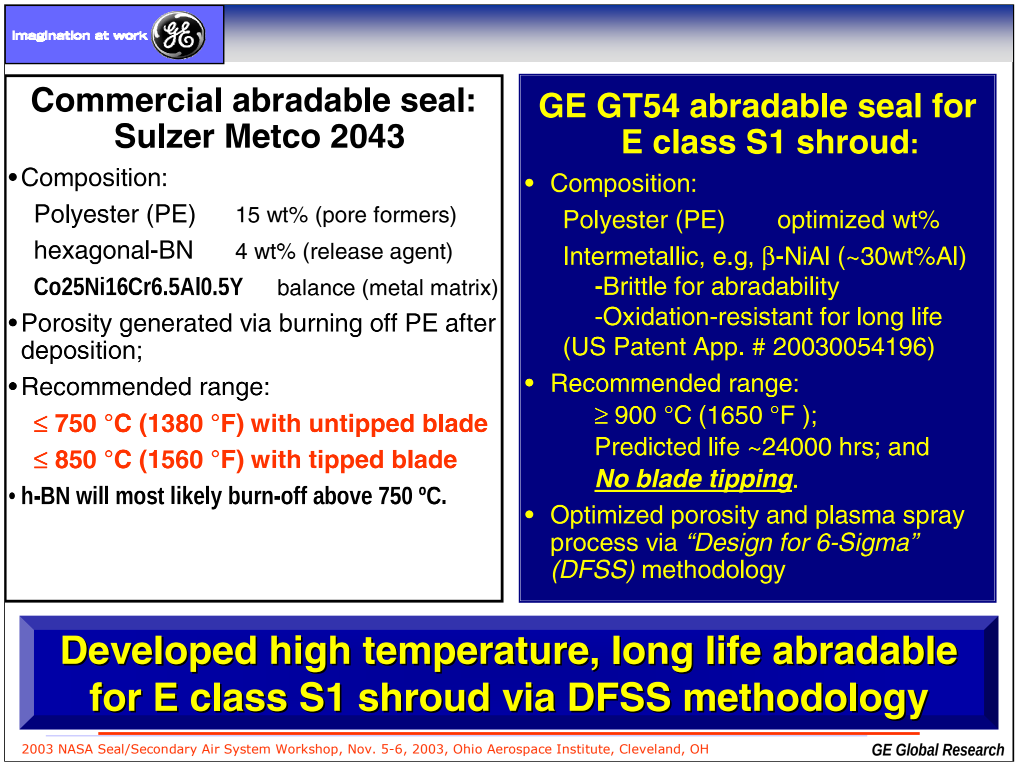

This chart gives a detailed comparison between SM2043 with the new GE abradable material GT54 targeted for temperatures ≥ 900 C (1650 F). Thus, this material increases the maximum use temperature with untipped blades by ~150 C (~270 F) that is needed for E-Class 1st stage shroud applications. This improvement is accomplished by increasing the Al content to 30% by weight, i.e., three times more Al, to give superior oxidation life above 850 C. This is done for similar levels of coating porosity to provide abradability.

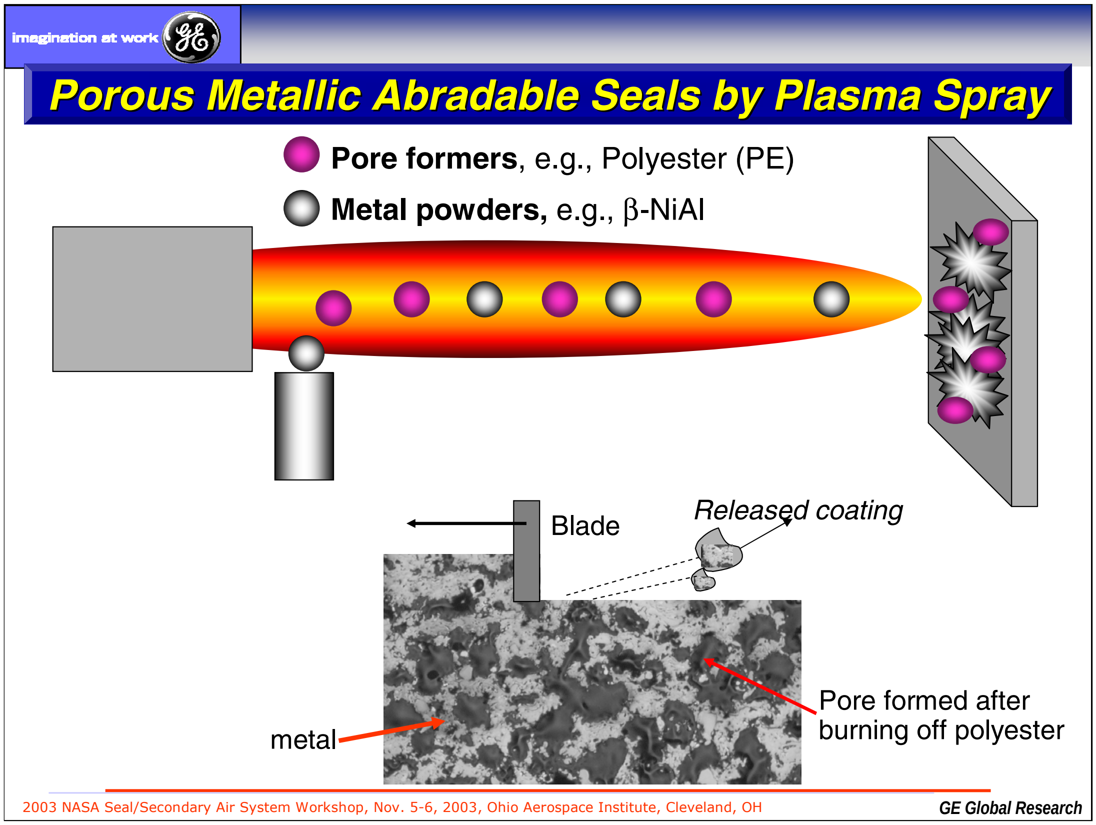

This chart shows how an abradable material is placed on a stationary shroud surface using a plasma spray process. A fugitive material is mixed in the powder to provide a controlled porosity in the resultant coating. The powder is then a composite of metal and polyester (pore former). It is feed into a plasma flame. Spray parameters, such as gun current, gas flow rate, standoff distance, spray movement rate, etc., are adjusted to give the desired coating properties. The resulting coating after burning off the remaining fugitive phase is a combination metal and pores that provides the desired level of porosity. This inherent porosity allows the coating to be abradable when cut by an untreated rotating blade tip. The spray powder and process is optimized to provide an appropriate porosity level for abradability while maximizing oxidation life.

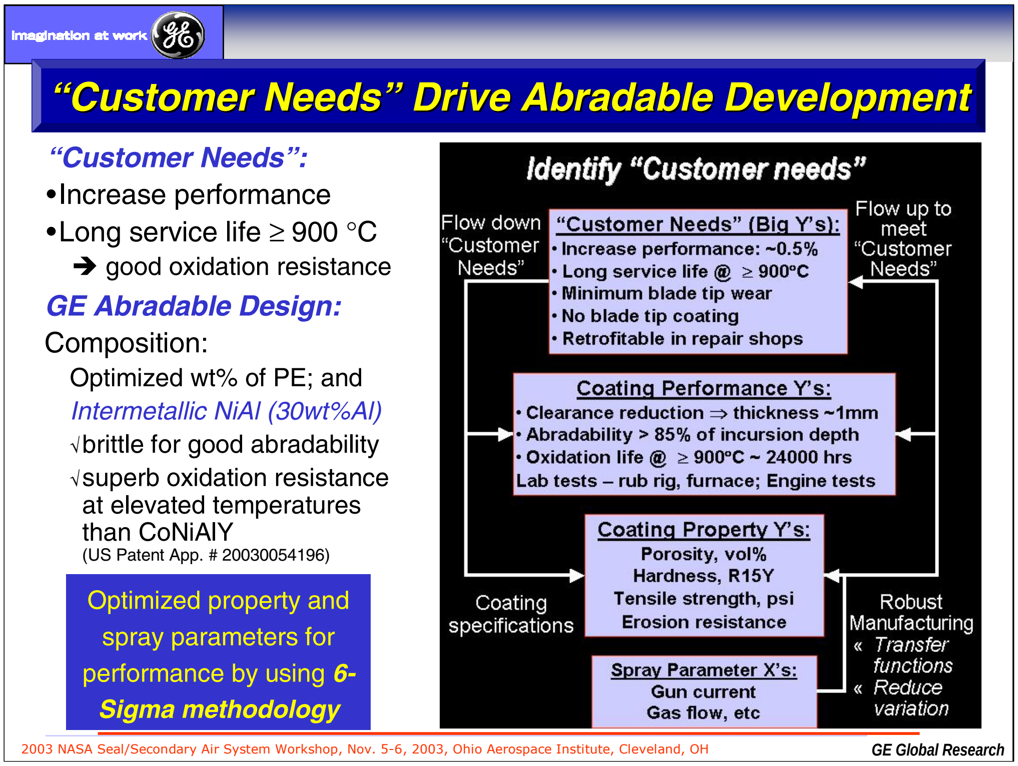

Abradable sealing systems must be designed to meet several customer requirements (Big Y's). The requirements of abradability (without blade tipping) vs. coating oxidation life are conflicting and drive the development process. These requirements (Big Y's) in turn lead to coating Performance Y's, i.e., abradability, oxidation life, erosion resistance. These Performance Y's are measurable and ensure the coating meets design requirements. The Performance Y's are in turn translated into specifications of coating properties such porosity and hardness. To achieve such properties, a robust spray process needed to be developed with optimized process X's (plasma conditions).

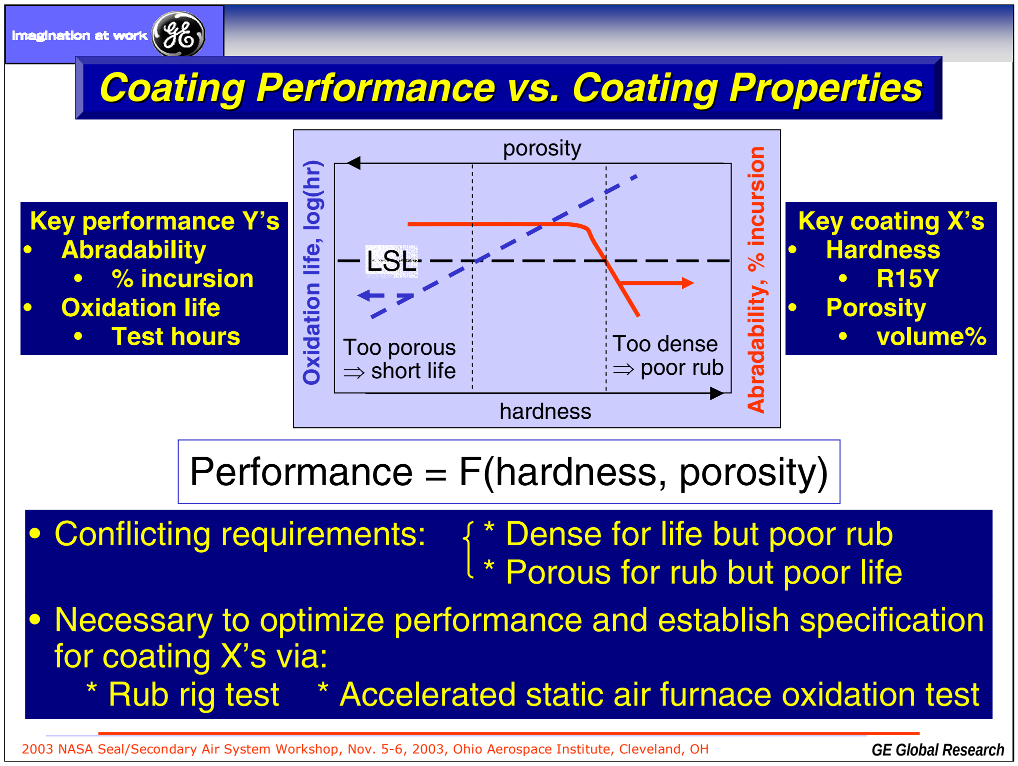

This chart shows how coating conflicting requirements of oxidation life vs. abradability are translated into coating property spec's.

From the lower spec limit (LSL) for oxidation (left side of chart) and abradability (right side), one can determine the corresponding spec levels for porosity and hardness using correlations from lab measurements. Thus, lab tests are done in the development effort to determine the correlations used later to determine a robust spray process.

imagination at work

Laboratory Tests of Candidate Abradables

- Abradable performance laboratory tests:
  - Abradability - Rub rig
  - Oxidation life - Accelerated static furnace oxidation test
- Abradable coating property tests:
  - Porosity - Image analysis
  - Hardness - R15Y hardness test
  - Tensile test using ASTM C633-79
  - Erosion test using ASTM G76

2003 NASA Seal/Secondary Air System Workshop, Nov. 5-6, 2003, Ohio Aerospace Institute, Cleveland, OH GE Global Research

This chart shows the lab tests performed to measure the coating properties. These tests will be described in more detail in the following charts.

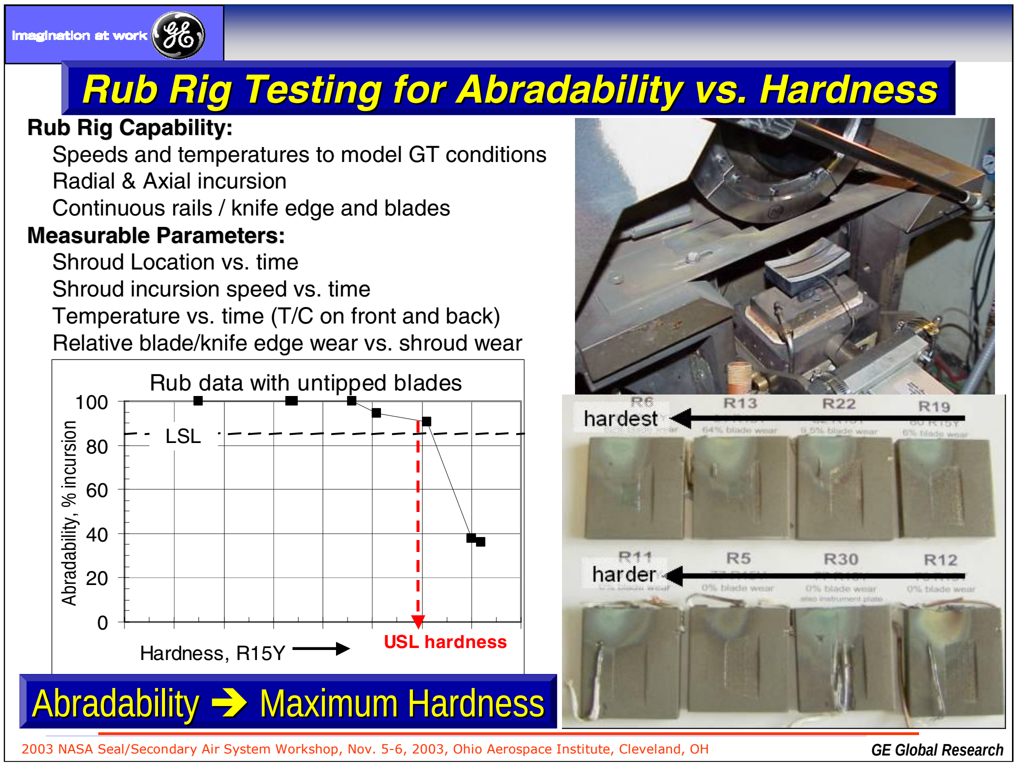

A versatile abradable rub rig has been designed, built and commissioned to evaluate various abradable materials. Both unshrouded and shrouded rotating blade tips can be simulated at nearly engine operating conditions. Representative axial and radial movements can be simulated. Various parameters are measured to quantify the tribopair wear characteristics. Initial testing was performed to verify the rig against other available rub rigs.

Abradability is defined as the % of abradable material removed in the rub vs. the total incursion. % blade tip wear then = 100% - % abradability.

In testing the new material, several rub samples were coated with GT54 having a range of hardness from soft to hard. The testing was done at simulated temperatures modeling the E-Class 1st stage shroud environment. The resulting data yielded an upper spec limit (USL) for acceptable hardness that matched the abradable LSL. For higher hardness values, the coating was not deemed to be abradable.

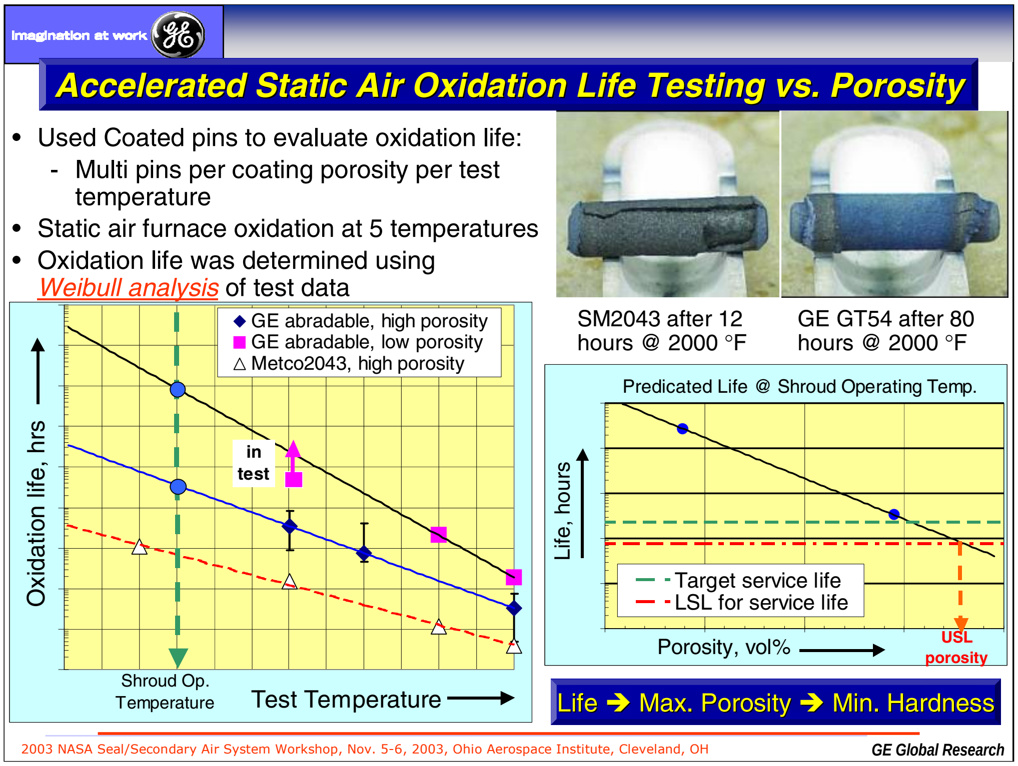

Oxidation life is determined via. furnace testing. Metallic pins made from the same material as the engine shrouds were coated with SM2043 and the new abradable coating; the latter with different levels of porosity, i.e., hardness. Pins were placed in furnaces set to different temperatures. The testing was accelerated by choosing temperatures higher than the application temperature.

Oxidation life is defined as the hours before coating crack initiation occurs. The photo on the left shows SM2043 after 12 hours with a major crack already initiated. The photo on the right is GT54 after 80 hours at the same temperature . This coating had a typical porosity level. The only cracks in the GT54 were on the end caps and not in the coating itself. These photos demonstrate the significant life increase of GT54 over the commercial coating.

The plot on the left is based on the furnace testing data. The two GT54 lines are for two different levels of coating porosity. The data are extrapolated to the shroud operating temperature and cross plotted on the right. The right-hand plot defines the coating porosity USL to achieve the desired LSL oxidation life. This USL porosity is translated to a coating hardness LSL from flat sample testing. The pin coating hardness was not readily measurable because of the curved surface of the pins.

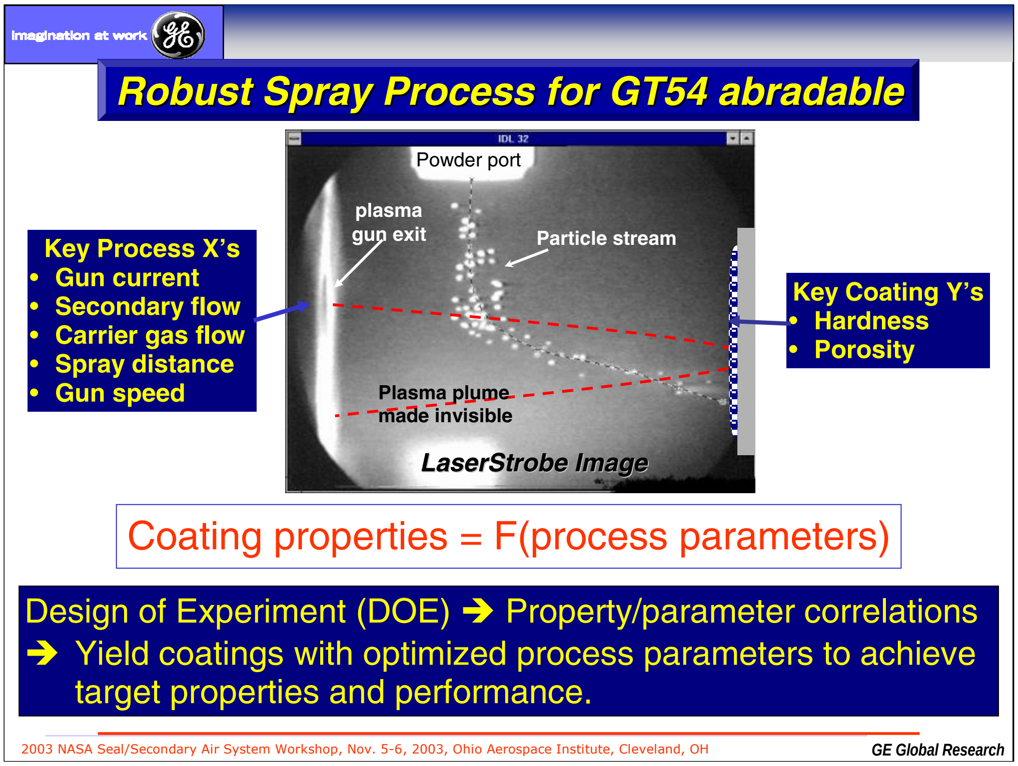

Once the abradable coating property spec's are known from the lab testing, a robust spray process can defined. This process has optimized process X's to achieve target coating Y's. This was done via.

(1) running a design of experiments (DOE) to generate data correlations between properties and the process parameters, and

(2) optimizing the process to achieve the desire properties and performance.

imagination at work

Spray Process Optimization via Design of Experiment (DOE)

- 2^{5-1} DOE: 5-factor 2-level half-factorial design with center points and repeats;
- Plasma parameters:
  - Gun current
  - Secondary flow
  - Carrier Flow
  - Spray Distance
  - Gun Speed
- Measured coating response:
  - Hardness, tensile,
  - Erosion resistance, and
  - Thickness per pass
- Data analysis by using DFSS tools.

	Plasma Parameters: High value (1), Low value (-1), center value (0)				
Run	Gun_amp	2nd_flow	Carrier_flow	Spray_dist.	Gun_speed
1	-1	-1	-1	-1	-1
2	1	-1	-1	-1	1
3	-1	1	-1	-1	1
4	1	1	-1	-1	-1
5	-1	-1	1	-1	1
6	1	-1	1	-1	-1
7	-1	1	1	-1	-1
8	1	1	1	-1	1
9	-1	-1	-1	1	1
10	1	-1	-1	1	-1
11	-1	1	-1	1	-1
12	1	1	-1	1	1
13	-1	-1	1	1	-1
14	1	-1	1	1	1
15	-1	1	1	1	1
16	1	1	1	1	-1
17	-1	-1	-1	-1	-1
18	1	-1	-1	-1	1
19	-1	1	-1	-1	1
20	1	1	-1	-1	-1
21	-1	-1	1	-1	1
22	1	-1	1	-1	-1
23	-1	1	1	-1	-1
24	1	1	1	-1	1
25	-1	-1	-1	1	1
26	1	-1	-1	1	-1
27	-1	1	-1	1	-1
28	1	1	-1	1	1
29	-1	-1	1	1	-1
30	1	-1	1	1	1
31	-1	1	1	1	1
32	1	1	1	1	-1
33	0	0	0	0	0
34	0	0	0	0	0

2003 NASA Seal/Secondary Air System Workshop, Nov. 5-6, 2003, Ohio Aerospace Institute, Cleveland, OH — GE Global Research

This chart shows a design of experiments (DOE) that was performed to determine a robust spray process. A 5-factor, 2-level half-factorial DOE was run. The plasma spray factors considered were: gun current, secondary flow, carrier flow, spray distance, and gun speed. Repeats were included to assess process variability. Center points were run to determine non-linearity effects. The measured coating parameters were hardness, tensile, erosion, and thickness per pass. The effect of the latter parameter is shown on the next chart.

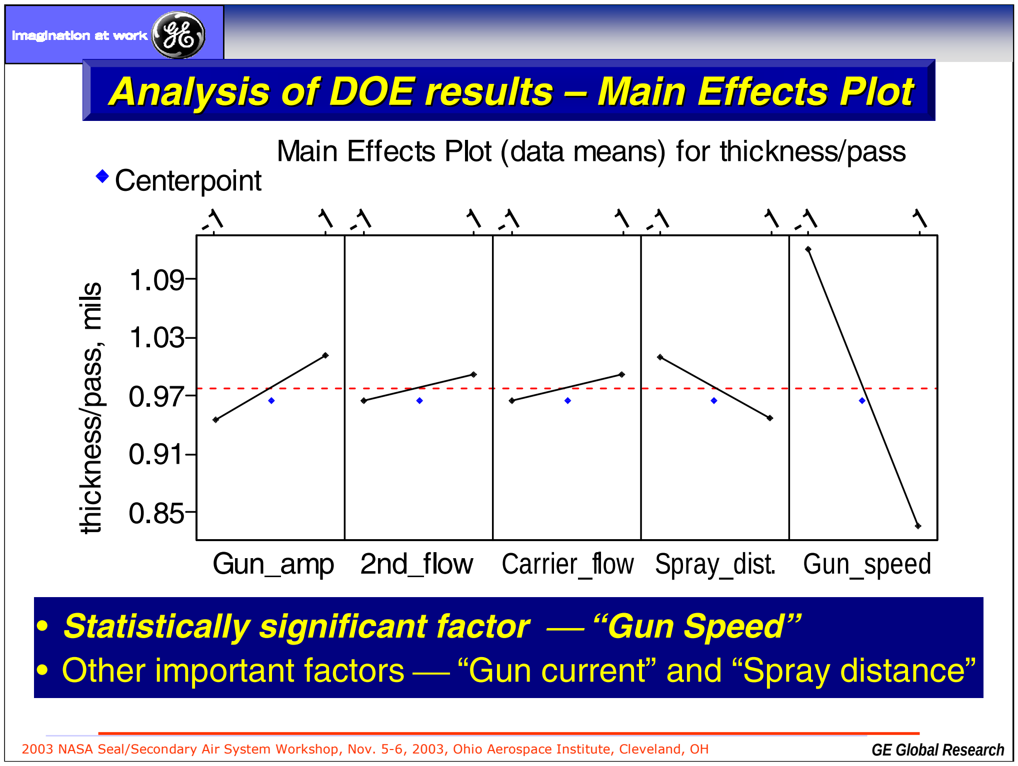

This chart shows the effects of various spray parameters on one of the coating properties measured, i.e., coating thickness per spray pass. As expected, gun speed is an important parameter. The center point results show that curvature is negligible so that linear regression of the DOE results can be used to generate data correlations.

imagination at work

Correlations → Optimum spray parameters

- Generated correlations for hardness, tensile, erosion, thickness per pass
- Used Excel Solver to optimize spray parameters and thus achieve target properties
- Performed validation runs and transition to shop.

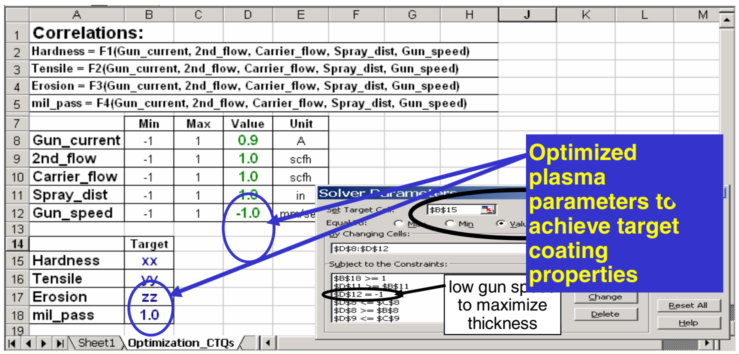

2003 NASA Seal/Secondary Air System Workshop, Nov. 5-6, 2003, Ohio Aerospace Institute, Cleveland, OH   GE Global Research

Data correlations are put in an analysis solver to optimize spray parameter to achieve target coating properties in a robust manner. This then facilitates transitioning the robust process for spraying engine parts in a production shop.

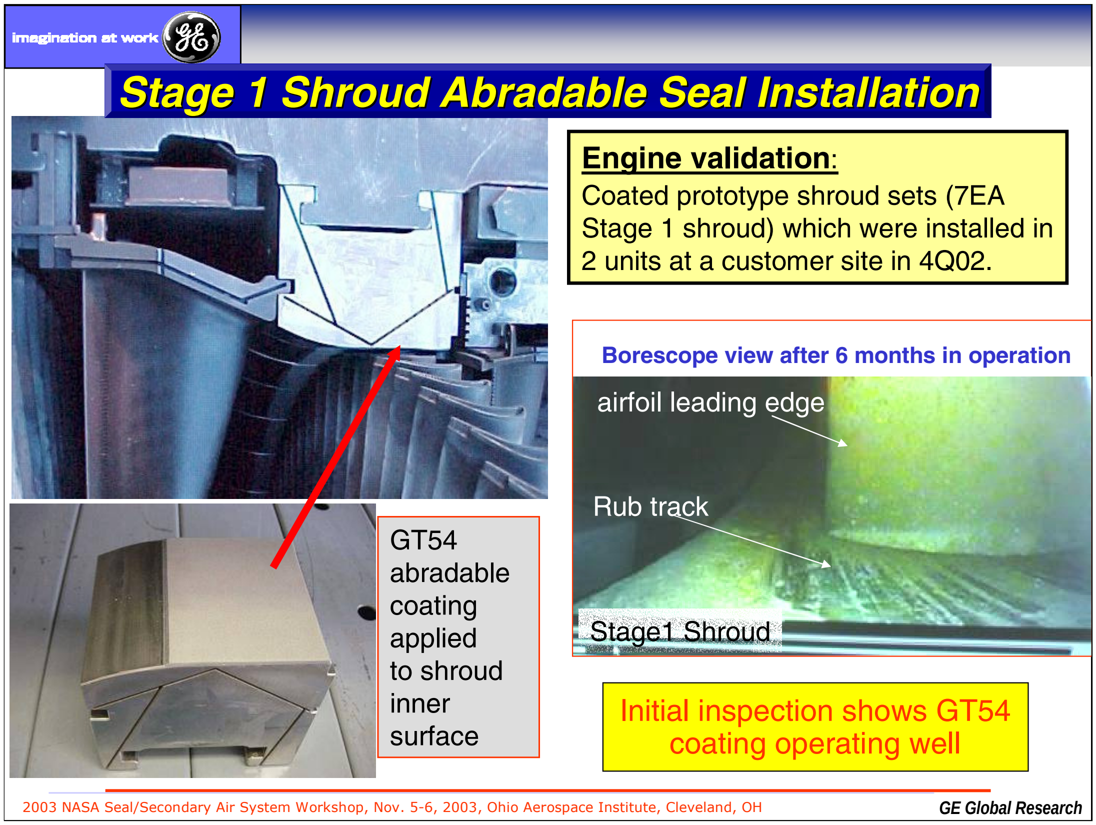

The new GT54 abradable coating is being validated in the stage 1 of E-Class gas turbines. The shrouds with GT54 on the inner surface were installed in the two units in late in 2002. The units were both borescope inspected in mid-2003. The inspections showed that where wear rubs occurred the coating was abradable without bucket tip wear. Coating life will be determined after longer operating hours. Thus, so far the GT54 coating is performing well.

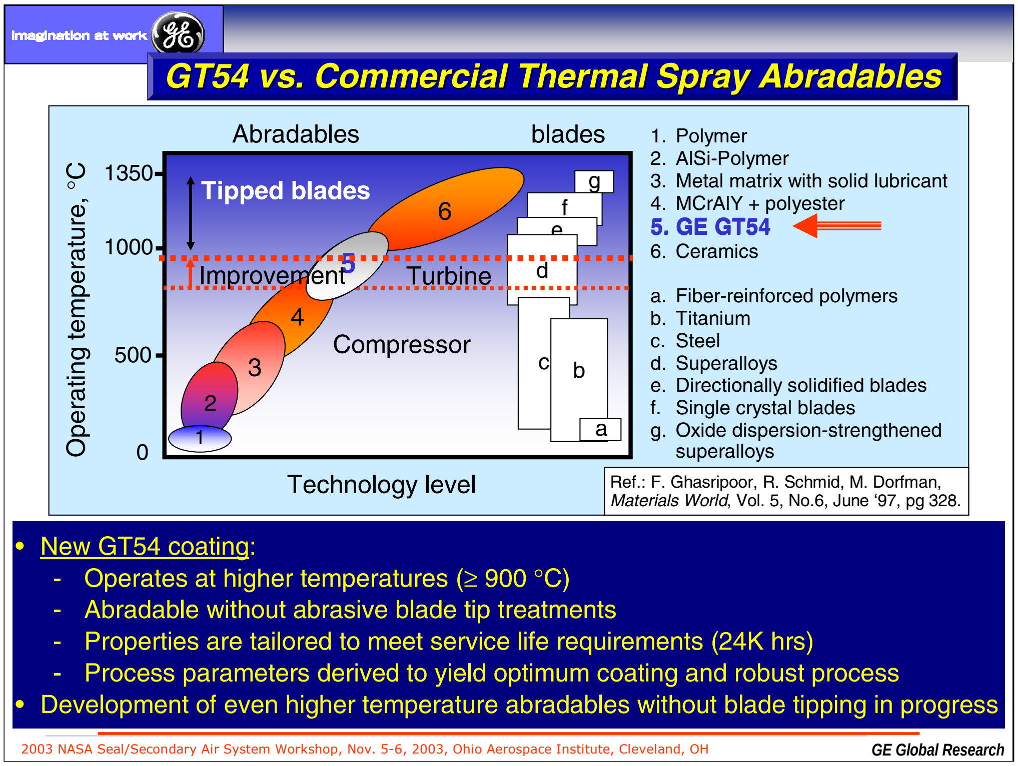

This chart is the same as the one shown earlier with GT54 abradable material added. This material was needed for E-Class 1st stage temperature range applications without using a ceramic material that would need blade tip treatments.

Development results to date show that the new GT54 coating meets the various target requirements, and thus customer expectations for E-Class stage 1 applications. Abradable development for F-Class stage 1 shrouds is in progress.

imagination at work

Summary—Status of Abradable Seal Applications

	Compressor	Stage 1 Turbine	Stage 2/3 Turbine
Benefits	TBD (~0.5 to 1%)	0.4 to 0.8%	0.4 to 0.6%
Materials	Material development complete Application processes selected	- GT50 for untipped E-Class GT temperatures - New coating (GT56) introduced for longer life - For higher temperatures, coating developed for tipped blades. - New coating has been developed for high temperature and untipped blades.	- Honeycomb (HC) in place - Longer life HC development in progress
Application Status	Cost/benefit being evaluated in the field	- GT50 – good initial penetration into E-Class GT fleet (> 300 units) - Two new coatings developed and introduced into E- and F-Class GT fleet	Good penetration of HC into E-Class GT fleet (~ 900 units) and F-Class GT fleet

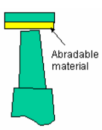

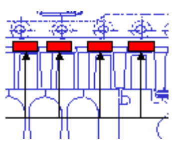

GT 50 Coated S1S
One of ~ 300 sets

GT 56 Coated S1S—1st set installed in 2003

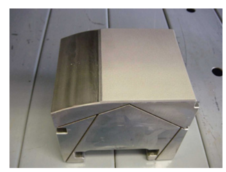

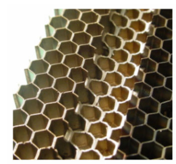

2003 NASA Seal/Secondary Air System Workshop, Nov. 5-6, 2003, Ohio Aerospace Institute, Cleveland, OH

GE Global Research

There is an organized, coordinated effort to develop and apply abradable seals to industrial gas turbines. E-Class turbines have been the primary focus of this presentation, but abradable seals are being considered for F-Class turbines as well. Compressor and turbine stage 2 & 3 applications are very similar for the two turbine classes. Considerable effort is being focused on the turbine stage 1 abradable tip sealing. Two generations of coatings have been introduced into E-Class turbines over the last three years. The F-Class stage 1 brings higher temperature challenges for the abradable sealing system developed for that location.

HIGH MISALIGNMENT CARBON SEALS FOR THE FAN DRIVE
GEAR SYSTEM TECHNOLOGIES

Dennis Shaughnessy and Lou Dobek
United Technologies
Pratt & Whitney
East Hartford, Connecticut

The Ultra Efficient Engine Technology (UEET) program is a NASA-funded program to develop and demonstrate technology for quiet, fuel-efficient, low-emissions next generation commercial gas turbine engines. An essential role for achieving lower noise levels and higher fuel efficiency is played by the power transmission gear system connected to the fan. Geared systems driving the fan will be subjected to inertia and gyroscopic forces resulting in extremely high angular and radial misalignments. Because of the high misalignment levels, compartment seals capable of accommodating angularities and eccentricities are required. Pratt & Whitney and Stein Seal Company selected the segmented circumferential carbon seal as the best candidate seal type to operate at highly misaligned conditions and developed a test program to determine misalignment limits of current segmented circumferential seals. The long-term goal is to determine a seal design able to withstand the required misalignment levels and provide design guidelines.

A technical approach is presented, including design modification to a "baseline" seal, carbon grade selection, test rig configuration, test plan and data acquisition. Near term research plans and back-up seal designs are also presented.

2003 NASA Seal/Secondary Air System Workshop

High Misalignment Carbon Seals

Background

Tomorrow's Engines with Geared Fans will be subjected to extreme conditions such as:

- High angular and radial seal misalignments
  - Gyroscopic loads - angular misalignment
  - Sun input gear orbiting - radial/eccentric misalignment
- Higher LPC shaft speed; ~10,000 RPM
- Large Diameter Fan Hub

Seals capable of accommodating high misalignment, high rubbing speeds, low pressure differentials and large diameters must be developed.

November 5-6, 2003

Background information on principal causes of extreme conditions in Advanced Commercial Engines. Such conditions impose on seals high misalignment, high rubbing speed, large diameters and low pressure differentials.

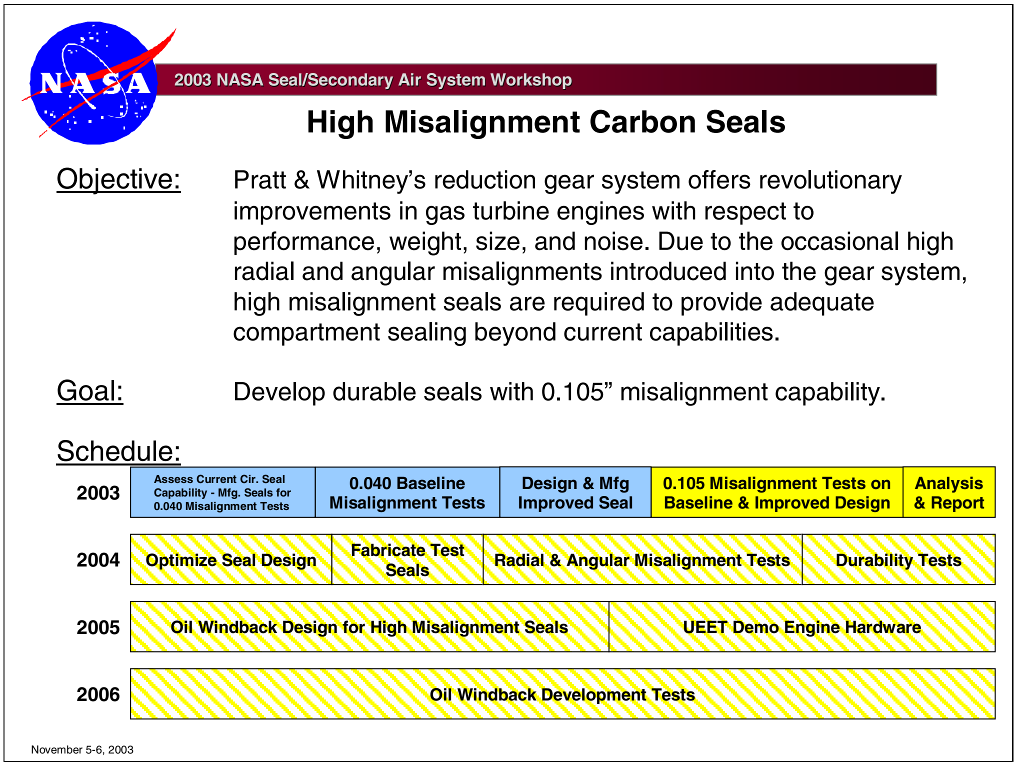

Objective – Development of seals capable of 0.105" misalignment for use in the Pratt & Whitney reduction gear system.

2003 NASA Seal/Secondary Air System Workshop

High Misalignment Carbon Seals

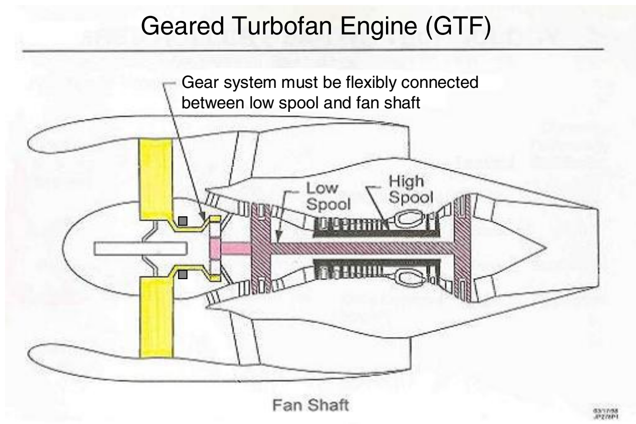

November 5-6, 2003

Misalignment seals are located along the flexible shaft between the low spool and fan shaft.

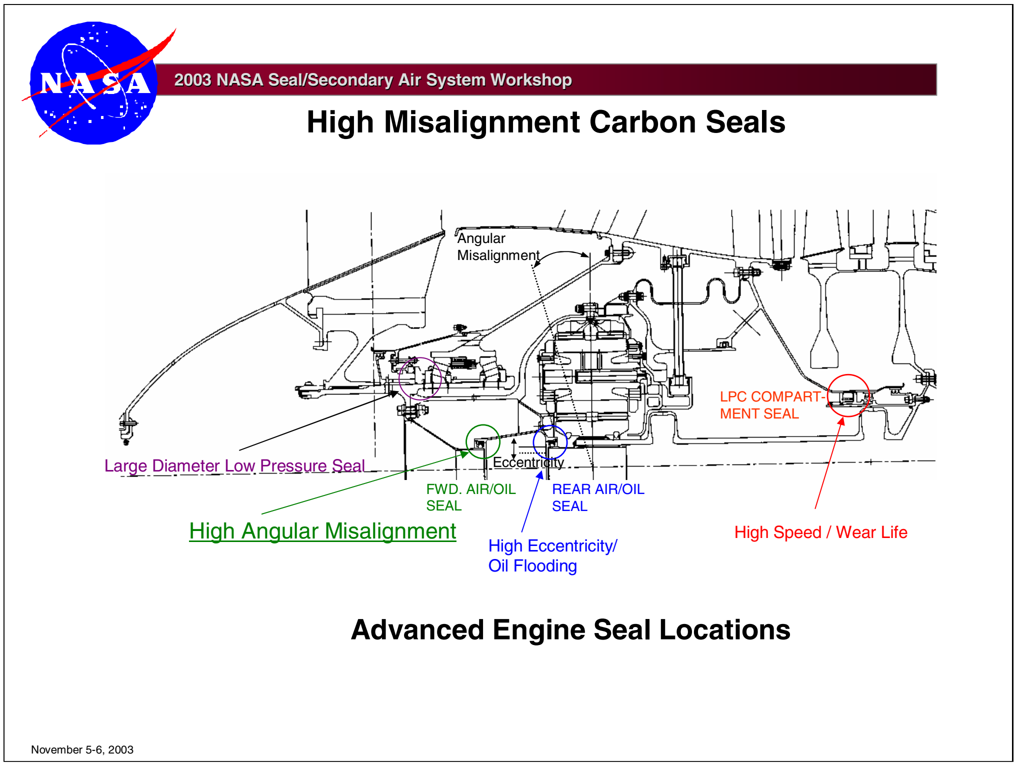

Seal locations within the forward compartments of the fan drive geared engine. Forward air/oil seal represents the location of the highest source of angular and radial misalignment.

2003 NASA Seal/Secondary Air System Workshop

High Misalignment Carbon Seals

	FWD. AIR/OIL SEAL	REAR AIR/OIL SEAL	FDGS/LPC COMPARTMENT SEAL
Required Life (hours)	30,000	30,000	30,000
Delta P (psi)	<50	<50	40-50
Surface Speed (ft/s)	33	90	345
Buffer Air Temperature (deg. F)	350	350	415
Angular Misalignment (deg)	0.5	0.2	0.1
Eccentricity (inches)	0.005	0.02	0.005
Sealing Diameter (inches)	2.95	2.95	11.2
Type	Segmented/ bellows/ other	Segmented/ other	Segmented/ ring/ other

Seal Operating Conditions

November 5-6, 2003

Seal operating conditions (required life, pressure differentials, speeds, misalignment levels and others).

Critical requirements are highlighted.

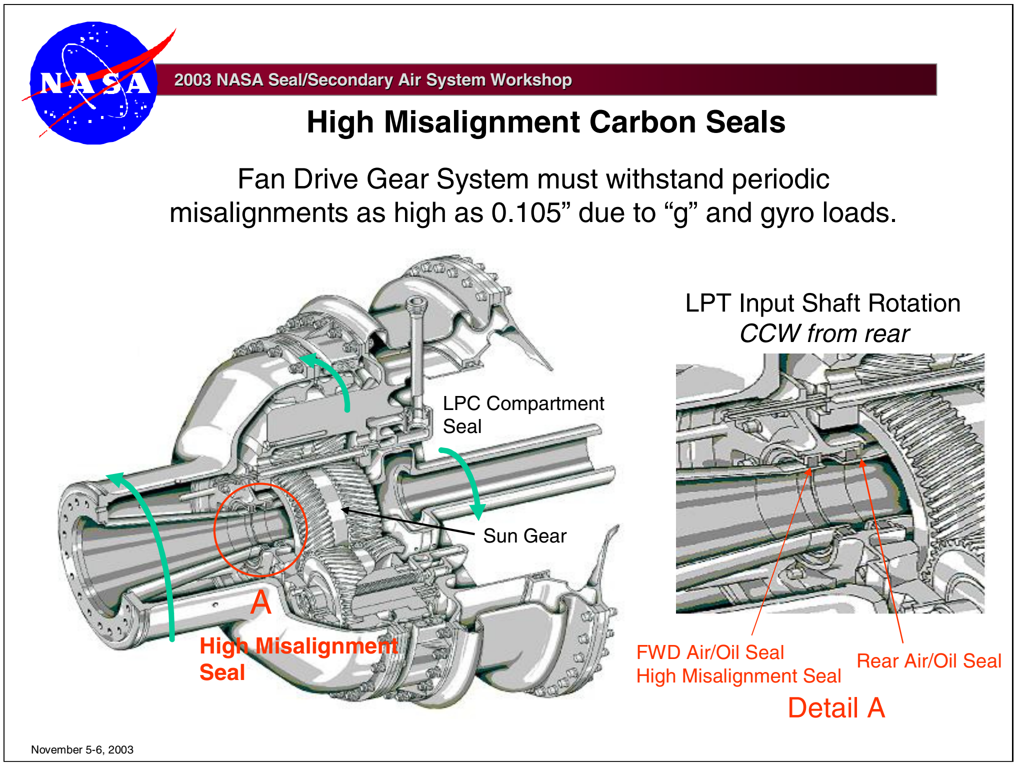

Fan drive gear systems must withstand periodic misalignments as high as 0.105” due to “g” and gyro loads.

2003 NASA Seal/Secondary Air System Workshop

High Misalignment Carbon Seals

Approach

Misalignment Seal Test Rig Program

Stein Seal selected as the seal supplier/tester.

Testing at supplier's facilities.

Step 1
- "Baseline" seal design
- Carbon grade "X" - high strength, low modulus.
- Misalignment increased in steps up to 0.020 in. radial & .5° angular misalignment

Step 2
- Misalignment increased in steps up to 0.040 in. radial & .5° angular misalignment

Step 3
- Alternate seal designed w/Carbon grade "X" tested
- Misalignment increase in steps from 0.060 to 0.105 in. radial & 0.5° angular misalignment

Step 4
- Alternate seal designed w/Carbon grade "Y" tested
- Misalignment increase in steps from 0.060 to 0.105 in. radial & 0.5° angular misalignment

November 5-6, 2003

Technical approach of misalignment seal development program. Four main steps will be followed starting from a "baseline" seal testing.

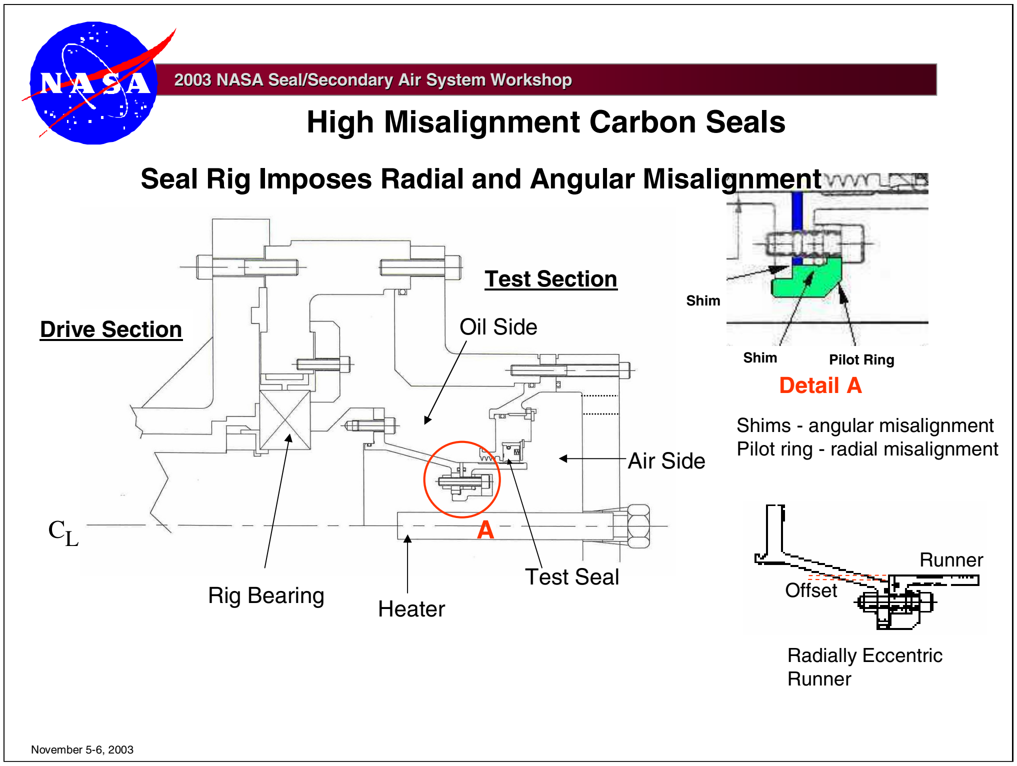

Seal test rig schematics used to impose radial and angular misalignment. Shims are used to impose angular misalignment and pilot rings are used to impose radial misalignment.

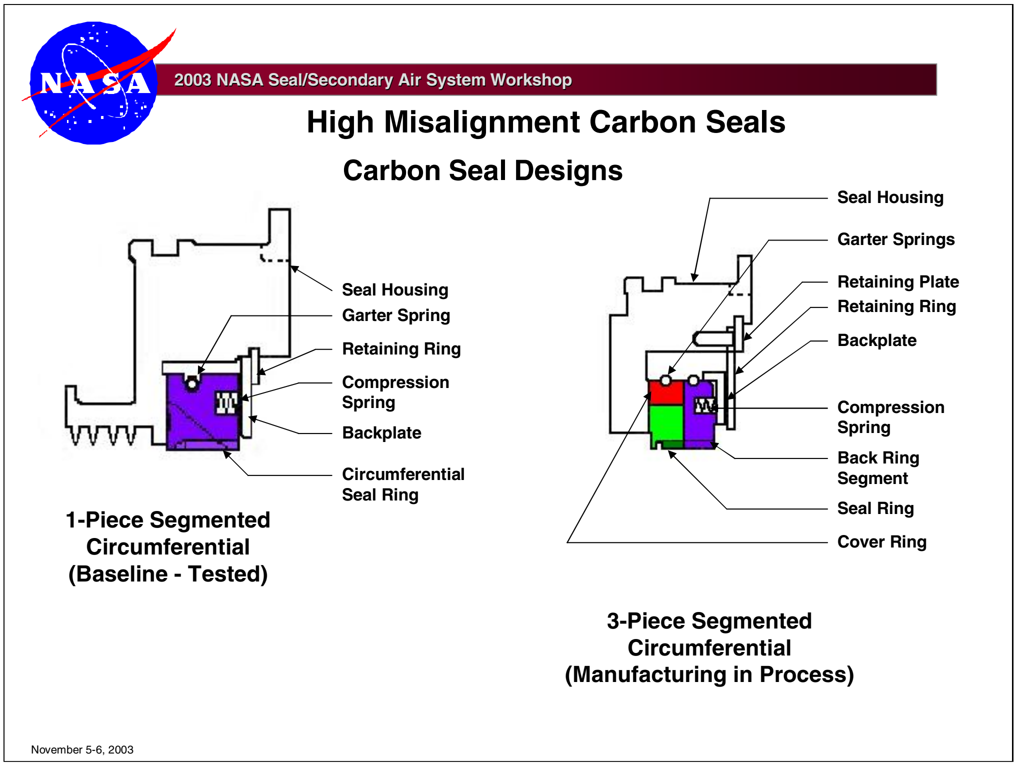

Baseline seal is compose of a one-piece 4 segmented seal. Alternate design is composed of a three-piece design, each piece consisting of four segments.

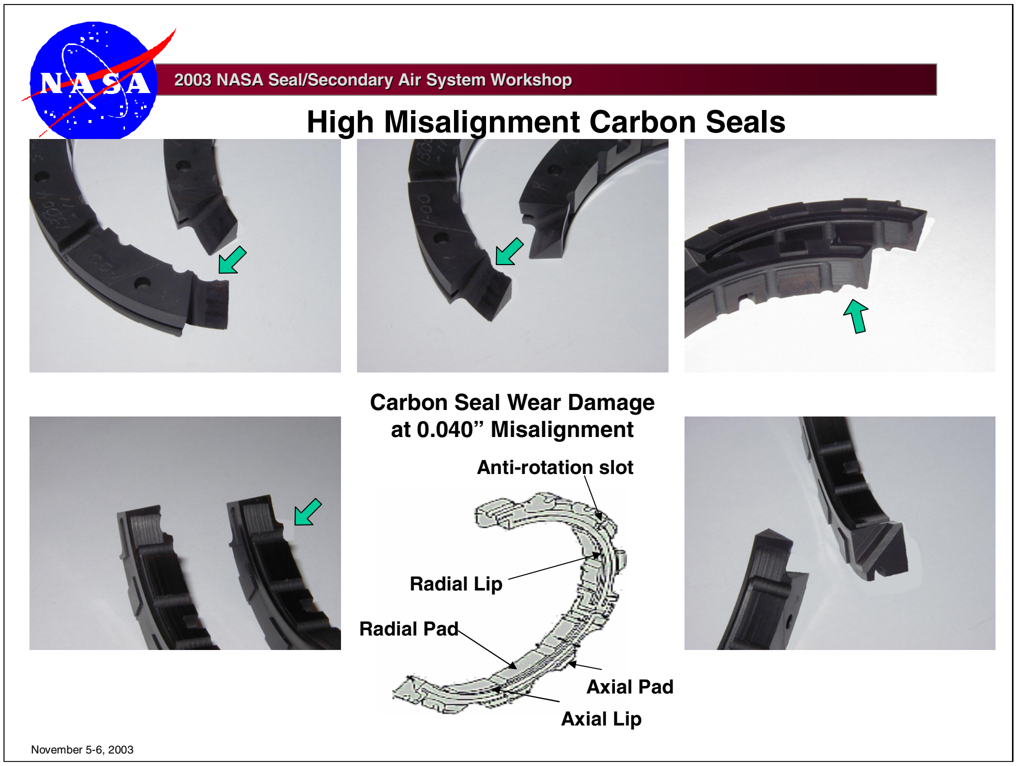

Step one Carbons indicate excessive wear and chipping along the tongue and sockets of the segments.

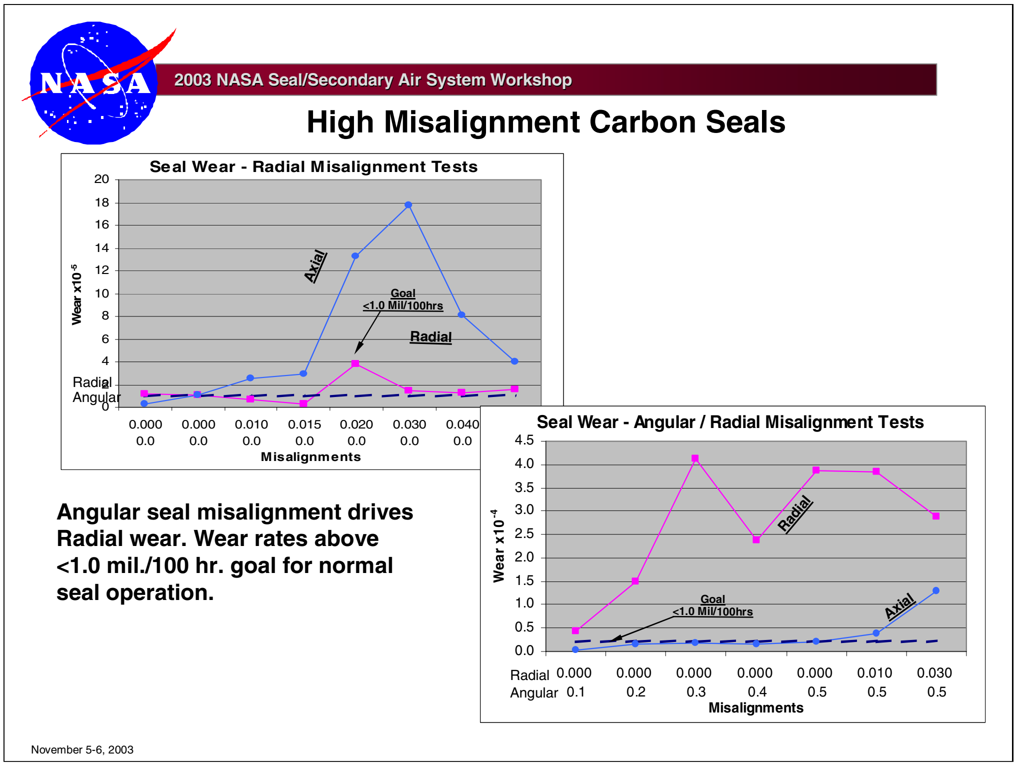

Step one test results indicate wear rates in excess of those desired. Unexpected reduction in wear rates at higher levels of misalignment under investigation.

2003 NASA Seal/Secondary Air System Workshop

High Misalignment Carbon Seals

Commercialization Aspects

Fan Drive Gear System development identified certain technologies as key requirements of which, High Misalignment Seals are extremely important.

Geared Turbo Fan Provides:

- **550lbs weight reduction over a conventional 67K thrust turbofan engine.**
- **3%-4% TSFC improvement over conventional turbofan engines.**
- **30db noise reduction.**

Gear System technology also lends itself to Rotorcraft transmissions.

The circumferential seals are Stein Seal designs that are being optimized in this program.

November 5-6, 2003

The Fan Drive Gear System offers significant advances in the areas of weight reduction, noise reduction and fuel consumption.

2003 NASA Seal/Secondary Air System Workshop

High Misalignment Carbon Seals

Plans for Next Year & Beyond

2004 Optimize seal designs
Fabricate test seals
Radial & angular misalignment tests
Optimized seal durability tests

2005 Oil windback design
UEET demo engine hardware

2006 Oil windback tests

November 5-6, 2003

Plans for continuation include design optimization, durability testing, and windback design and testing.

2003 NASA Seal/Secondary Air System Workshop

High Misalignment Carbon Seals

Conclusion(s)

The initial one-piece circumferential seal design has limited misalignment capability as demonstrated in the seal rig testing.

To meet the misalignment goal, a more compliant design with an improved carbon material is required.

November 5-6, 2003

Conclusions thus far indicate limited capabilities of the one-piece segmented carbon seal. Alternate Carbon materials may yield more compliant results.

COMPLIANT FOIL SEAL INVESTIGATIONS

Margaret P. Proctor
National Aeronautics and Space Administration
Glenn Research Center
Cleveland, Ohio

Irebert Delgado
U.S. Army Research Laboratory
Glenn Research Center
Cleveland, Ohio

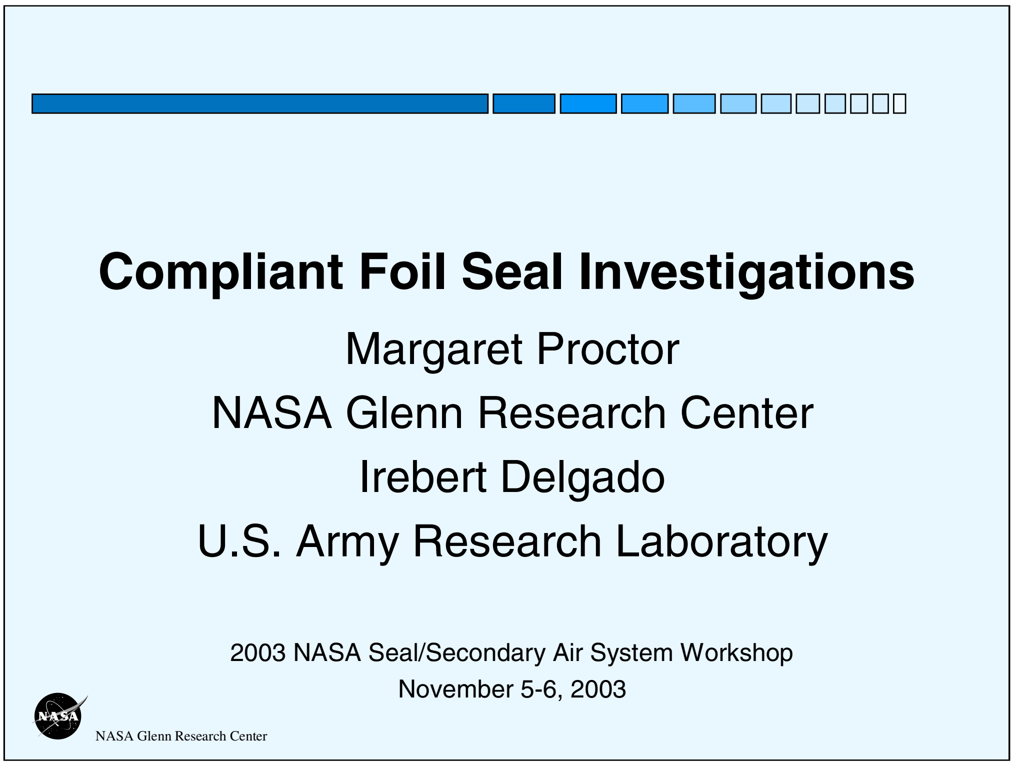

Room temperature testing of an 8.5 inch diameter foil seal was conducted in the High Speed, High Temperature Turbine Seal Test Rig at the NASA Glenn Research Center. The seal was operated at speeds up to 30,000 rpm and pressure differentials up to 75 psid. Seal leakage and power loss data will be presented and compared to brush seal performance. The failure of the seal and rotor coating at 30,000 rpm and 15 psid will be presented and future development needs discussed.

Compliant Foil Seal Investigations

Margaret Proctor
NASA Glenn Research Center
Irebert Delgado
U.S. Army Research Laboratory

2003 NASA Seal/Secondary Air System Workshop
November 5-6, 2003

NASA Glenn Research Center

NASA Glenn Research Center has been working with Mohawk Innovative Technology, Inc. (MiTi) to develop a Compliant Foil Seal for use in gas turbine engines. MiTi was awarded phase I and phase II SBIR contracts to analyze, develop, and test foil seals. As part of the Phase II contract, MiTi delivered an 8.5 inch diameter foil seal to NASA GRC for testing. Today I will be presenting some results of testing the 8.5 inch foil seal at NASA.

Mohawk's 8.5 inch Foil Seal Prior to Test

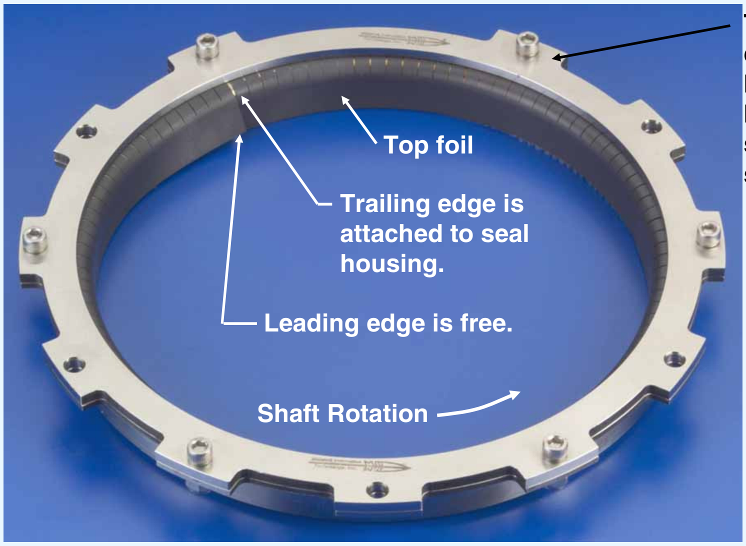

Top foil is clamped to seal housing on high pressure side of seal by seal clamp.

NASA Glenn Research Center

This foil seal is an extension of MiTi's foil bearing technology. The foil seal is essentially a foil bearing that uses a pair of top foils with slotted extensions to block the axial flow from passing thru the bump foils located behind the top foils. The two top foils are clocked to each other so that the extension tabs of one top foil block the slots of the other. The trailing edge of the top foil is fixed to the seal housing and the leading edge is free. Rotor rotation is counter clockwise looking from the high pressure side. The top foil is coated with MiTi's Korolon 800 coating.

Down Stream Edge of Foil Seal

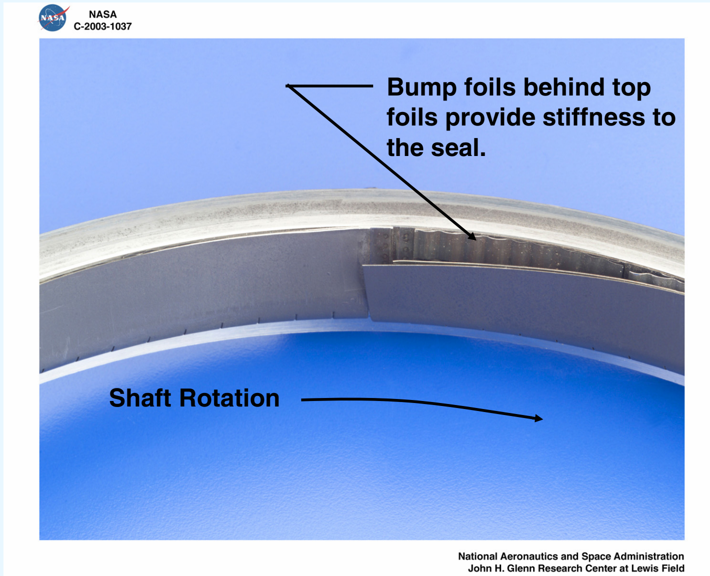

NASA Glenn Research Center

The bump foils can be seen behind the top foil in this view of the downstream side of the seal near the leading edge. When the seal is installed over the rotor the top foil conforms to the rotor od.

Test Summary of 8.5 inch Foil Seal

- **Tests Completed: Room temperature static, 7-17-03**
  Room temperature performance 7-21-03

- **Leakage and Power Loss measured at: 0,10, 15, 20, 25 Krpm**
  0 to ~70 psid
  Pressure cycled up and down twice at each speed.

- **Shaft orbits indicated problem at 30,000 rpm, 15 psid**
  - folded “figure 8”-shape, decreased speed to 25 Krpm
  - orbits worsened, aborted turbine drive
  - very large orbits during deceleration

- **Seal and rotor coating severely damaged.**

NASA Glenn Research Center

Room temperature static and performance tests were conducted on the 8.5 inch foil seal. Results were obtained at speeds up to 25000 rpm and pressure differentials from 0 to 70 psid. At each speed the pressure was cycled up and down twice. 2 psid was applied during the initial rotation to ensure air flow to carry away the heat generated due to rubbing between the top foil and the CrC coated rotor that occurs prior to top foil lift off. At 30,000 rpm and 15 psid, the rig shaft orbits indicated a problem. Speed was decreased to 25000 rpm. The orbits worsened and we shutdown the air turbine. The shaft orbits became very large during deceleration. Post test inspection found the seal and rotor coating were severely damaged.

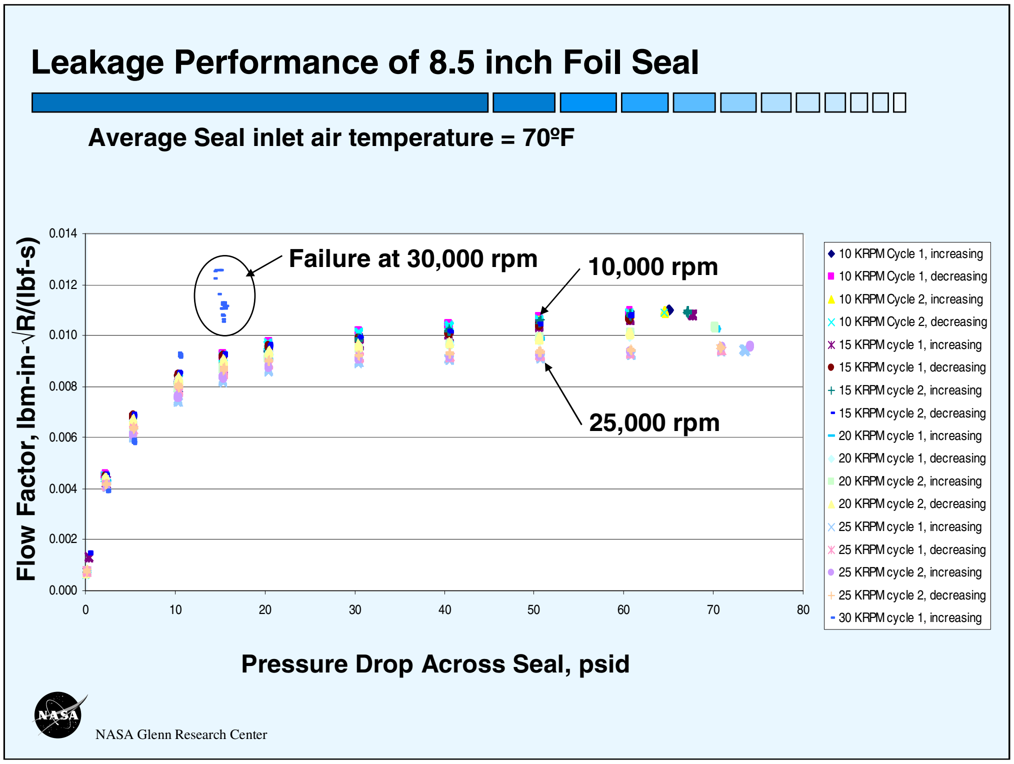

This is a plot of the seal leakage flow factor versus pressure drop across the seal obtained during the performance test. For all speeds the flow factor increases with increasing pressure differential until about 25-30 psid where it levels off indicating that the flow is choked. The flow factor decreases as speed increases due to reduced clearance cause by centrifugal growth of the rotor. During the failure event at 30,000 rpm and 15 psid the flow factor increased substantially and rapidly. This sudden increase in flow factor indicates an opening of the seal clearance caused by either loss of the seal coating or wear of the seal top foil.

Leakage Performance Comparison

- The 8.5 inch foil seal flow factor levels out between 0.009 to 0.011.
- Previous testing has shown finger and brush seals to have flow factors at 0.004 to 0.006.
- MiTi previously tested a 2.84 inch foil seal and found its leakage performance to be much better than a brush seal.
- The leakage performance of the 8.5 inch foil seal is about twice that of finger or brush seals. Since this is counter to previous findings at smaller diameter seals, it is concluded that there are some scale up issues that need to be addressed.

Foil Seal and Brush Seal Leakage Data
2.84 in. Dia. Journal; 68 °F
SBIR Phase 1

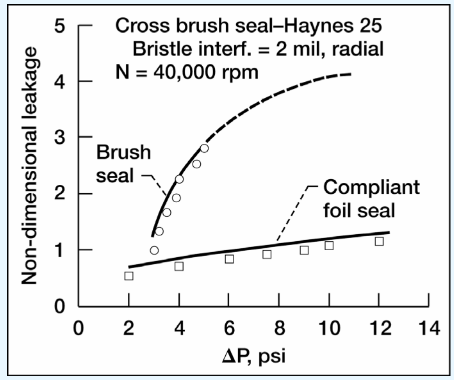

NASA Glenn Research Center

From the previous chart we see that the flow factor for the 8.5 inch foil seal leveled out between 0.009 and 0.011.

Previous testing at NASA has shown that finger and brush seals have flow factors of 0.004 to 0.006.

MiTi previously tested a 2.84 inch foil seal and found its leakage performance to be much better than a brush seal.

The leakage performance of the 8.5 inch foil seal is about twice that of a brush or finger seal. Since this is counter to previous findings at smaller diameter seals, it is concluded that there are some scale up issues that need to be addressed.

Power Loss of 8.5 inch Foil Seal

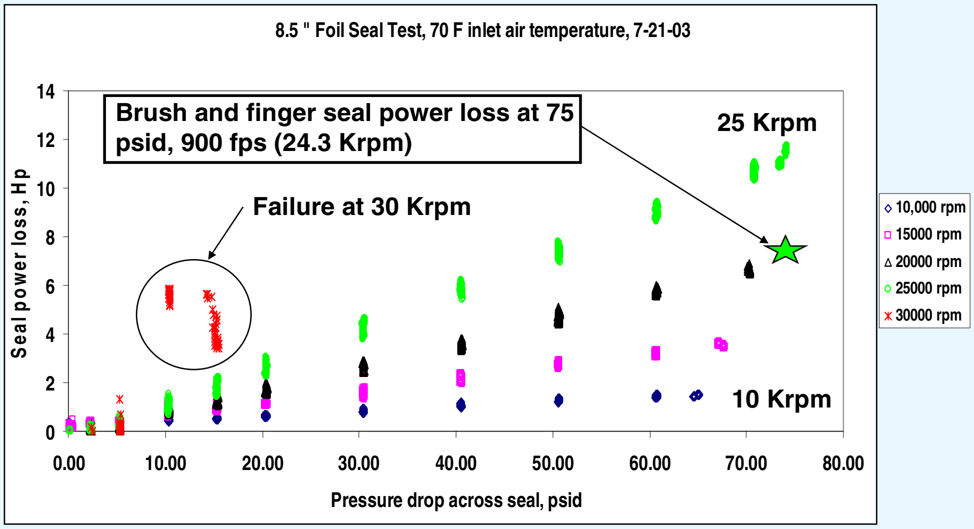

NASA Glenn Research Center

This is a plot of the measured 8.5 inch foil seal power loss versus pressure drop across the seal for each speed tested. A torquemeter was used to measure the total torque of the seal test rig with the seal installed. The tare torque of the seal test rig without a test seal installed is subtracted from the total torque to derive the seal torque. The seal power loss is computed as the seal torque multiplied by speed. The seal power loss increases with speed and with pressure differential.

Noting that the seal power loss of the 8.5 inch foil seal at 25,000 rpm or 927 ft/s and 75 psid is 11-12 Hp and comparing it to previously published data for the finger and brush seal at 1200 F inlet air temperature, 900 ft/s and 75 psid which had a seal power loss of 7.5 to 8 Hp, it is concluded that the 8.5 inch foil seal tested has a higher power loss than a brush or finger seal.

The seal power loss at 30,000 rpm and 15 psid was higher than one might expect based on the data for lower speeds. Also the power loss at 30,000 rpm and 10 psid was quite high and indicates rubbing was occurring at that point.

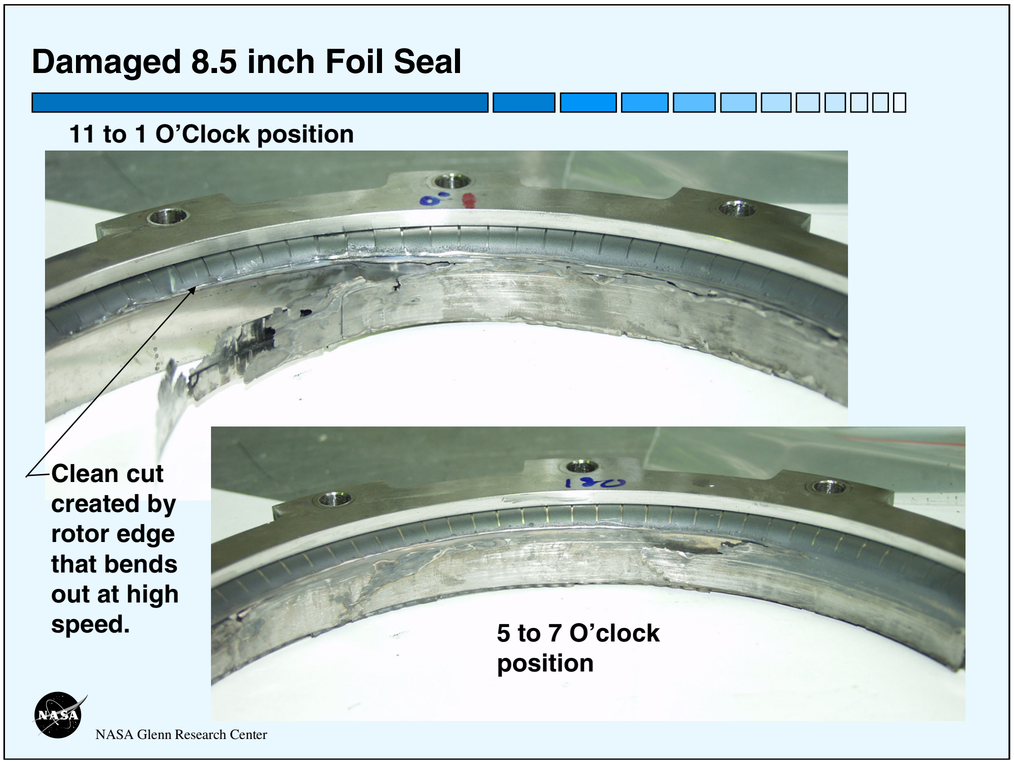

This is the 8.5 inch foil seal after room temperature testing to 30,000 rpm. The seal is damaged beyond use. Parts of the top foils and bump foils were found blown behind the rotor at disassembly. The Korolon coating is rubbed off and the top foil was burned through at places. Note the clean cut at the bend in the top foil. This cut aligns with the edge of the test rotor. The test rotor has an I-beam cross section at the rim. Hence at high speeds the edges of the rotor rim bend out radially farther than the axial center of the rim. This displacement combined with the chamfer on the edge of the rotor makes a nice cutting tool.

Damaged Rotor Coating

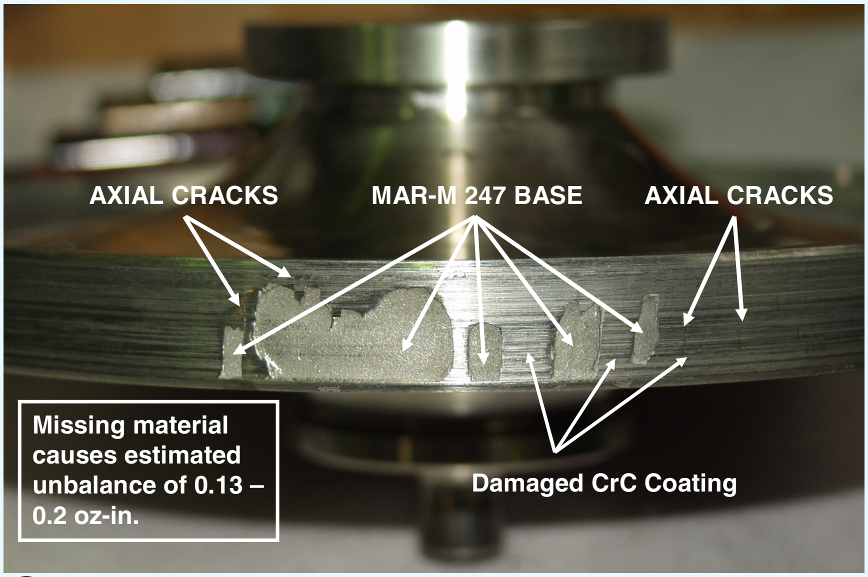

NASA Glenn Research Center

The rotor coating failed. The Mar M-247 rotor had a 0.010 inch thick CrC coating applied by high velocity oxygen fuel thermal spraying. By measuring the areas of the missing coating and the depth of the damage, the unbalance of the missing material is estimated to be 0.13-0.2 oz-in, which is 27-40 times greater than the balance specification for the rotor. Some hairline axial cracks are visible.

Rotor under fluorescent penetrant dye inspection

Axial cracks, typical of heat checking, indicate fatigue failure of the coating.

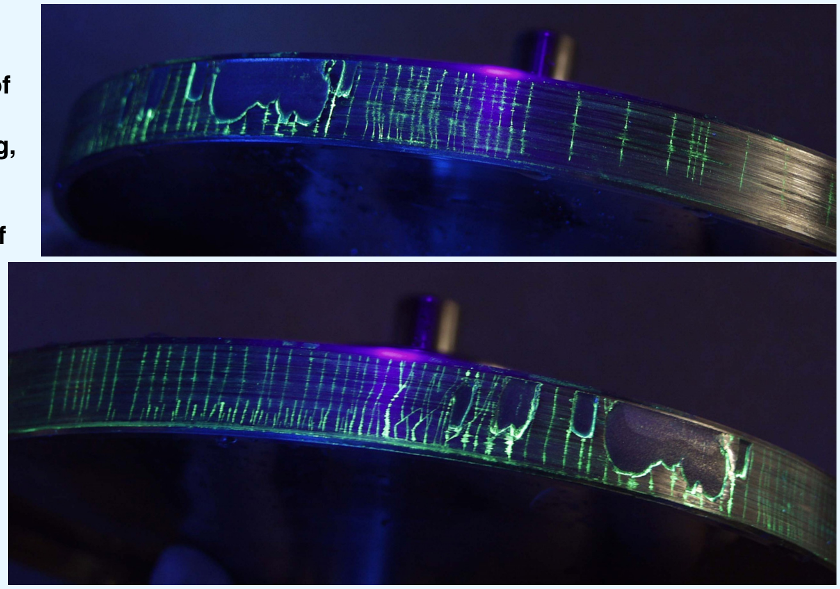

NASA Glenn Research Center

Many axial cracks are visible in the rotor coating under fluorescent penetrant dye inspection. These axial cracks are typical of heat checking and indicate fatigue failure of the coating. The fatigue failure is likely due to the mismatch in coefficients of thermal expansion for the rotor material Mar M-247 and the CrC coating.

Conclusions

- 8.5 inch foil seal leakage is higher than brush or finger seals and smaller foil seals. More optimization of the seal is needed to reduce leakage for large diameter seals and to understand scaling issues.
- Power loss of the 8.5 inch foil seal increases with speed and pressure differential and is about 50 percent higher than brush or finger seals at 900 fps and 75 psid.
- The foil seal was successfully tested at speeds to 25,000 rpm which corresponds to a DN of 5.4 million, surpassing previous maximum DN demonstrations of foil bearing technology.
- The damage to the seal was likely caused by a loss of clearance due to centrifugal growth of the rotor and fatigue failure of the coating, which initiated a thermal runaway condition.
- Rotor coating selection and application needs a redesign.
- A good understanding of the seal operating environment and operating limits is paramount to success.

NASA Glenn Research Center

Self-explanatory.

TEST RIG FOR EVALUATING ACTIVE TURBINE BLADE TIP CLEARANCE CONTROL CONCEPTS

Scott B. Lattime
Ohio Aerospace Institute
Brook Park, Ohio

Bruce M. Steinetz
National Aeronautics and Space Administration
Glenn Research Center
Cleveland, Ohio

Malcolm G. Robbie and Arthur H. Erker
Analex Corporation
Brook Park, Ohio

Test Rig For Evaluating Active Turbine Blade Tip Clearance Control Concepts

Scott B. Lattime
Ohio Aerospace Institute, Cleveland, Ohio

Bruce M. Steinetz
NASA Glenn Research Center, Cleveland, Ohio

Malcolm G. Robbie and Arthur H. Erker
Analex Corp., Cleveland, Ohio

2003 NASA Seal/Secondary Air System Workshop
November 5, 2003
Cleveland, Ohio

Glenn Research Center
UEET – Rotating Machinery Clearance Management
at Lewis Field

Overview

- **Objectives**
  - ACC System Concept
  - ACC Concept Evaluation Test Rig
- **ACC Concept System/Test Rig Design Overview**
  - Rig Specifications
  - Design Criteria
- **Test Rig and Support Systems**
  - Design of Main Components
  - Control Logic
  - Fabrication Status
- **Conclusions/Discussion**

Glenn Research Center
UEET – Rotating Machinery Clearance Management at Lewis Field

Objectives

- **Design a mechanical ACC system for HPT tip seal clearance management**
  - Improve upon slow thermal response of "case cooling" methods used today.
  - Provide continuous ACC throughout entire flight profile.

- **Design a test rig to evaluate ACC system concepts.**
  - Evaluate actuator concept response and accuracy under appropriate thermal and pressure conditions in a non-rotating environment.
  - Evaluate clearance sensor response and accuracy in a non-rotating "hot" environment.
  - Measure secondary seal leakage due to segmented shroud design, shroud actuation, and case penetration.

- **Test Rig Capabilities:**
  - Chamber temperatures up to 1500 °F.
  - Seal carrier backside pressure up to 120 psi (simulate cooling air Δp).
  - Sized for actual seal hardware (20" diameter turbine).
  - Simulate realistic tip seal clearance changes due to mechanical and thermal loading (electronically).
  - Positioning feedback sensing, rig construction, and actuation system designed to achieve positioning accuracy ≤ 0.004-in.

Glenn Research Center
UEET – Rotating Machinery Clearance Management
at Lewis Field

Multiple Independent Actuator ACC System Design

- Provides best potential for high positional accuracy requirements (< 0.005-in).
- Fuel-draulic actuators utilize engine high pressure fuel to power system (> 3000-psi).
- Number of actuators/shroud segments is scalable to engine size (force and accuracy requirements).
- Overcomes thermal binding and positional accuracy issues identified with other mechanically linked concepts (e.g., unison ring).
- Independent actuators can provide both axisymmetric and asymmetric clearance adjustments depending on load condition (e.g., backbone bending, flight loads, non-uniform thermal loads).

Glenn Research Center
UEET – Rotating Machinery Clearance Management
at Lewis Field

We have focused our efforts on designing mechanical ACC systems that articulate the seal shroud via mechanical linkages connected to actuators that reside outside the extreme environment of the HPT. We opted for this style of design due to a lack of high temperature/low profile actuators that are presently available.

We have also selected multiple hydraulic actuators for this first generation ACC system. Fuel-draulic actuators are already a well established technology.

Test Rig/ ACC System Specifications

- **Temperature**
  - The backside of the HPT shroud (blade outer-air-seal) is generally cooled with compressor discharge air (P3 air: **1200 to 1300-ºF**)
- **Pressure**
  - The cooling air is also used to purge the leading and trailing edges of the shroud segments, providing a positive backflow margin from the hot rotor inlet flow.
  - P3 is highest during maximum thrust events such as takeoff and re-accel. For large commercial engines this translates to a maximum cooling air pressure differential of up to **150-psid** across the shroud.
- **Actuation Range and Rate**
  - Maximum tip clearance changes due to axisymmetric and asymmetric loads on the rotor and stator components are on the order of 0.050-in.
  - FAA requires that engines have the ability to reach 95% rated takeoff power from flight idle (or from 15% rated takeoff power) in 5.0 seconds.

  → **0.01-in/s**

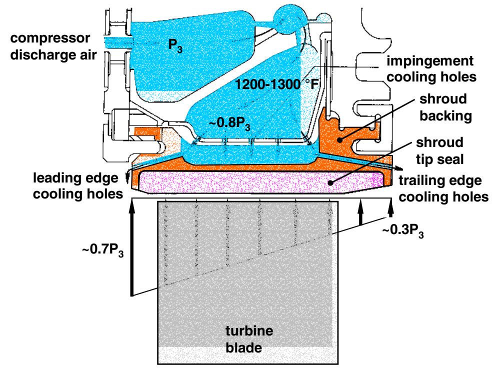

Glenn Research Center
UEET – Rotating Machinery Clearance Management
at Lewis Field

The design was concentrated on simulating the temperature and pressure conditions that exist on the backsides of the seal segments, without the need for a rotating turbine. This greatly simplified the rig design. We plan to assess the response of the ACC system to the effects of a turbine wheel (i.e., rapid clearance closures due to mechanical and thermal loads) by simulating closures electronically, as will be discussed in a later.

Design Criteria

- **The substantial diameter of the segmented shroud structure (~20-in), under moderate pressures (~120-psi), gives rise to significant loads, and hence stresses, to which the actuation system and components must react.**
- **These stresses coupled with high temperatures (1200 to 1300-°F) can significantly reduce component cycle life due to creep.**
- **Managing these stresses with adequate materials and geometry to improve component cycle life was a driving factor in the rig component design.**
- **Larson-Miller parameter data for a variety of high temperature, super alloys was utilized to design components to achieve a desired minimum cycle life.**
  - Inconel 718 utilized for most of the hot section components.
  - Components were designed for less than 0.5% creep strain, resulting in a 15-ksi limiting stress.
  - **15-ksi stress level corresponds to over 100,000 hours life at 1300-˚F and approximately 300 hours life at 1500˚F.**

Glenn Research Center
UEET – Rotating Machinery Clearance Management
at Lewis Field

ACC Concept Evaluation Rig

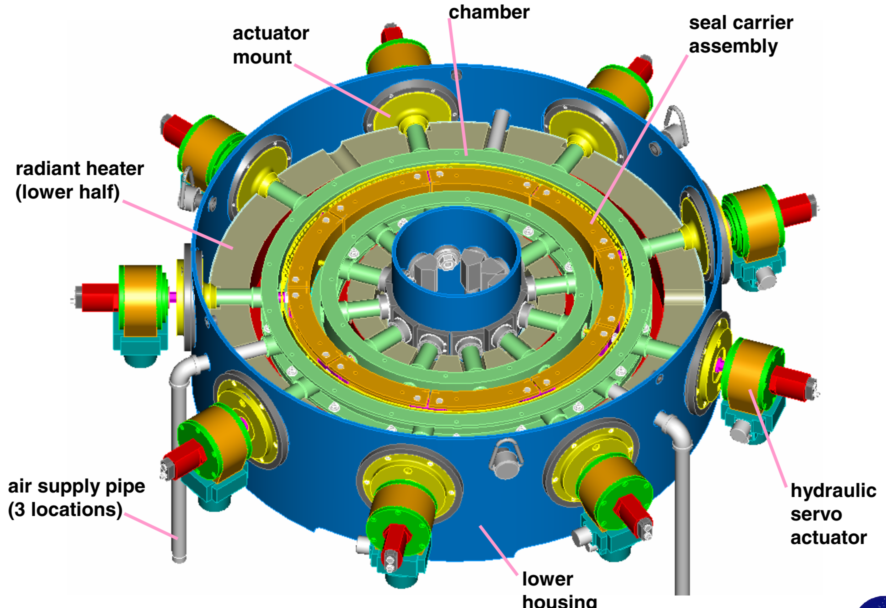

Glenn Research Center
UEET – Rotating Machinery Clearance Management
at Lewis Field

Here we see the Gen 1 ACC System Concept and Test rig.

The test rig comprises six main components: the housing, the radiant heater, the pressurized chamber, the seal carrier assembly, the actuator rod assemblies, and the hydraulic actuators.

At the heart of the rig is a segmented shroud structure (seal carrier) that would structurally support the tip seal shroud segments in the engine. Radial movement of the seal carriers controls the effective position/diameter of the seal shroud segments, thereby controlling blade tip clearance.

The rig housing consists of two concentric cylinders, which form an annular cavity. An annular radiant heater made of upper and lower halves surrounds the segmented seal carrier structure to simulate the HPT tip seal backside temperature environment. A pressurized chamber encloses the carrier segments inside the annular heater through which heated pressurized air is supplied to simulate the P3 cooling/purge air pressure on the seal backsides. Heated air enters the chamber via three pipes that are fed from a manifold at the air heater exhaust through radial inlet ports as shown.

ACC Rig Cutaway

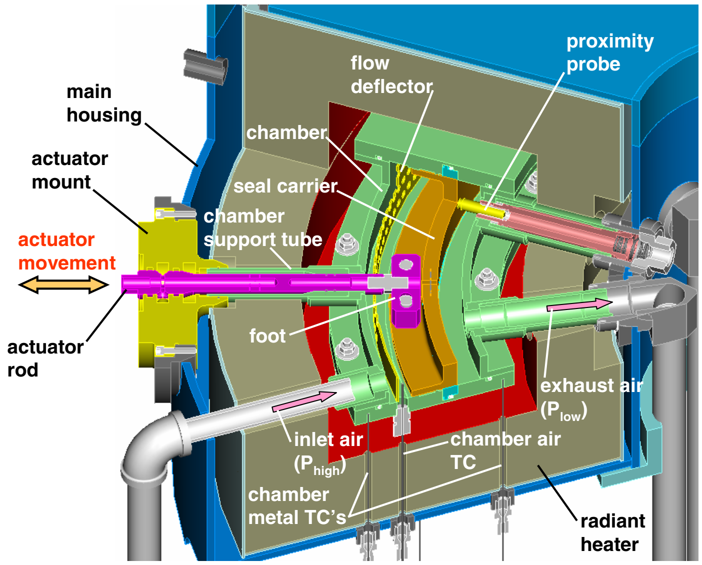

Glenn Research Center

UEET – Rotating Machinery Clearance Management at Lewis Field

The carrier segments are connected to independent hydraulic actuators through an actuator rod assembly. The foot of the actuator rod assembly positions the carrier segments in the radial direction, while allowing relative circumferential movement or dilation of the seal carrier segments through a pinned and slotted arrangement.

A series of radial tubes projecting outward from the chamber's inner and outer side walls serve as supports, air supply and exhaust ports, probe fixtures, and the actuator rod guides. The chamber functions to support and align the carrier segments and actuator rods, as well as to house instrumentation and to seal the pressurized air from the radiant heater which is not designed to carry any pressure loading.

The inlet flow is baffled circumferentially around the outer chamber wall by a flow deflector to achieve uniform heating of the seal carrier assembly. The pressurized air is sealed along the sides of the seal carrier segments by contacting face seals that are energized via metal "E"-seals imbedded in the upper and lower chamber plates. The joints between adjoining carrier segments are sealed with thin metal flexures. Air that escapes over and between the carrier segments is vented out of the rig through a number of exhaust pipes that protrude radially along the inner chamber wall. The number and inner diameter of exhaust pipes were chosen to eliminate the possibility of backpressure at the exhaust ports.

High temperature proximity probes measure the radial displacement of the seal carriers at various circumferential locations. These measurements provide direct feedback control to the independent actuators and allow the desired radial position (clearance) to be set. The direct feedback control system allows for simulation of realistic transient tip clearance changes in lieu of a rotating turbine wheel. Superimposing a mission-clearance-profile over the actual clearance measurement input to the actuator controllers will allow researchers to assess the system's response to the most dramatic transient events such as mechanical and thermal loading of the rotor during takeoff and re-accel.

The proximity probes are held at a constant standoff to the chamber inner wall via a spring-loaded piston arrangement. The spring-loaded mounting keeps the proximity sensor at a relatively constant position to the chamber inner sidewall during the initial heating of the rig. This arrangement also allows for easy removal of the probes without dismantling the housing.

The chamber air temperatures will be measured at three circumferential locations on the high-pressure side of the carriers to show how well the pressurized air is mixed by the chamber baffle. The chamber flange metal temperatures will be measured via two surface thermocouples attached to the inner and outer flange on the lower cover plate.

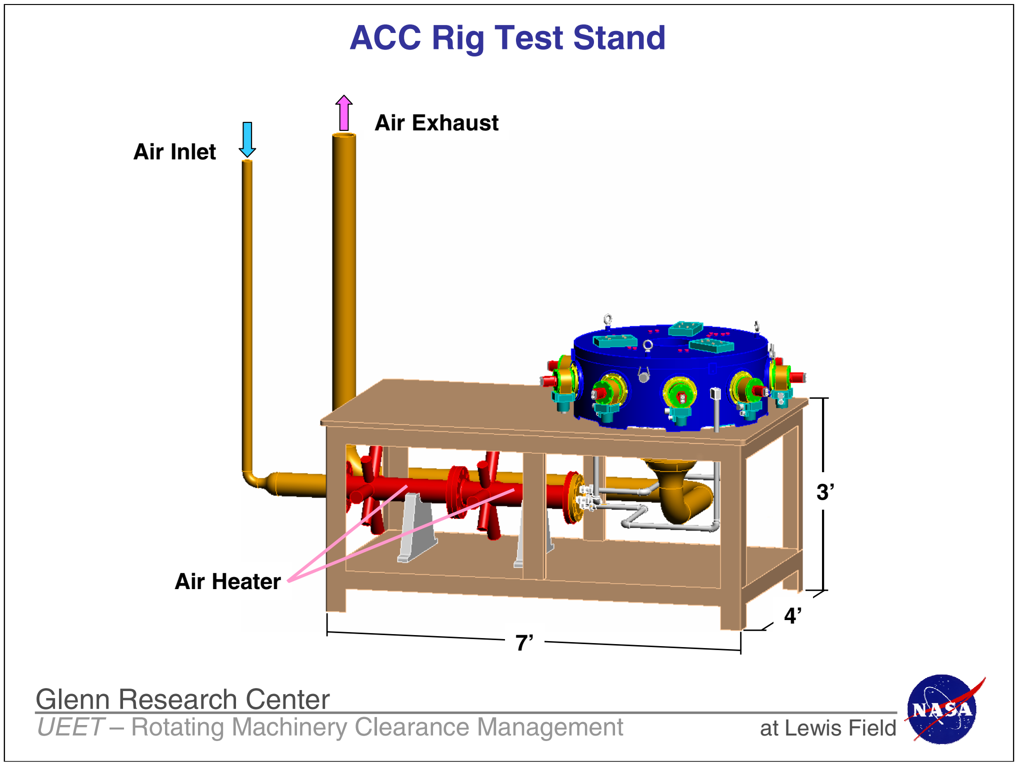

This slide shows the rig's air supply and exhaust plumbing layout as well as the test stand dimensions.

The air heater system comprises two 36-kW, inline, flanged heaters, manufactured by Osram Sylvania. It is designed to supply up to 75-scfm of air at 120-psi and 1500 °F.

Carrier-Actuator Rod Assembly

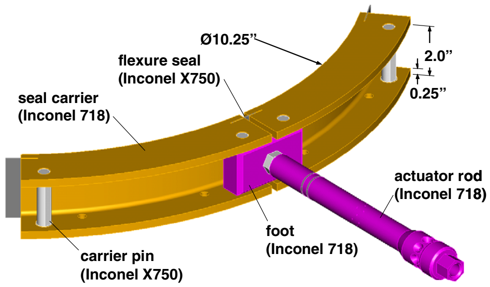

- **The slots are cut on a tangent to the radius on which the carrier pinholes are located.**
- **Prevents the carrier segment from cocking while it is displaced radially and circumferentially.**
- **The length of the slot allows a radial displacement of 0.2-in for each of the nine segments.**

Glenn Research Center
UEET – Rotating Machinery Clearance Management
at Lewis Field

Because the carriers are constrained by a pinned connection at one end and a slotted connection at the other, the segments must shift circumferentially as they are displaced in the radial direction. The slots in the feet are cut on a tangent to the radius on which the carrier pinholes are located. This keeps the carrier segments from cocking while it is displaced in both the radial and circumferential directions. The circumferential length of the carrier segments as well as the length of the slot in the actuator rod foot allows a radial displacement of 0.2-in for each of the nine segments. The slots for the flexure seals have adequate clearance to prevent the segments from becoming arch-bound as the segments are moved radially inward.

The pins are made of Inconel X750. This material was selected to help minimize galling against adjacent Inconel 718 components. The pins have flats machined on the diameter that contacts the slots, providing a bearing surface and reducing the contact stress developed between the pin and foot

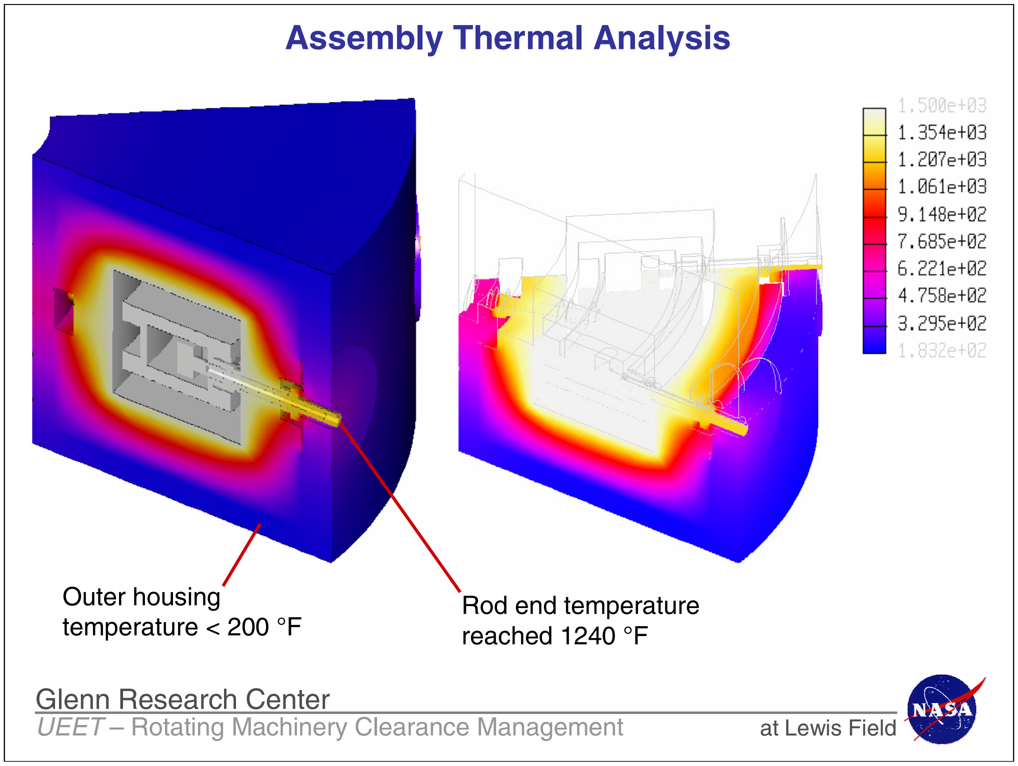

A steady-state thermal analysis estimated rod-end temperatures above 1240 °F with the radiant heater and chamber at 1500 °F. This rod-end temperature greatly exceeds the upper operating temperature (~250 °F) allowed by conventional hydraulic actuators. A cooling scheme for the rod end was then designed to allow the use of conventional actuators.

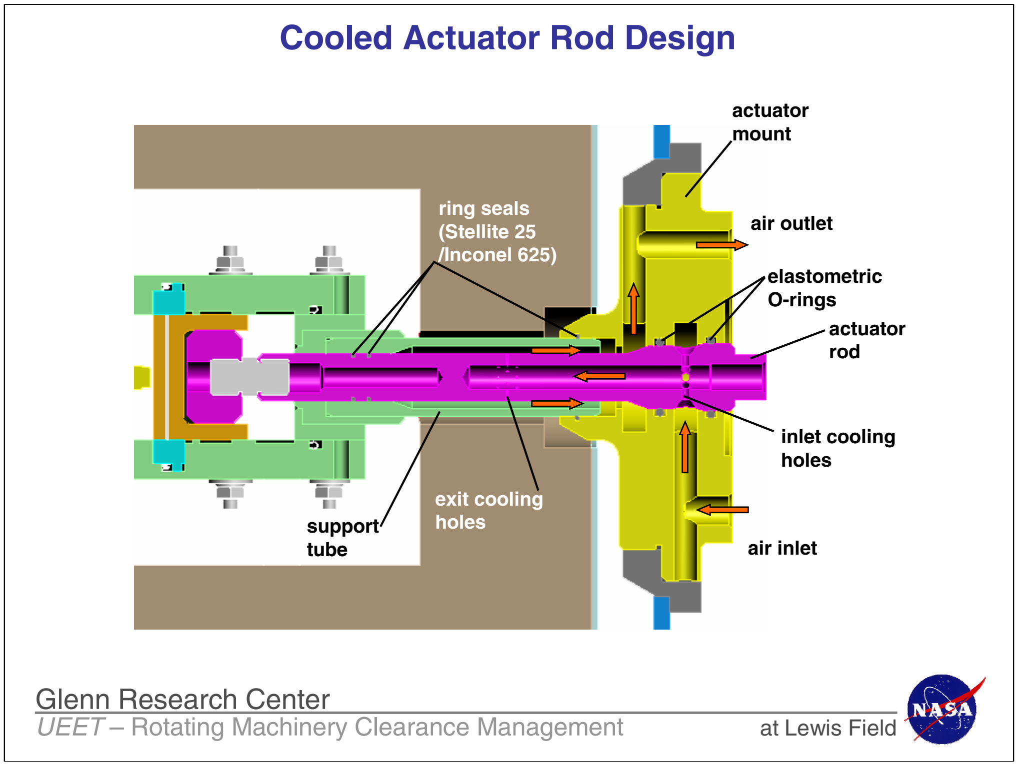

The cooling scheme allows the actuator rod and support tube to function as a tube-in-tube heat exchanger using a small flow rate of ambient air to cool the assembly.

The cooling holes were made from three sets of six, 0.03-in diameter holes drilled around the circumference of the hollow rod. Ambient air, supplied at the rod end through features in the actuator mount, travels axially through the center of the rod, passes radially through the cooling holes, and exits between the support tube and outer diameter of the rod.

Rod Cooling Scheme Validation

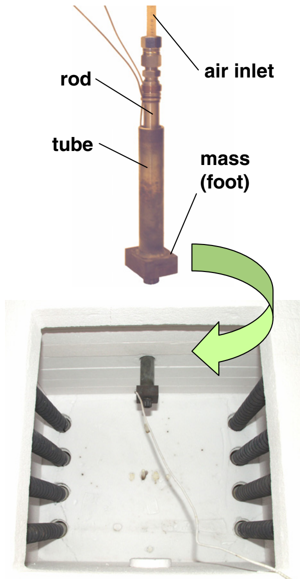

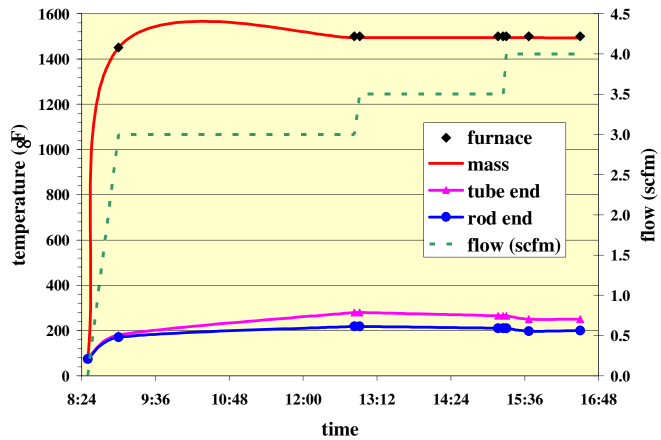

test hardware in furnace

Air flow of 4.0 scfm kept both rod and tube ends < 250 °F.

Glenn Research Center
UEET – Rotating Machinery Clearance Management
at Lewis Field

A mockup of the cooled actuator rod design was built to validate the design. A solid steel block (simulating the actuator foot) was bolted to one end of a stainless steel tube (simulating the rod). Another larger tube was welded to the block (simulating the support tube) in a concentric arrangement. An air supply line was attached to the end of the inner tube from which the assembly was supported and inserted into a box furnace. The insulation thickness of the furnace closely approximated that of the radiant heater designed for the rig. A plastic supply line was used minimize heat loss through the supply tube. Thermocouples were attached to measure the temperatures of the mass, the end of the inner rod, and the end of the outer tube. The furnace was heated to 1500 °F and after the mass temperature stabilized at 1500 °F, ambient air at approximately 70 °F was supplied to the assembly. Temperatures of the furnace, mass, tube end, and rod end are shown as a function of time on the left vertical axis. The cooling air volumetric flow is shown on the right vertical axis. The chart shows that for minimal air flow (3.0 to 4.0-scfm) both the tube and rod end temperatures were kept below 250 °F. Thus the cooling scheme design was successfully validated and implemented into the rig design to allow the use of conventional actuators.

Chamber Seal Locations & Leakage

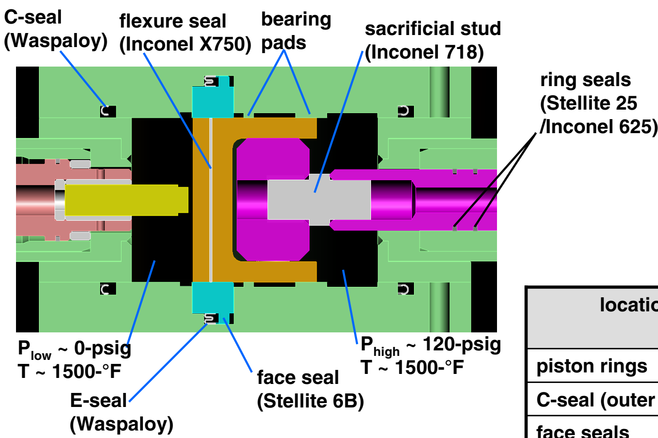

location	ΔP (psi)	Temp (°F)	Flow (scfm)
piston rings	120	1500	0.65
C-seal (outer flange)	120	1500	1.61
face seals	120	1500	2.10
E-seals (behind face)	120	1500	5.40
flexure seals	120	1500	23.34
Total			33.1

Glenn Research Center
UEET – Rotating Machinery Clearance Management   at Lewis Field

The nature of this ACC concept with its segmented shroud design and case penetration requires multiple high temperature seals. The test rig will allow the development and evaluation of these seals that will eventually be required in an engine. Obviously the leakage created by the use of these secondary seals must be minimized to gain the benefits of the ACC system. For the test rig, the secondary seal leakage drove the design of the air heater.

Flexure seals are used to prevent the radial flow of pressurized air between the carrier segment joints. The 2.0-in wide by 0.9-in long flexures are made of 0.02-in Inconel X750 sheet stock. This material was chosen for its galling resistance to the carrier material. The carrier slits that contain the flexures are designed with a 0.01-in clearance.

The chamber contains four “C-seals”, two on the upper and lower outer diameter flanges and two on the upper and lower inner diameter flanges of the cover plates. The seals are made of Waspalloy and have a cross sectional thickness of 0.015-in. The seals were designed by Perkin-Elmer to seal against a 120-psi pressure at 1500 °F and they require a 150-lbf/in seating load per seal at assembly.

The upper and lower cover plates also house a metal face seal assembly. These seals act to block the pressurized air from flowing between the cover plates and carrier segments. The face seal, made of Stellite 6B, is a pressure balanced design and utilizes an “E-seal” as a preload and secondary seal device. Stellite 6B was selected for the face seal material due to its high temperature properties and anti-galling performance against Inconel 718. The E-seals, also designed by Perkin-Elmer Fluid Sciences and made of Waspalloy, provide a closing force to the face seal on the carrier segments and prevent air from leaking between the face seal and cover plate. Each E-seal provides about 10-lbf/in preload to its corresponding face seal. The face seal was designed with a generous cross section, due to its large diameter, to provide stiffness for operation as well as manufacturing.

The actuator rod contains two pairs of expanding concentric ring seal sets on its bearing surface. Each pair is made of an outer Stellite 25 ring and an inner Inconel 625 ring. The seals were designed by Precision Rings, Inc. (Indianapolis, IN) for a 120-psi at 1500 °F.

ACC Actuator Development

Gen 1 Actuator: Custom hydraulic-servo actuator

Capabilities	Min Req.	Actual
Stroke	0.1-in	0.2-in
Accuracy	0.001-in	0.0006-in
Load	1800 lbf	3000 lbf
Rate	0.01-in/s	0.04-in/s

- Compact, Lightweight
- Failsafe (retracts, fails open – avoids blade rubs)
- P_{high}, P_{low}, position measurement

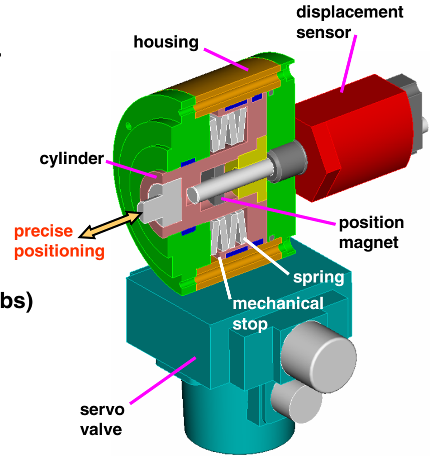

Gen 2 Actuator: Currently evaluating advanced designs using piezo, SMA, magneto-strictive and other technologies.

Can "Smart" actuators out perform "standard" technology ???

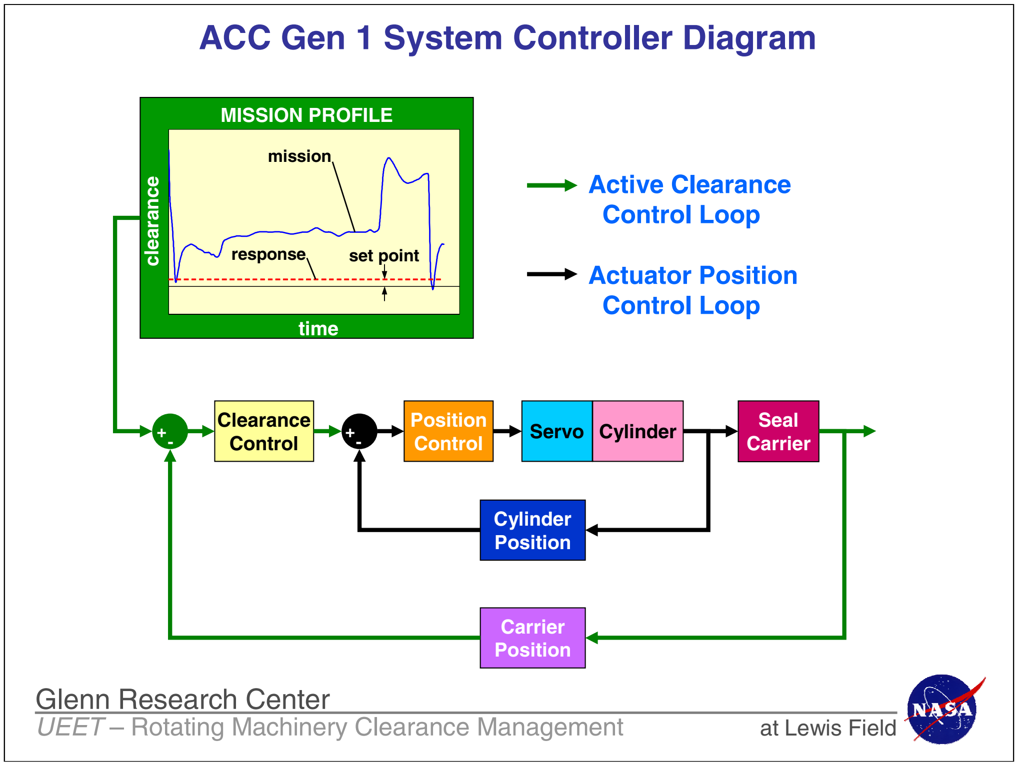

This slide shows a diagram of the control system strategy that will employed to operate and evaluate this first generation ACC system as well as future systems. Each of the nine independent hydraulic actuators will have its own feedback control allowing the positioning of each cylinder or actuator. An outer loop will be monitoring the position of the carrier segments. The outer loop will determine the minimum clearance off of which the desired clearance will be measured. The control system will be used to evaluate the accuracy and response of the ACC system to both steady state and transient clearance profiles.

Our next speaker, Mr. Kevin Melcher of the Controls and Instrumentation Branch at NASA GRC, will provide a more in depth discussion on his development of this control system and his work on defining control system requirements and architecture for advanced ACC systems.

Test Rig Fabrication Status

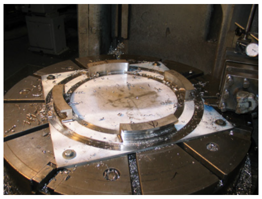

Carrier Segments

Radiant Heater Housing

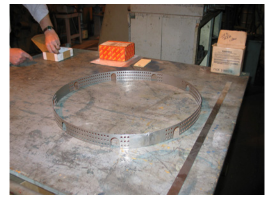

Flow Deflector

Chamber

Main Housing

Main Housing Lid

Glenn Research Center
UEET – Rotating Machinery Clearance Management
at Lewis Field

Here we can see some of the main components of the test rig as they are currently being fabricated. The components are about 75% complete. We expect assembly to occur at the end of the month, with rig check out occurring towards the end of December.

Future Work

- **The ACC system performance will be evaluated under a series of HPT simulated temperature and pressure conditions.**
  – Actuator stroke, rate, accuracy, repeatability
  – System concentricity, synchronicity
  – Component wear
  – Secondary seal leakage
  – Clearance sensor response and accuracy

- **The results of this testing will be used to further develop/refine the current actuator design as well as other actuator concepts.**
  – SMA’s, piezoelectric, magnetostrictive, other

- **Optimization of ACC system components for future flight hardware development.**
  – increased cycle life
  – reduced size and weight

APPENDIX

Glenn Research Center
UEET – Rotating Machinery Clearance Management
at Lewis Field

HPT Blade Tip Clearance Variation

- **Load Mechanisms**
  - Engine Loads (centrifugal, thermal, internal engine pressure, thrust)
  - Flight (inertial, aerodynamic, and gyroscopic)
- **Wear Mechanisms**
  - Rubs
  - Erosion

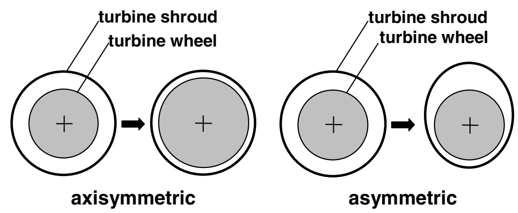

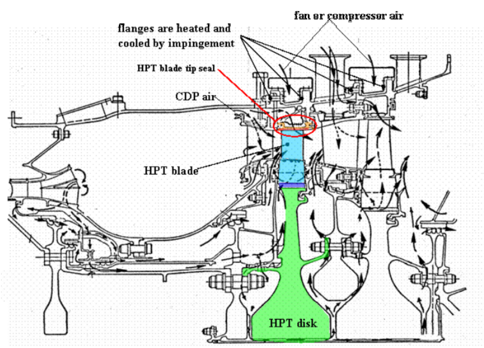

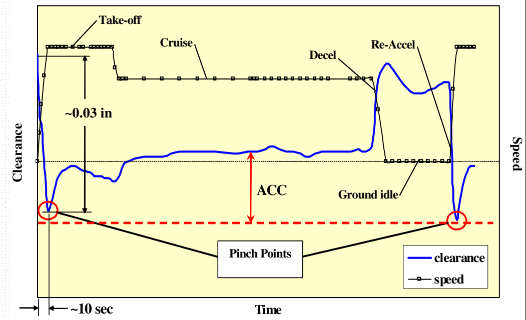

Motivation (Benefits of ACC for HPT)

- **Fuel Savings/ Reduced Emissions**
  - 0.010-in tip clearance is worth ~1% SFC
  - Less fuel burn, reduces emissions
- **Increased Cycle Life (Reduced Maintenance Costs)**
  - Deterioration of exhaust gas temperature (EGT) margin is the primary reason for aircraft engine removal from service.
  - 0.010-in tip clearance is worth ~10 ºC EGT.
  - Allows turbine to run at lower temperatures, increasing cycle life of hot section components and engine TOW (~1000 cycles).
- **Increased Efficiency/Operability**
  - Increased payload and mission range capabilities
- **HPT Reaps the Most Benefit Due to ACC**
  - Improved tip clearances in the HPT resulted in Life Cycle Cost reductions 4x > LPT and 2x > HPC. (Kawecki, 1979)

CONTROLS CONSIDERATIONS FOR TURBINE ACTIVE CLEARANCE CONTROL

Kevin J. Melcher
National Aeronautics and Space Administration
Glenn Research Center
Cleveland, Ohio

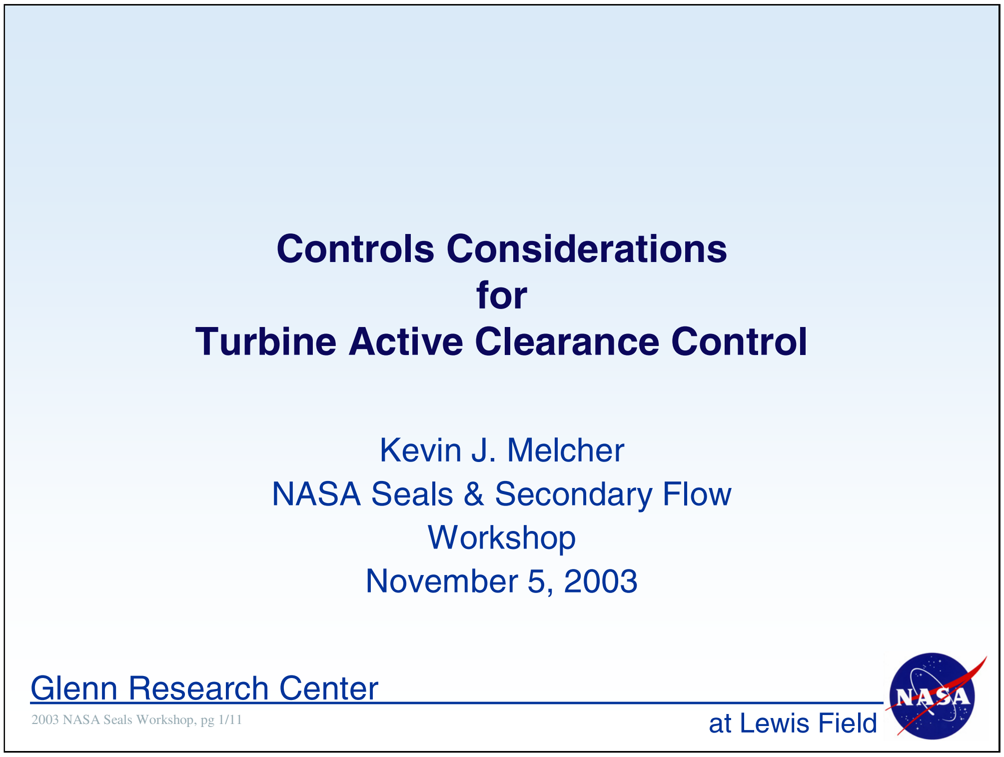

This presentation discusses active control of turbine tip clearance from a control systems perspective. It is a subset of charts that were presented at the 2003 meeting of the International Society of Air Breathing Engines which was held August 31 through September 5 in Cleveland, Ohio. The associated reference paper is cited at the end of the presentation. The presentation describes active tip clearance control research being conducted by NASA to improve turbine engine systems. The target application for this effort is commercial aircraft engines. However, it is believed that the technologies developed as part of this research will benefit a broad spectrum of current and future turbomachinery. The first part of the presentation discusses the concept of tip clearance, problems associated with it, and the benefits of controlling it. It lays out a framework for implementing tip clearance controls that enables the implementation to progress from purely analytical to hardware-in-the-loop to fully experimental. And it briefly discusses how the technologies developed will be married to the previously described ACC Test Rig for hardware-in-the-loop demonstrations. The final portion of the presentation, describes one of the key technologies in some detail by presenting equations and results for a functional dynamic model of the tip clearance phenomena. As shown, the model exhibits many of the clearance dynamics found in commercial gas turbine engines. However, initial attempts to validate the model identified limitations that are being addressed to make the model more realistic.

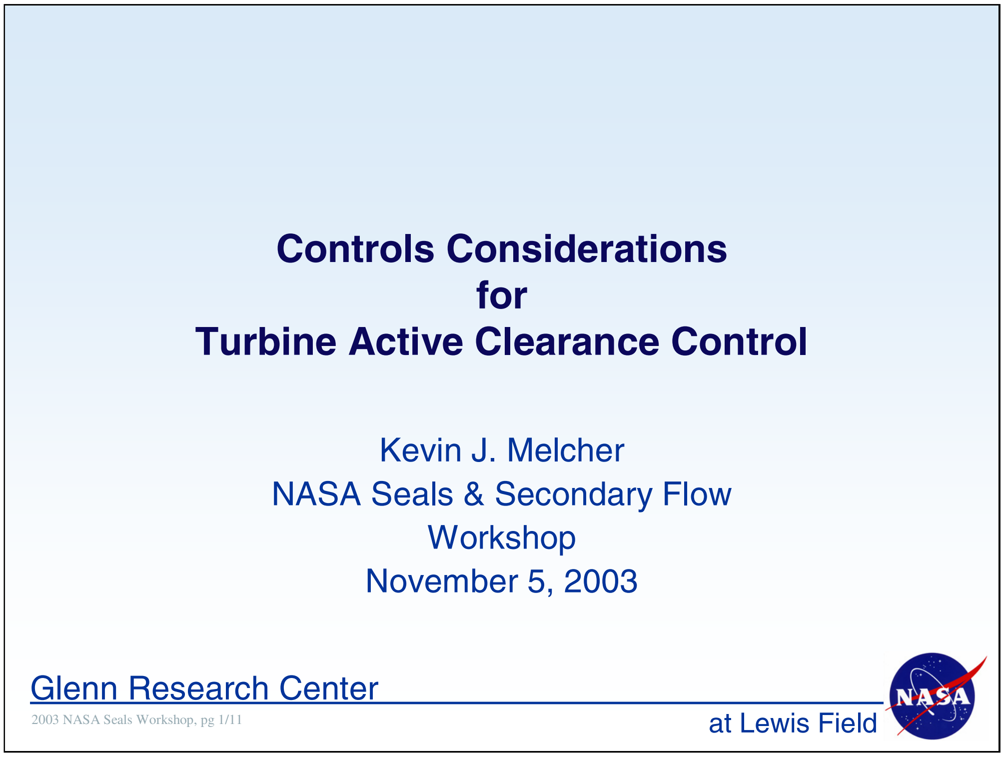

This presentation discusses active control of turbine tip clearance from a control systems perspective. It is a subset of charts that were presented at the 2003 meeting of the International Society of Air Breathing Engines which was held in Cleveland, Ohio. The associated reference paper is cited at the end of the presentation.

Kevin J. Melcher is a member of the Controls and Dynamics Technology Branch at NASA Glenn Research Center. He is currently the team lead for the development and implementation of controls software and hardware in support of a fast-acting turbine tip clearance control system. Other team members are: Mr. Jonathan DeCastro and Dr. Javier Kypuros. Mr. DeCasto works for QSS Group Inc. as a performance-based contractor to NASA Glenn Research Center. He is currently working on control law development and implementation for the project. Dr. Kypuros is an associate professor in the Department of Mechanical Engineering at the University of Texas-Pan American. He is working on developing first-principles-based models of the clearance dynamics.

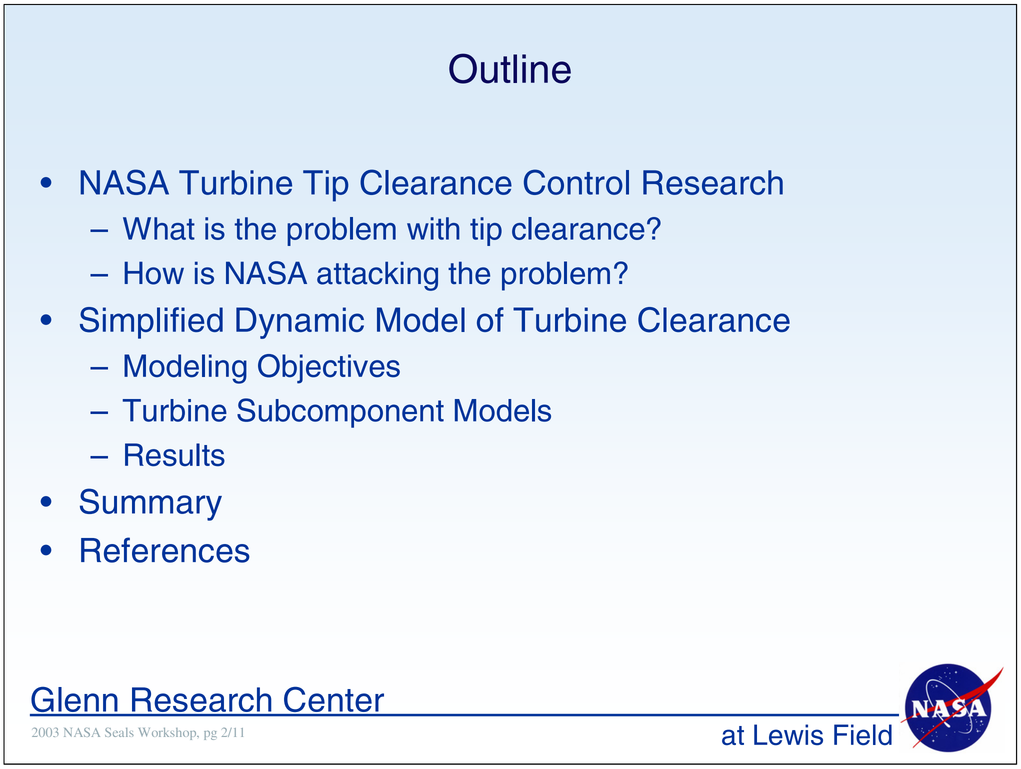

The presentation describes active tip clearance control research being conducted by NASA to improve turbine engine systems. The target application for this effort is commercial aircraft engines. However, it is believed that the technologies developed as part of this research will benefit a broad spectrum of current and future turbomachinery. The first part of the presentation discusses the concept of tip clearance, problems associated with it, and the benefits of controlling it. It lays out a framework for implementing tip clearance controls that enables the implementation to progress from purely analytical to hardware-in-the-loop to fully experimental. And it briefly discusses how the technologies developed will be married to the previously described ACC Test Rig for hardware-in-the-loop demonstrations. The final portion of the presentation, describes one of the key technologies in some detail by presenting equations and results for a functional dynamic model of the tip clearance phenomena. As shown, the model exhibits many of the clearance dynamics found in commercial gas turbine engines. However, initial attempts to validate the model identified limitations that are being addressed to make the model more realistic.

So, “What is the problem with tip clearance?”

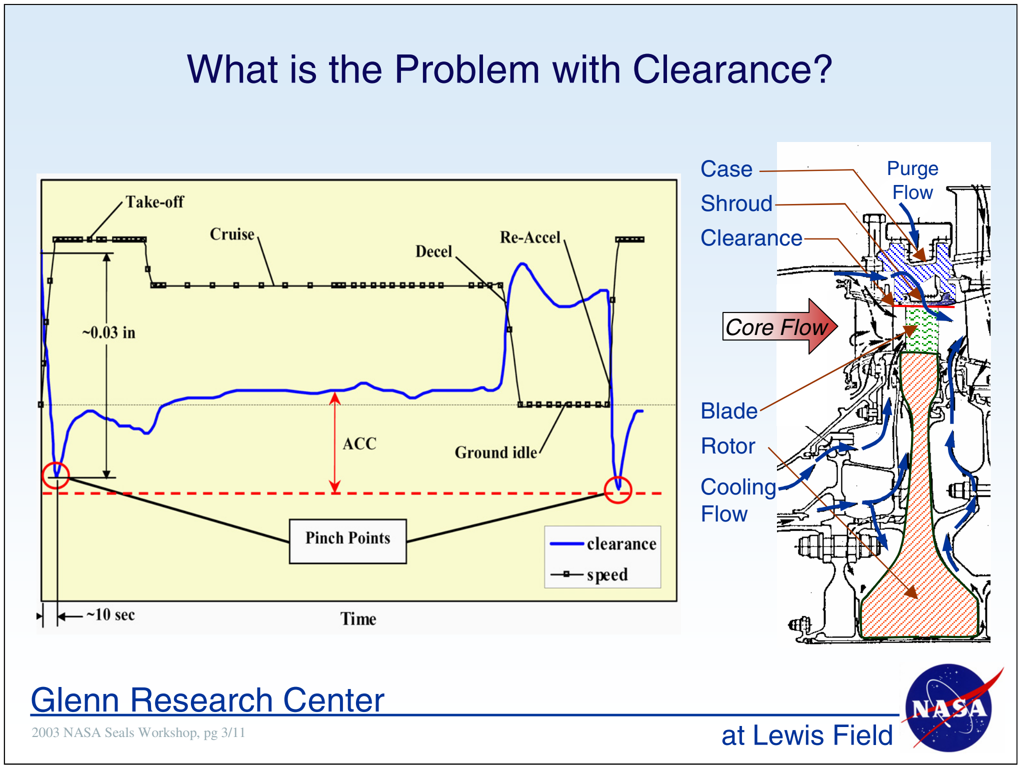

This slide illustrates changes in tip clearance during a notional mission. The clearance transient is the result of changing engine operating conditions and axisymmetric loads. The main operating regimes are takeoff, cruise, decel, and re-accel. The transient may be described as follows.

A cold engine is designed to have a large amount of turbine clearance. This clearance is rapidly diminished as engine speed is increased from ground idle to maximum power during takeoff. In fact, changes of over 30 mils are not uncommon during takeoff and reaccel events in large commercial engines. During this event, the rotor/blade assembly expands rapidly causing the rotating components to grow radially outward. The rotor grows primarily due to rotational forces, and the blade due to rapid heating. The case/shroud surrounding the rotating components also expands radially due to heating, but at a much slower rate due. The result is a minimum clearance condition known as a “pinch point”. The rotor and blade growth eventually reach steady conditions while the case/shroud continues to grow somewhat allowing the clearance to increase. As the engine approaches cruise conditions, the radial growth reaches thermal and mechanical equilibrium and the clearance remains relatively constant. However, throttle transients that can occur will also effect the clearance and must be accounted for when designing in the cold clearance in order to avoid rubbing the blades on the case. Of particular concern is the decl/re-accel transient that can generate pinch points with less clearance than takeoff.

Unfortunately, the additional clearance added to accommodate the pinch point results in excess clearance and reduced performance during what is typically the longest portion of the mission, cruise. In addition, EGT blooms tend to occur just after the pinch point. These blooms can use up EGT margin and cause the engine to be pulled for maintenance prematurely. The red-dashed line illustrates the objective of active clearance control – That is to maintain tight clearances throughout the flight decreasing fuel use and EGT bloom.

Active clearance control systems exist on some of the more advanced engine systems. However, state-of-the-art systems are based on a thermal approach that uses cooling air to manage the growth of the shroud, and hence the clearance. These systems tend to be slow due to the large thermal masses involved and so, cannot eliminate the pinch points. The systems do not use direct sensor measurements resulting in limited or no ability to handle unanticipated events during the flight. Our goal is to develop an advanced fast-acting clearance control system addresses the important concerns by using direct sensor feedback to maintain optimally minimal clearance throughout a given mission.

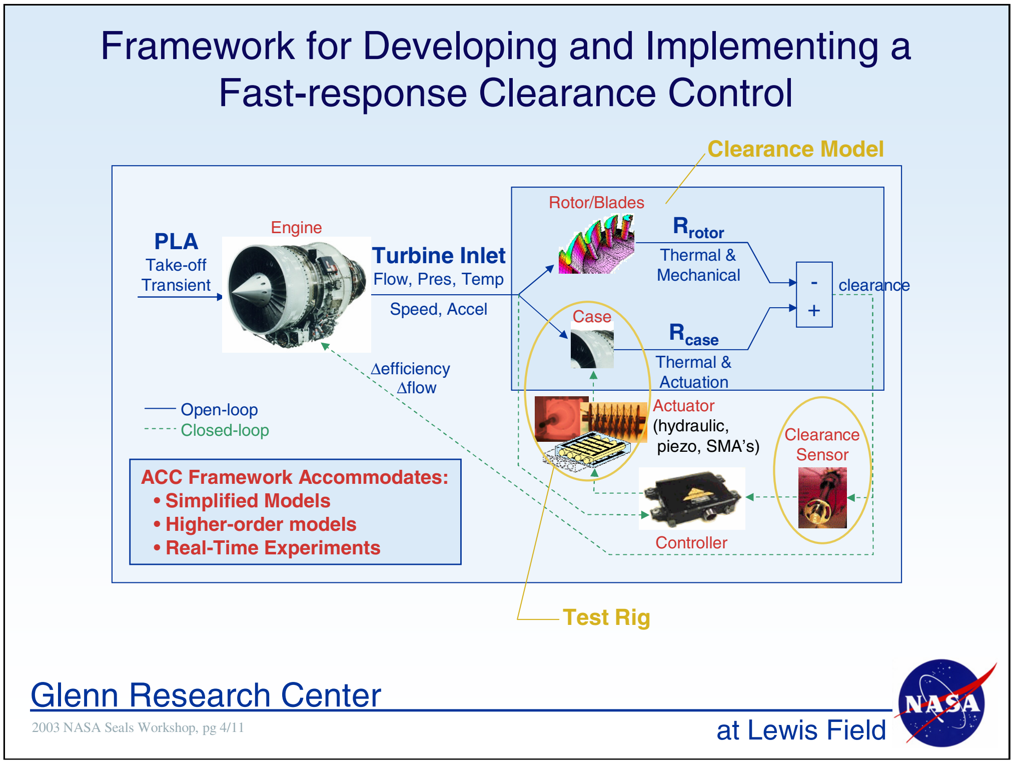

This slide shows the framework we have developed for implementing a fast-response clearance control system. In this frame work, the engine provides inputs to the turbine. The various parts of the turbine expand or contract in response to the changing engine conditions. A clearance sensor measures the changing gap between the case and the blades and provide that information to the controller which adjusts the actuator to maintain the desired clearance.

The intent of this framework is allow the individual elements to be represented by simplified models, higher-order models, and real-time experiments. And so, provide a path for moving the technology development from analytical simulation to hybrid analytical/experimental simulation to engine test. Elements of the framework are label in red. Critical technology gaps are highlighted in gold.

Bruce Steinetz from NASA Glenn's Mechanical Components Branch and Scott Lattime of QSS Group Inc. have developed a method for mechanically actuating the turbine shroud to control clearance. This is the ACC Test Rig identified in the previous presentation.

Clearance sensor technology is another technology gap. Current clearance sensors do not have the desired accuracy or reliability needed to meet strict turbine engine applications. Under the UEET Program, NASA is working with its industry partners to fill this gap.

Another critical technology gap is dynamic modeling of the clearance phenomenon. Dynamic models are critical elements in the design and development of advanced control systems. Existing models of the clearance phenomena are proprietary models that are not generally available and are not documented in the open literature. These range from high-fidelity finite element models to more simple empirical approximations.

The following slide shows how this framework will be used to tie the test rig, models, and real-time controller together for a hardware-in-the-loop demonstration of our ACC system.

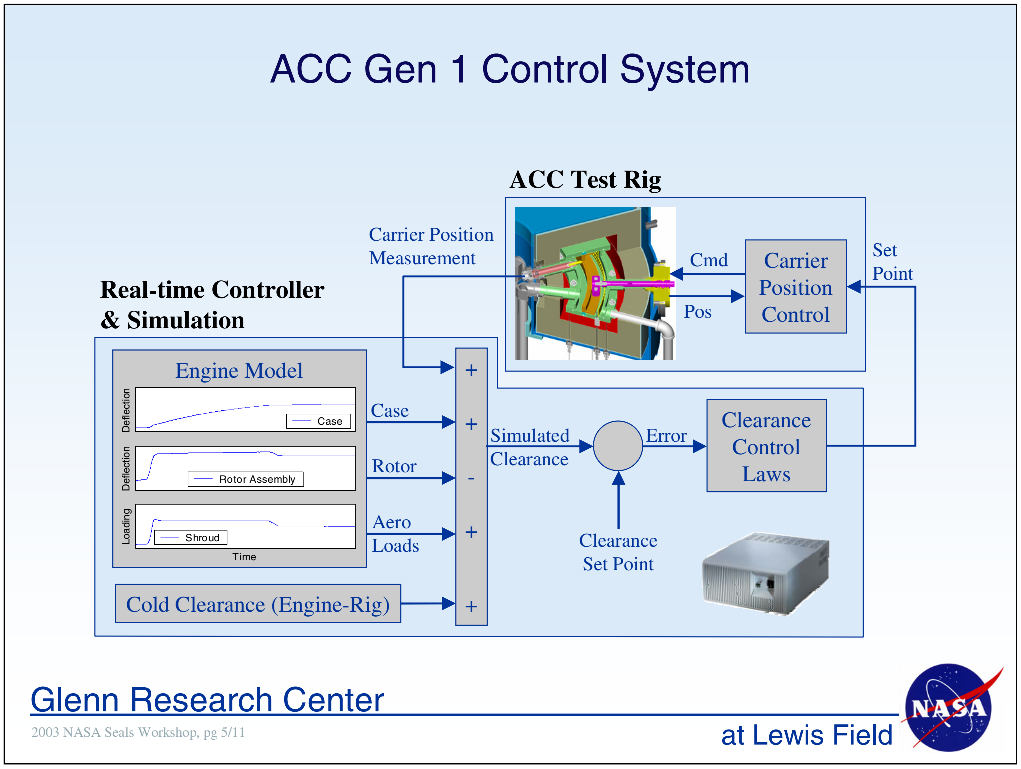

As envisioned in this slide, the research control system consists of two blocks – the real-time control and the test rig. The test rig includes the seal carrier, the clearance sensor, and the actuator with position control. The control block contains a dynamic model of pertinent time-varying engine parameters and the control laws.

For a given mission, the engine model calculates deflections for the case and rotor assembly due to thermal and mechanical loads. Thus simulating the rotational effects absent in the test rig. It also calculates the changing pressure loads that the actuator would be exposed to if it were in a real-engine. An ongoing trade study suggests that these loads have a larger effect on transient performance of the control system than the thermal or mechanical loads. They must be taken into account when designing the control laws. The cold build clearance of both the engine and the test rig must also be considered when computing the error between the clearance set point and the measured clearance. The control laws use the error to compute a new set point for the actuator.

The carrier position control adjusts the position of the seal carrier. The resulting change in gap is measured by the sensor, and fed back to the error closing the loop on clearance. The initial implementation will focus on controlling changes in axisymmetric clearance.

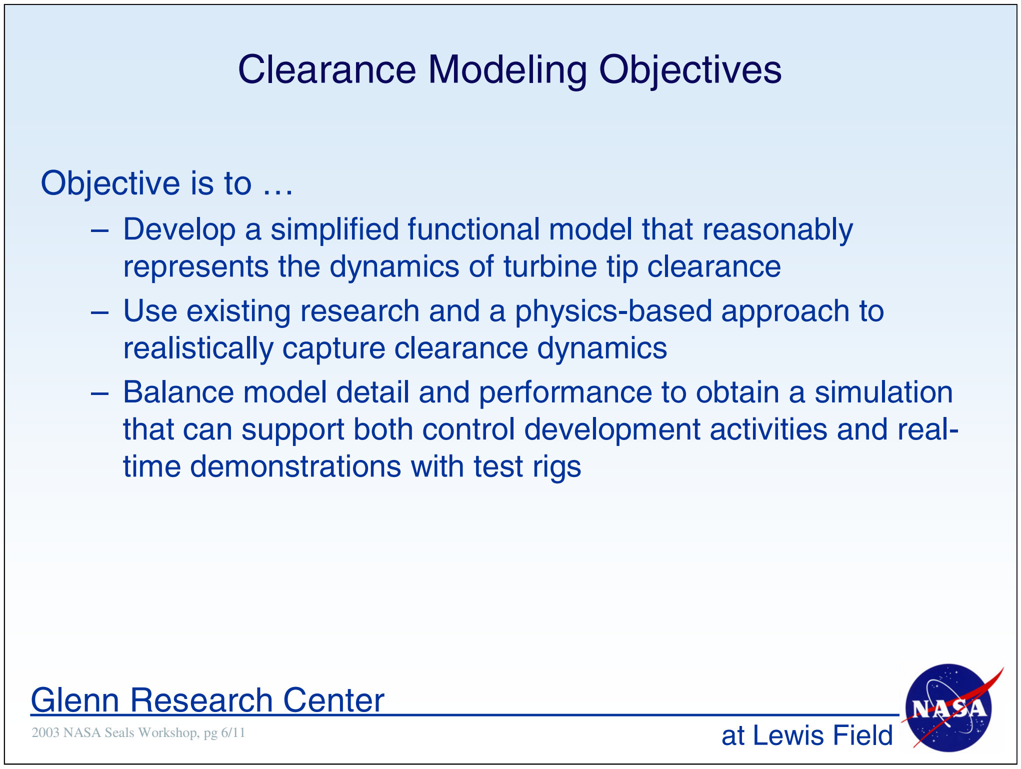

Objectives for the clearance modeling effort are shown on this slide. The primary goal is to create a model that reasonably reflects the steady state trends and dynamic response of turbine tip clearance to changes in engine operating condition. A model of this sort is all that is necessary to develop and demonstrate the control laws for proof-of-concept. In order to adequately model the system, a physics-based approach that captures the first-order effects is preferred. Modeling efforts will balance model detail with computational performance so that the model can be used to support both development of a realistic controller and real-time demonstration of the controller with the ACC test rig being developed at NASA Glenn.

The next slide will provide a brief overview of the approach used to develop the clearance model by examining the turbine rotor.

Simplified Dynamic Model – Turbine Rotor

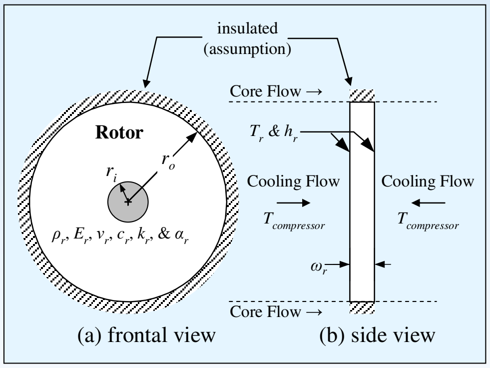

Simplifying Assumptions:
- Can be represented as disk of uniform thickness
- Primary heat transfer through the circular surface
- Temperature of rotor at air interface does not vary circumferentially or radially
- Thermal gradient across width is negligible – metal temperature is constant throughout

Radial Deflection due to Thermal Stresses:

$$u_{r1} = \alpha_r r_o (T_r - T_{ref})$$

Radial Deflection due to Rotation:

$$u_{r2} = \frac{\rho_r \omega^2 r_o}{4E}\left[(1-\nu_r) r_o^{\,2} + (3-\nu_r) r_i^{\,2}\right] = C_r \frac{\omega^2(t)}{E(T_r)}$$

Glenn Research Center

2003 NASA Seals Workshop, pg 7/11

at Lewis Field

In general, the rotor (or disk) has a complex shape that requires rather complex finite element analysis to define the thermal and mechanical deformations. To simplify the analysis for controls purposes, a number of assumptions and constraints are implemented. First, the rotor is treated as a disk of uniform thickness simplifying the calculation of the deformation due to mechanical and thermal stresses. Second, since the circumferential tip are of the disk is relatively small compared to the radial cross section, heat transfer is assumed to occur primarily across the radial cross section. Third, the circular surface is assumed to be at the same temperature, that is , the temperature does not vary circumferentially or radially. Finally, the thermal gradient across the width is assumed negligible, potentially ignoring the thermal inertia of this large mass.

The rotor is stressed radially by thermal stresses due to changing engine temperatures and by centrifugal forces that change with engine speed. In this simple representation, the radial deflection due to thermal stresses is a function of the coefficient of thermal expansion (α_r,), the difference between the bulk metal temperature (T_r) and a reference temperature (T_{ref}), and the rotor radius (r_o) at the specified reference temperature. The total radial deflection of the rotor is thus a sum of the deflections due to temperature and rotation.

The shroud (tip seal) and the blade are modeled with similar simplifying assumptions. Similar to the rotor, the blade deforms radially due to both rotational and thermal loads. However, deformation of the shroud is caused by variations in temperature and pressure. Models for the blade and shroud are described in reference 1 at the end of this presentation.

Simplified Dynamic Model – Clearance Calculation

$$\delta(t) = r_{shroud}(t) - r_{rotor}(t) - l_{blade}(t)$$
$$= (r_a + u_{s1} + u_{s2}) - (r_o + u_{r1} + u_{r2}) - (l_0 + u_{b1} + u_{b2})$$

$$= \delta_{cold} + \left[\Delta r_{shroud}(t) - \Delta r_{rotor}(t) - \Delta l_{blade}(t)\right]$$
$$= \left(r_a - r_o - l_0\right) + \left[\left(u_{s1} + u_{s2}\right) - \left(u_{r1} + u_{r2}\right) - \left(u_{b1} + u_{b2}\right)\right]$$

$$Note: u = u(t)$$

Glenn Research Center

2003 NASA Seals Workshop, pg 8/11

at Lewis Field

This slide shows simple algebraic equations used to obtain clearance from the computed deformation of the turbine subcomponents. In the first form, the radius of the rotor assembly (rotor radius + blade length) is subtracted from the radius of the shroud. In the second form, the deflection of the turbine subcomponents are summed to obtain the change in clearance relative to the constant cold-build clearance. This is summed with the cold-build clearance to obtain the clearance as a function of time.

The following slide shows results from a Matlab/Simulink implementation of the model just described.

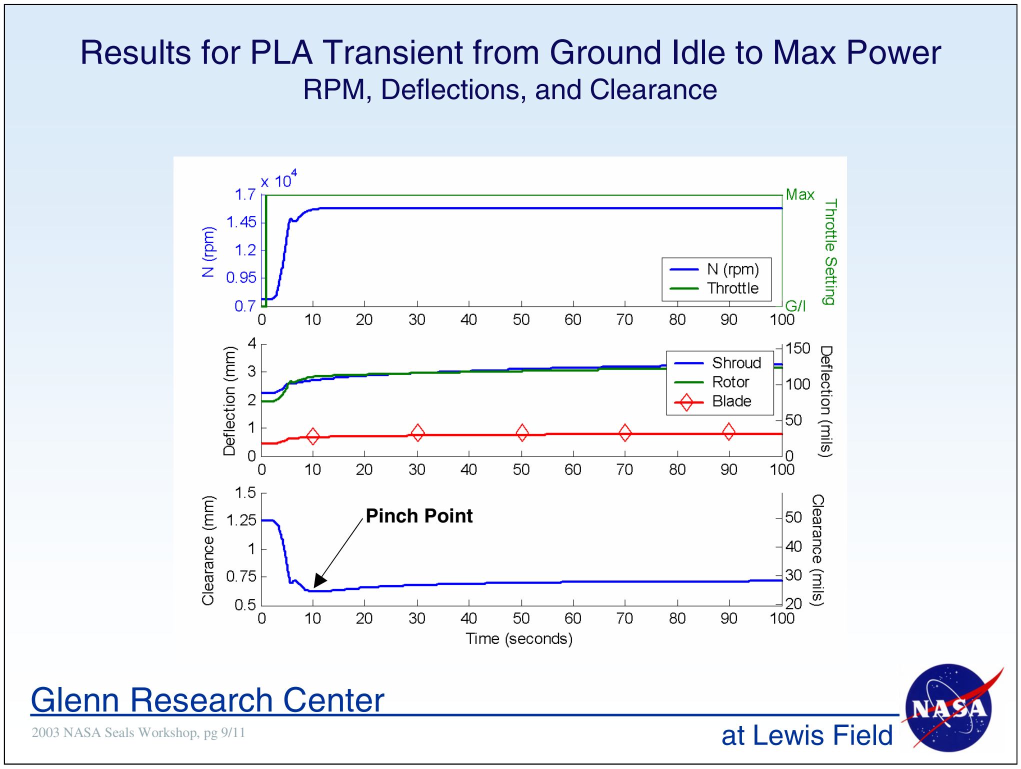

Shown here are preliminary results from the clearance model for a transient where the engine power command was stepped from ground idle conditions to maximum power. To generate the results, a dynamic model of a “fighter-like” aircraft engine was used to generate temperatures, pressures, and rotor speed as a function of time. The time-dependent engine operating conditions were used as input to the clearance model described in previous charts. Some of the expected trends are evident in these results.

The upper plot shows the step in power lever angle and the associated change in engine turbine speed. In addition to these inputs, compressor exit pressure & temperature, and turbine inlet pressure & temperature were used to define changes in engine operating condition during the transient.

The middle plot shows the simulated response of the shroud, rotor, and blades to the changing engine operating conditions. The blades elongate rather quickly due, primarily, to the large thermal transients. The rotor initially expands quickly in the radial direction as the rotational loads dominate the response. At about 5 seconds, the growth slows as the rotational loads reach steady state and the thermal stresses dominate the rate of deformation. The shroud response is initially dictated by the pressure loads which peak at about 5 seconds. After that, the large thermal inertia of the shroud provides continued sustained growth due to thermal stresses. The changing growth rates of the shroud and rotor+blades produces the pinch point shown on the lower plot.

Ongoing efforts are focused on validating and improving the model. The following slide highlights some of the work that still needs to be done by comparing the NASA/UTPA model with a validated empirical model.

Comparison of Clearance Model (ACC) with Validated Simulation of Commercial Engine (CES)

- Deflection of Turbine Subcomponents -

ACC calculates metal temperatures | ACC uses CES metal temperatures

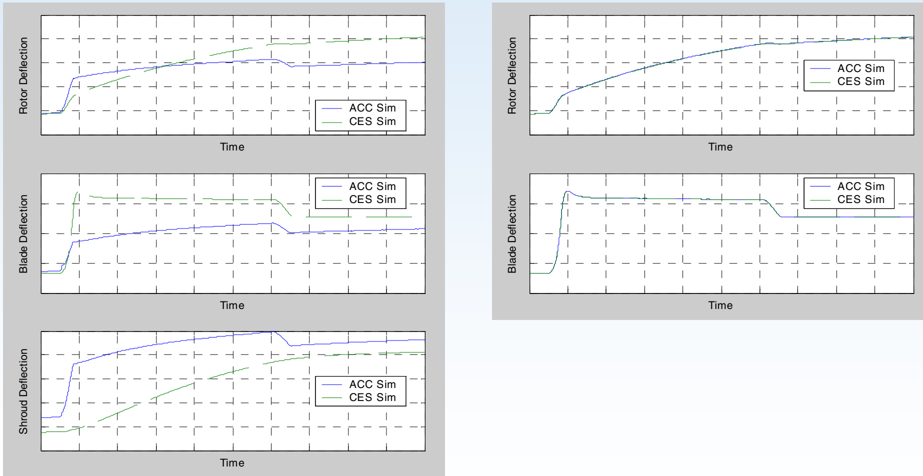

Glenn Research Center

2003 NASA Seals Workshop, pg 10/11

at Lewis Field

Here, output from the NASA/UTPA clearance model (ACC Sim) is compared with that from the simulation of a large commercial engine (CES). Comparisons are made for two different cases. The results on the left show the radial deflection of the turbine subcomponents as a function of time for both the CES and ACC simulations. For this case, bulk metal temperatures for the ACC Sim were computed by heat transfer equations derived for the model. Results on the right are for the case where bulk metal temperatures computed by the CES Sim were used by the ACC Sim to compute thermal deformations. The fact that plots on the left are mismatched and those on the right are not points to un-modeled temperature dynamics in the ACC Sim as the source of the mismatch. In fact, due to the simplifying assumptions used in the ACC Sim, the thermal inertia of the individual subcomponents are un-modeled. The result is that deflections computed by the ACC simulation are faster than those for the baseline CES simulation. Also un-modeled is the heat transfer to/from the cooling flow that occurs between the compressor and the turbine. This is likely the cause of the steady-state errors. Ongoing efforts by NASA and the University of Texas Pan American are focused on resolving these issues to improve the simulation.

Summary

- Fast-response active clearance control identified as a critical technology for improving performance and increasing engine on-wing life.
- Identified gap technologies required to support active clearance control
  – clearance modeling, actuation, and sensing
- Defined framework for developing, implementing, and maturing critical ACC technologies
- Working toward integrating critical ACC technologies in test rig for proof-of-concept demonstration
- Developed functional model of a clearance dynamics that:
  – Captures many of the essential dynamics – good start
  – Has simplified form that meets requirements for real-time implementation
  – With modifications (identified) can provide realistic model for control design and implementation

Glenn Research Center

2003 NASA Seals Workshop, pg 11/11

at Lewis Field

References

1. Melcher, Kevin J.; and Kypuros, Javier A.: "Toward A Fast-response Active Turbine Tip Clearance Control", ISABE2003-1102, 16th International Symposium on Air-breathing Engines, August 31-September 1, 2003.
2. Kypuros, Javier A.; and Melcher, Kevin J.: "A Reduced Model for Prediction of Thermal and Rotational Effects on Turbine Tip Clearance", NASA TM-2003-212226, March 2003.

NON-CONTACTING FINGER SEAL DEVELOPMENTS AND DESIGN CONSIDERATIONS

M. Jack Braun, Hazel M. Pierson, Dingeng Deng, and Fred K. Choy
University of Akron
Akron, Ohio

Margaret P. Proctor
National Aeronautics and Space Administration
Glenn Research Center
Cleveland, Ohio

GEOMETRY

ATIGAT

a)

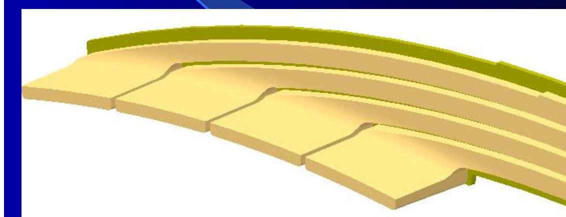

b)

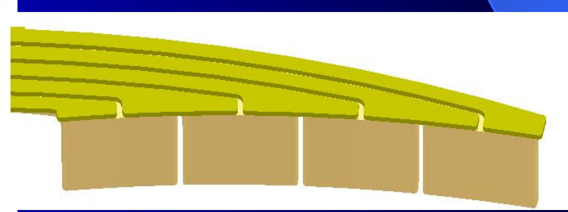

c)

GEOMETRY (cont'd)

ATIGAT

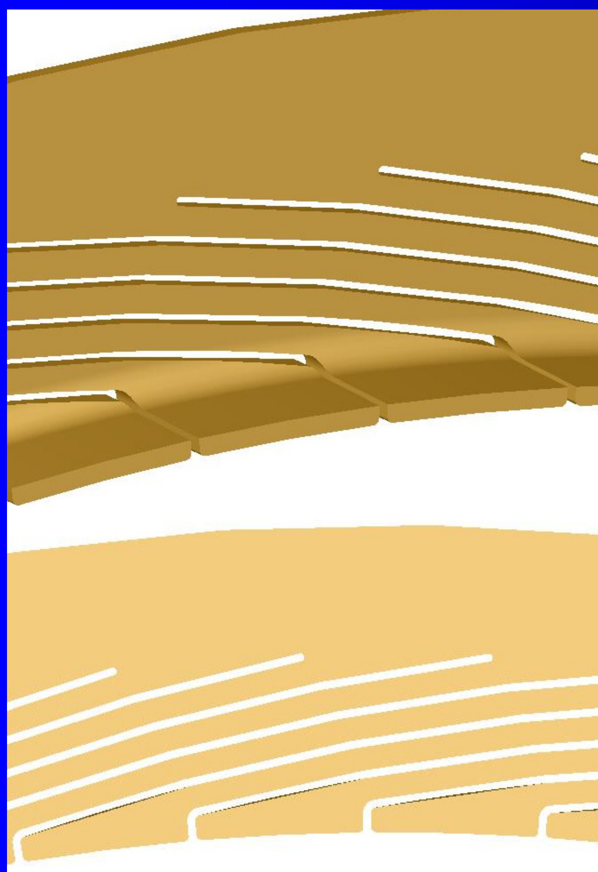

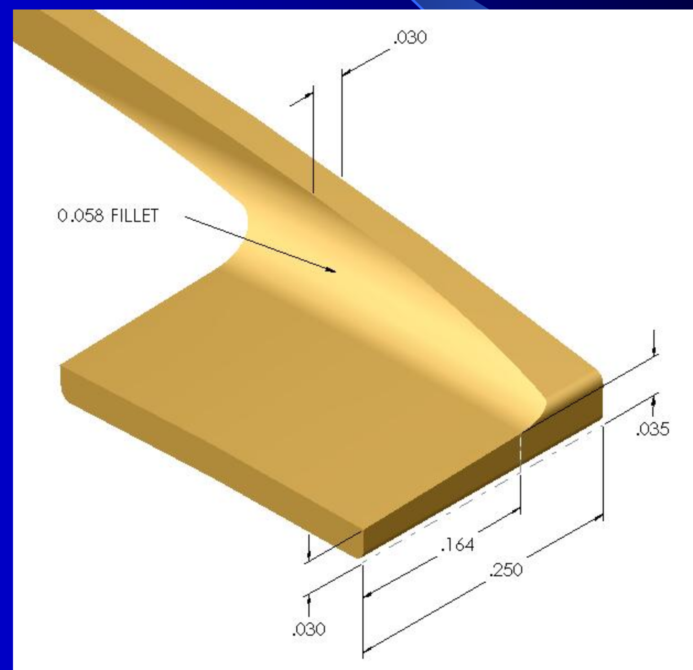

c)

UNDERSTANDING BOUNDARY CONDITIONS

ATIGAT

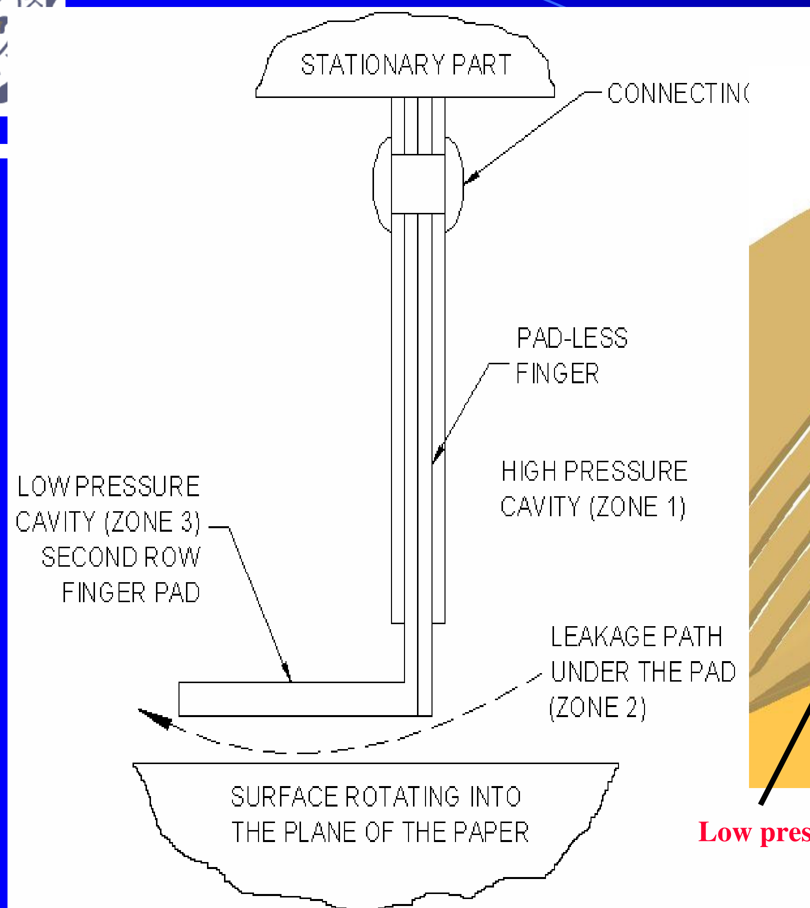

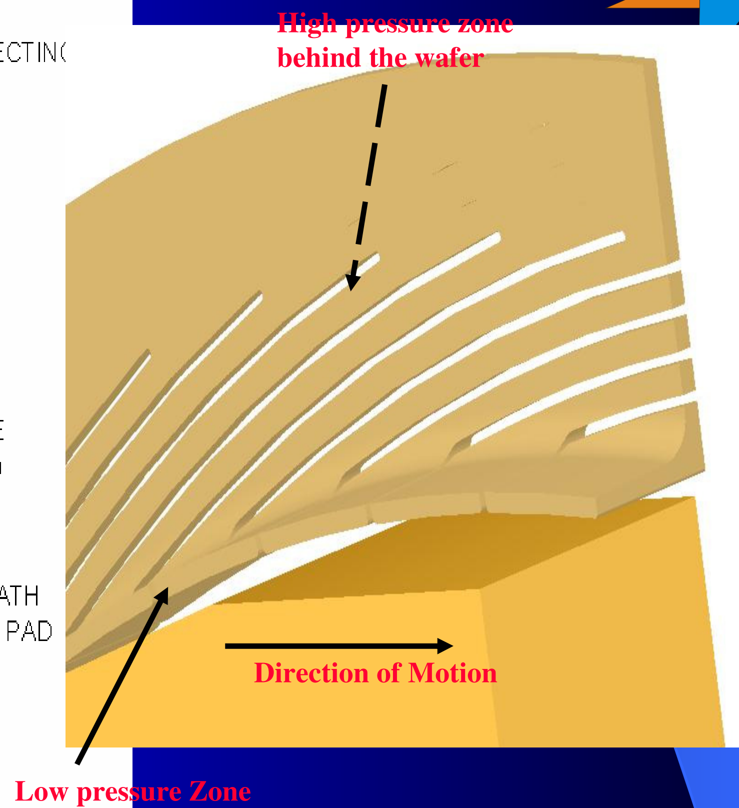

Boundary conditions for the Finger Seal.

Schematic Cross Section with Two Rows of Padded Low- and Pad-less High Pressure Fingers and definition of the pressure zones

Solid model showing the high and low pressure zones

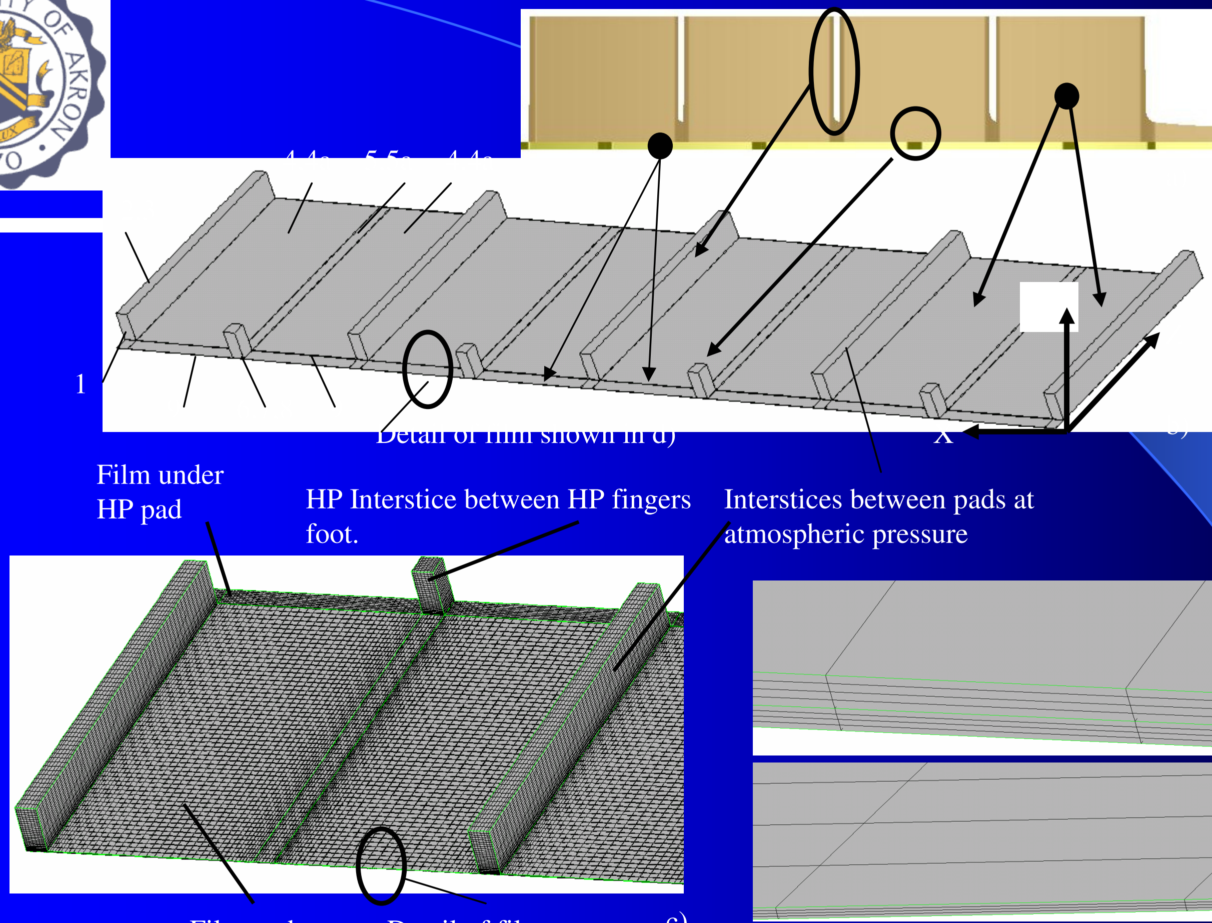

Grid Details for the Pressure, Flow and Temperature Calculations.
a) Solid representation of the two rows of fingers viewed from below
b) Corresponding representation of the fluid film contained between the rotor and the assembly of fingers.
c) Detail of the cell structure in the fluid film below and in-between HP and LP pads.
d) Fluid film grid structure under the HP finger
e) Fluid film grid structure under the LP finger

BLOCK GRIDDING DETAILS AND BOUNDARY CONDITIONS

ATIGAT

Label No.	Number of cells	Remarks	Boundary condition type
1	324	Single block of film between the rotor and the HP finger pad-less foot	Solid wall, top; Rotating wall, bottom
2, 3	17523	Top block of the film, in-between the LP pads	Solid walls, top Interface, bottom
	2124	Bottom block of the film, in-between the LP pads, directly above the rotor; 2 and 3 are contiguous	Outlet, side, LP; Interface, top Rotating wall, bottom
4,4a	9204	Top block of the film, directly under the LP pad	Solid wall, top Interface, bottom
	9204	Bottom block of the film, directly above the rotor; 4 and 4a are contiguous	Interface, top; Rotating wall, bottom
5,5a	2124	Top block of the film, in-between the LP pads	Solid wall, top Interface, bottom
	2124	Bottom block of the film, in-between the LP pads, directly above the rotor, 5a is contiguous with 5	Interface, top Rotating wall, bottom
6,7,8	2349	Top block of the film, in-between the HP fingers' feet	Solid wall, top Interface, bottom
	324	Middle block of the film, in-between the HP fingers' feet	Interface, top Interface, bottom
	324	Bottom block of the film, in-between the HP fingers' feet, directly above the rotor 6,7 and 8 are contiguous between themselves	Interface, top Rotating wall, bottom
9	1404	Single block of film between the rotor and the HP finger pad-less foot	Solid wall top, Rotating wall bottom

BLOCK GRIDDING DETAILS AND BOUNDARY CONDITIONS

Label No.	Number of cells	Remarks	Boundary condition type
1	324	Single block of film between the rotor and the HP finger pad-less foot	Solid wall, top; Rotating wall, bottom
2, 3	17523	Top block of the film, in-between the LP pads	Solid walls, top Interface, bottom
	2124	Bottom block of the film, in-between the LP pads, directly above the rotor; 2 and 3 are contiguous	Outlet, side, LP; Interface, top Rotating wall, bottom
4,4a	9204	Top block of the film, directly under the LP pad	Solid wall, top Interface, bottom
	9204	Bottom block of the film, directly above the rotor; 4 and 4a are contiguous	Interface, top; Rotating wall, bottom
5,5a	2124	Top block of the film, in-between the LP pads	Solid wall, top Interface, bottom
	2124	Bottom block of the film, in-between the LP pads, directly above the rotor, 5a is contiguous with 5	Interface, top Rotating wall, bottom
6,7,8	2349	Top block of the film, in-between the HP fingers' feet	Solid wall, top Interface, bottom
	324	Middle block of the film, in-between the HP fingers' feet	Interface, top Interface, bottom
	324	Bottom block of the film, in-between the HP fingers' feet, directly above the rotor 6,7 and 8 are contiguous between themselves	Interface, top Rotating wall, bottom
9	1404	Single block of film between the rotor and the HP finger pad-less foot	Solid wall top, Rotating wall bottom

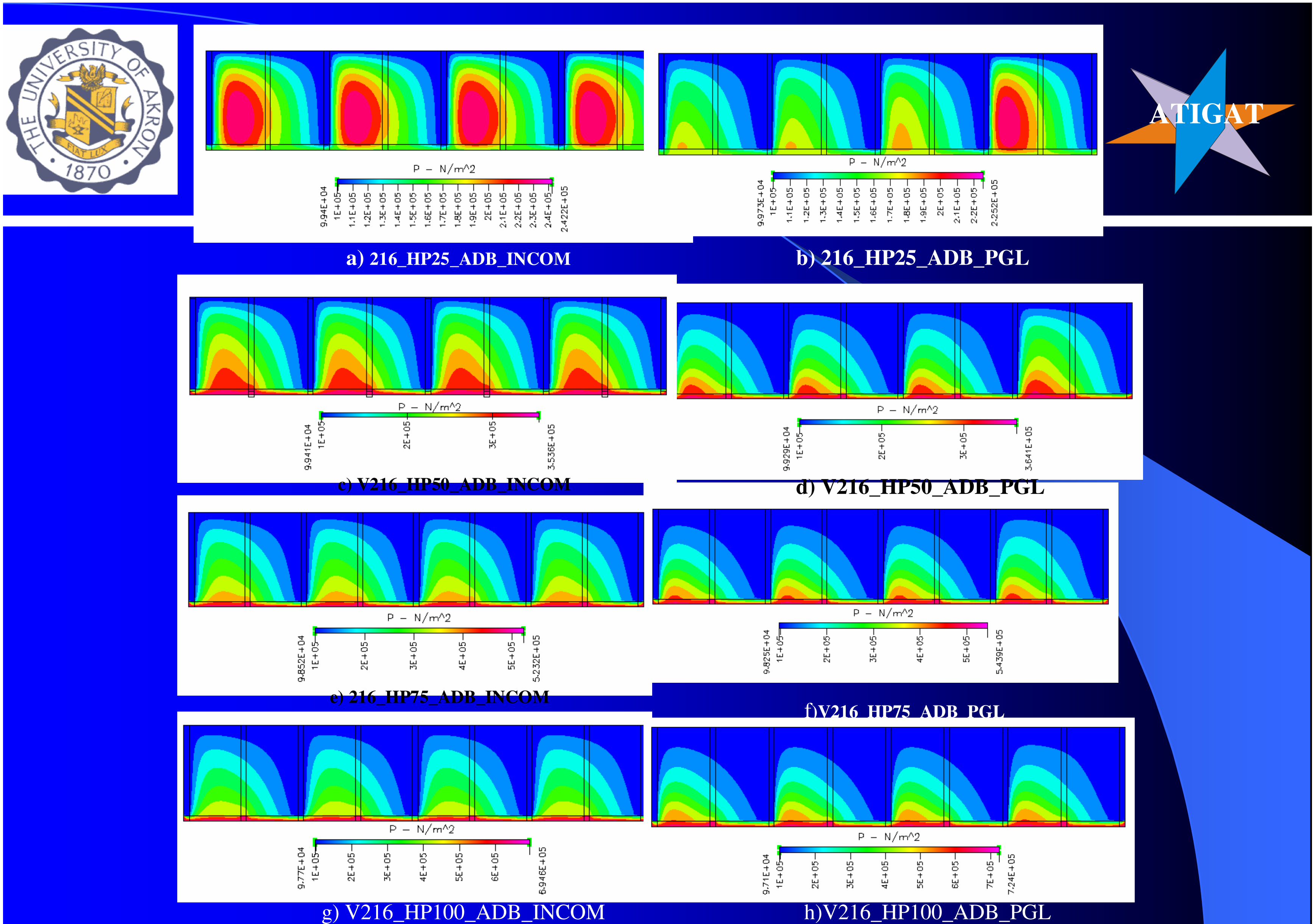

Figure 10. Flow Patterns Under The Finger Seal For Adiabatic Incompressible And Adiabatic Compressible Regimes

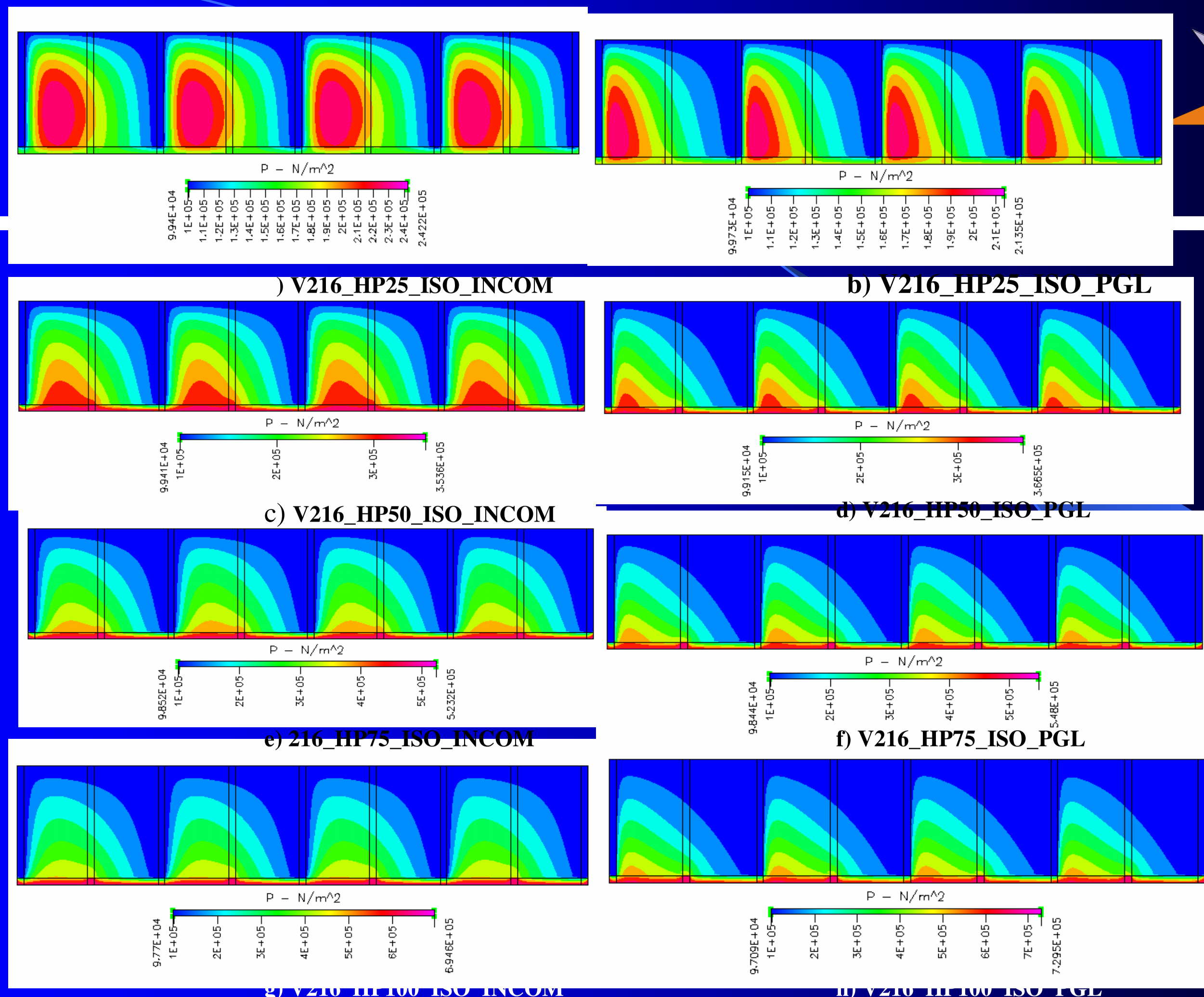

Flow Patterns Under The Finger Seal For Isothermal Incompressible And Isothermal Compressible Regimes

a), c), e),g) Isothermal, incompressible cases; V=216 m/s; HP side (25, 50, 75, 100 psi;

b), d), f), h) Isothermal, compressible, perfect gas law; V=216 m/s; HP side (25, 50, 75, 100 psi

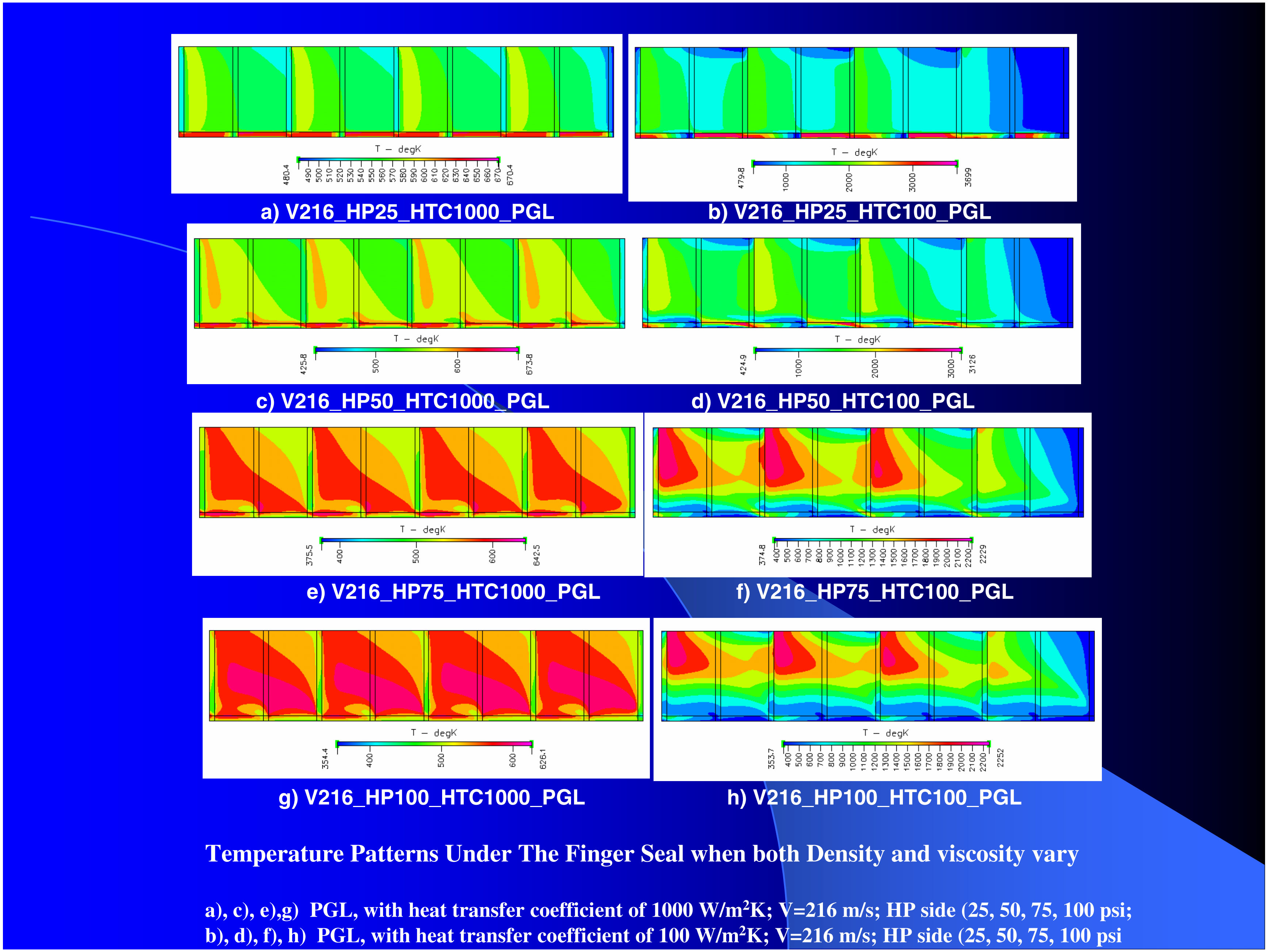
a) V216_HP25_HTC1000_PGL
b) V216_HP25_HTC100_PGL
c) V216_HP50_HTC1000_PGL
d) V216_HP50_HTC100_PGL
e) V216_HP75_HTC1000_PGL
f) V216_HP75_HTC100_PGL
g) V216_HP100_HTC1000_PGL
h) V216_HP100_HTC100_PGL
T – degK
Temperature Patterns Under The Finger Seal when both Density and viscosity vary
a), c), e),g) PGL, with heat transfer coefficient of 1000 W/m²K; V=216 m/s; HP side (25, 50, 75, 100 psi;
b), d), f), h) PGL, with heat transfer coefficient of 100 W/m²K; V=216 m/s; HP side (25, 50, 75, 100 psi

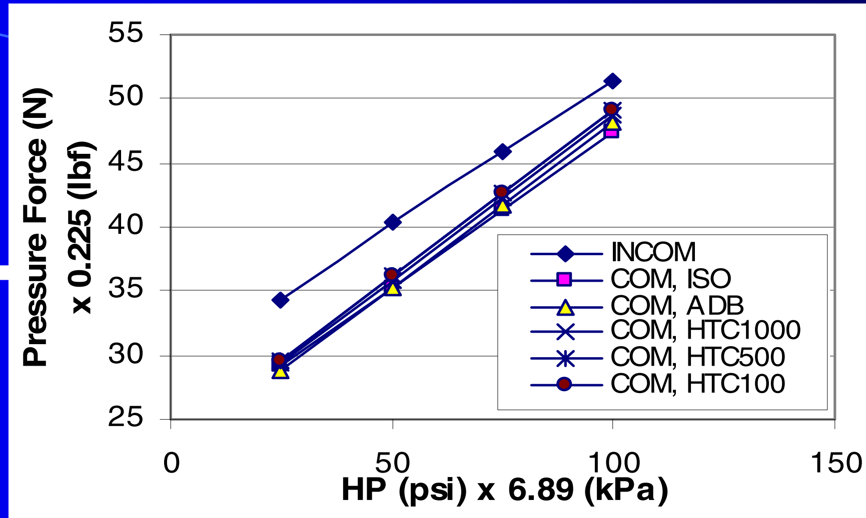

(a)

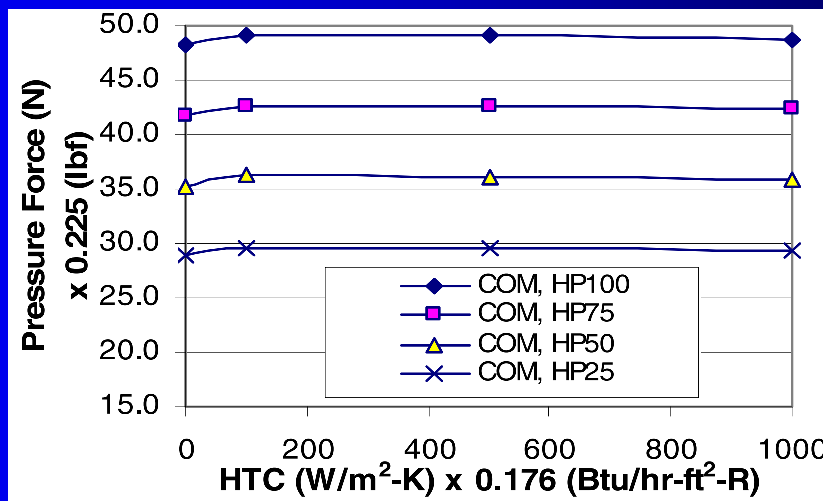

(b)

A Parametric Study of Lifting forces Generated under the 4 HP-4LP pads assembly.

a) **Force variation versus variation of HP side pressure**

b) **b) Force variation versus the heat transfer coefficient when the HP side is varied parametrically**

ATIGAT

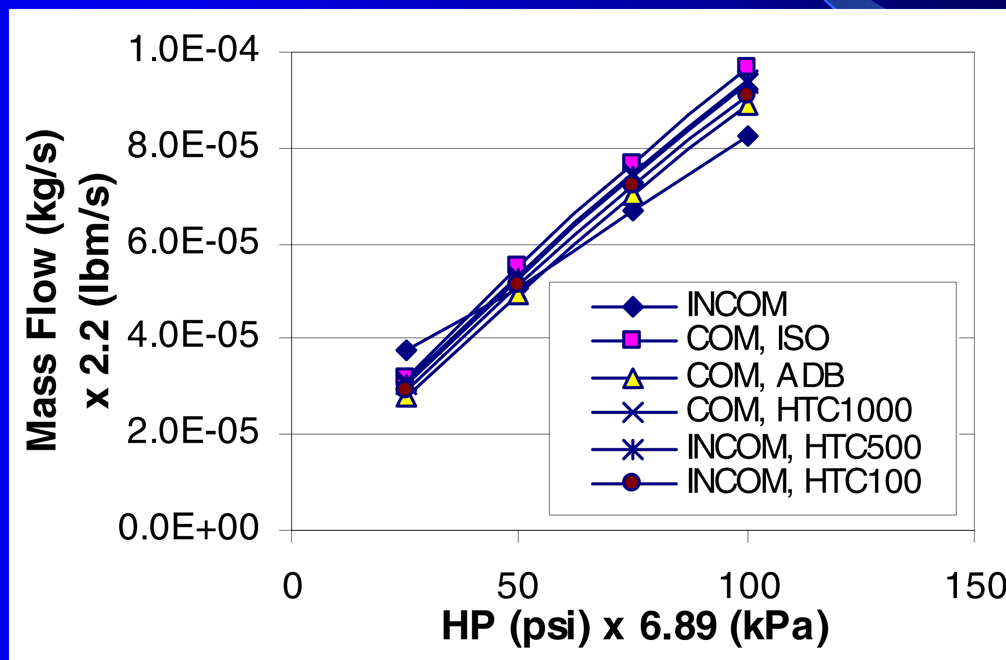

Mass Flow as a Function of the HP side Pressure

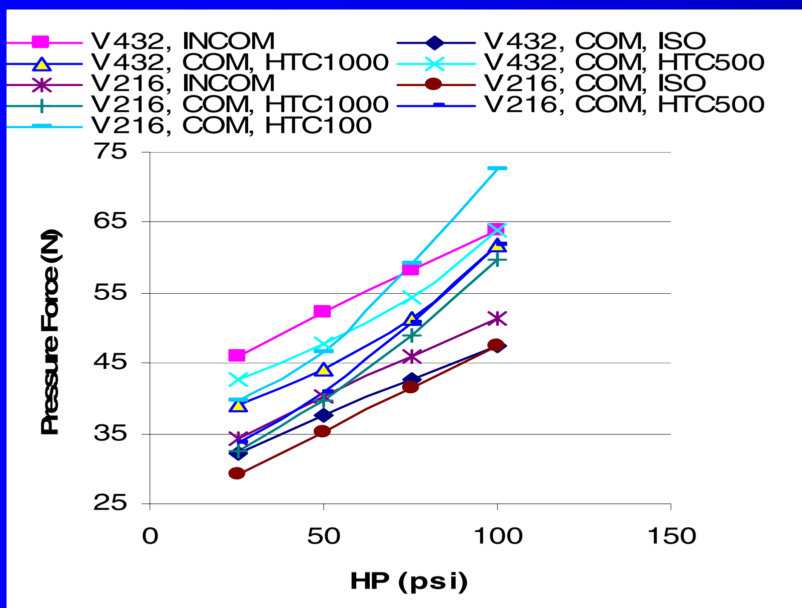

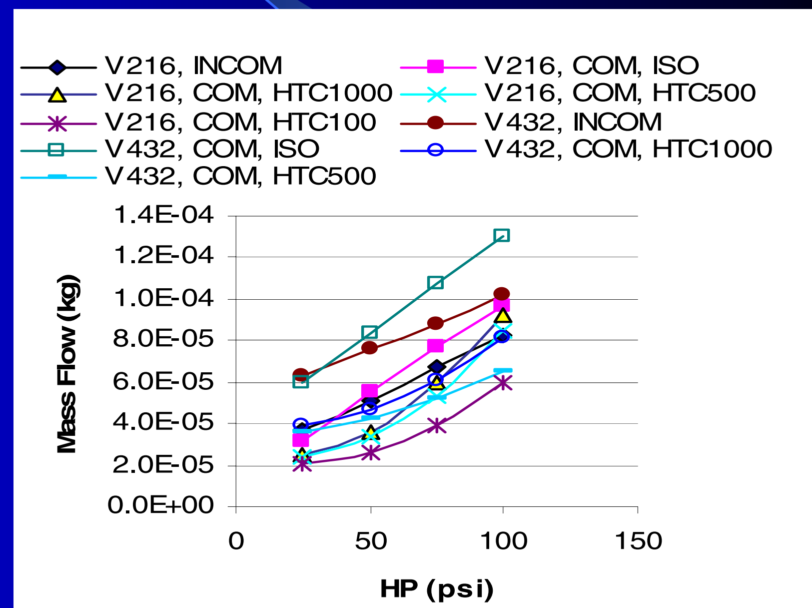

A Parametric Study of Lifting Forces and Mass Flows as a Function of the HP side and Thermal Boundary Conditions when Viscosity is allowed to vary

PARTIAL CONCLUSIONS

ATIGAT

It was found that:

- the interplay between the rotation induced pressure generation and the axial pressure drops controlled by the HP side, is dominated by rotation at low HP side pressure, but it is then taken over by the axial pressure drop when the latter becomes larger then 173kPa at 216mps.
- the effect of allowing the dynamic viscosity to vary with temperature is to introduce strong non-linearities both in the behavior of the leakage flow and the load carrying capability.

PARTIAL CONCLUSIONS

ATIGAT

- the numerical experiments showed that the FS behaves more like a bearing at low axial ΔPs and like a seal at high ones
- that the increase in the rotational velocity causes increased LCC, but
- the increase in the heat transfer coefficient causes more leakage and diminishes the load carrying capability.
- that the temperature maps showed that the high temperature regions shift from under the HP fingers at low ΔPs and towards the outer regions of the LP finger pad when the axial ΔPs increase

ATIGAT

DYNAMIC SIMULATION CONCEPTS AND RESULTS

FINGER SEAL EQUIVALENT MODEL FOR DYNAMIC SIMULATION

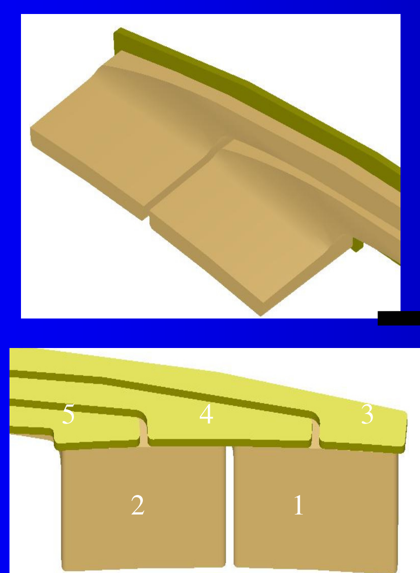

a)

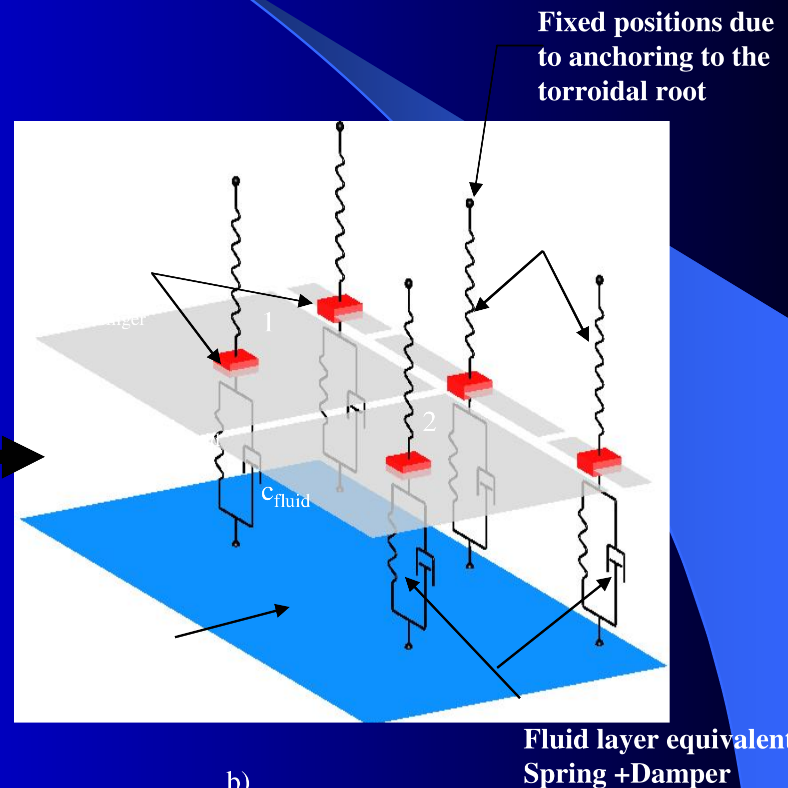

b)

Solid model and Equivalent Spring-Mass-Spring/Damper representation for use in the equation of motion simulation

ONE DEGREE OF FREEDOM MODEL

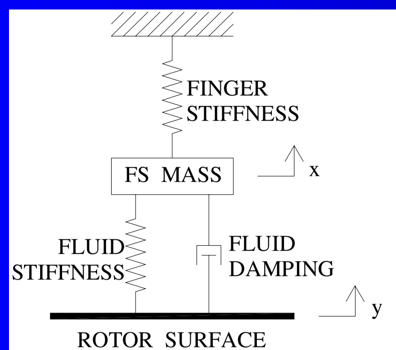

a)

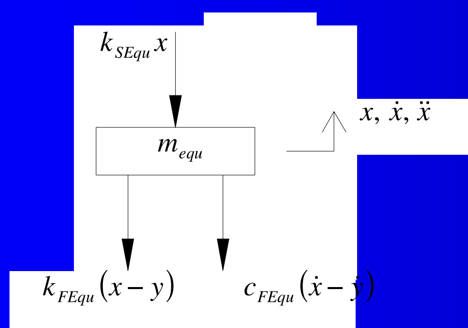

b)

Equivalent Damping and Stiffness Characteristics of the Model Shown in Figure 10

a) Equivalent Spring Dash-pot model

b) Free Body diagram for Derivation of the Equation of Motion

STIFFNESS AND DAMPING COEFFICIENTS

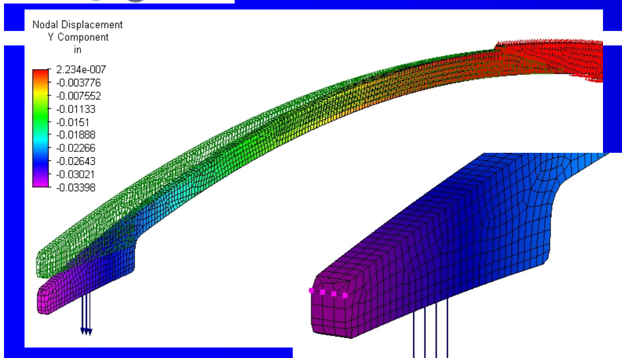

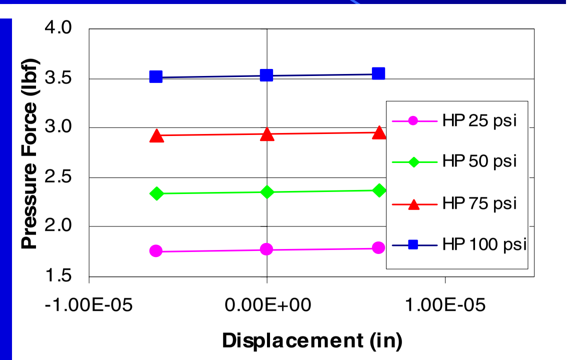

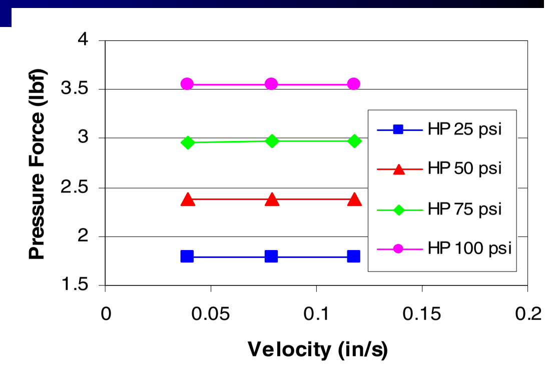

Determination of the fluid stiffness and damping coefficients using CFD-ACE+ modeling

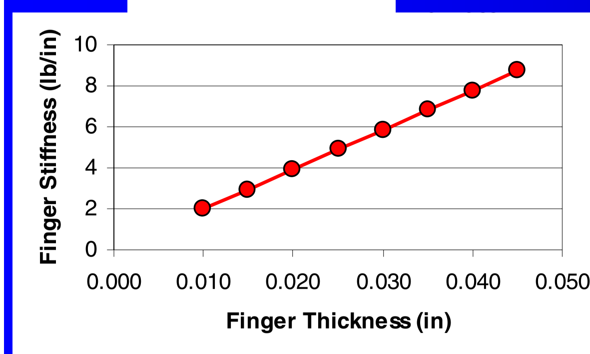

c)

Parametric Determination of the HP Finger Stiffness when Loaded Under With .011lbf
Finger loading points and subsequent displacement
Nodal displacement points for a 0.030" thick finger
Finger displacement versus changes in the cross section finger thickness (axial)

EQUIVALENT STIFFNESS, DAMPING AND FINGERS MASS; THE GOVERNING EQUATION

$$k_{SEqu} = k_{S1} + k_{S2} + k_{S3} + k_{S4} + k_{S5} = 2k_{S1} + 3k_{S3}$$

Solid fingers equivalent stiffness

$$k_{FEqu} = k_{F1} + k_{F2} + k_{F3} + k_{F4} + k_{F5} = 2k_{F1} + k_{F4} + 2k_{F3}$$

Fluid film equivalent stiffness

$$c_{FEqu} = c_{F1} + c_{F2} + c_{F3} + c_{F4} + c_{F5} = 2c_{F1} + c_{F4} + 2c_{F3}$$

Fluid film equivalent damping

$$m_{Equ} = m_{LP1} + m_{LP2} + m_{HP3} + m_{HP4} + m_{HP5} = 2m_{LP1} + 2m_{HP4}$$

Fingers equivalent mass

$$m_{Equ}\ddot{x} + c_{FEqu}\dot{x} + (k_{FEqu} + k_{SEqu})x = c_{FEqu}\dot{y} + k_{FEqu}y$$

Governing Equation

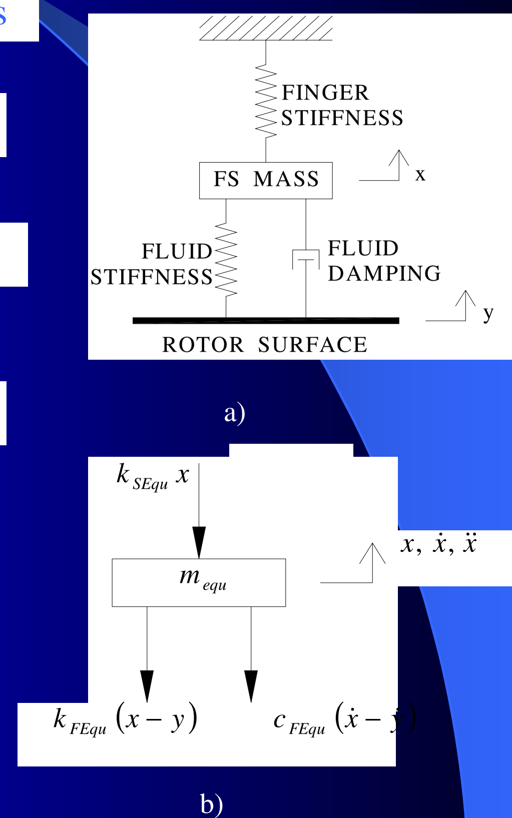

TRANSMISSIBILITY AND PHASE SHIFT

If one applies now a harmonic motion to the rotor surface in the form,

$$y(t) = Y\sin(\omega t)$$

then

$$m_{Equ}\ddot{x} + c_{FEqu}\dot{x} + k_{TEqu}x = $$
$$= k_{FEqu}Y\sin(\omega t) + c_{FEqu}\omega Y\cos(\omega t)$$

And solving for X

$$x_p(t) = X\cos(\omega t - \phi_1 - \phi_2)$$

$$X = Y\left[\frac{k_{FEqu}^2 + (c\omega)^2}{\left(k_{TEqu} - m_{Equ}\omega^2\right)^2 + \left(c_{FEqu}\omega\right)^2}\right]^{1/2}$$

$$\phi_1 = \tan^{-1}\left(\frac{c_{FEqu}\omega}{k_{TEqu} - m_{Equ}\omega^2}\right)$$

$$\phi_2 = \tan^{-1}\left(\frac{k_{FEqu}}{c_{FEqu}\omega}\right)$$

Transmissibility
and
Phase shift

$$T = X/Y$$

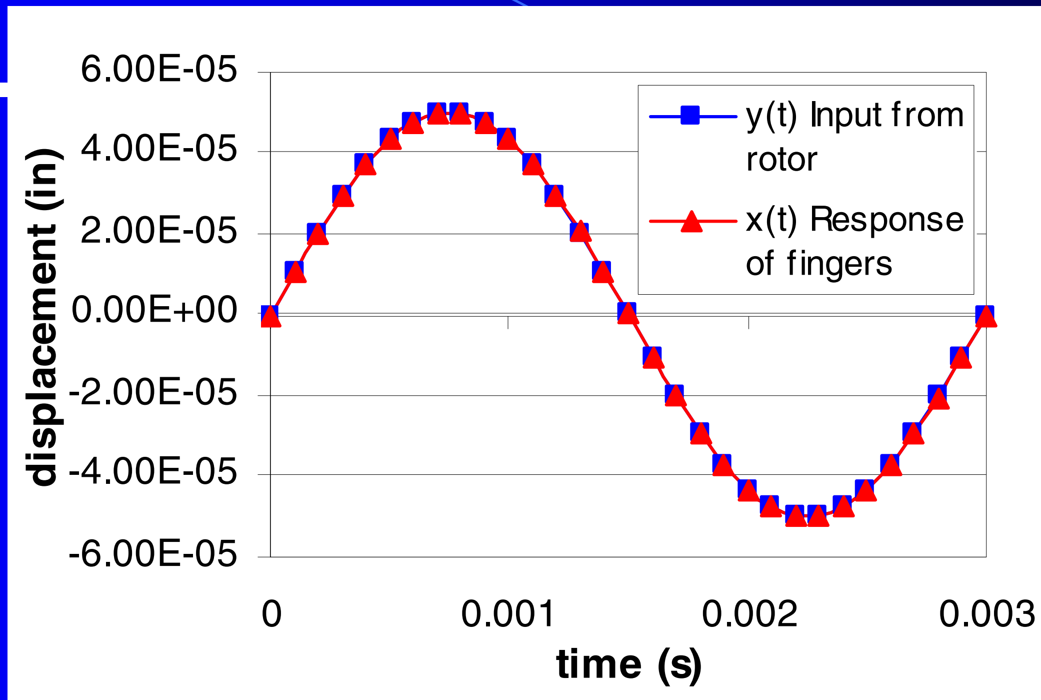

Response of the finger seal model to a harmonic input motion of the rotor.

$$k_{SEqu} = 23.44\frac{\text{lbf}}{\text{in}}(4105\frac{\text{N}}{\text{m}});\ k_{FEqu} = 6852\frac{\text{lbf}}{\text{in}}(6E5\frac{\text{N}}{\text{m}})$$

$$c_{FEqu} = .1\frac{\text{lbf}\cdot\text{s}}{\text{in}}(17.5\frac{\text{N.s}}{\text{m}});$$

$$m_{Equ} = 3.701\text{x}10^{-3}\text{lbm}(1.68\text{E}-3\text{kg})$$

$$\boldsymbol{Y} = 5\cdot 10^{-5}\,\boldsymbol{in}(1.27\boldsymbol{E}-3\boldsymbol{mm});$$

$$\omega = 20{,}000\boldsymbol{rpm} = 2094\frac{\boldsymbol{rad}}{\boldsymbol{s}};\ \boldsymbol{y}(\boldsymbol{t}) = 5\cdot 10^{-5}\sin(2094\,\boldsymbol{t})$$

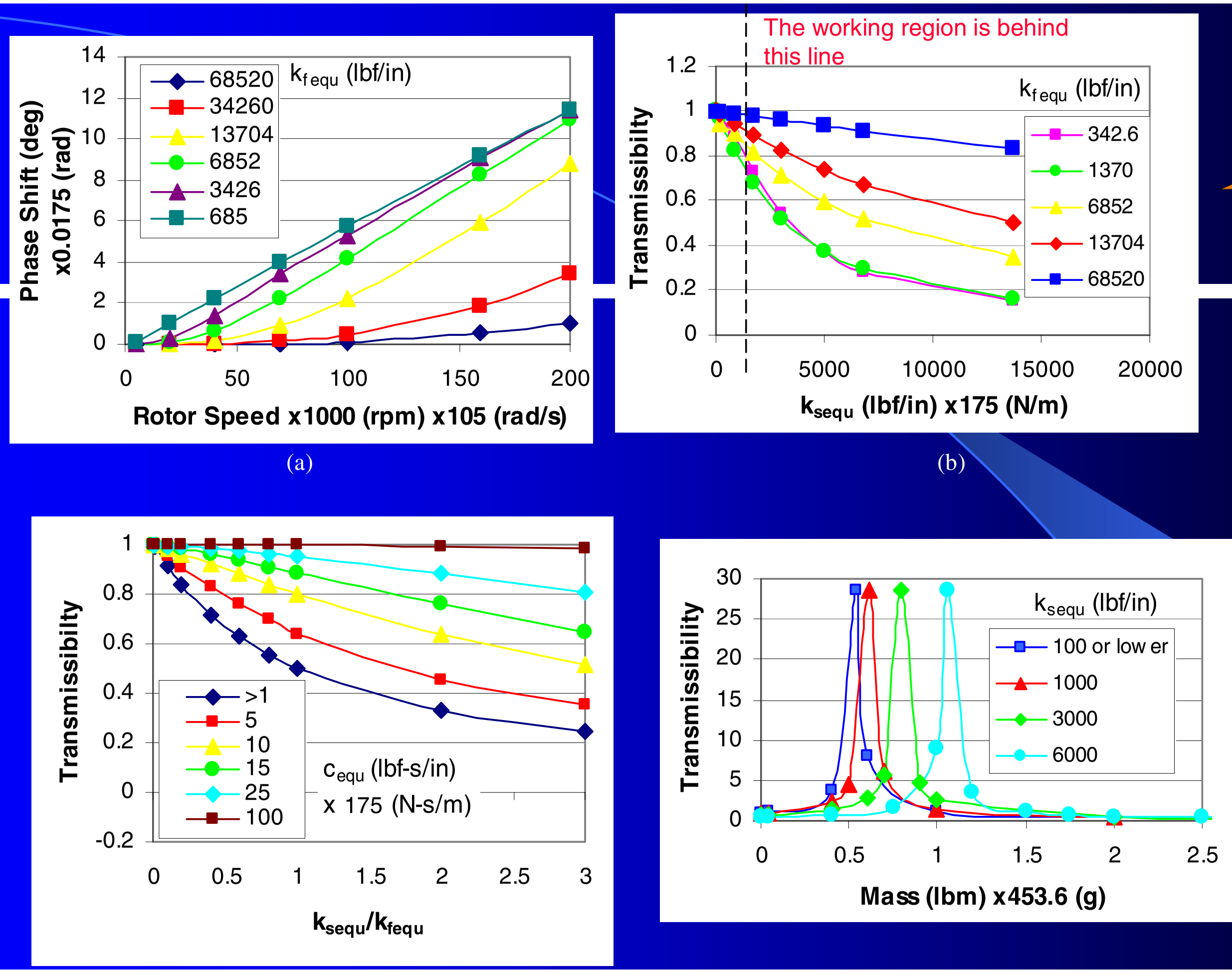

Variations in Displacement Transmissibility and Phase Shift as a Function of the Dynamic System Parameters.
(a) Phase shift of the finger response (ϕ) as a function of the rotor speed for increasing values of the fluid stiffness (kfequ). mequ=0.0037 lbm; ksequ=20.5 lbf/in; cfequ=0.1lbf-s/in.
(b) Transmissibility as a function of the stick stiffness (ksequ) for increasing values of fluid stiffness (kfequ). mequ=0.0037 lbm; cfequ=0.1 lbf-s/in; ω=20,000rpm.
(c) Transmissibility as a function of the stick stiffness/fluid stiffness ratio (ksequ/kfequ) for increasing values of fluid damping (cequ). mequ=0.0037 lbf; ω=20,000rpm.
(d) Transmissibility as a function of the finger mass (mequ) for increasing values of the stick stiffness (ksequ). kfequ=6000 lbf/in; cfequ=0.1 lbf-s/in; ω=20,000rpm

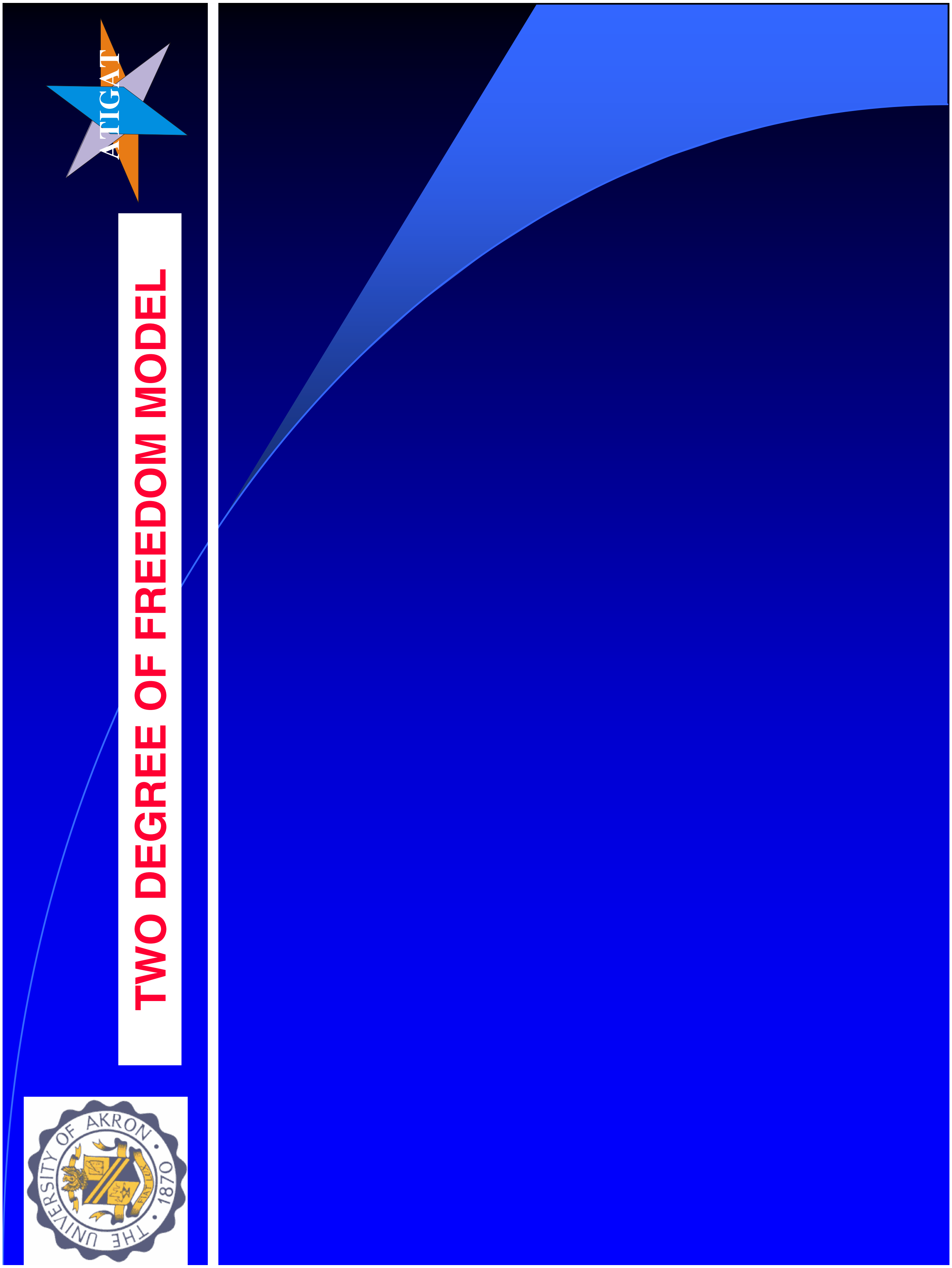
ATIGAT
TWO DEGREE OF FREEDOM MODEL
THE UNIVERSITY OF AKRON 1870

ATIGAT

$$\begin{bmatrix} m_R & 0 \\ 0 & m_{FS} \end{bmatrix} \begin{Bmatrix} \ddot{x}_1 \\ \ddot{x}_2 \end{Bmatrix} + \begin{bmatrix} c_f & -c_f \\ -c_f & c_f \end{bmatrix} \begin{Bmatrix} \dot{x}_1 \\ \dot{x}_2 \end{Bmatrix} + \begin{bmatrix} k_f & -k_f \\ -k_f & k_f + k_s \end{bmatrix} \begin{Bmatrix} x_1 \\ x_2 \end{Bmatrix} = \begin{Bmatrix} F_1 \\ 0 \end{Bmatrix}$$

$$x_1(t) = \mathrm{X}_1 e^{i\omega t}$$
$$x_2(t) = \mathrm{X}_2 e^{i\omega t}$$

$$\begin{bmatrix} \mathrm{Z}_{11} & \mathrm{Z}_{12} \\ \mathrm{Z}_{21} & \mathrm{Z}_{22} \end{bmatrix} \begin{Bmatrix} \mathrm{X}_1 \\ \mathrm{X}_2 \end{Bmatrix} = \begin{Bmatrix} F_0 e^{iwt} \\ 0 \end{Bmatrix}$$

When the Coulomb friction model is activated it replaces the zero right hand side

where

$$\mathrm{Z}_{11} = -\omega^2 m_R + i\omega c_f + k_f$$
$$\mathrm{Z}_{12} = \mathrm{Z}_{21} = -i\omega c_f - k_f$$
$$\mathrm{Z}_{22} = -\omega^2 m_{FS} + i\omega c_f + (k_f + k_s)$$

Then the solution is

$$\vec{\mathrm{X}} = [\mathrm{Z}(i\omega)]^{-1} \vec{F}$$

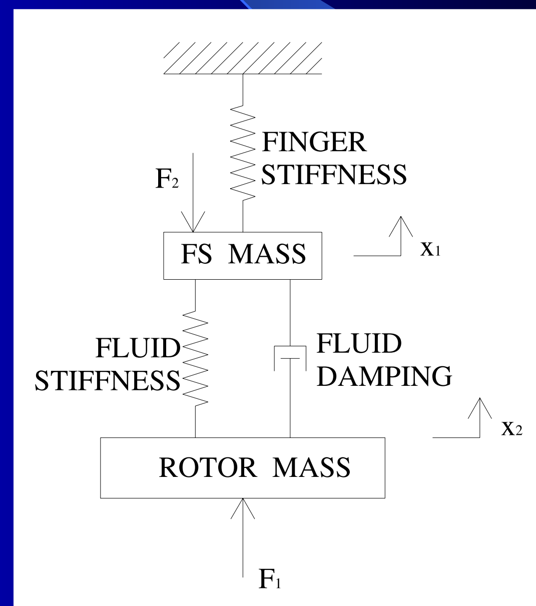

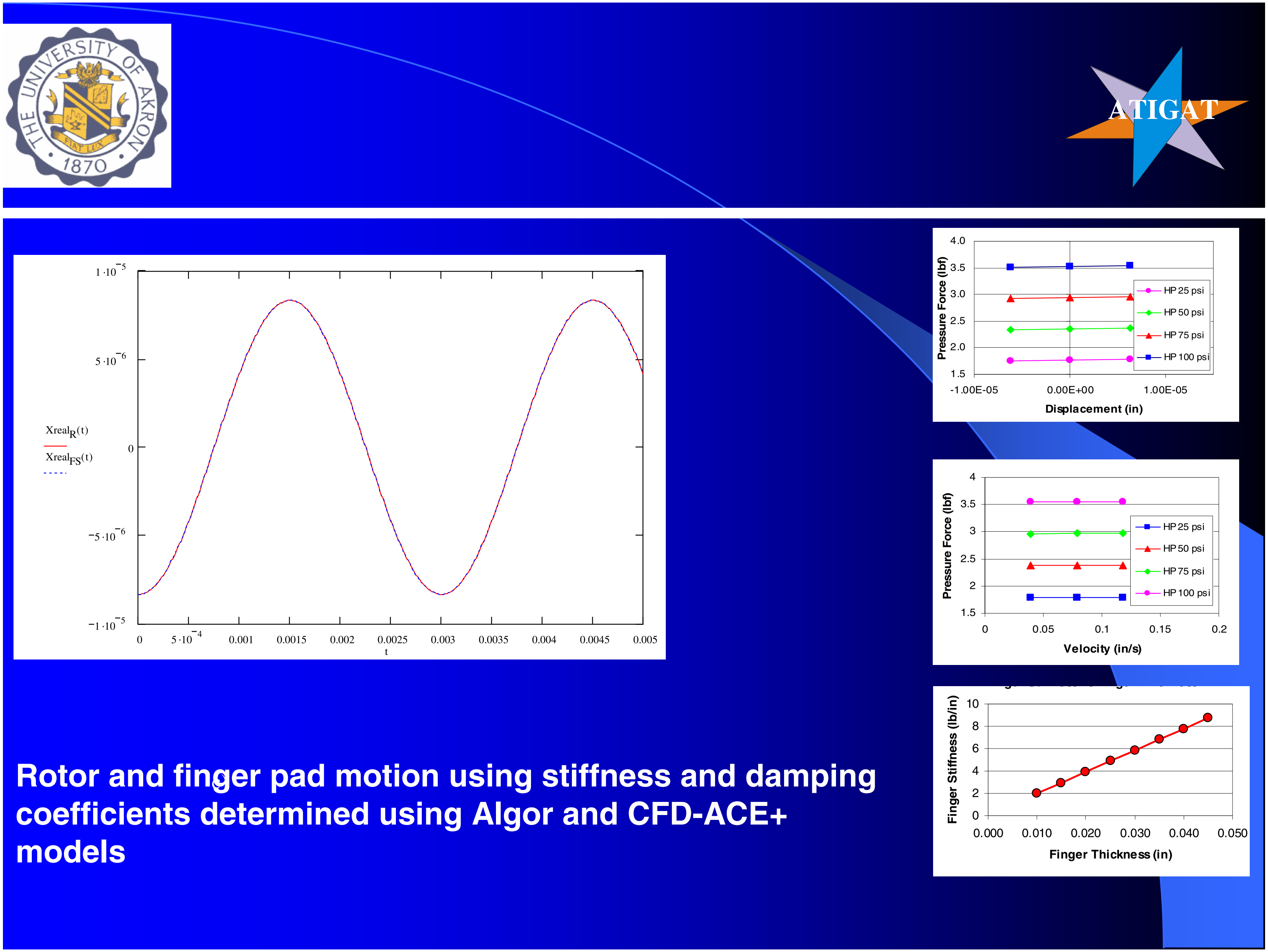

ATIGAT
THE UNIVERSITY OF AKRON 1870
$Xreal_R(t)$
$Xreal_{FS}(t)$
t
Pressure Force (lbf)
Displacement (in)
HP 25 psi
HP 50 psi
HP 75 psi
HP 100 psi
Pressure Force (lbf)
Velocity (in/s)
Finger Stiffness (lb/in)
Finger Thickness (in)
Rotor and finger pad motion using stiffness and damping coefficients determined using Algor and CFD-ACE+ models

Pad and Rotor motion when the stiffness of the stick is increased

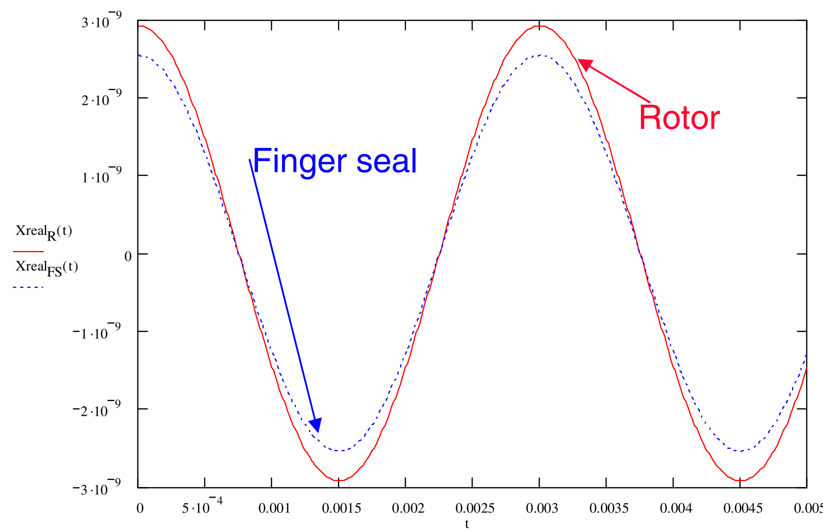

Pad and Rotor motion when the mass of the pad is increased

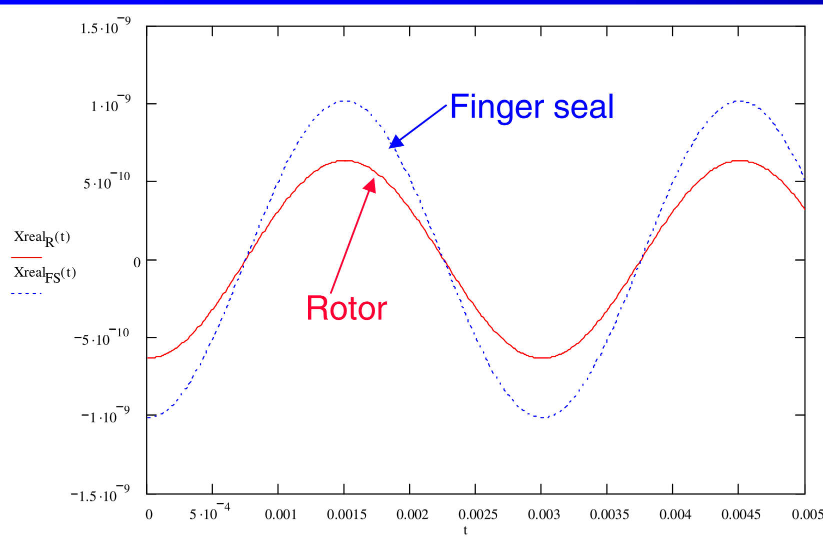

MODEL OF THE ASSEMBLY FOR THE SEAL GLOBAL DYNAMIC COEFFICIENTS

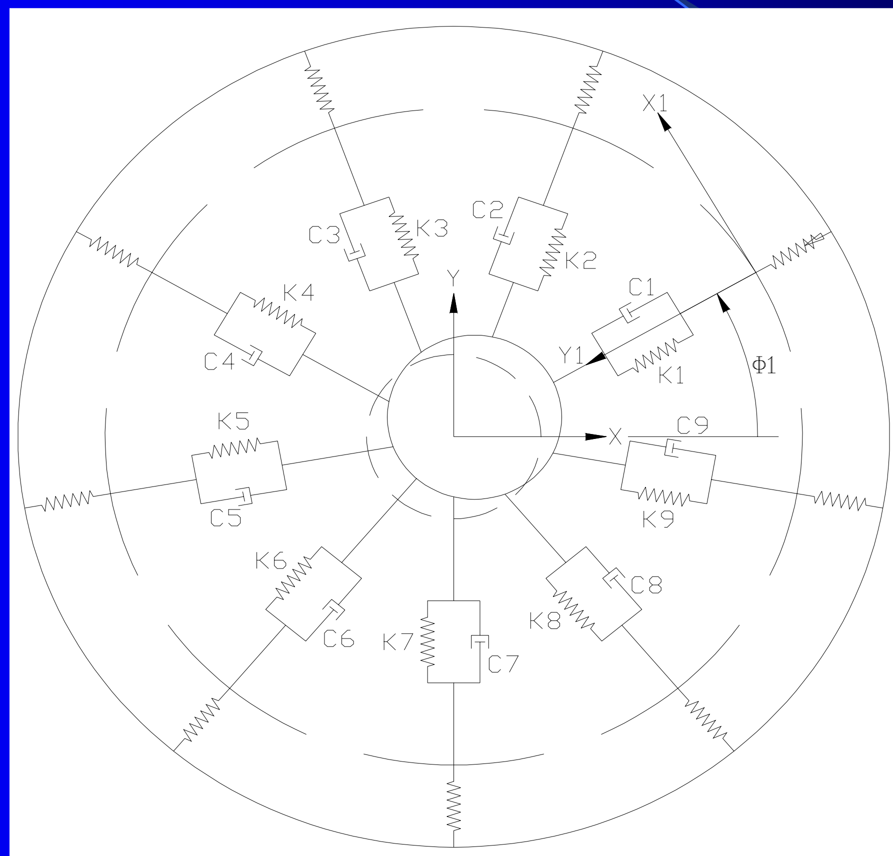

MODEL OF THE ASSEMBLY FOR THE SEAL GLOBAL DYNAMIC COEFFICIENTS

Defining the steady-state equilibrium point of the journal to be the origin for a translated coordinate system

$$(X', Y')$$

the equations of motion for the journal can be written by summing the forces acting on the journal in the

X' and Y'

directions. shows these forces associated with the i^{th} pad, where

F_{ki} = force from i^{th} spring due to a change in rotor position and

F_{ci} = force from i^{th} damper due to a change in rotor velocity.

The forces due to the rotor position and velocity are

$$F_{ki} = K_i y_i'$$
$$F_{ci} = C_i \dot{y}_i'$$

where y_i' and $\dot{y}_i'$ are the radial position and velocity of the journal in i^{th} rotated coordinate system

MODEL OF THE ASSEMBLY FOR THE SEAL GLOBAL DYNAMIC COEFFICIENTS

Given the position and velocity of the rotor in the (X', Y') coordinate system, it is necessary to perform a coordinate transformation, which yields

$$F_{ci} = C_i(-\dot{X}'\cos\phi_i + \dot{Y}'\sin\phi_i)$$

$$F_{ki} = K_i(-X'\cos\phi_i + Y'\sin\phi_i)$$

Summing forces the differential equation of motion can be written as

$$\delta\dot{x} = A\delta x$$

$$A = \begin{bmatrix} 0 & 0 & 1 & 0 \\ 0 & 0 & 0 & 1 \\ A_{31} & A_{32} & A_{33} & A_{34} \\ A_{41} & A_{42} & A_{43} & A_{44} \end{bmatrix}$$

$$A_{31} = \left(\sum_{i=1}^{9} -K_i\cos^2(\phi_i)\right)/m$$

$$A_{32} = 0$$

$$A_{33} = \left(\sum_{i=1}^{9} -C_i\cos^2(\phi_i)\right)/m$$

$$A_{34} = 0$$

$$A_{41} = 0$$

$$A_{42} = \left(\sum_{i=1}^{9} -K_i\sin^2(\phi_i)\right)/m$$

$$A_{43} = 0$$

$$A_{44} = \left(\sum_{i=1}^{9} -C_i\sin^2(\phi_i)\right)/m$$

$$K_{xx} = -A_{31}$$
$$K_{yy} = -A_{42}$$
$$C_{xx} = -A_{33}$$
$$C_{yy} = -A_{44}$$

THE TEST SECTION ASSEMBLY

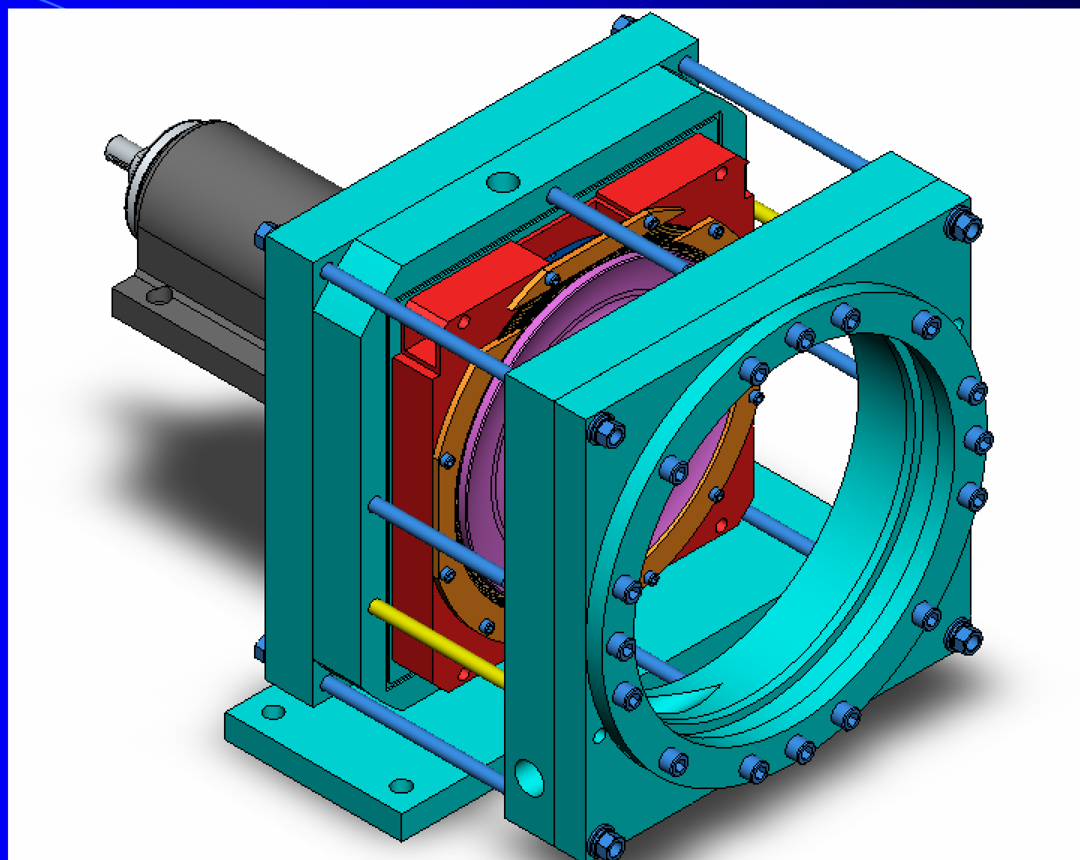

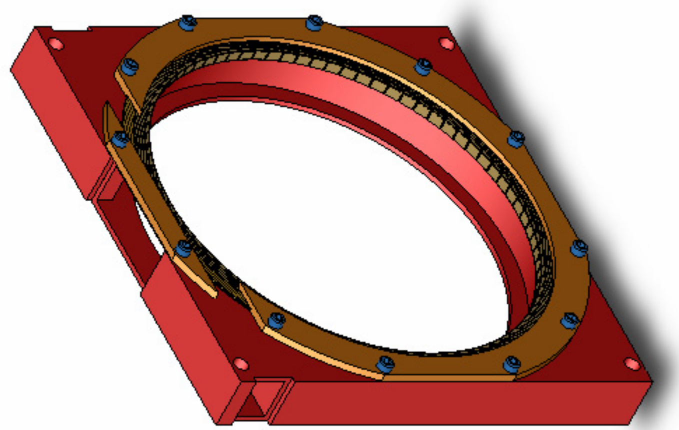

COULOMB FRICTION EVALUATION TEST SECTION

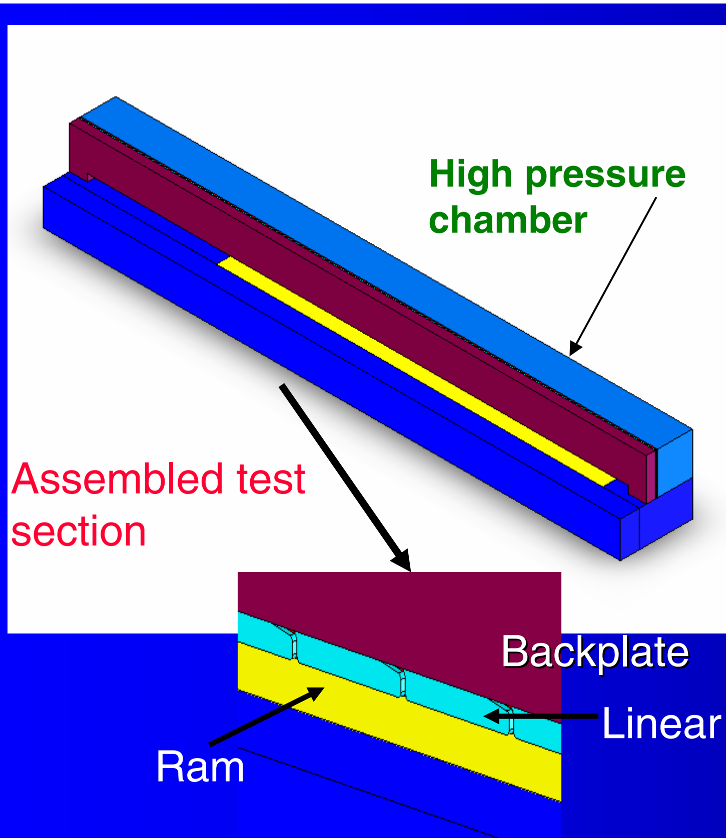

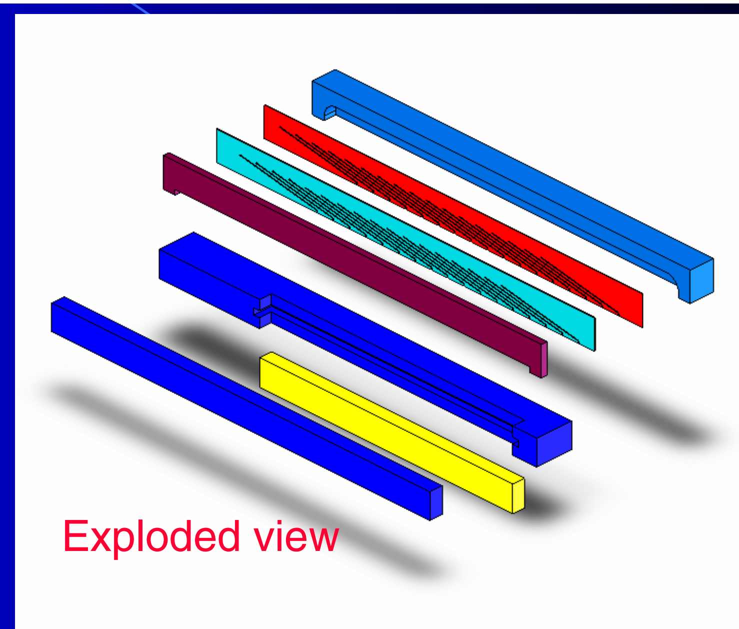

CONCLUSIONS

A three dimensional Navier-Stokes based code (CFD-ACE+/FEMSTRESS) was utilized to analyze the thermofluid behavior of a modified FS[1].

- The pressure patterns, mass flows and load carrying capabilities of this structure were assessed. It was found that even at a lower linear velocity of 216mps (708 fps) the geometry proposed has good lifting capability.

CONCLUSIONS (cont'd)

- The interplay between the rotation induced pressure generation and the axial pressure drops controlled by the HP side, is dominated by rotation at low HP side pressure, but it is then taken over by the axial pressure drop when the latter becomes larger then 173kPa at 216mps.

- The pressure patterns generated by this geometry at low pressure drops prove that the seal behaves in the fashion of a mini-slider bearing.

CONCLUSIONS (cont'd)

The dynamic model introduced a simplified spring-mass-damper equivalent to the complicated structure presented by the FS.

The numerical experiments concentrated on the determination of the phase shift and displacement transmissibility Y .

These two parameters indicate how well and under what conditions the finger will follow the rotor.

CONCLUSIONS (cont'd)

ATIGAT

It was found that

(i) the phase shift values increased when fluid stiffness was low and comparable to that of the stick,

(ii) the phase shift value decreases with fluid damping increase,

(iii) the combination of small *k*SEqu and large *k*FEqu amounts to a transmissibility Y=1,and a reversal in role leads to very small Ys,

(iv) for damping values lower than 175 N.s/m2 (1 lbf.s/in2) damping has no effect on Y and

CONCLUSIONS (cont'd)

ATIGAT

(v) certain combinations of mass and fluid and solid stiffness lead to very large Y when the rotor speed approaches the natural frequency of the system.

EFFECT OF FLOW-INDUCED RADIAL LOAD ON BRUSH SEAL/ROTOR CONTACT MECHANICS

Haifang Zhao and Robert J. Stango
Marquette University
Milwaukee, Wisconsin

Effect of Flow-Induced Radial Load on Brush Seal/Rotor Contact Mechanics

NASA Seal/Secondary Air System Workshop
November 5-6, 2003 Cleveland, Ohio
NASA Glenn Research Center

by

Haifang Zhao[*], and Robert J. Stango[**]

Department of Mechanical and Industrial Engineering
Marquette University
1515 W. Wisconsin Ave.
Milwaukee, WI
robert.stango@mu.edu

*Graduate Research Assistant and Doctoral Candidate
**Professor and Director, Deburring and Surface Finishing Research Laboratory

This paper is concerned with modeling and evaluating bristle deformation, bending stress, and bristle/rotor contact forces that are generated at the interface of the fiber and rotor surface due to radial fluid flow, and augments previous work reported by the author's, which assessed filament tip forces that arise solely due to interference between the bristle/rotor. The current problem derives its importance from aerodynamic forces that are termed "blow-down," that is, the inward radial flow of gas in close proximity to the face of the seal. Thus, bristle deformation, bristle tip reaction force, and bristle bending stress is computed on the basis of an in-plane, large-displacement mechanics analysis of a cantilever beam that is subjected to a uniform radial load. Solutions to the problem are obtained for which the filament tip is constrained to lie on the rotor surface, and includes the effect of Coulombic friction at the interface of the fiber tip and rotor. Contact forces are obtained for a range of brush seal design parameters including fiber lay angle, flexural rigidity, and length. In addition, the governing equation is cast in non-dimensional form, which extends the range of applicability of solutions to brush seals having a more general geometry and material composition.

Effect of Flow-Induced Radial Load on Brush Seal/Rotor Contact Mechanics

NASA Seal/Secondary Air System Workshop
November 5-6, 2003 Cleveland, Ohio
NASA Glenn Research Center

by

Haifang Zhao*, and Robert J. Stango**

Department of Mechanical and Industrial Engineering
Marquette University
1515 W. Wisconsin Ave.
Milwaukee, WI
robert.stango@mu.edu

*Graduate Research Assistant and Doctoral Candidate
**Professor and Director, Deburring and Surface Finishing Research Laboratory

This work focuses on the evaluation of:

- bristle deformation
- bristle bending stress
- bristle/rotor interface contact forces

due to *radial fluid flow* associated with aerodynamic forces that are termed *"blow-down"* … i.e., inward radial flow of gas in close proximity to the face of the seal.

The mechanics formulation is based upon constrained, large-displacement of a cantilever beam subjected to planar deformation caused by uniform radial load, and includes Coulombic friction at interface of fiber tip and rotor.

A non-dimensional form of governing equation is obtained, which extends range of applicability of solutions to brush seals having a more general geometry and material composition.

Bristle tip/rotor contact forces and bristle bending stress are reported for both interference and transition brush seals for a range of brush seal design parameters including fiber lay angle, flexural rigidity, and length.

MARQUETTE UNIVERSITY

In-situ Brush Seal

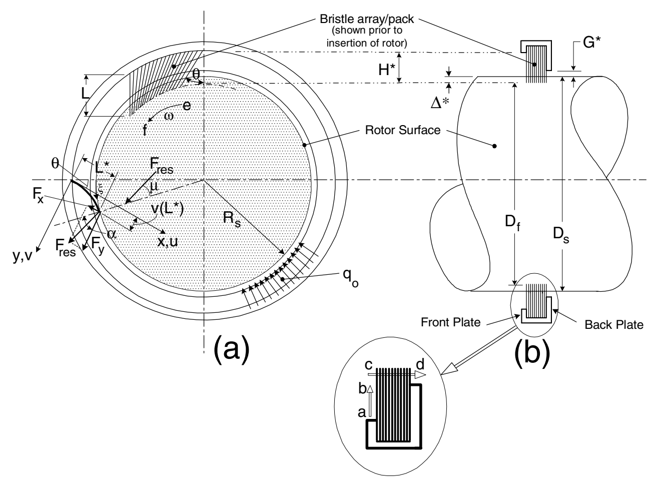

Several flow fields of particular interest are identified above:

<u>Radial fluid flow across the face of the seal (i.e., along path a-b)*</u>

Inward radial flow of gas along the face of the seal is often termed *blow-down*. Since this component of fluid flow is inclined across the bristle length L, filament tips are displaced inward, toward the rotor surface. This, in turn, can promote closure of the seal, while increasing both the bristle tip/contact force and bristle bending stress.

<u>Axial fluid flow through the bristle network of the seal (i.e., along path c-d)</u>

Gases that escape the upstream chamber must pass through the annular region G*, where the brush seal is positioned. Thus, the densely packed fibrous barrier can impede flow/leakage due to the inherent stiffness of the fibers, and the reinforcing constraint offered by the back plate.

<u>Circumferential (rotor-induced) fluid flow (i.e., along curved path e-f)</u>

Rapid rotation of the rotor can give rise to a flow field at/along the shaft surface, in the direction of shaft rotation. This flow field has been termed *rotor-induced swirl* and can be of sufficient strength to cause bristle tips to lift off of the rotor surface.

* The topic of current presentation.

Bristle load/geometry

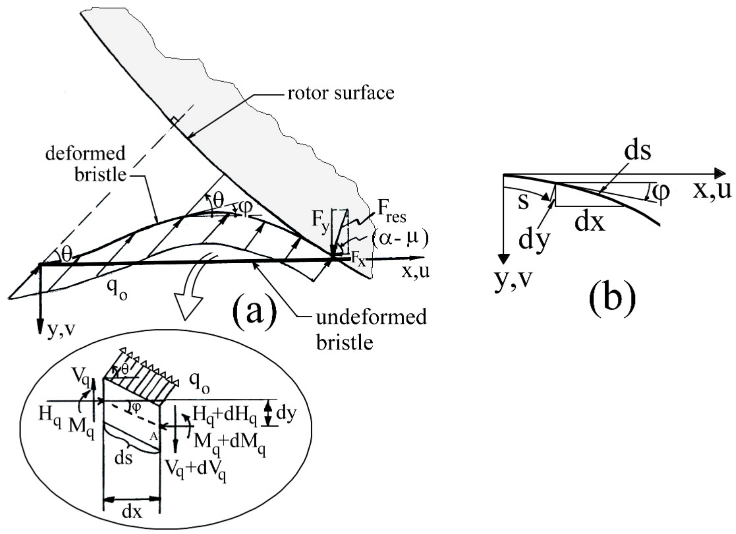

The geometry and loading for the current problem is depicted above whereby a single bristle within the radial flow field is isolated and examined. The undeflected bristle having length L (solid horizontal line) is oriented at the fiber lay angle θ and penetrates the rotor having radius R_s by an amount Δ^*, where $\Delta^* \geq 0$ is the nominal interference.

Also shown is the distributed load of arbitrary magnitude q_o (force per unit length), which represents the uniform bristle loading induced by an inward radial flow of gas. One may observe that, in the deformed configuration, both the magnitude and direction of load q_o is preserved along the entire fiber length, while the fiber tip is constrained to lie along the rotor surface.

Mechanics Formulation of Problem

The Bernoulli-Euler Law: $EI\kappa = M_q + M_F$

Curvature-moment relation: $\kappa = \dfrac{d\phi}{ds}$

$$dM_q = q_0 (L - s)\sin(\theta + \phi) ds$$

$$dM_F = -F_{res} \cos(\alpha - \mu - \phi) ds$$

Governing Equation:

$$EI \frac{d^2\phi}{ds^2} = q_o (L - s)\sin(\theta + \phi) - F_{res}\cos(\alpha - \mu - \phi)$$

The governing equation for the bristle elastica is given by the Bernoulli-Euler equation, where κ is the bristle curvature, ϕ is the bristle slope angle, s is the arc-length coordinate along the fiber, EI is the flexural rigidity, and the component moments M_q and M_F are internal moments associated with the distributed load q_o and bristle-rotor contact force F_{res}, respectively.

Distributed load component dM_q and differential moment associated with rotor/bristle contact force dM_F are obtained by satisfying bristle equilibrium, which leads to the governing equation above for bristle deformation.

MARQUETTE UNIVERSITY

Mechanics Formulation, cont'd

Boundary Conditions:

Φ=0 at s=0; $d\Phi/ds=0$ at s=L

Additional Constraints:

$$\begin{Bmatrix} x_\xi \\ y_\xi \end{Bmatrix} = \begin{bmatrix} \cos\theta & -\cos\left(\theta + \frac{\xi}{R_s}\right) \\ -\sin\theta & \sin\left(\theta + \frac{\xi}{R_s}\right) \end{bmatrix} \begin{Bmatrix} R_s + H^* - \Delta^* \\ R_s \end{Bmatrix} \quad ; \quad \begin{cases} y_t = \int_0^L \sin\phi ds \\ x_t = \int_0^L \cos\phi ds \end{cases}$$

$$\boxed{\left|x_t - x_\xi\right| < \varepsilon \quad ; \quad \left|y_t - y_\xi\right| < \varepsilon}$$

Constraint equations are formulated that ensure the bristle terminus (x_t, y_t) lies along the rotor surface (x_ξ, y_ξ). Details concerning the basic algorithm that is used for obtaining convergent solutions to the current problem can be found in *ASME Journal of Tribology* (2003), 125, pp. 414-421.

MARQUETTE UNIVERSITY

Mechanics Formulation, cont'd

Dimensionless form of Governing Equation:

$$\frac{d^2\phi}{ds^{*2}} = \left(\frac{q_0 H^{*3}}{EI}\right) s^* \sin(\theta + \phi) - \left(\frac{F_{res} H^{*2}}{EI}\right) \cos(\alpha - \mu - \phi)$$

"Complementary Load" relationship

$$\left(\frac{F_{res} H^{*2}}{EI}\right)_1 = \left(\frac{F_{res} H^{*2}}{EI}\right)_2 \quad ; \quad \left(\frac{q_0 H^{*3}}{EI}\right)_1 = \left(\frac{q_0 H^{*3}}{EI}\right)_2$$

The governing equation can be rendered into the above dimensionless form, which leads to the above "complementary load" relationships. These relations can be useful for exploring alternative brush seal design configurations and can enable engineers to forecast the role that flow-induced load q_0, flexural rigidity, and bristle/rotor geometry play in generating contact forces in the system.

Numerical Results & Discussion

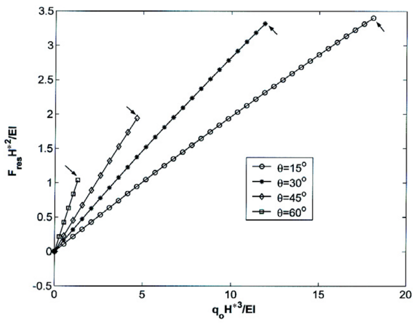

Figure 3 (Δ*/H* =0)

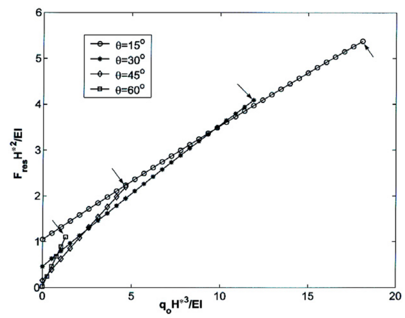

Figure 4 (Δ*/H* =0.14)

Relationship between dimensionless bristle resultant force and dimensionless flow-induced load for lay angles of 15, 30, 45 and 60 degrees. Arrows denote point at which bristle yield curvature/stress is reached. (Results shown are for μ = 0.21, Rs/H* = 8.9).

In Figure 3, the relationship between the non-dimensional contact force and non-dimensional flow-induced distributed load is shown for a transition seal ()*/H* = 0) having the bristle lay angles θ = 15°, 30°, 45°, and 60°. These results indicate that lay angle θ is a key design parameter for regulating the magnitude of bristle/rotor contact force and bristle stress. Similarly, in Figure 4 the non-dimensional relationship between contact force and flow-induced load is reported for the deepest interference parameter ()*/H" = 0.14).

Numerical Results & Discussion, cont'd

Common characteristics of Fig. 3 & Fig. 4, and the direct use of *Complimentary Load* relations:

- To a first order of approximation, the reported data can be regarded as a linear response throughout the entire load history
- The slope of the response is approximately the same for any given (i.e. fixed) lay angle θ.
- The slope of the response for any given angle is independent of the interference parameter Δ*/H*

Thus:

$$\left(\frac{F_{res} H^{*2}}{EI}\right) = m\left(\frac{q_0 H^{*3}}{EI}\right) + \frac{F_0 H^{*2}}{EI}$$

and it follows that

$$\boxed{F_{res} = mH^* q_o + F_o}$$

The above observations suggest that coupling exists between the two different non-dimensional loads involving F_{res} and q_0. Thus, shaft/bristle contact forces that arise due to flow-induced load q_0 are regulated by *scale factor* mH*, where m is the slope of the response curve(s) shown in Figures 3 and 4, and H* is the radial length of the bristle.

Thus, for a given (i.e., fixed) radial load q_o, the magnitude of shaft contact force is principally regulated by the three parameters m, H*, and F_o. This finding suggests that least contact force can be obtained by the use of shallowest lay angle θ = 15° (i.e., the minimum slope, m_{min}), least radial bristle length exposure H^*_{min} , and least design interference $)^*_{min}$ (i.e., F_0=0).

MARQUETTE UNIVERSITY

Numerical Results & Discussion, cont'd

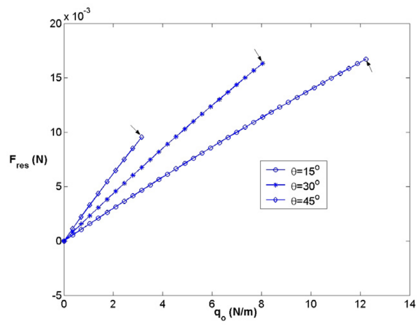

Fig. 5 $\Delta^*/H^*=0$

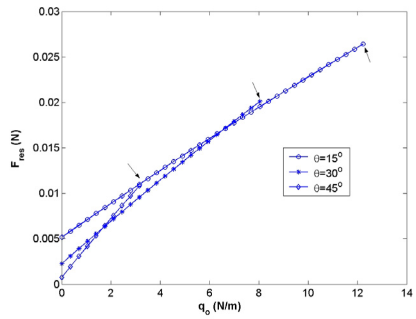

Fig. 6 $\Delta^*/H^*=0.14$

Relationship between actual bristle resultant force F_{res} and actual flow-induced load q0 for lay angles of 15, 30 and 45 degrees. Arrows denote point at which bristle yield stress is reached. (Results shown are for $\mu = 0.21$, $R_s/H^*=8.9$)

For the purpose of illustrating the actual magnitude and range of loads that are feasible prior to the onset of bristle yield, Figures 3 and 4 are recast in Figures 5 and 6 in terms of the flow-induced distributed load q_o and the bristle tip resultant force F_{res} for three different lay angles. These data have employed the brush seal parameters R_s = 64.77 mm, H^* = 7.2644 mm, and flexural rigidity EI = 2.5930 x 10^{-7} N·m^2. One may observe that the same trends that appeared in Figures 3 and 4 also appear in Figures 5 and 6, and that the location where bristle yield stress is reached (arrows) provides a basis for identifying the acceptable range of q_o that can be sustained by the bristle.

MARQUETTE UNIVERSITY

Numerical Results & Discussion, cont'd

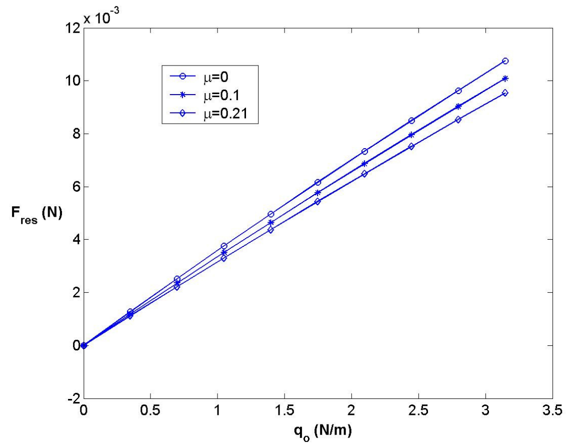

Fig. 7 Relationship between actual bristle resultant force F_{res} and actual flow-induced load q_o for coefficients of friction μ =0, 0.1 and 0.21. (Results shown are for lay angle of 45 degrees, R_s/H^*=8.9 and Δ^*/H^*=0)

In Figure 7 the role that friction plays in the contact problem is examined for a brush seal having lay angle $\theta = 45^o$ and interference $\Delta^* = 0$. It is noted that the successive increase of friction coefficient $\mu = 0.0$, $\mu = 0.1$, and $\mu = 0.21$, leads to the successive reduction of the resultant filament contact force F_{res}. This result, while somewhat unexpected, is characteristic of large displacement mechanics problems involving deformation of a fiber whose tip is constrained to lie along a surface having light to moderate friction. A detailed explanation of this phenomenon has been discussed in *ASME Journal of Tribology* (2003), 125, pp. 414-421.

MARQUETTE UNIVERSITY

Numerical Results & Discussion, cont'd

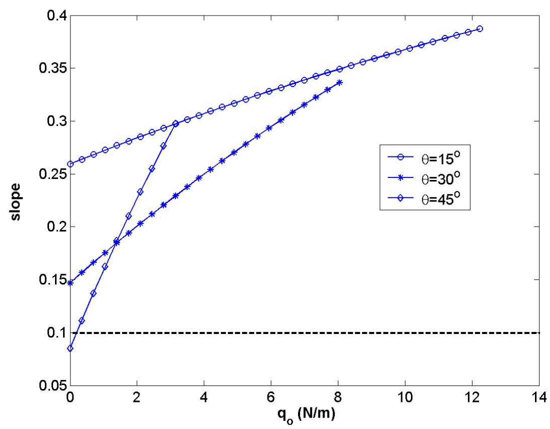

Figure 8 Relationship between slope at bristle tip and actual flow-induced load q_o for lay angles of 15, 30 and 45 degrees. (Results shown are for μ=0.21, R_s/H^*=8.9 and Δ^*/H^*=0.07)

The relevance of utilizing linear beam theory for analysis of the current problem is examined in Figure 8 for the case of a brush seal subjected to variable flow-induced load q_o and moderate interference parameter The vertical axis records the slope of the bristle tip (i.e., ϕ(s=L)), and a horizontal line has been placed along ϕ = 0.1, which is often taken as the upper bound for accurate use of linear beam theory. Thus, the results indicate that use of non-linear beam theory is required for bristle mechanics analysis of the current problem.

MARQUETTE UNIVERSITY

Numerical Results & Discussion, cont'd

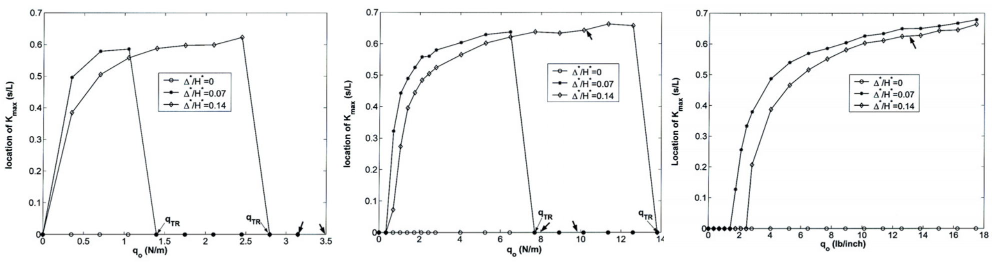

(a) (b) (c)

Fig. 9 Relationship between the location at which maximum bristle curvature (or stress) occurs and actual flow-induced load q_o for interference parameters Δ^*/H^* = 0.0, 0.07, and 0.14 for (a) 45 degree lay angle, (b) 30 degree lay angle, and (c) 15 degree lay angle. Bold arrows denote point at which bristle yield stress is reached. (Results shown are for μ = 0.21, and Rs/H^* = 8.9).

Both the *location* and *magnitude* of maximum bristle bending stress is an important design consideration for evaluating life and failure mode of the brush seal. In Figures 9a, 9b, and 9c the *location* where maximum stress occurs within the bristle is examined for three different lay angles $\theta = 45^o$, $\theta = 30^o$, and $\theta = 15^o$, respectively. Since the direction of the fluid load q_o *opposes* the direction of the force at the bristle tip, stress at the fiber root must progressively unload, while the position of maximum stress migrates toward the mid-bristle location. The continual growth of q_o gives rise to further redistribution of the bristle bending stress, and the location of maximum stress inevitably returns to the fiber root. The magnitude of the flow-induced load at which an abrupt transition of bending stress location occurs has been labeled q_{TR} in the above figures.

MARQUETTE UNIVERSITY

Conclusion

- C*omplementary load* relations have been derived that can provide insight into the relationship among bristle geometry, flexural rigidity, bristle/rotor contact force, and flow-induced radial load.

- Bristle/rotor contact force:
  - The magnitude of interface contact force is principally regulated by the selection of bristle lay angle, bristle length, and brush seal interference.
  - minimum bristle/rotor contact force can be obtained by selecting the shallowest bristle lay angle, least filament length, and least bristle/rotor interference.

MARQUETTE
UNIVERSITY

Conclusion, Cont'd

- Mechanics analysis of the current problem necessarily warrants the use of nonlinear beam theory for the evaluation of bristle stress and deformation.

- Bristle bending stress:
  - The location of maximum bending stress within a bristle can vary, and depends upon the selection of bristle lay angle, brush/rotor interference, and the magnitude of flow-induced load.
  - As a consequence of the above statement, it is feasible that bristle fatigue failure can occur at the fiber root or at some intermediate position along the fiber length.
  - Minimal bending stresses are obtained for the brush seal that utilizes the shallowest bristle lay angle, and least rotor/bristle interference.

GOLDEN EAGLE

SEAL DEVELOPMENTS AT FLOWSERVE CORPORATION

Andrew Flaherty, Lionel Young, and William Key
Flowserve Corporation
Temecula, California

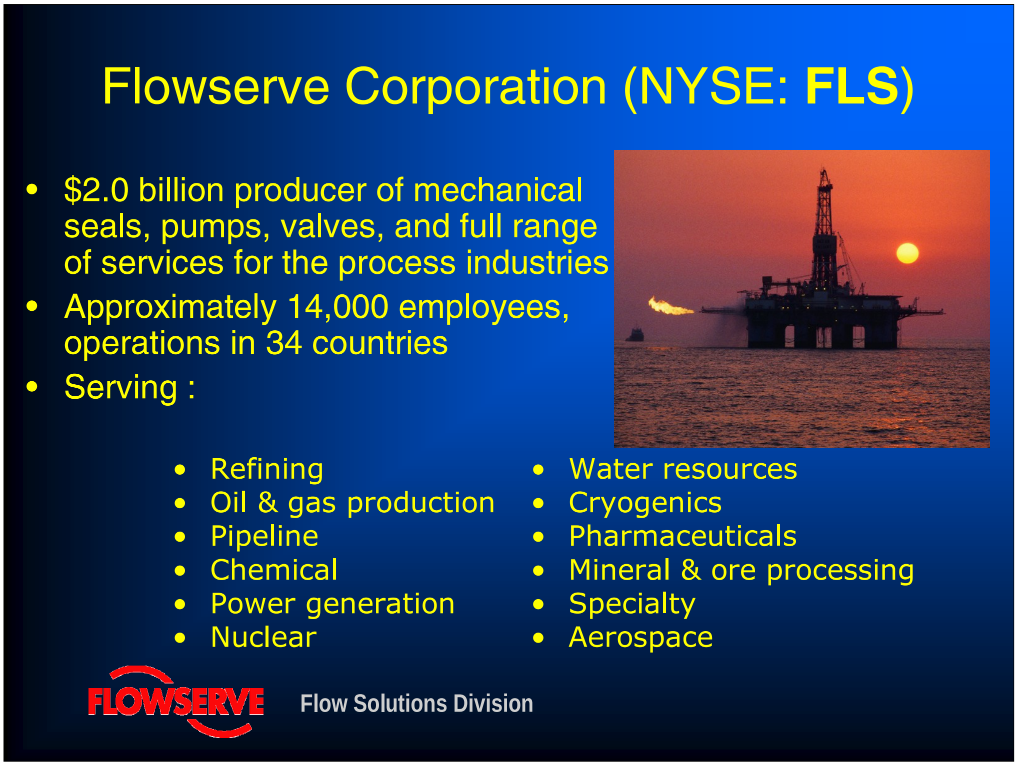

•Flowserve Corporation is a global supplier of mechanical seals, pumps and valves.

•Flowserve supports a wide range of markets – from the chemical market and hydrocarbon processing industry to the aerospace market.

•To meet the requirements of the various markets, Flowserve's Flow Solutions Division, which is focused on mechanical seals, is ISO9001 certified, compliant with the Nuclear Industry's 10CFR50 Appendix B, and is currently working to comply with Aerospace's AS9100.

•Flowserve produces a range of mechanical sealing solutions, which includes mechanical end-face seals (in both bellows and o-ring pusher versions), circumferential seals, and other custom configurations.

•Most of the seals can be designed to be contacting or non-contacting, depending on the application requirements.

- Today's presentation will focus on the Laser Machining process that was developed to create the next generation of non-contacting seals.
- Non-contacting, or lift-off type face seals have been around since the 1970's. In the aerospace market, they have been used in commercial applications since about 1995.
- The lift-off features in aerospace tend to be 2-D (a Rayleigh step of uniform depth) and are generally produced with potentially labor intensive processes.
- Laser machining opens the door for a whole new realm of possibilities.

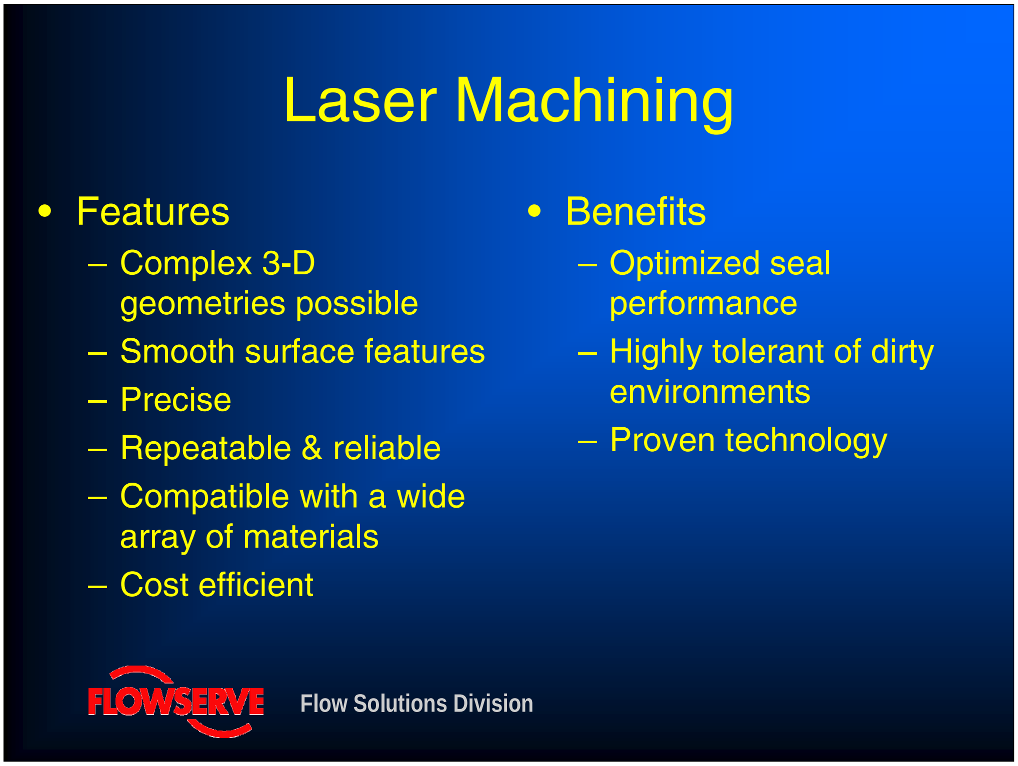

•Using an in-house developed, proprietary laser system, Flowserve is able to create complex features on the order of 0.5 microns.

•This highly reliable & repeatable system allows Flowserve to optimize seal performance for each application.

•Flowserve has been implementing this process in production since 1999.

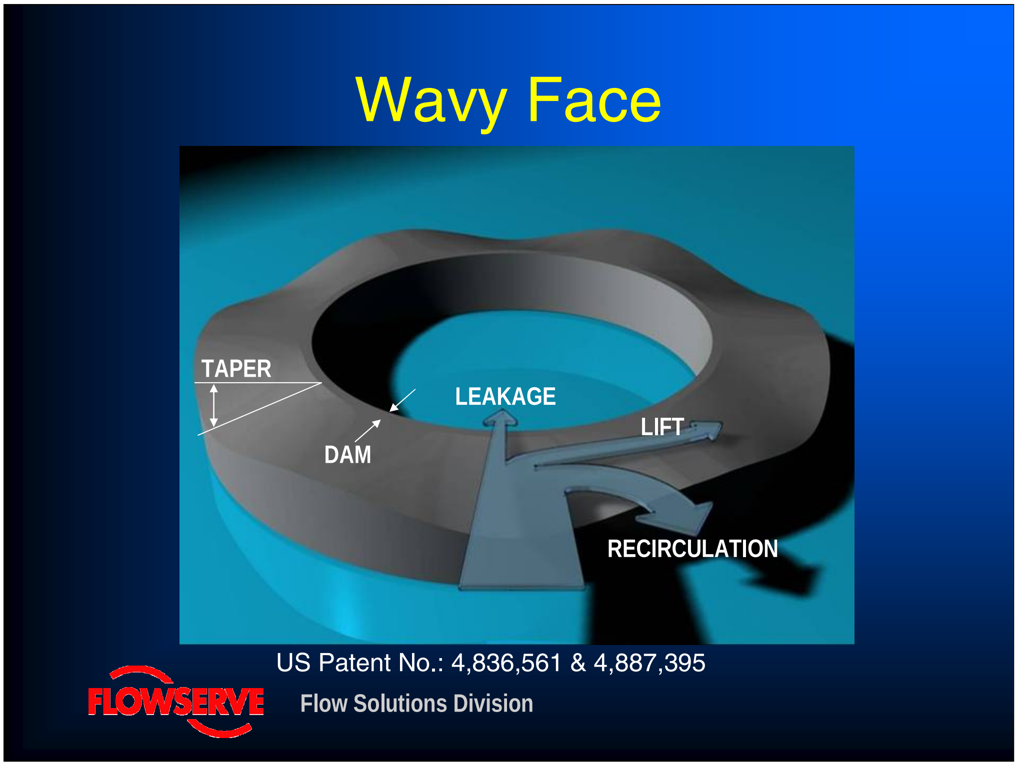

•The Wavy Face design is a good of example of how to take advantage of the laser machining process.

•The pattern, a sinusoidal wave that varies in both the circumferential & radial directions offers:

- Bi-directional rotation
- Hydrostatic and hydrodynamic load support
- Contamination resistance
- Non-aggressive condition should incidental contact occur
- The ability to operate in variety of fluids, including gases, liquids, mixed phase fluids, volatile hydrocarbons & dirty steam to name a few.

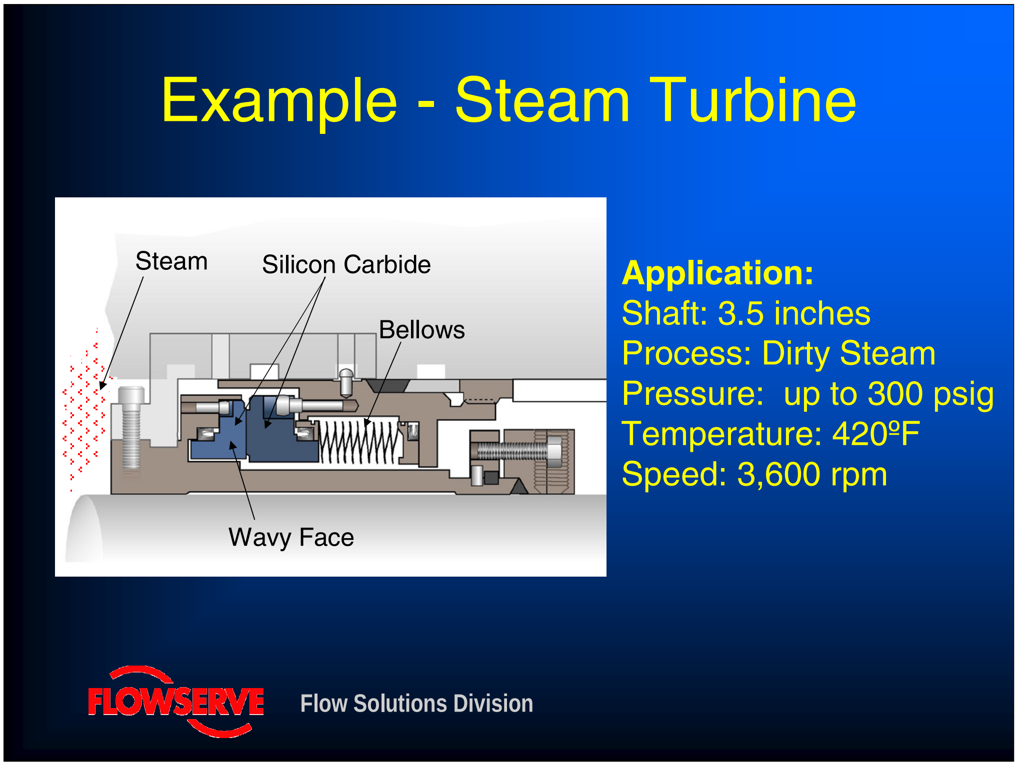

- Traditionally, steam turbine applications have been difficult to seal:
    - The environment is hot.
    - The quality of steam is generally poor.
    - Conditions can vary depending on if the turbine is operating or in standby mode.
- Seals often failed due to abrasive wear at the seal interface or due to hang-up, resulting from calcium carbonate precipitating out of solution.
- One solution to wear problem was to use a Wavy Face design.

•A seal was tested in dirty steam for almost 1,400 hours under typical application operating conditions, including slow roll and full speed & pressure.

•At the conclusion of the test, the faces exhibited no wear and were comparable to a brand new face.

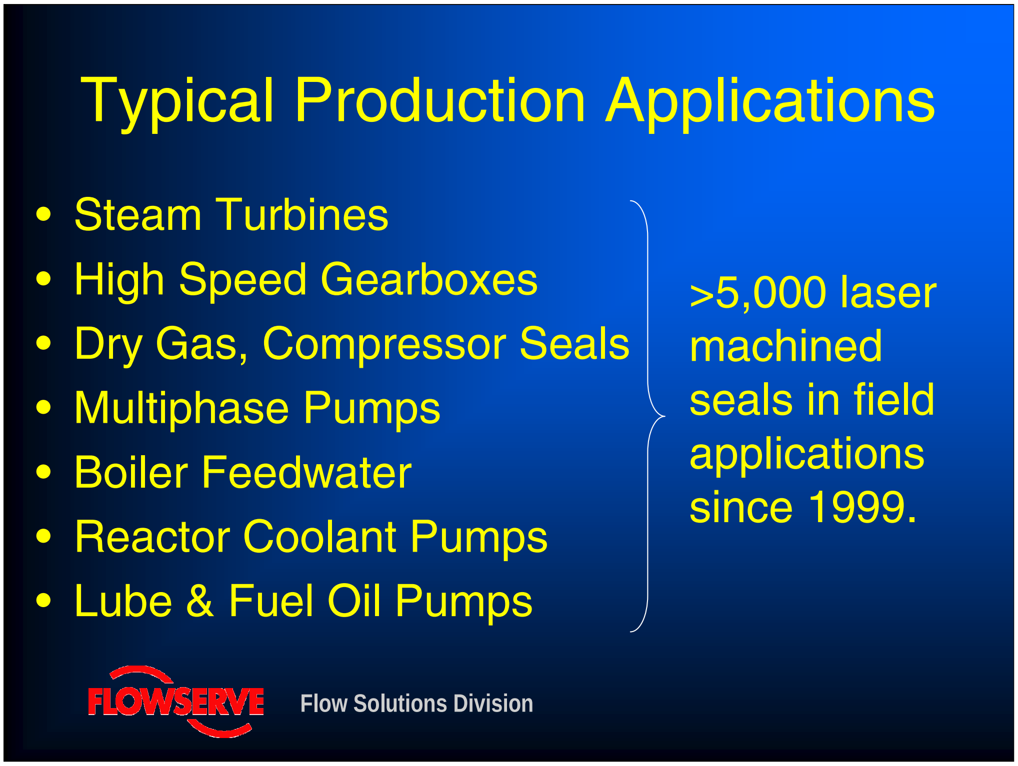

- In addition to Steam Turbines, laser machined faces have been able to enhance the performance of seals in several difficult applications.
- Currently, there are more than 5,000 laser machined seals in service.

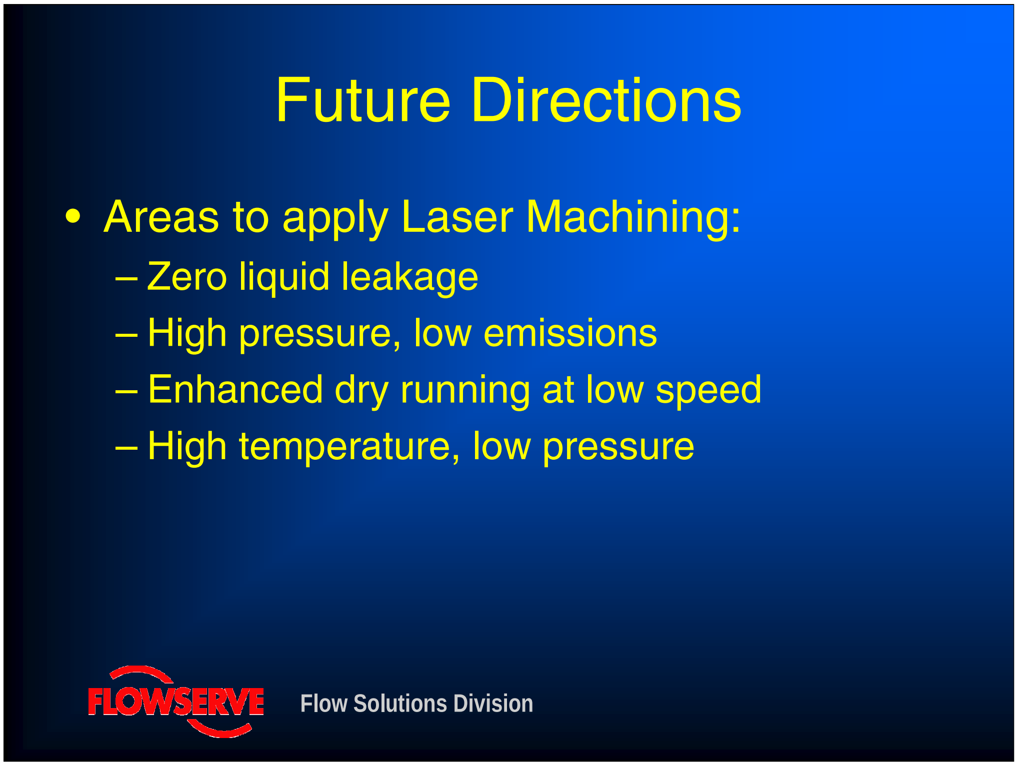

•Laser machining is being investigated for applications to address several other needs from zero liquid leakage to optimized non-contacting seals for high temperature, low pressure applications.

INVESTIGATIONS OF HIGH PRESSURE ACOUSTIC WAVES IN RESONATORS WITH SEAL-LIKE FEATURES

Christopher C. Daniels
Ohio Aerospace Institute
Brook Park, Ohio

Bruce M. Steinetz and Joshua R. Finkbeiner
National Aeronautics and Space Administration
Glenn Research Center
Cleveland, Ohio

Xiaofan Li and Ganesh Raman
Illinois Institute of Technology
Chicago, Illinois

Investigations of High Pressure Acoustic Waves in Resonators With Seal-like Features

C. Daniels
Ohio Aerospace Institute
Cleveland, OH 44142

B. Steinetz and J. Finkbeiner
NASA John H. Glenn Research Center
Cleveland, OH 44135

Xiaofan Li and Ganesh Raman
Illinois Institute of Technology
Chicago, IL 60616

NASA Seal / Secondary Air Flow System Workshop
November 5-6, 2003

Presentation

- Background
- Program Objective
- Research Objective
- Baseline Configuration
  - Experimental Setup
  - Results
- Closed Configuration with Blockages
  - Experimental Setup
  - Results
- Open Resonator Configuration
  - Experimental Setup
  - Results
- Open Resonator Configuration with Δp
  - Experimental Setup
  - Results
- Summary
- Future Work

Background

- Linear acoustic theory limits pressure waves to approximately 10% overpressure. Shock formation dissipates any additional wave energy.
- Dr. Timothy Lucas discovered a method to produce high-amplitude pressure waves in acoustic resonators in 1990.
- Using specially shaped resonating cavities, dynamic gas pressures exceeding 500 psi can be generated shock-free.
- Lucas focused on creating refrigeration compressors and formed Macrosonix Corporation to develop the technology.
- Most previously published work focused mainly on using refrigerant as the working fluid.

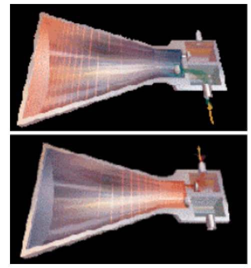

Mechanical Engineering Magazine "Sound Waves at Work" March, 1998

Program Goal

Development of a non-contacting seal that would overcome two fundamental problems of conventional seals:

- Leakage
- Wear

Exploit recent developments in non-linear acoustics

- Specially shaped acoustic resonator is driven at resonance
- Generation of high-amplitude pressures

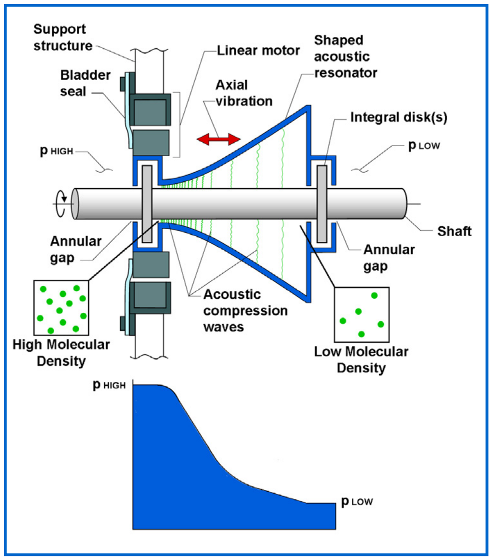

Research Objective

- Extend the research of non-linear acoustics in resonators:
  - Lawrenson, et al. (1998)
    - **Experimentally generated high overpressure unshocked waveforms**
    - **Peak acoustic pressures of 1446kPa (209 psia)**
  - Ilinskii, et al. (1998)
    - **1-Dimensional numerical prediction**
    - **Non-linear acoustics with shaped resonators**
  - Chun, et al. (2000)
    - **Additional resonator shapes**
- Determine if high-amplitude standing pressure waves can be generated:
  - using air as the working fluid
  - in resonators containing seal-like features
    - **blockages (shaft)**
    - **ventilation holes (annular clearance)**

Dimensionless Variables

Dimensionless **Pressure**

– $\mathbf{p / p_0} = p_{INSTANTANEOUS} / p_{AVE\ QUIET\ CONDITION}$

– $\mathbf{p_{MAX} / p_0} = p_{CYCLE\ MAXIMUM} / p_{AVE\ QUIET\ CONDITION}$

- Dimensionless **Frequency**
  – $\mathbf{\Omega} = 2 \cdot f \cdot l_{RESONATOR} / (\gamma \cdot 8314 \cdot T_K / MW)^{1/2}$

- Dimensionless **Time**
  – $\boldsymbol{\tau} = f \cdot t / (2 \cdot \pi)$

Baseline Configuration

Baseline Configuration: Experimental Setup

- **Electrodynamic Shaker Table**
  - **500lbf (2220N) capacity**
- **Conical Resonator**
  - **$r(z) = 0.0056 + 0.2680 \cdot z$ [m]**
  - **Aluminum 7075T6 with 0.14inch (3.6×10^{-3}m) wall thickness**
  - **Containing air (ambient conditions)**
- **Instrumentation**

  A. Dynamic pressure sensors (2)

  B. Static pressure transducers (2)

  C. Accelerometer (2)

  D. Thermocouples (2)

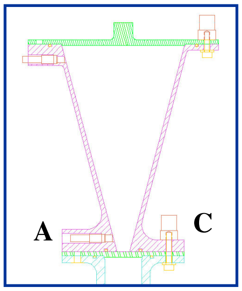

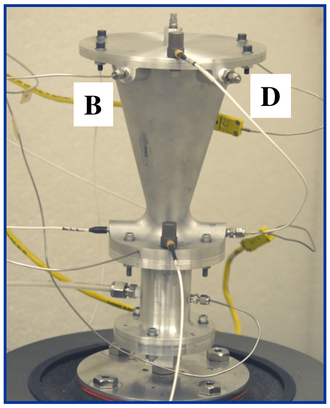

Baseline Configuration: Experimental Results

- Non-linear frequency shift with increasing acceleration amplitude
- Moderate hysteresis evident (hardening)

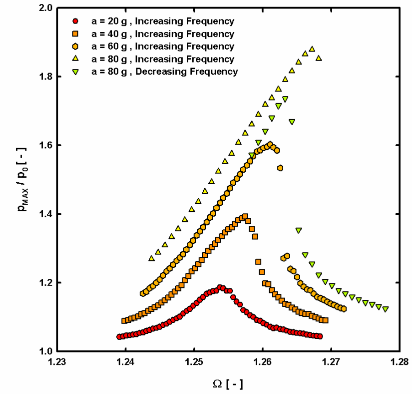

Cylinder shocks below Pmax/Po < 1.1

Baseline Configuration: Experimental Results

- Non-linear frequency shift with increasing acceleration amplitude
- Moderate hysteresis evident (hardening)

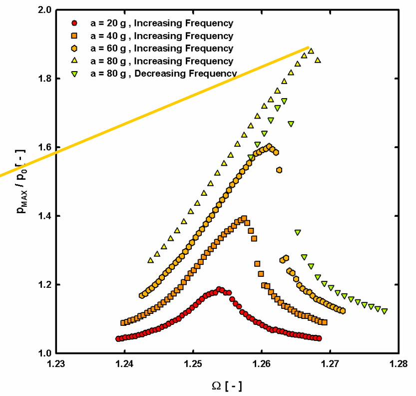

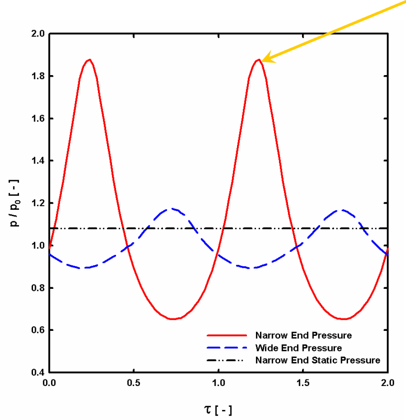

- Constant max acceleration: 80g
- P_o = 100.2 kPa (14.5 psia)
- No microshocks evident
- P_{MAX} / P_0=1.88 (188.3kPa / 27.3psia)
- Static Pressure rise of 8.4 kPa (1.2psi)

Cylinder shocks below Pmax/Po < 1.1

Closed Resonator Configuration With Blockages

Closed Configuration w/ Blockages: Experimental Setup

- Identical hardware and instrumentation used in Baseline experiments
- Baseline end caps (no ventilation holes)
- Additionally
  - Centrally located cylindrical blockage
    - **ϕ 0.403 inch (1.255 cm)**

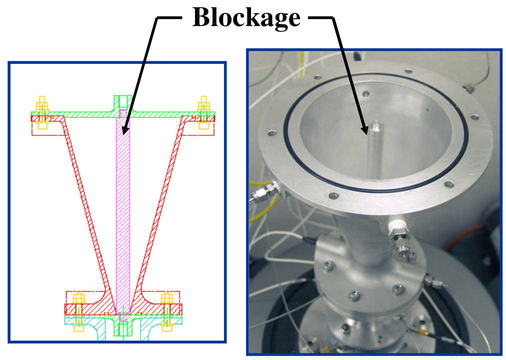

Closed Configuration w/Blockages: Experimental Results

- Blockage Diameter: ϕ 0.403 inch (1.255 cm)
- No apparent hysteresis
- No frequency shift with increasing acceleration amplitude

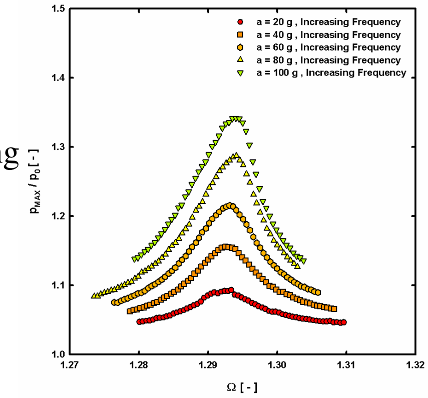

Closed Configuration w/Blockages: Experimental Results

- Blockage Diameter: ϕ 0.403 inch (1.255 cm)
- No apparent hysteresis
- No frequency shift with increasing acceleration amplitude

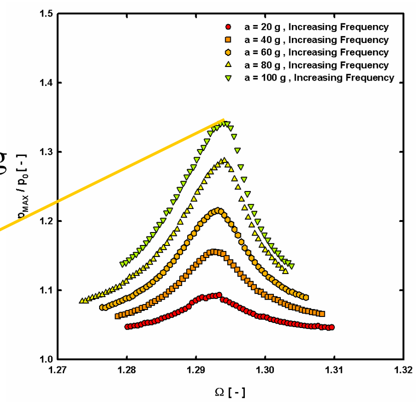

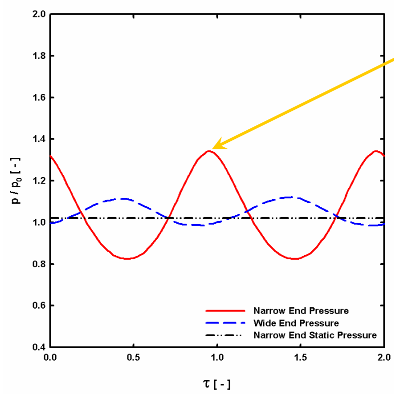

- No microshocks evident
- $P_o = 97.6$ kPa
- $P_{MAX} / P_0 = 1.34$ (130.8 kPa)
- Static Pressure rise of 2.1 kPa

Open Resonator Configuration

Open Resonator Configuration: Experimental Setup

- Identical hardware and instrumentation used in baseline experiments
- End caps
  - Aluminum 7075T6
  - 0.188inch (4.77×10^{-3}m) thickness
- Additionally
  - Wide end cap:
  - one (1) ventilation hole ϕ0.100in ($\phi 2.54 \times 10^{-3}$m)
  - Narrow end cap:
  - eight (8) ventilation holes ϕ0.025in ($\phi 6.35 \times 10^{-4}$m)

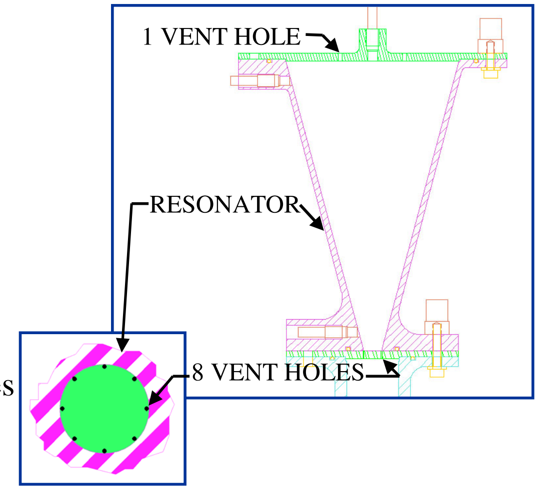

Wide and narrow ventilation have similar areas

Open Configuration: Experimental Results

- Max acceleration: 100g
- No apparent hysteresis
- No frequency shift with increasing acceleration amplitude

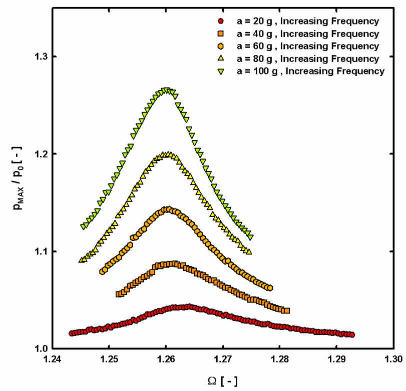

Open Configuration: Experimental Results

- Max acceleration: 100g
- No apparent hysteresis
- No frequency shift with increasing acceleration amplitude

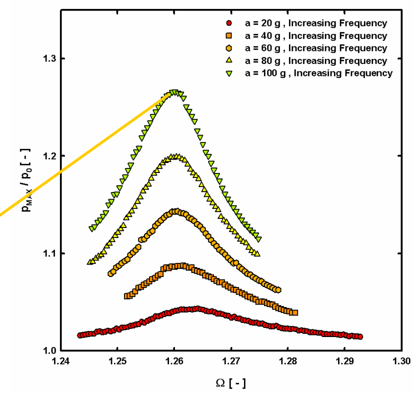

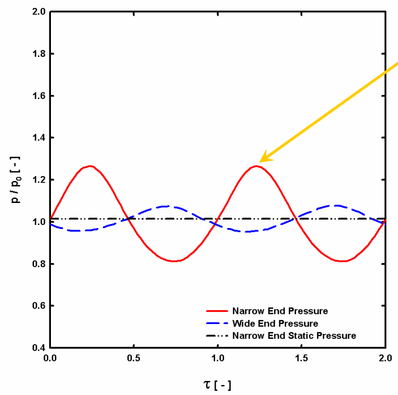

- No microshocks evident
- P_o = 99.2 kPa
- P_{MAX} / P_0 = 1.26 (125.5 kPa)
- Static Pressure rise of ~ 0.5 kPa

Open Resonator Configuration with Pressure Differential

Open Resonator Configuration: Experimental Setup

- Identical hardware and instrumentation used in open resonator experiments
- Additionally
  - Plenum pressurized
  - Air flow metered
- Oscillation conditions:
  - No Oscillation
  - Off Resonance
  - On Resonance

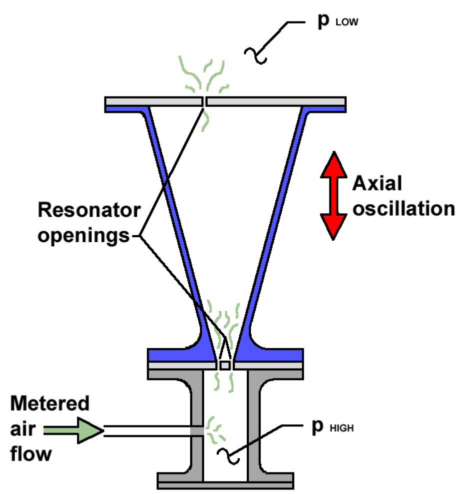

Open Resonator with Differential Pressure Results

- No Oscillation
- Off Resonance
- On Resonance

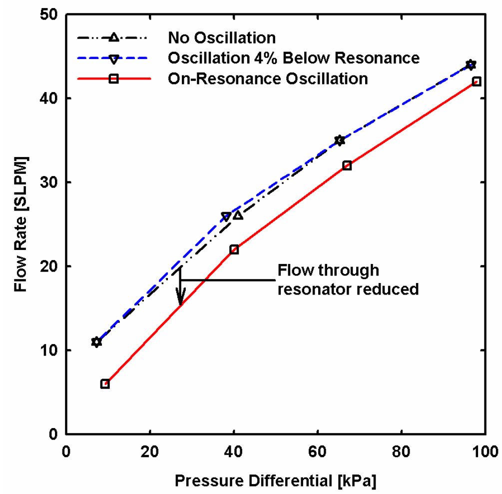

1.5 psi seal

Open Resonator with Differential Pressure Results

- No Oscillation
- Off Resonance
- On Resonance

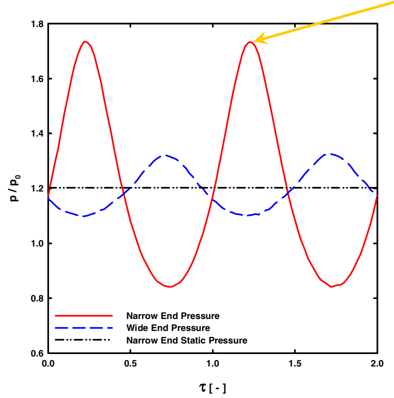

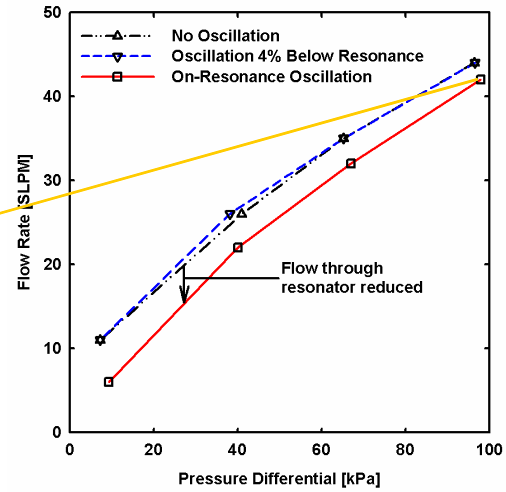

Feasibility of reducing air-flow using acoustic pressurization demonstrated

Summary

1. Standing waves with maximum pressures of 188 kPa have been produced in resonators containing ambient pressure air.
2. Addition of structures inside the resonator shifts the fundamental frequency and decreases the amplitude of the generated pressure waves.
3. Addition of holes to the resonator does reduce the magnitude of the acoustic waves produced, but their addition does not prohibit the generation of large magnitude non-linear standing waves.
4. The feasibility of reducing leakage using non-linear acoustics has been confirmed.

Future Work

- Other resonator shapes are known to produce higher pressure amplitudes (shown right).
- Other advanced seal concepts have been identified and are expected to have greater pressure blocking ability.

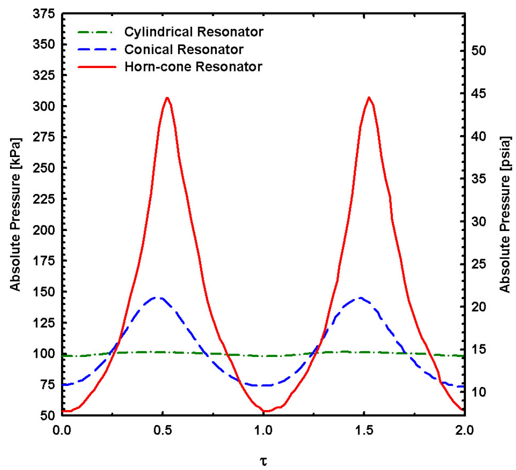

End of Presentation

Appendix

Shock Formation in a Cylindrical Resonator

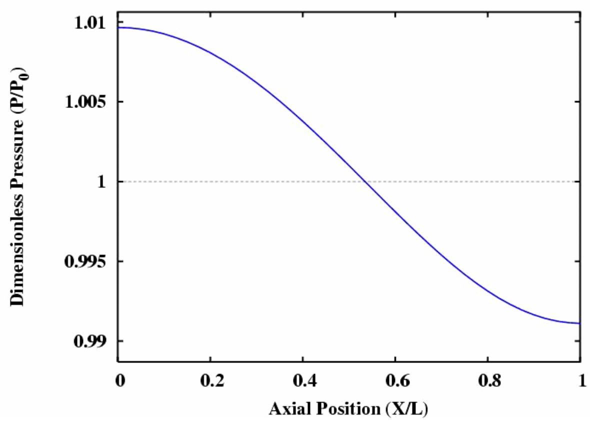

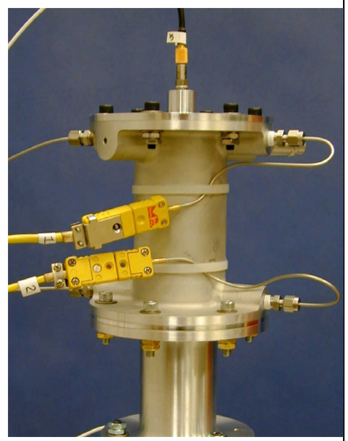

<u>Off</u> Resonant Frequency Oscillation

Shock Formation in a Cylindrical Resonator

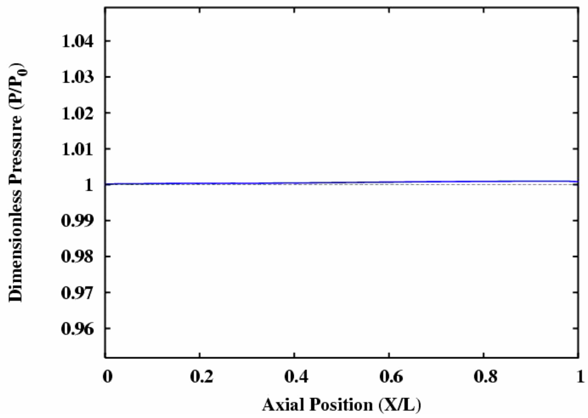

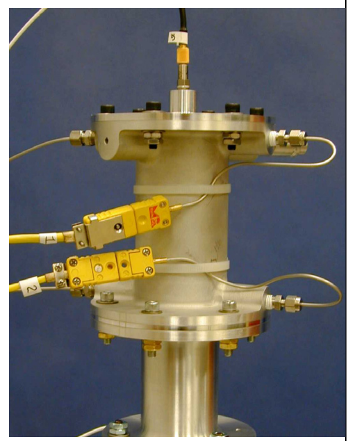

<u>On</u> Resonant Frequency Oscillation

Pressure Waveform in a Horn-cone Resonator

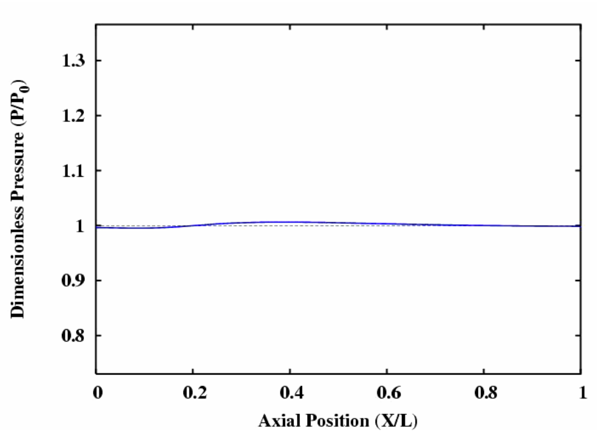

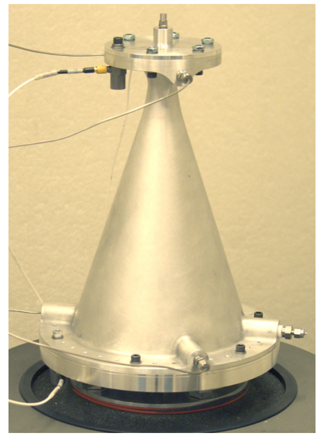

On Resonant Frequency Oscillation

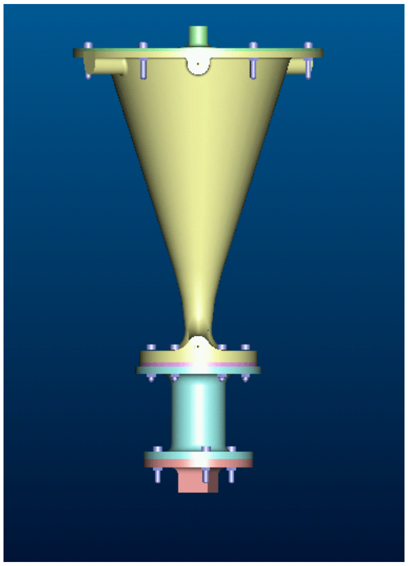

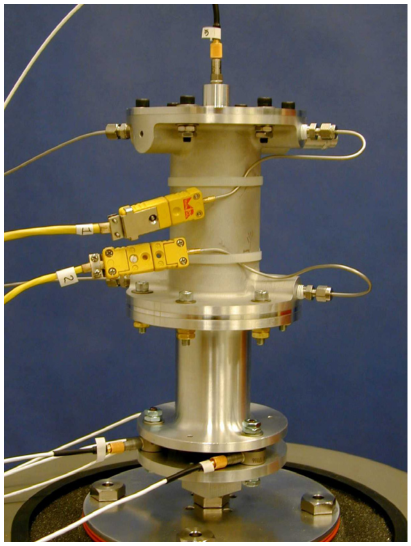

Horn-cone resonator results

Using New Glenn Acoustic Seal Lab:

- Demonstrated high acoustic pressures **(~45psi)** suitable for seals can be generated in closed resonators with **air** as working fluid (Literature: high molecular weight refrigerant)
- Demonstrated high acoustic pressures possible with addition of central shaft blockage

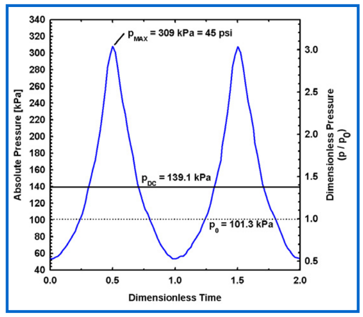

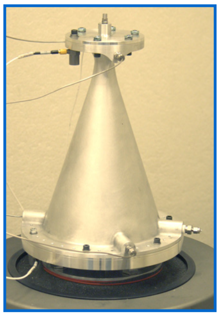

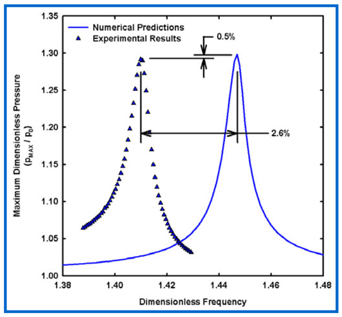

Developed / validated

- 1-Dimensional acoustic resonator analysis/design tool for closed resonators**.**
  - **Good agreement between experimental and predicted pressure amplitudes and resonant frequency**

Closed Configuration w/Blockages: Experimental Results

- Constant maximum sinusoidal acceleration: 80g
- Increasing blockage diameter:
  - Reduces P_{MAX}
    - **$P_{MAX} / P_0 = 1.65$ (ϕ0.403 inch)**
    - **$P_{MAX} / P_0 = 1.57$ (ϕ0.443 inch)**
  - Increases fundamental resonant frequency
    - **$\Omega_1 = 1.293$ (ϕ0.403 inch)**
    - **$\Omega_1 = 1.299$ (ϕ0.443 inch)**

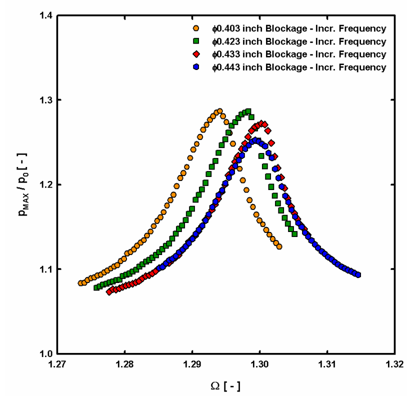

Comparison of Results

- Maximum Acceleration Amplitude: 80g
- From the baseline configuration:
  - P_{MAX} reduced 31% with addition of openings
  - P_{MAX} reduced 36% with addition of blockages
  - Ω increased 2% with addition of blockages

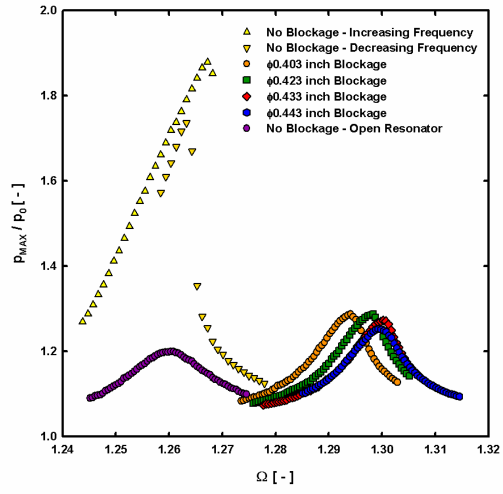

NUMERICAL INVESTIGATIONS OF HIGH PRESSURE ACOUSTIC WAVES IN RESONATORS

Mahesh Athavale and Maciej Pindera
CFD Research Corporation
Huntsville, Alabama

Christopher C. Daniels
Ohio Aerospace Institute
Brook Park, Ohio

Bruce M. Steinetz
National Aeronautics and Space Administration
Glenn Research Center
Cleveland, Ohio

CFD Research Corporation, 215 Wynn Dr., Huntsville, Al 35805 - www.cfdrc.com

Enabling Better Products
By Simulation & Innovation

NUMERICAL INVESTIGATIONS OF HIGH PRESSURE ACOUSTIC WAVES IN RESONATORS

M. Athavale, M. Pindera
CFD Research Corp., Huntsville, AL
C. Daniels, B. Steinetz
NASA GRC, Cleveland, OH

November 5-6, 2003
2003 NASA Seal/Secondary Air System Workshop
OAI, Cleveland, OH

This presentation presents work on numerical investigations of nonlinear acoustic phenomena in resonators that can generate high-pressure waves using acoustic forcing of the flow. Time-accurate simulations of the flow in a closed cone resonator were performed at different oscillation frequencies and amplitudes, and the numerical results for the resonance frequency and fluid pressure increase match the GRC experimental data well. Work on cone resonator assembly simulations has started and will involve calculations of the flow through the resonator assembly with and without acoustic excitation. A new technique for direct calculation of resonance frequency of complex shaped resonators is also being investigated. Script-driven command procedures will also be developed for optimization of the resonator shape for maximum pressure increase.

OUTLINE

- Overview and Objectives
- Description of Methodology
- Closed Cone Resonator, Bomb Tests
- Flow in Cone Resonator Assembly
- Summary

OVERVIEW AND OBJECTIVES

- **Acoustic Resonators are Used to Build Large Pressure Changes by Nonlinear Amplification of Small/Acoustic Disturbances**
  - acoustic forcing at resonance frequency sets up re-enforcement of pressure waves
  - different resonator shapes for better performance
  - gas compressors, e.g. in refrigeration systems,
  - fluid sealing..
- **Current Available Design Tools Consist of 1-D Numerical and/or Analytical Models**
  - for estimation of resonance freq., pressurization
  - limited usefulness in complex flow systems+resonators

OVERVIEW AND OBJECTIVES

- **Objectives of this Project is to Test and Adapt a High-Fidelity CFD Code for Analysis and Design Prototyping of Acoustic Resonators**
  - calculation of resonance frequencies of complex-shaped resonators
  - estimation of the pressure performance of resonators
  - optimization of resonator shapes using script-driven automated analysis procedures
  - simulations of full resonator assemblies to predict flow-performance in actual systems

DESCRIPTION OF METHODOLOGY

- Utilize an Advanced CFD Solver CFD-ACE+ for Fully-Resolved Flow Analysis of Resonators;

  Salient Features are:

  - finite volume, pressure based
  - high-order spatial and temporal resolution
  - moving grid formulation for oscillator excitation
  - conjugate heat transfer; real gas effects,
  - script-based code execution for automated grid generation, code execution, and for optimization of resonator shape

DESCRIPTION OF RESONATOR SET UP

- Acoustic Resonators are Typically Axisymmetric Tubes with Different Shapes
  - cylindrical, conical, half-cosine shaped

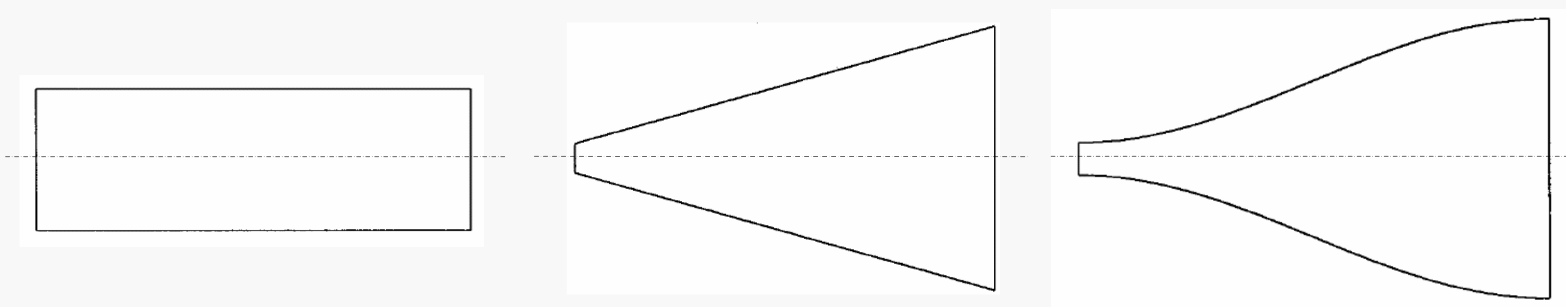

- Shape of the Wall and Tube Length are Key Parameters that Decide Pressurization, Resonance Frequency
- Vibrate the Entire Resonator to Input Acoustic Energy
- Cone Resonator Analyzed
  - pressure history at different frequencies
  - numerical results compared with GRC experimental data

CONE RESONATOR SCHEMATIC

- The GRC Cone Resonator Setup Was Used in the Simulations, for both Closed Resonator and Resonator with Flow

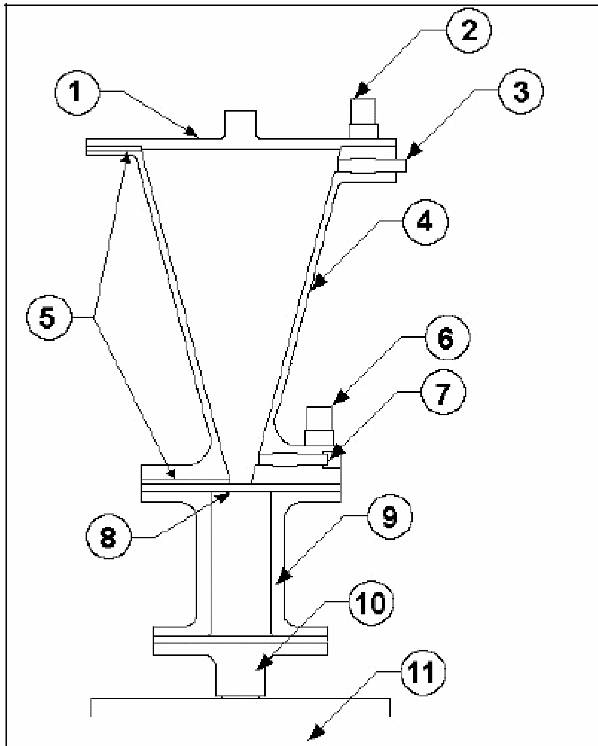

1. Sealed wide end cap
2. Wide end accelerometer
3. Wide end dynamic pressure transducer
4. Acoustic resonator
5. Static pressure and thermocouple ports
6. Narrow end accelerometer
7. Narrow end dynamic pressure transducer
8. Sealed narrow end cap
9. Attachment to shaker table
10. Attachment to shaker table
11. Electrodynamic shaker

©CFD Research Corporation – http://www.cfdrc.com

CLOSED CONE RESONATOR MODEL SETUP

- 2-D Axisymmetric Representation of Resonator
- Computational Grid: 50x18 Cells
- Flow and Boundary Parameters:
  - air as compressible working fluid, laminar flow
  - acoustic forcing through a sinusoidal motion imposed on all walls, @ different accelerations
  - 3-rd order convective fluxes, time step @ ~ CFL = 0.5
  - two acceleration amplitudes : 10 and 50g
  - different frequencies: between 1285-1295 Hz

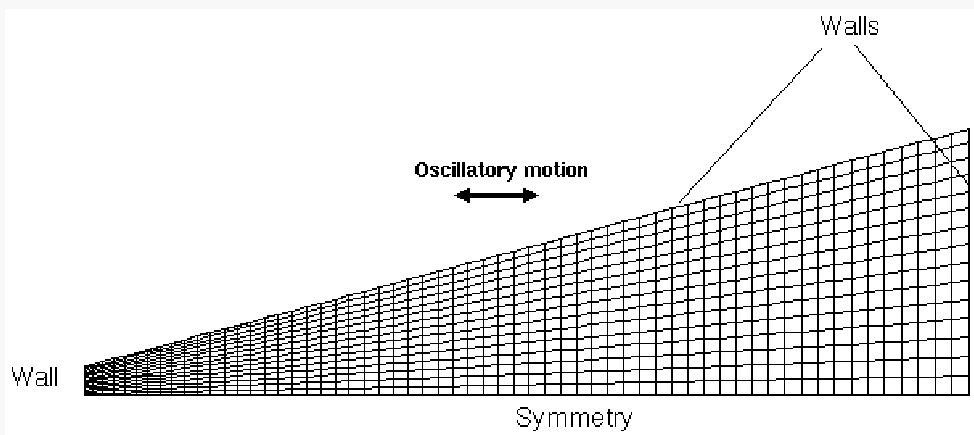

CONE RESONATOR RESULTS

- Static Pressure Field in the Resonator, at Resonance, Oscillation Frequency = 1288 Hz, Accel. Ampl. = 50g

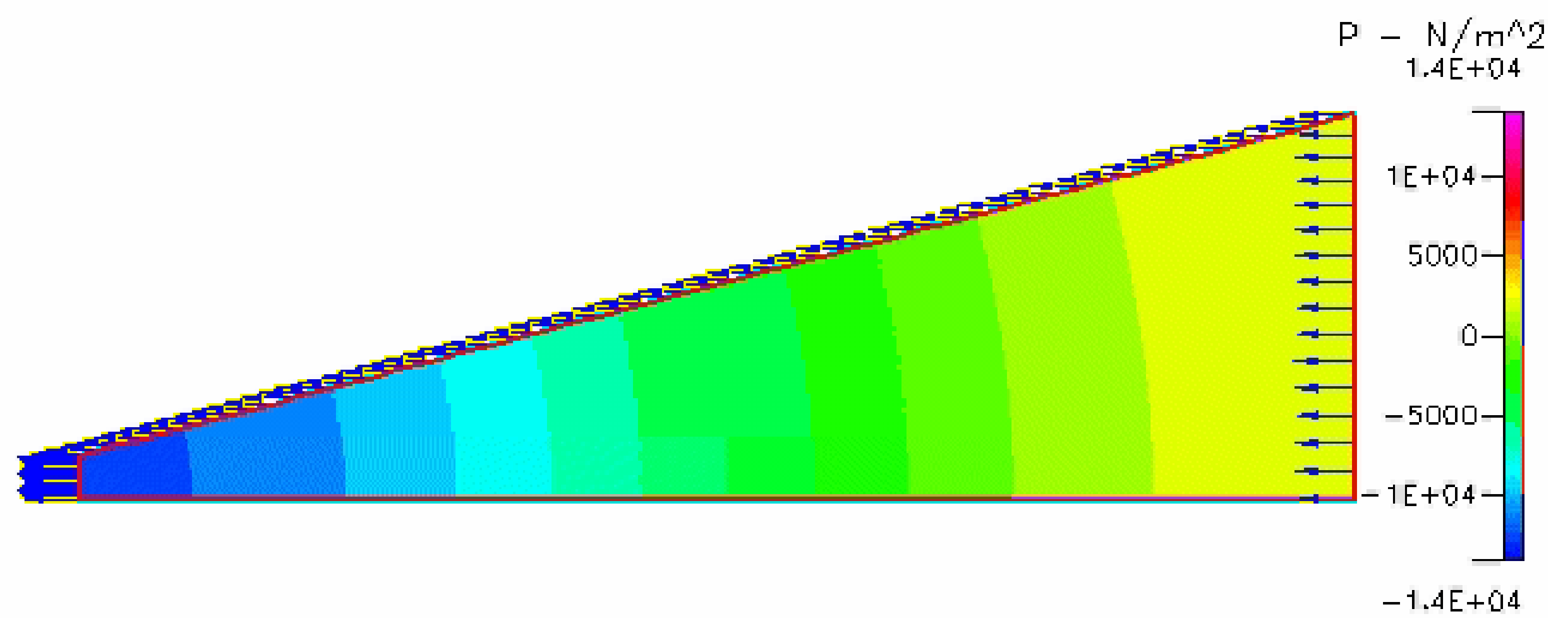

CONE RESONATOR RESULTS

- **Static Pressure Trace at the Narrow End; Plotted for Different Frequencies near Resonance, Accel. Ampl. = 10g**

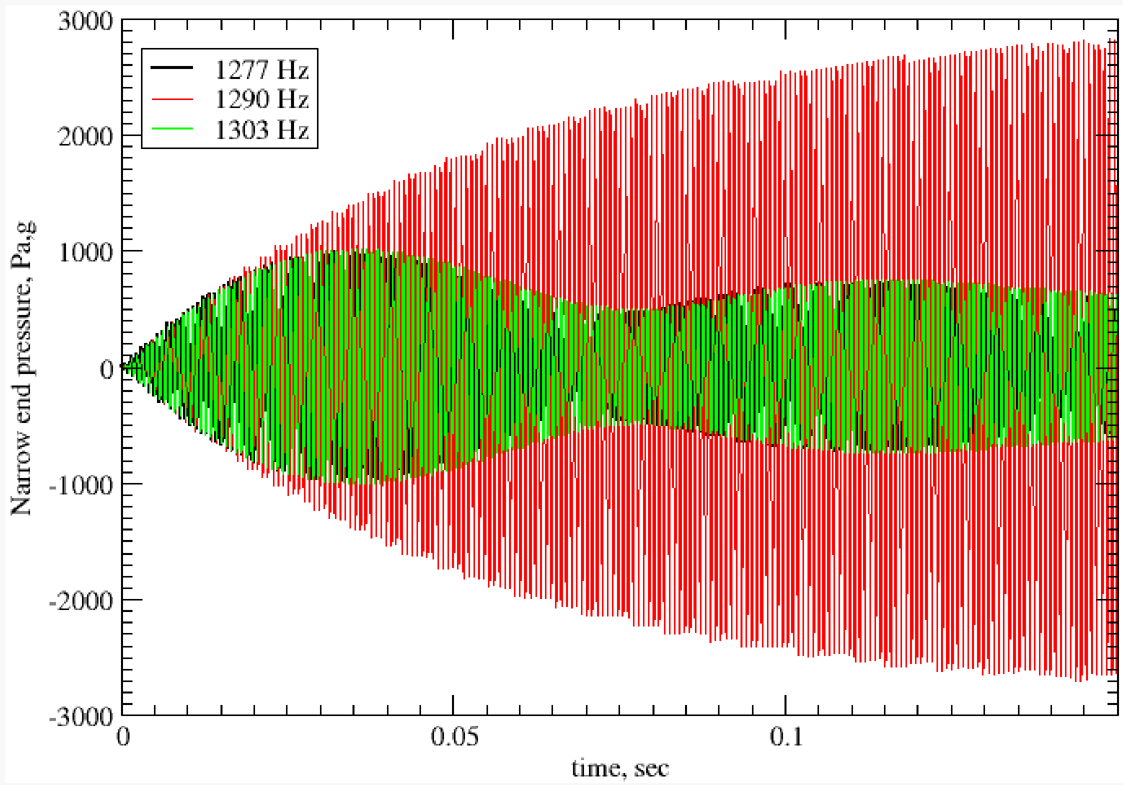

CONE RESONATOR RESULTS

- **Static Pressure Trace at the Narrow End; Plotted for Different Frequencies near Resonance, Accel. Ampl. = 50g**

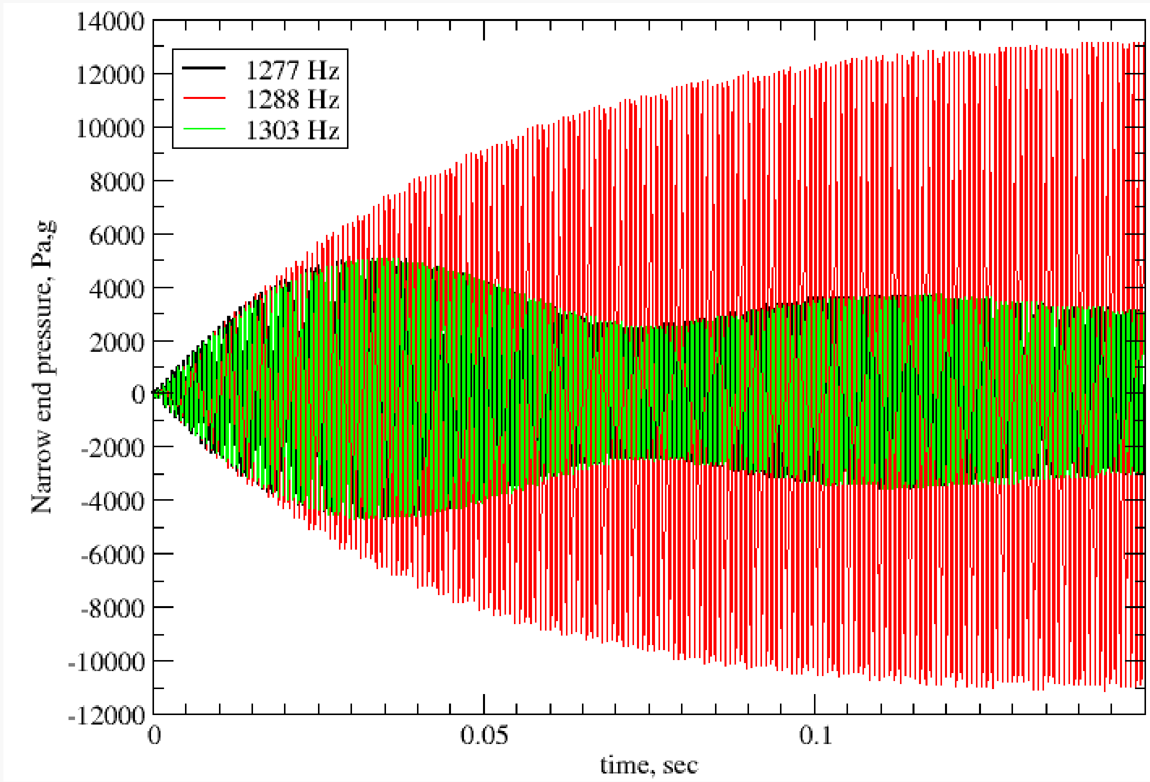

CONE RESONATOR RESULTS

- Calculated and Experimental Results for the Cone Resonator: Pressurization and Resonance Frequencies
  - the experimental and computed resonance frequencies match well
  - pressurization amplitude is also reasonably well predicted

Acceleration Amplitude	Resonance Frequency, Hz Experimental	Resonance Frequency, Hz Numerical	Maximum Pressure, kPa Experimental	Maximum Pressure, kPa Numerical
10 g	1287-1293	1288	118.331	114.5
50 g	1287-1293	1290	104.148	103.28

CONE RESONATOR BOMB TESTS

- Resonance Frequency of Resonator is a Key Parameter
  - treatment of complex shaped resonators is difficult
  - frequency-scanning is one approach: calculate pressurization @ different frequencies
- Proposed New Method: Based on Bomb Tests
  - impose an initial pressure distribution in the resonator; typically a half-cosine wave with a large amplitude
  - calculate the time-accurate flow field as the initial pressure wave settles into an oscillatory response at the resonance frequency
- Trial and Error for Resonance Frequencies is Not Needed

BOMB TEST RESULTS

- Sample Pressure Field and Pressure Trace at the Narrow End of the Resonator, Initial Pressure Amplitude 6 MPa
  - Fourier transform of pressure trace → resonance frequency
  - no trial and error needed for frequency calculations
- Preliminary Results Show Predicted Frequencies Within 3%, Further Refinements in Progress

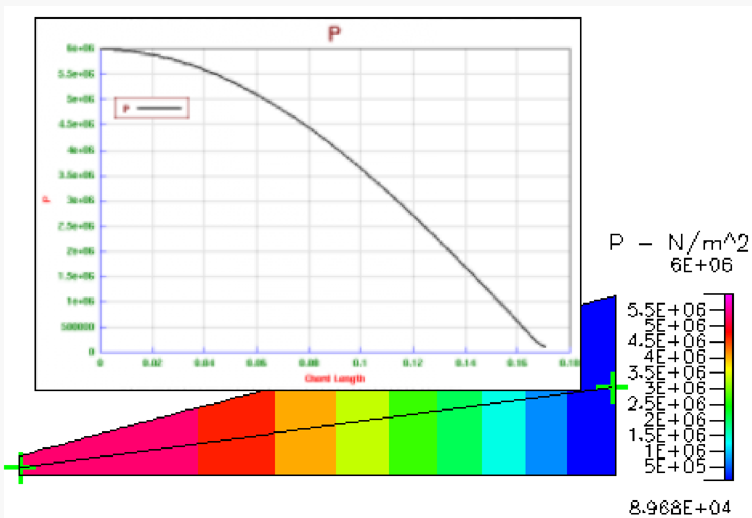

Initial pressure distribution

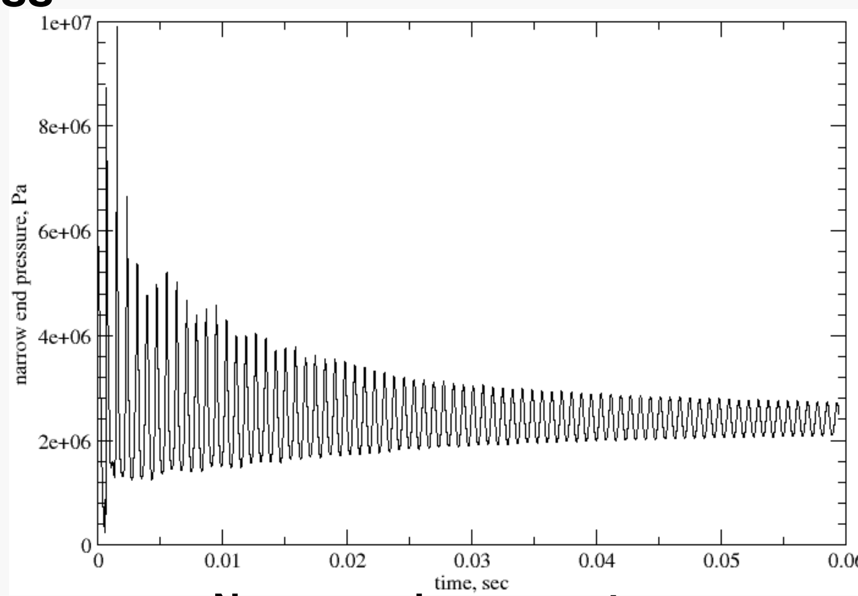

Narrow end pressure trace

©CFD Research Corporation – http://www.cfdrc.com

RESONATOR ASSEMBLY FLOW SETUP

- Work on the GRC Resonator Flow Experimental Setup Was Started and is in Progress
- Schematic of the Computational Model Shown
  - 2-D axisymmetric representation of the assembly used
  - flow passages (holes) represented by 2-d slits
  - slit widths initially matched flow areas, subsequently changed to match steady-state flow rates
  - pressure differential across the assembly generates airflow through the resonator
- Air as Working Fluid, Laminar Flow, Ambient Pressure @ 99 kPa, Plenum Pressurization of 7.3, 41.3, 65.6 kPa and 96.9 kPa above Ambient

RESONATOR ASSEMBLY FLOW SETUP

- **Computational Geometry, Grid and Boundary Condition Setup**

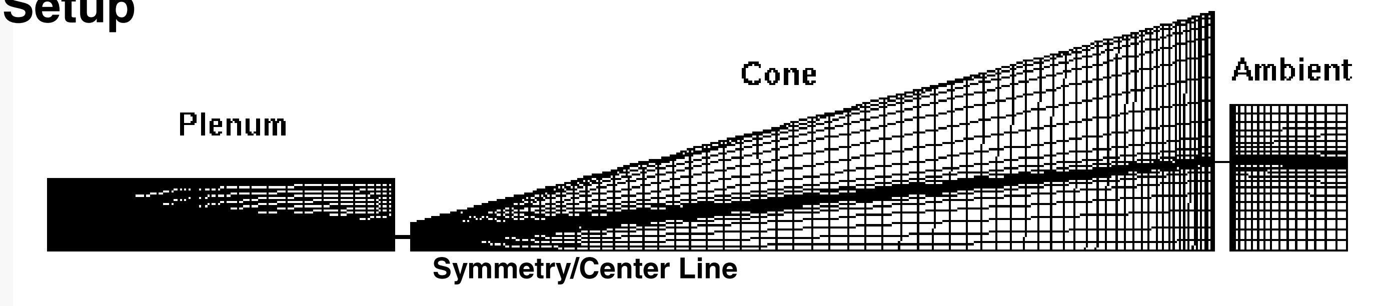

Full Model

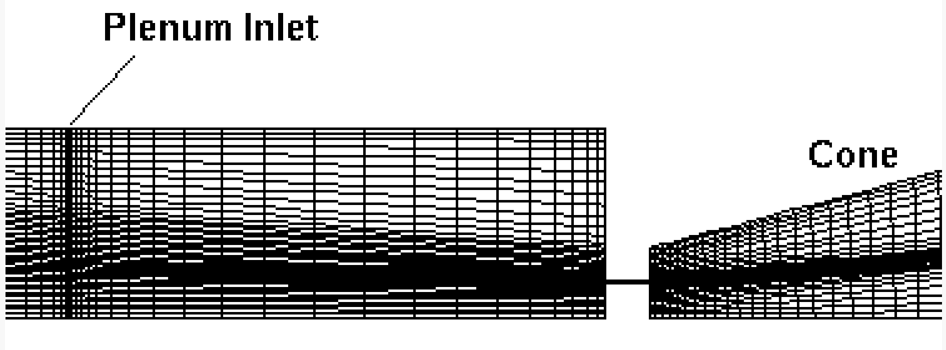

Detail Near Plenum

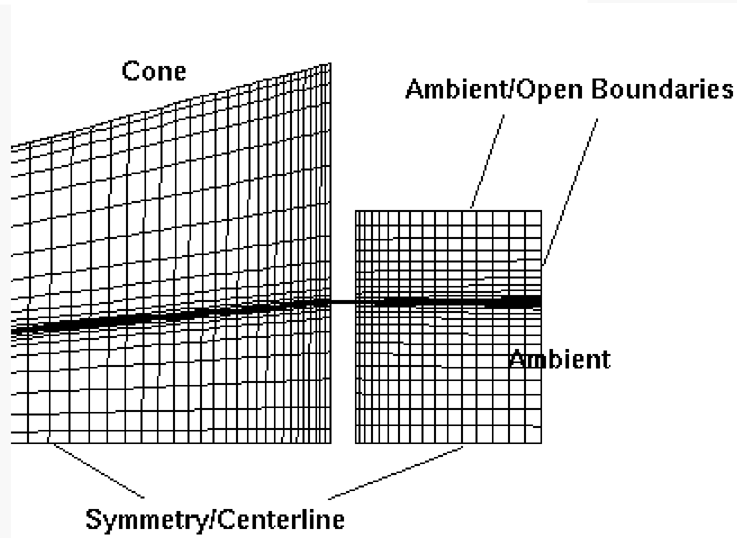

Detail Near Exhaust

RESONATOR ASSEMBLY STEADY-STATE RESULTS

- **Steady-State Results Obtained at Four Plenum Pressure Levels: 7.3, 41.3, 65.6 and 96.9 kPa**
  - **calculated mass flow rates compared with GRC experiments**
  - **2-D flow slit widths were adjusted to match experimental flow rates**
- **Sample Results for Plenum Pressurization of 97 kPa:**

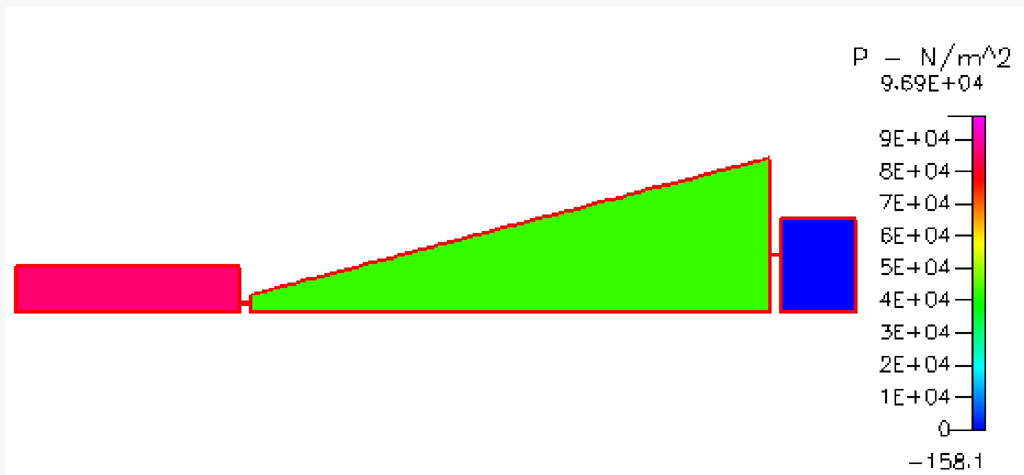

©CFD Research Corporation – http://www.cfdrc.com

RESONATOR ASSEMBLY TRANSIENT RESULTS

- Starting With the Steady-State Flow Results, Assembly Oscillations were Imposed as Moving Wall Conditions
- Oscillation Frequency Initially Set to 1300 Hz (Experimental value)
  - for initial runs, two plenum pressurization cases were used: lowest (7.3 kPa) and highest (96.9 kPa)
  - static pressure trace at narrow end of the cone used to assess the resonance frequency
  - numerical results showed that the resonance was at a much lower frequency of approximately 1280 Hz

RESONATOR ASSEMBLY VELOCITY FIELDS

- Resonator Oscillations Generate Time-Dependent Pressure Fields in the Plenum and Resonator
- Transient Velocity and Pressure Field @ 96.9 kPa and 1280 Hz

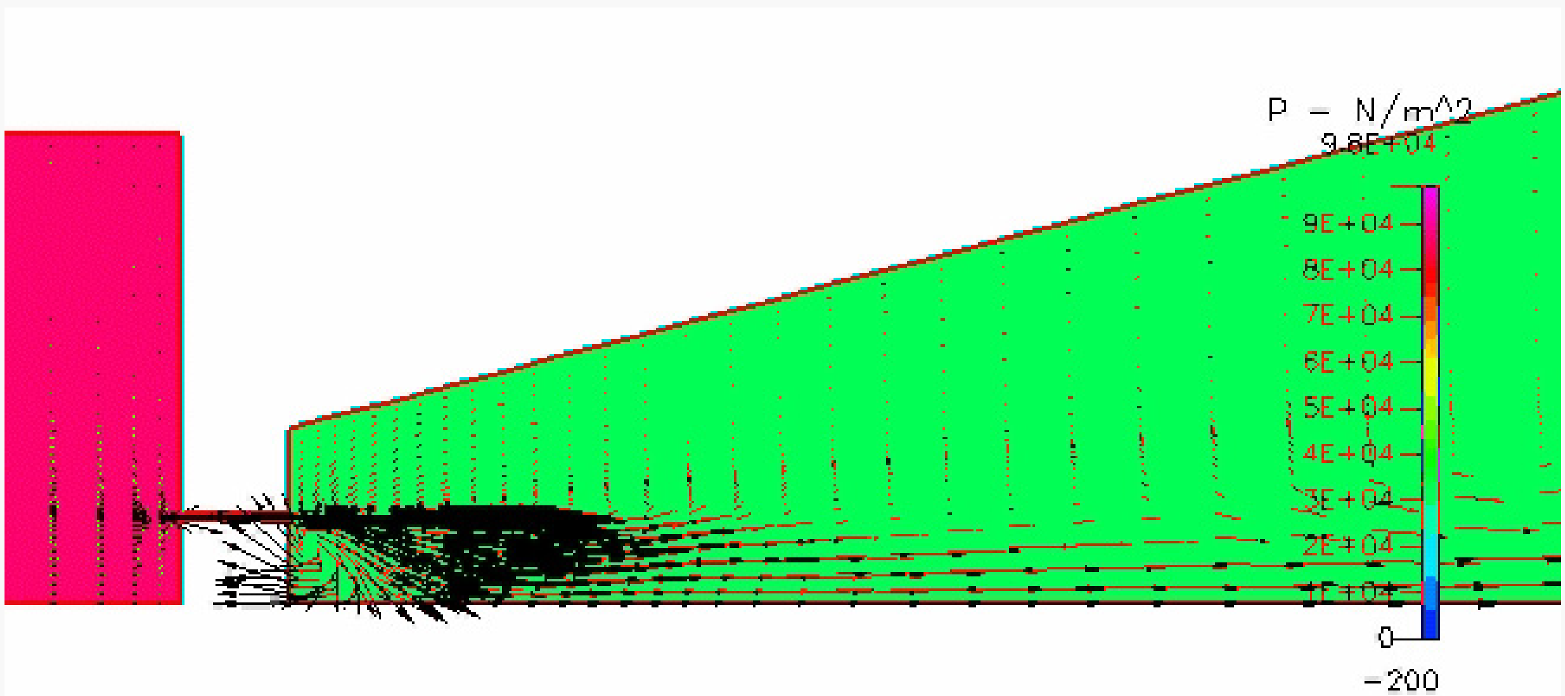

RESONATOR ASSEMBLY VELOCITY FIELDS

- **Transient Velocity and Pressure Fields @7.3 kPa and 1288 Hz**

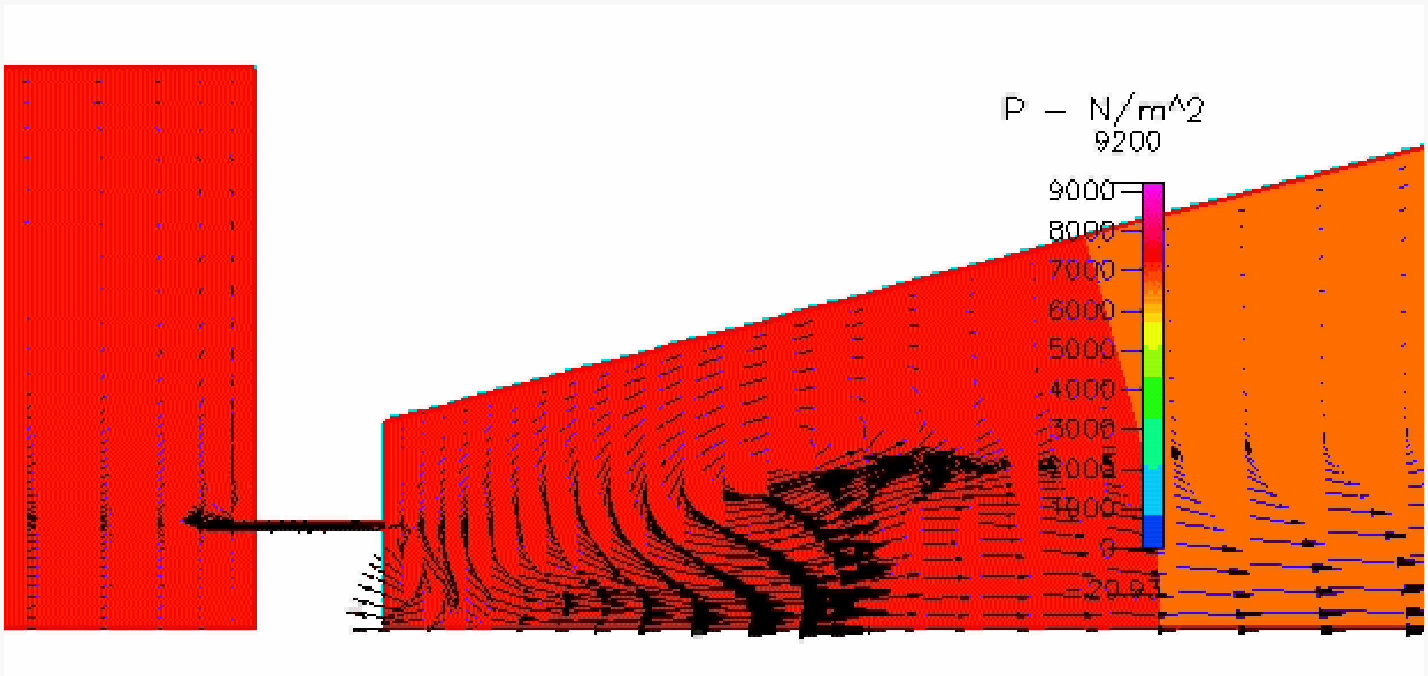

RESONATOR ASSEMBLY TRANSIENT RESULTS

- Cone Narrow End Pressure Trace for Different Oscillation Frequencies Used to Estimate Resonance Conditions
  - sample results for 96.9 kPa plenum pressurization shown

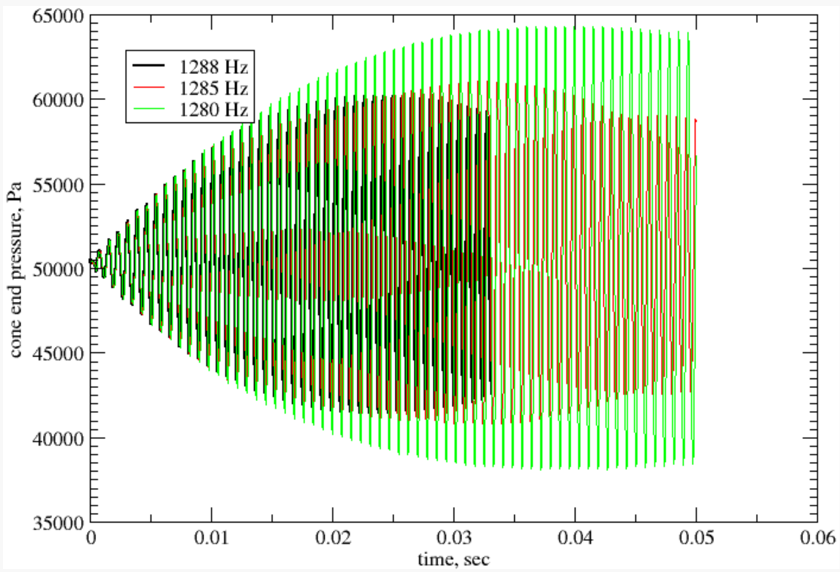

Narrow end pressure trace

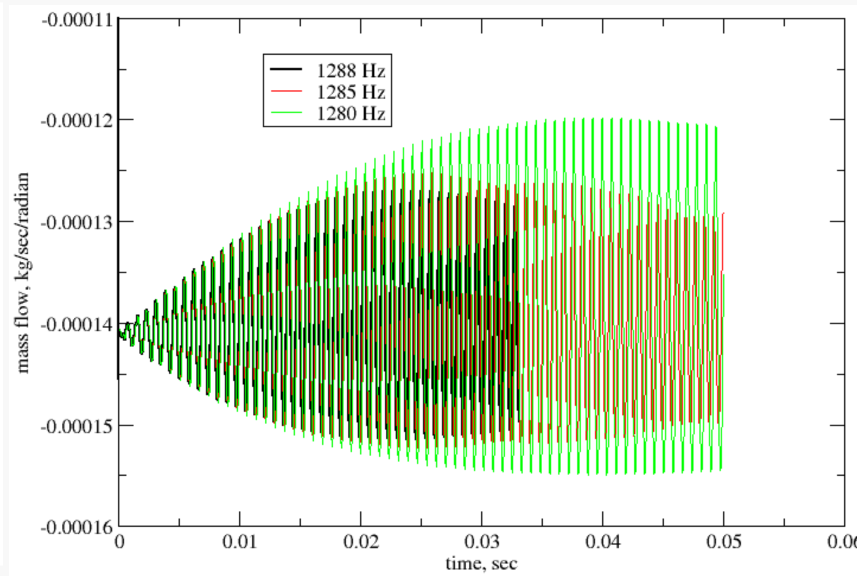

Resonator mass flow

©CFD Research Corporation – http://www.cfdrc.com

RESONATOR ASSEMBLY TRANSIENT RESULTS

- The Variable Velocity Field Results in a Different Mass Flow Going Through the Resonator Assembly
- Experiments Show a Net Reduction in the Resonator Mass Flows When Oscillating at the Resonance Conditions
- Numerical Results Also Show a Net Reduction in the Mass Flow Rates When Oscillations are Turned on.
  - predicted values of flow reduction are smaller than those seen in experiments
- Numerical Predictions of the Resonance Frequency is also Lower than the Experimental Value
- Currently Several Aspects are Being Explored to Reconcile Numerical and Experimental Results
  - assessment of the 2-d slit representation of the oscillator
  - effects of air heating seen during experiments

SUMMARY

- Successfully Demonstrated Use of a CFD Code for Calculations of Non Linear Acoustics in a Cone Resonator
  - resonance frequencies, resonator pressurization compared with experiments
  - ‘bomb’ test could be used for resonance predictions
- Resonator Assembly Simulations with Flow in Progress
  - initial steady-state and transient results
  - validation against experiments underway
- Work in Progress Towards Establishing a CFD Code for Design Prototyping and Optimization of Resonators

FELTMETAL® SEAL MATERIAL THROUGH-FLOW

Doug Chappel
Technetics Co.
DeLand, Florida

Technetics CORPORATION

Feltmetal® Seal Material Through - Flow

What Is Feltmetal®?

Micron Size Fiber Sinter Bonded Into A Continuous Felt

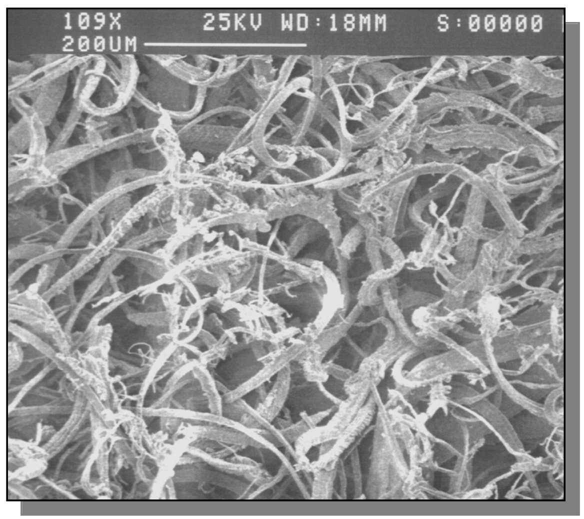

- Typically Hast-X or FeCrAlY
- Density Range 10 - 50%
- UTS Range 500 – 3000 psi
  (3.5 – 20.7 MPa)

Feltmetal® Abradable Materials Improve Turbomachinery Performance By Minimizing Operating Clearances

- Over 250M Hours Operating Experience
- Capable To 1400 F (760 C)
- Properties Can Be Tailored To Specific Customer Application

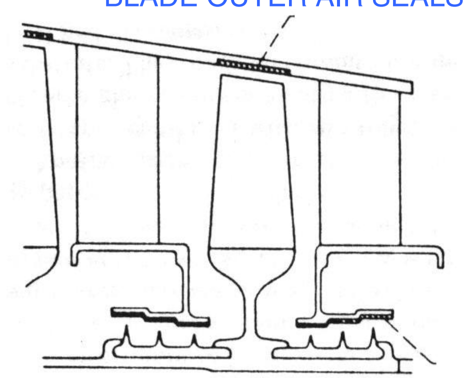

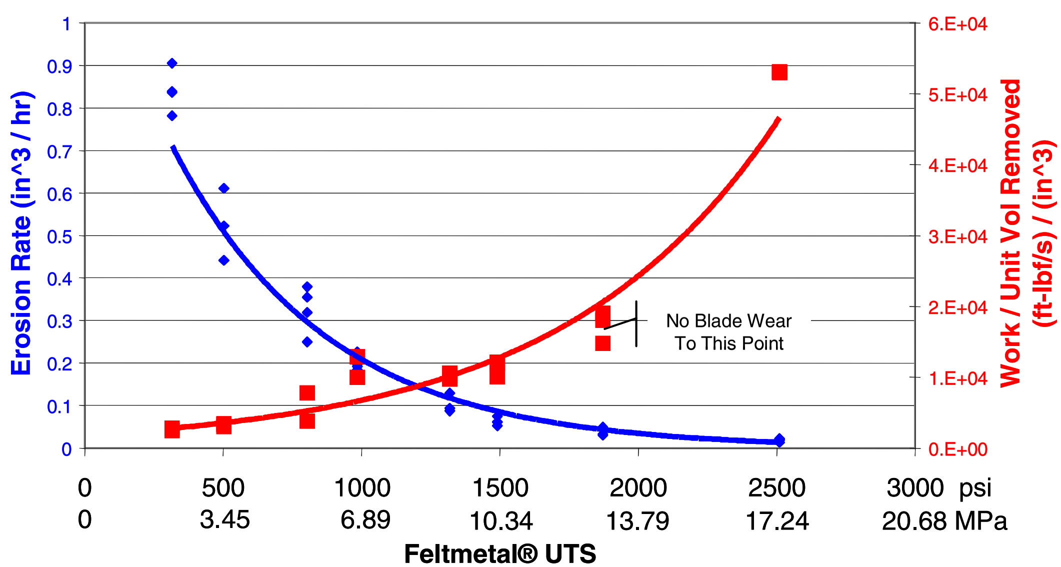

Being A Porous Material, There Will Be Some Leakage Flow Through The Feltmetal® Material Itself

One Engineer At A Large Aero Engine
Manufacturer Recalls His Boss Blowing Pipe
Smoke Through A Feltmetal Sample.

Simple Test Fixture Used To Compare Material Permeability

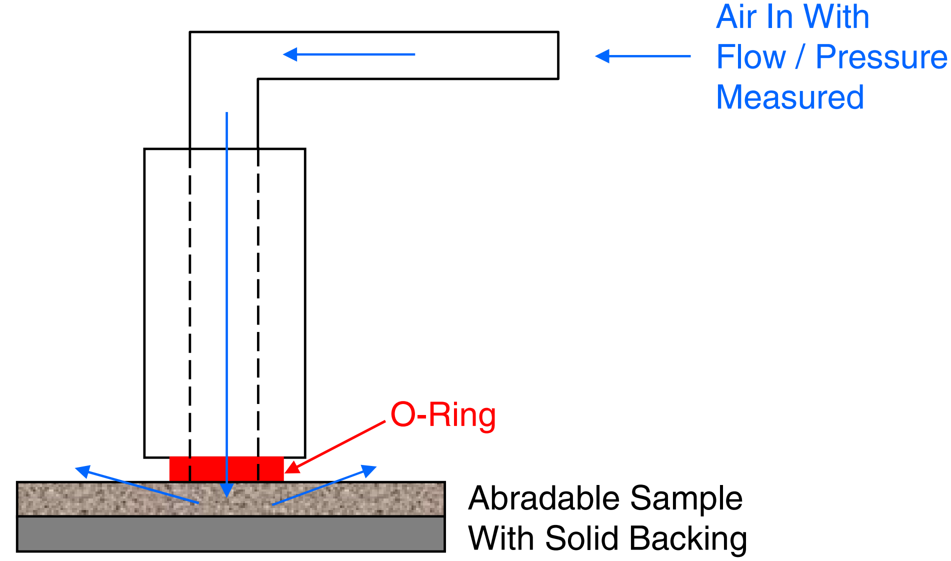

Increasing FM Density Decreases Leakage Flow

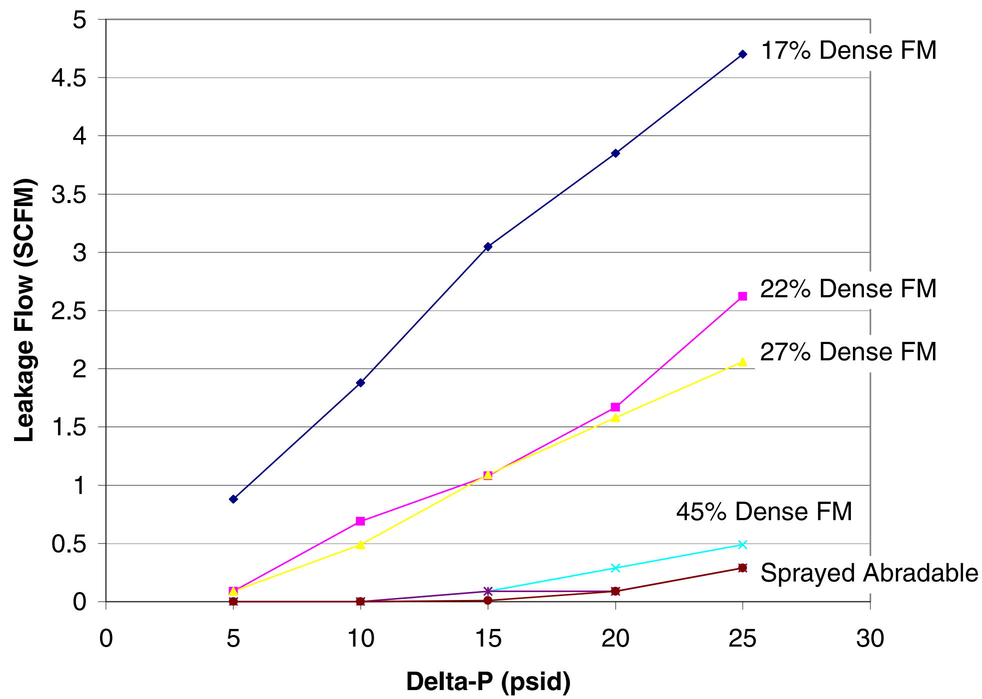

Abradability Properties Are Dependent On
Felt Tensile Strength NOT Felt Density

Technetics Test Rig Was Used To Evaluate Through – Flow In A Labyrinth Seal Configuration

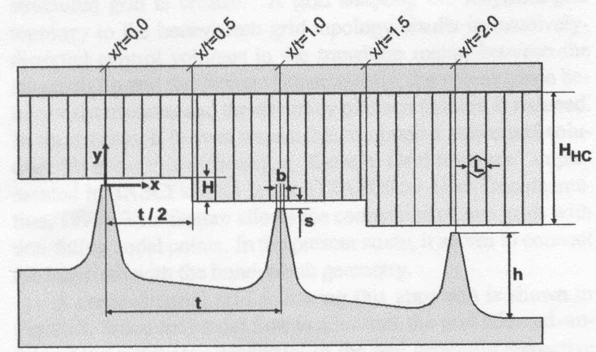

Figure 1. GEOMETRY OF LABYRINTH SEAL: h/t=0.46 , H/t=0.14, b/t=0.047, HC/t=0.86, L/t=0.23, s/t=0.043 . . . 0.114, $t = 28mm$

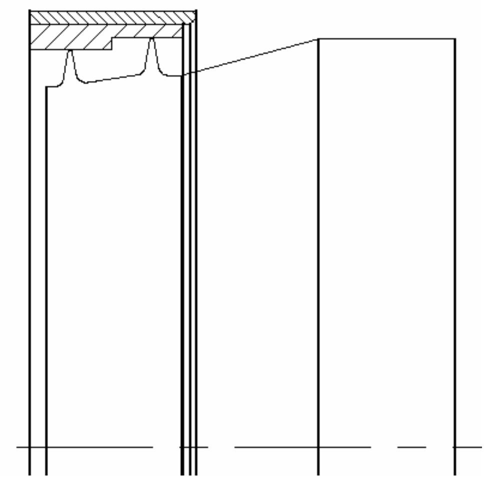

Seal Geometry Modeled After Universität Karlsruhe Test Configuration (2000-GT-0291)

Flow Comparison:
19% Dense Material vs. Simulated 100% Dense Material

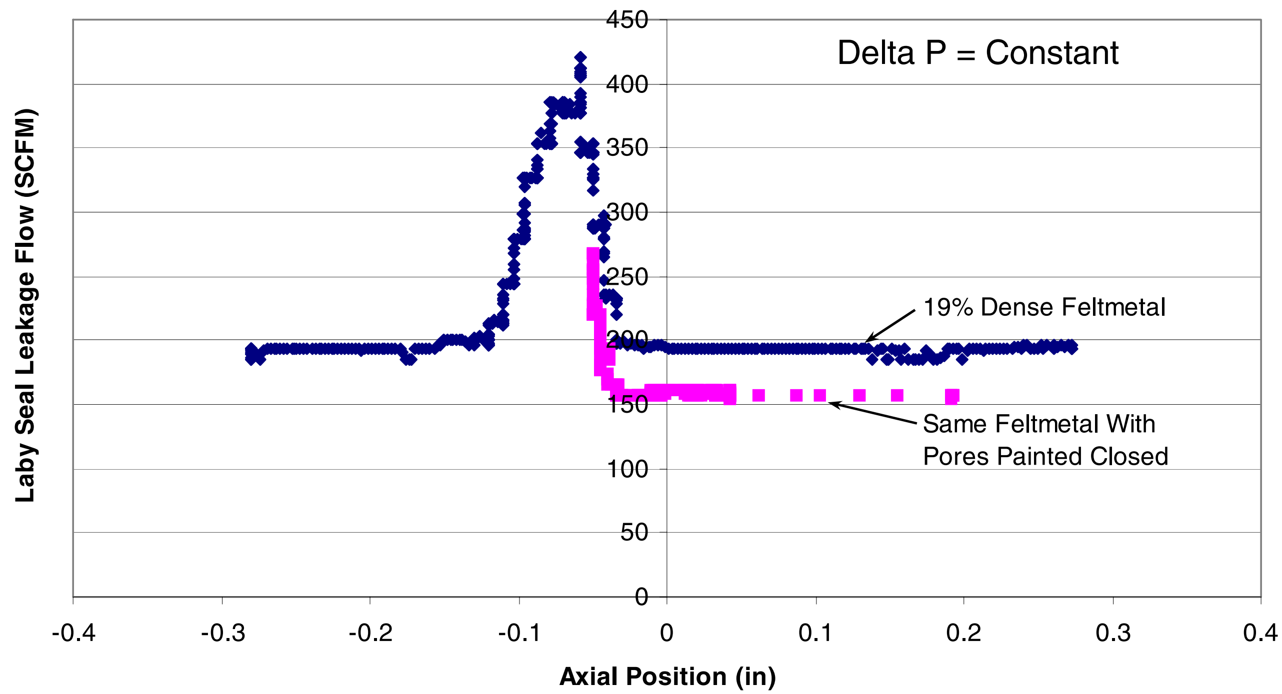

~18% Of Total Flow Attributed To Through-Flow

Increasing FM Density Will Improve Leakage Performance

“BIMODAL” NUCLEAR THERMAL ROCKET (BNTR) PROPULSION
FOR FUTURE HUMAN MARS EXPLORATION MISSIONS

Stan Borowski
National Aeronautics and Space Administration
Glenn Research Center
Cleveland, Ohio

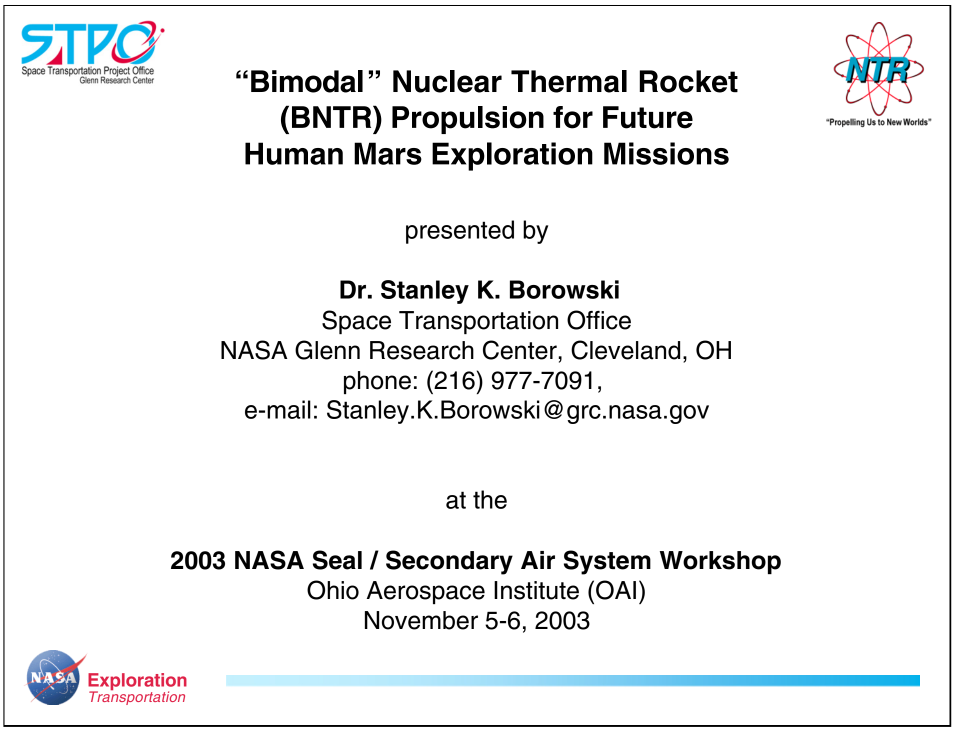

Space Transportation Project Office
Glenn Research Center

Artificial Gravity “Bimodal” NTR Crew Transfer Vehicle (CTV) for Mars DRM 4.0 (1999)

“Propelling Us to New Worlds”

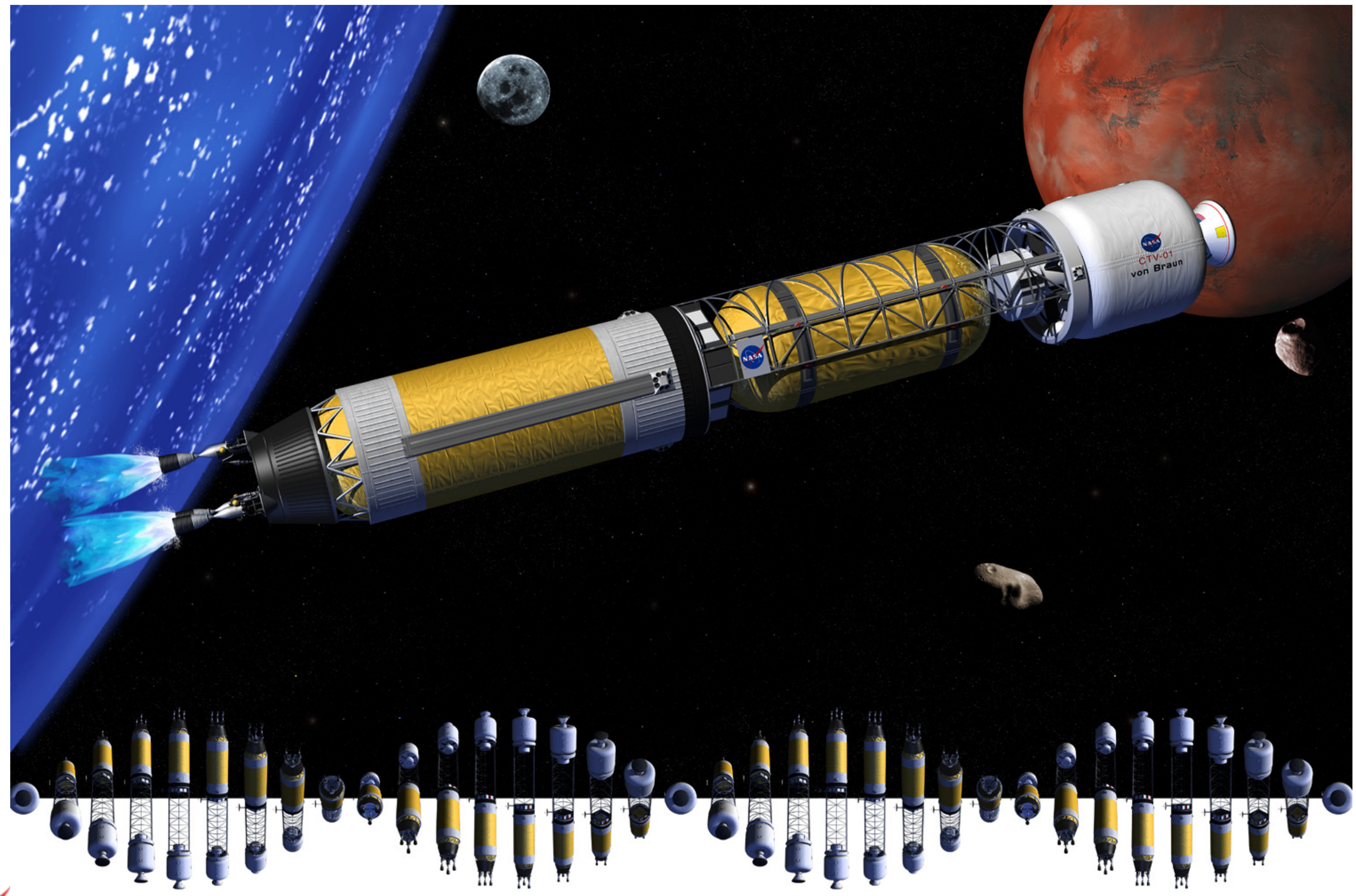

Exploration
Transportation

The "Bimodal" NTR (BNTR) Integrated Space Propulsion & Power System -- Smarter Systems Engineering --

Space Transportation Project Office
Glenn Research Center

"Propelling Us to New Worlds"

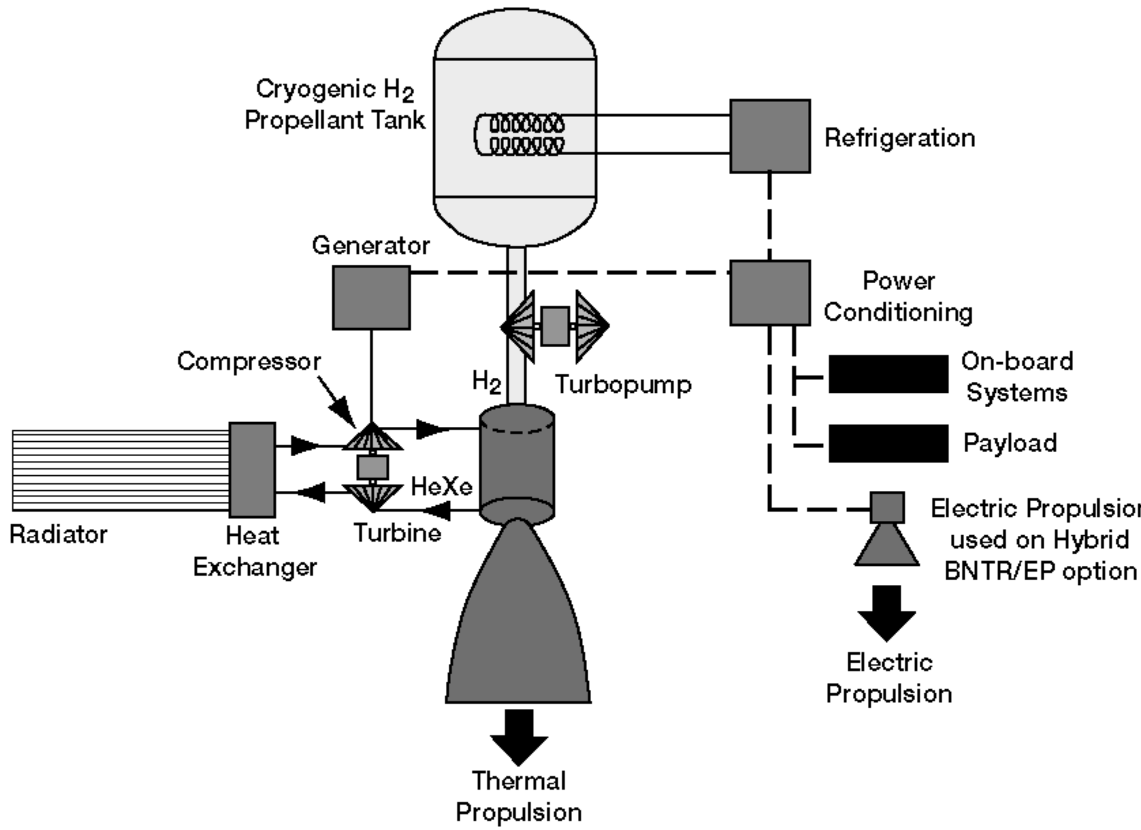

- During short, high thrust propulsion phase, each BNTR produces ~340 MW_t and ~15 klb_f of thrust
- During long, power generation phase, each BNTR operates in "idle mode" producing just ~150 kW_t
- A Brayton conversion unit on each BNTR produces up to 25 kW_e to enhance stage capabilities

Exploration Transportation

Space Transportation Project Office
Glenn Research Center

"Propelling Us to New Worlds"

Rover/NERVA* Program Summary (1959-1972)

- **20 Rocket/reactors designed, built and tested at cost of ~ $1.4 billion**
- **Engine sizes tested**
  - 50-250 klb_f
- **H_2 exit temperatures achieved**
  - 2,350-2,550 K (Graphite fuel)
- **I_{sp} capability**
  - 825-850 sec (hot bleed cycle)
- **Burn duration**
  - 62 mins. (NRX-A6 -- single burn)
  - >4 hrs. (NRX-XE -- 28 burns) (accumulated)
- **Engine thrust-to-weight**
  - ~3 for 75 klb_f NERVA
- **"Open Air" testing at Nevada Test Site**

**NERVA: Nuclear Engine for Rocket Vehicle Applications*

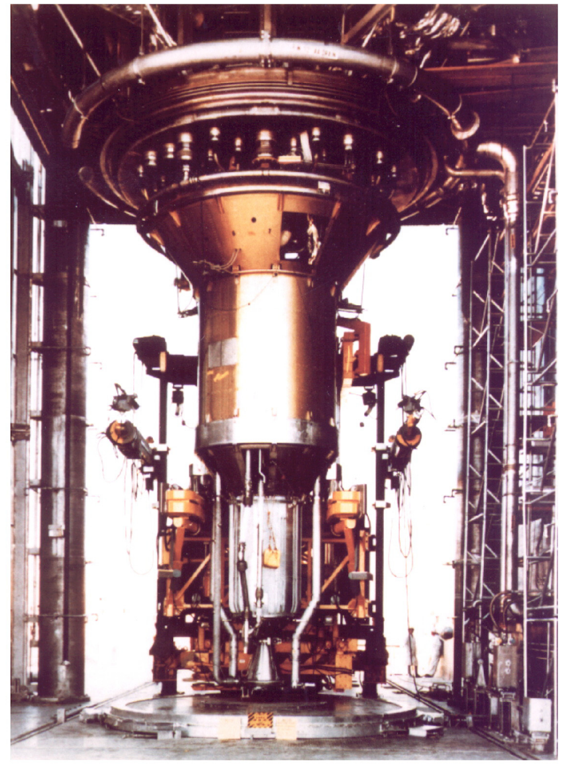

NERVA program experimental engine (XE) demonstrated 28 startup/shutdown cycles during tests in 1969.

Exploration Transportation

Nuclear Thermal Rocket (NTR) Propulsion

What's New?

Then (Rover/NERVA:1959–72)		Now
• **Engine sizes tested** – 50–250 klbf	Smaller, Higher Performance	• **"Current" focus is on smaller NTR sizes** – 5–15 klbf (Code S science–humans)
• **H_2 exit temps achieved** – 2,350–2,550K (Graphite)		• **Higher temp. fuels being developed** – 2,700K (Composite), 2,900K (Cermet) and ~3,100K (Ternary Carbides)
• **Isp capability** – 825–850 sec (hot bleed)	Easier to test	• **Isp capability** – 915–1005 sec (expander cycle)
• **Engine thrust-to-weight** – ~3 for 75 klbf NERVA		• **Advances in chemical rockets/materials** – ~2–6 for small NTR designs
• **Testing (Rover/NERVA)** – "Open Air" exhaust at Nevada test site	Environmentally "Green" For Public Acceptance	• **Small NTR allows full power testing in** – "Contained Test Facility" at INEL with "scrubbed" H_2 exhaust

"Propelling Us to New Worlds"

Space Transportation Project Office
Glenn Research Center

Exploration Transportation

Space Transportation Project Office
Glenn Research Center

Nuclear Thermal Rocket (NTR) Propulsion
-- Key Technology / Mission Features --

"Propelling Us to New Worlds"

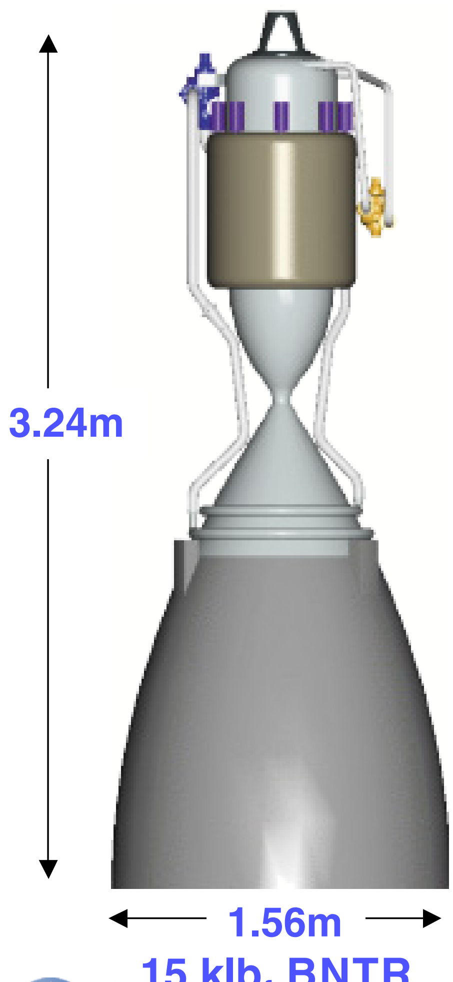

- NTR engines have negligible radioactivity at launch / simplifies handling and stage processing activities at KSC
  - < 10 Curies / 3 NTR Mars stage vs ~400,000 Curies in Cassini's 3 RTGs
- High thrust / Isp NTR uses same technologies as chemical rockets
- Short burn durations (~25-50 mins) and rapid LEO departure
- Less propellant mass than all chemical implies fewer ETO launches
- NTR engines can be configured for both propulsive thrust and electric power generation -- **"bimodal" operation**
- Fewest mission elements and much simpler space operations
- Engine size aimed at maximizing mission versatility
  -- robotic science, Moon, Mars and NEA missions
- NTR technology is evolvable to reusability and "in-situ" resource utilization (e.g., **LANTR -- NTR with LOX "afterburner" nozzle**)

Exploration Transportation

“Bimodal” NTR Cargo & Crew Transfer Vehicles for 1999 Mars Design Reference Mission (DRM) 4.0

6 - “80 t” SDHLVs plus Shuttle for Crew & TransHab Delivery

Space Transportation Project Office
Glenn Research Center

“Propelling Us to New Worlds”

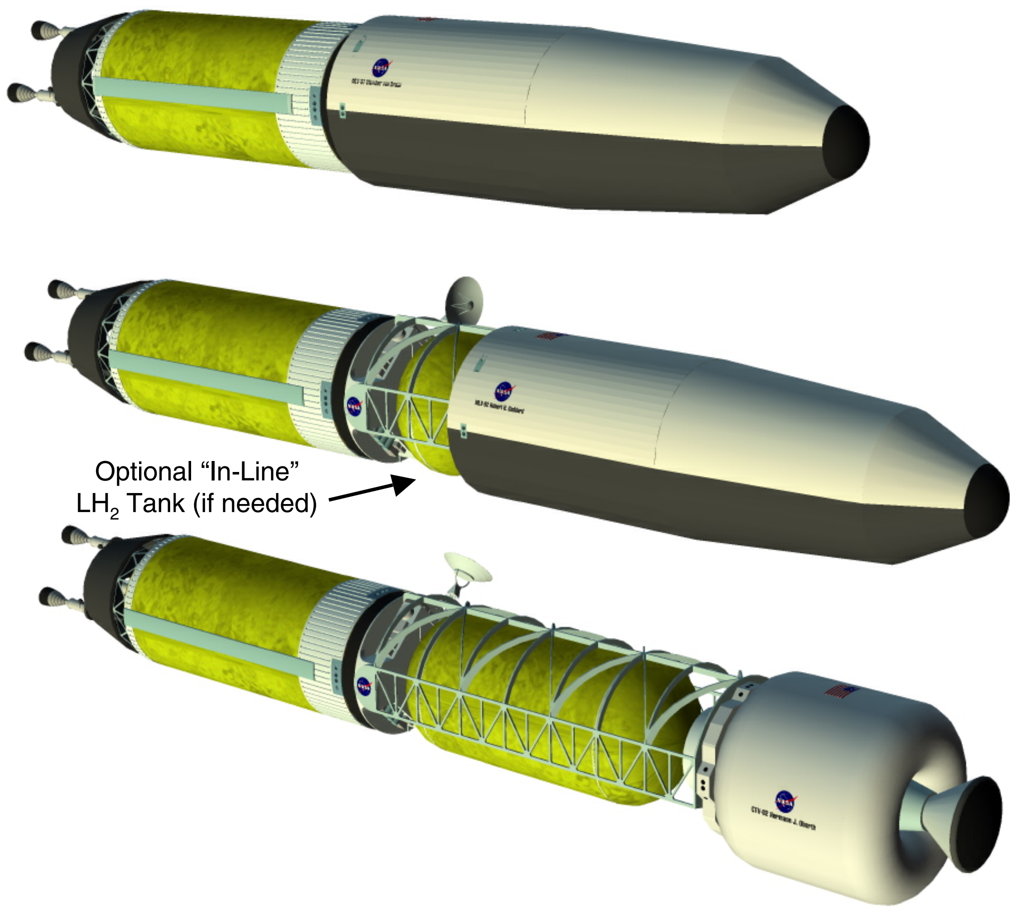

2011 Cargo Mission 1
Habitat Lander
IMLEO= 131.0 t

2011 Cargo Mission 2
Cargo Lander
IMLEO= 133.7 t

2014 Piloted Mission
Artificial Gravity
Crew Transfer Vehicle
IMLEO= 166.4 t

Exploration
Transportation

Modular "Bimodal" NTR Transfer Vehicle Design for Mars Cargo and Piloted Missions

"Propelling Us to New Worlds"

Bimodal NTR: High thrust, high I_{sp} propulsion system utilizing fissioning U^{235} produces thermal energy for propellant heating and electric power generation enhancing vehicle capability

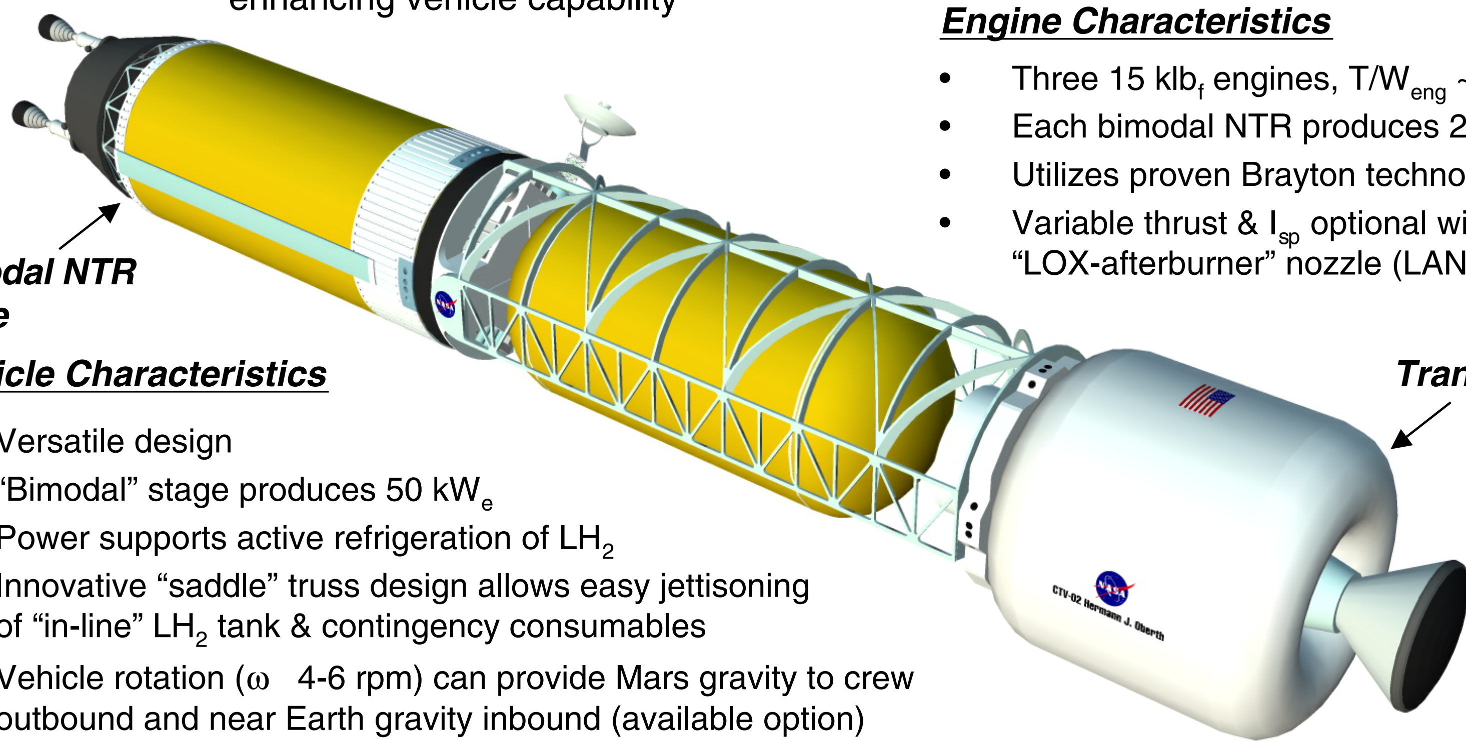

Engine Characteristics

- Three 15 klb_f engines, T/W_{eng} ~3.1
- Each bimodal NTR produces 25 kW_e
- Utilizes proven Brayton technology
- Variable thrust & I_{sp} optional with "LOX-afterburner" nozzle (LANTR)

Vehicle Characteristics

- Versatile design
- "Bimodal" stage produces 50 kW_e
- Power supports active refrigeration of LH_2
- Innovative "saddle" truss design allows easy jettisoning of "in-line" LH_2 tank & contingency consumables
- Vehicle rotation (ω 4-6 rpm) can provide Mars gravity to crew outbound and near Earth gravity inbound (available option)
- Propulsive Mars capture and departure on piloted mission
- Fewest mission elements, simple space ops & reduced crew risk
- Bimodal NTR vehicles easily adapted to Moon & NEA missions

Exploration Transportation

Mars DRM 4.0: "Bimodal" NTR Crew Transfer Vehicle (CTV) with Inflatable "TransHab" Module & Artificial Gravity Capability

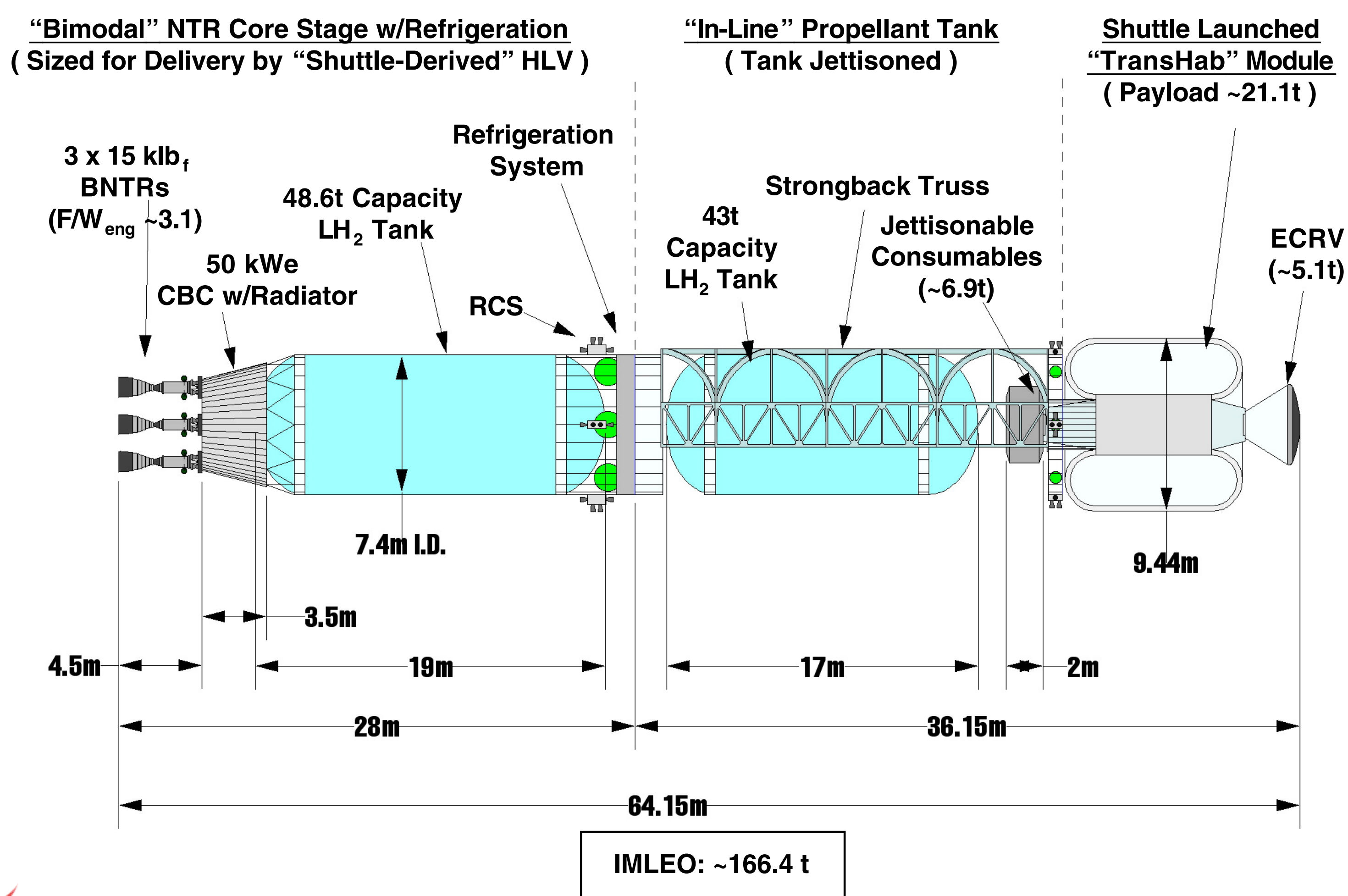

"Bimodal" Crew Transfer Vehicle Earth Orbit Assembly Sequence

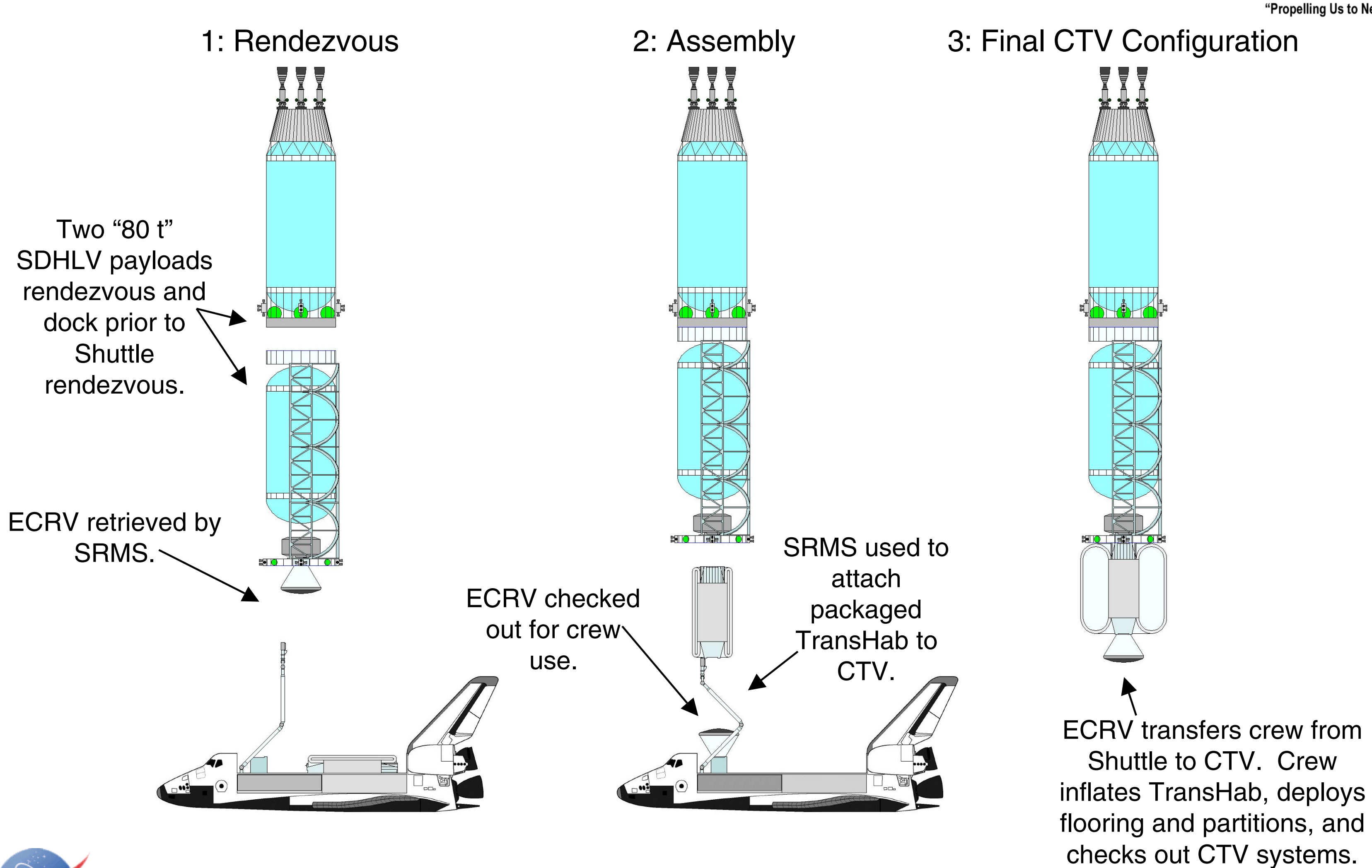

"Artificial Gravity" BNTR Mars Crew Transfer Vehicle (CTV) Mission Scenario

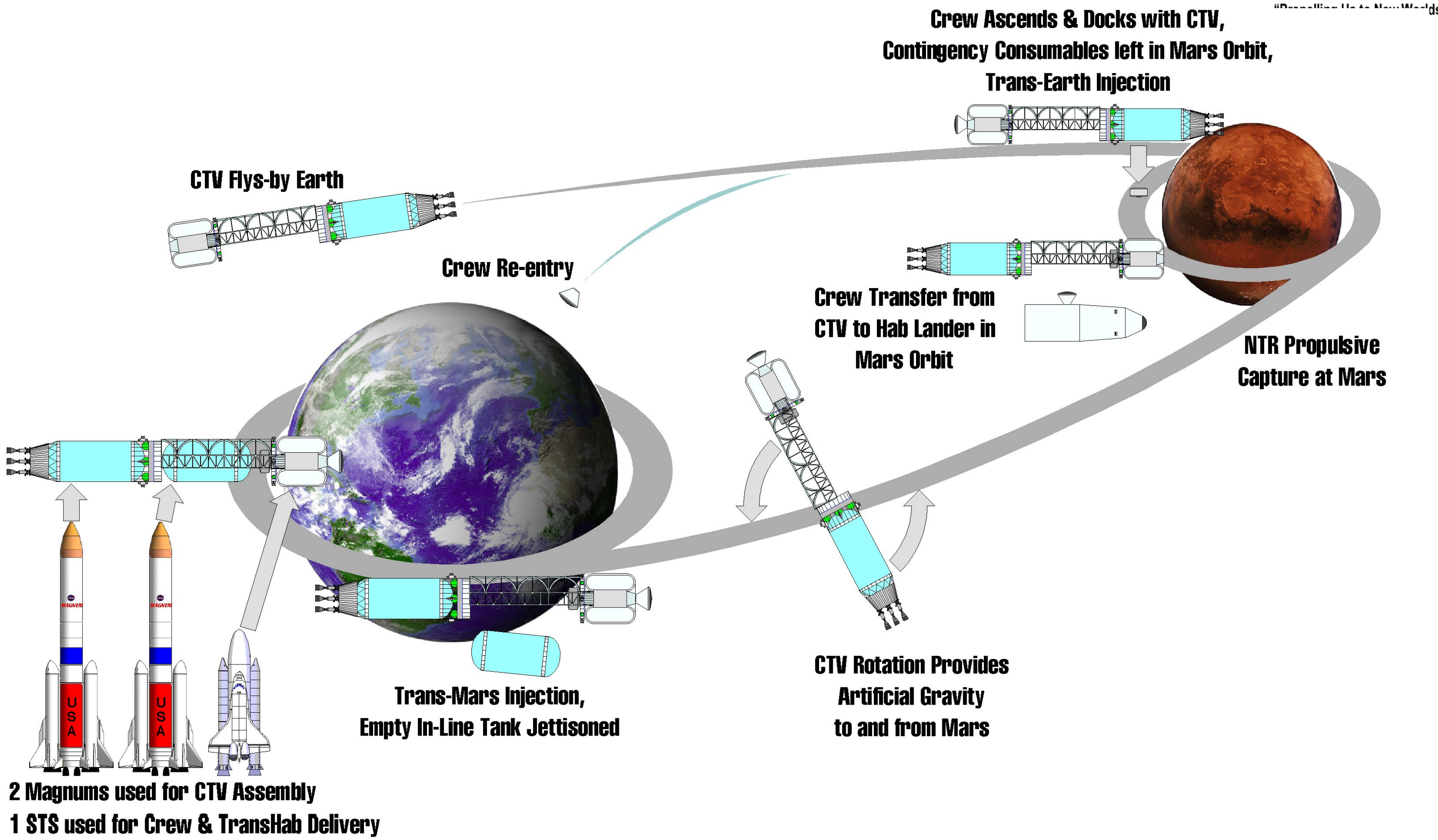

Space Transportation Project Office
Glenn Research Center

"Bimodal" NTR Crew Transfer Vehicle (CTV) in Artificial Gravity Mode

"Propelling Us to New Worlds"

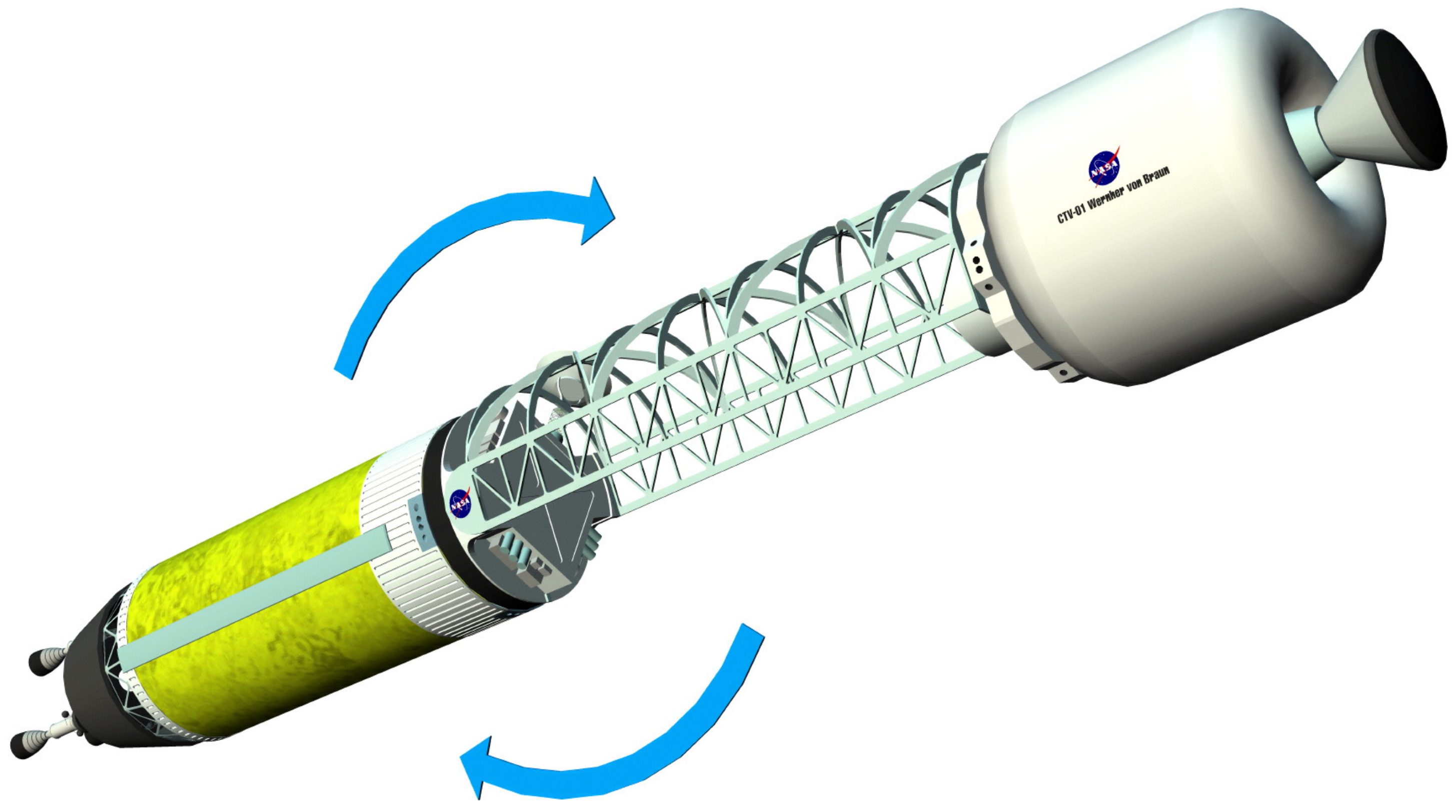

Exploration
Transportation

2014 “Bimodal” NTR Piloted Flight Profile (210 Day Transit Out, 190 Day Return)

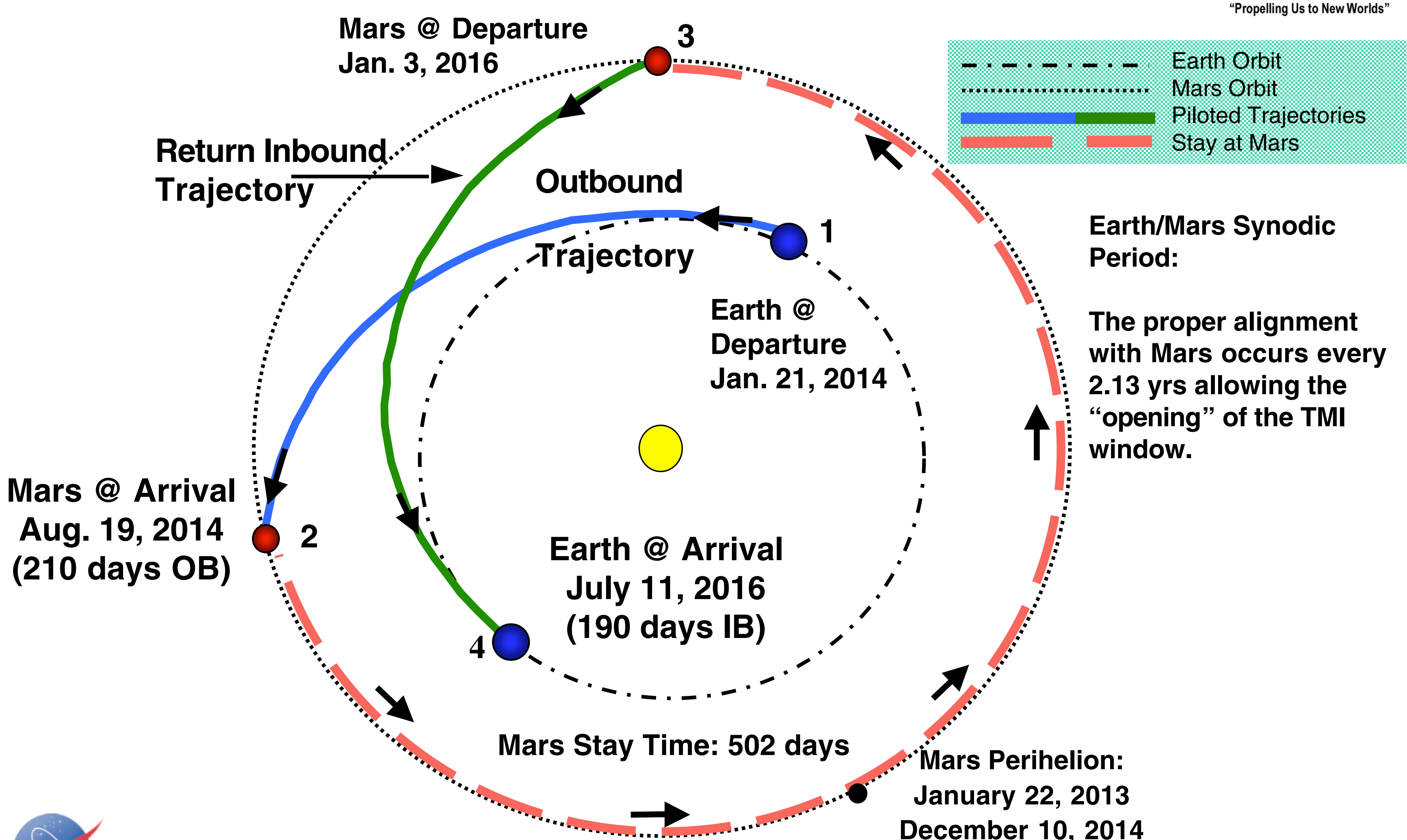

Earth/Mars Synodic Period:

The proper alignment with Mars occurs every 2.13 yrs allowing the “opening” of the TMI window.

Human Mars Mission Architecture Mass Comparison

(Shown at 80 t steps)

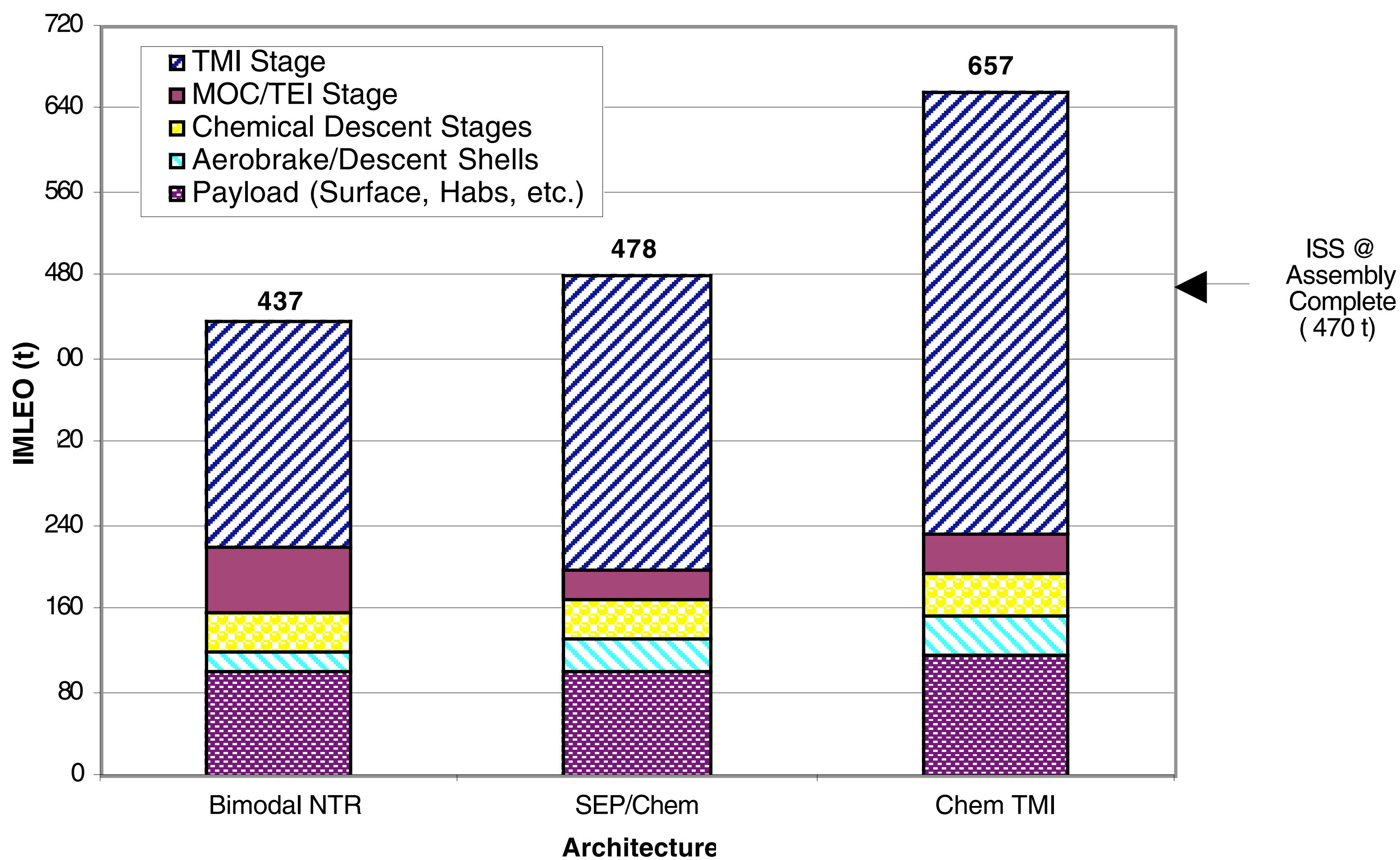

Space Transportation Project Office
Glenn Research Center

"LOX-Augmented" NTR (LANTR) Concept
--Operational Features and Characteristics--

"Propelling Us to New Worlds"

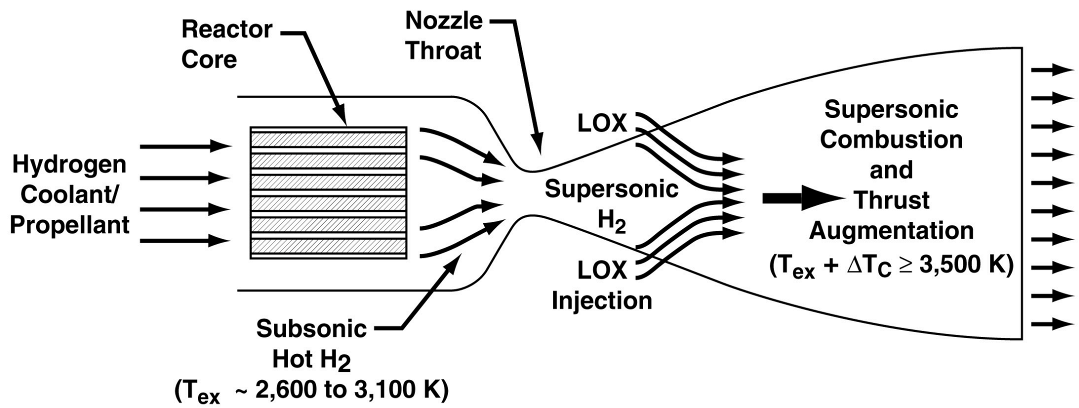

Life (hrs)	I_{sp} (sec) 5	10	35	Tankage	T/W$_{eng}$
T_{ex} (°K)	2,900	2,800	2,600	Fraction (%)	Ratio
O/H MR = 0.0	941	925	891	14.0	3.0*
1.0	772	762	741	7.4	4.8
3.0	647	642	631	4.1	8.2
5.0	576	573	566	3.0	11.0
7.0	514	512	508	2.5	13.1

*For 15 klbf LANTR with chamber pressure = 2,000 psia and ε = 500 to 1

Exploration Transportation

"LOX-Augmented" Nuclear Thermal Rocket (LANTR) "Afterburner" Nozzle Concept Demonstration

"Propelling Us to New Worlds"

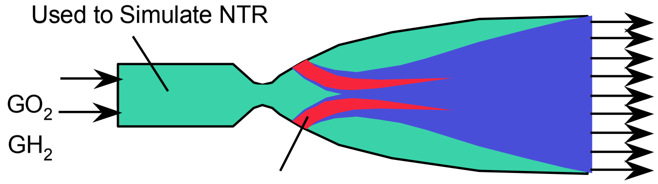

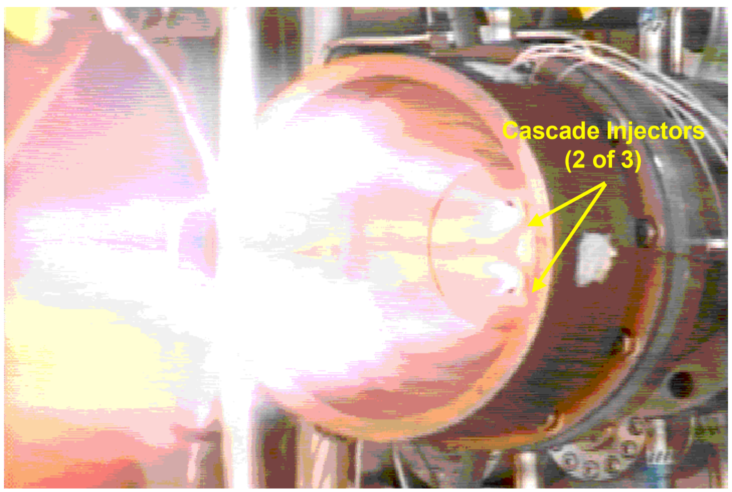

Baseline H/O Thrust: 2100 lbf at 1000 psia and MR = 1.5. With GO_2 injection into nozzle, measured thrust due to supersonic combustion is 3200 lbf (~52% thrust augmentation achieved at 50:1 and MR_L~3.0)

LANTR Concept and Benefits:
- "Afterburner" nozzle increases thrust by injecting & combusting GO_2 downstream of the NTR throat
- Enables NTR with variable thrust and Isp capability by varying the nozzle O/H mixture ratio (MR)
- Operation at modest MRs (<1.0) helps increase bulk propellant density for packaging in smaller volume launch vehicles
- LANTR's bipropellant operation enables smaller, faster Moon / Mars vehicles when using extraterrestrial sources of H_2 and O_2

LANTR Test Program Objectives: (Aerojet & GRC)
- Measure thrust augmentation from oxygen injection and supersonic combustion using small, fuel-rich H/O engine with two different area ratio nozzles (@ 25:1 and 50:1) as "non-nuclear" NTR simulator.
- Use results to calibrate reactive CFD assessment of bimodal LANTR engine

Status: LANTR afterburner nozzle demonstrated
- Oxygen injection into hot supersonic flow
- Supersonic combustion in the nozzle
- Elevated nozzle pressures measured
- Benign nozzle wall environment observed
- Increase O2 consumption rate with nozzle length
- Thrust augmentation >50% measured

Space Transportation Project Office
Glenn Research Center

Fully Reusable NTR-Powered Transfer Vehicle "The Key to Affordable Lunar Transportation"

"Propelling Us to New Worlds"

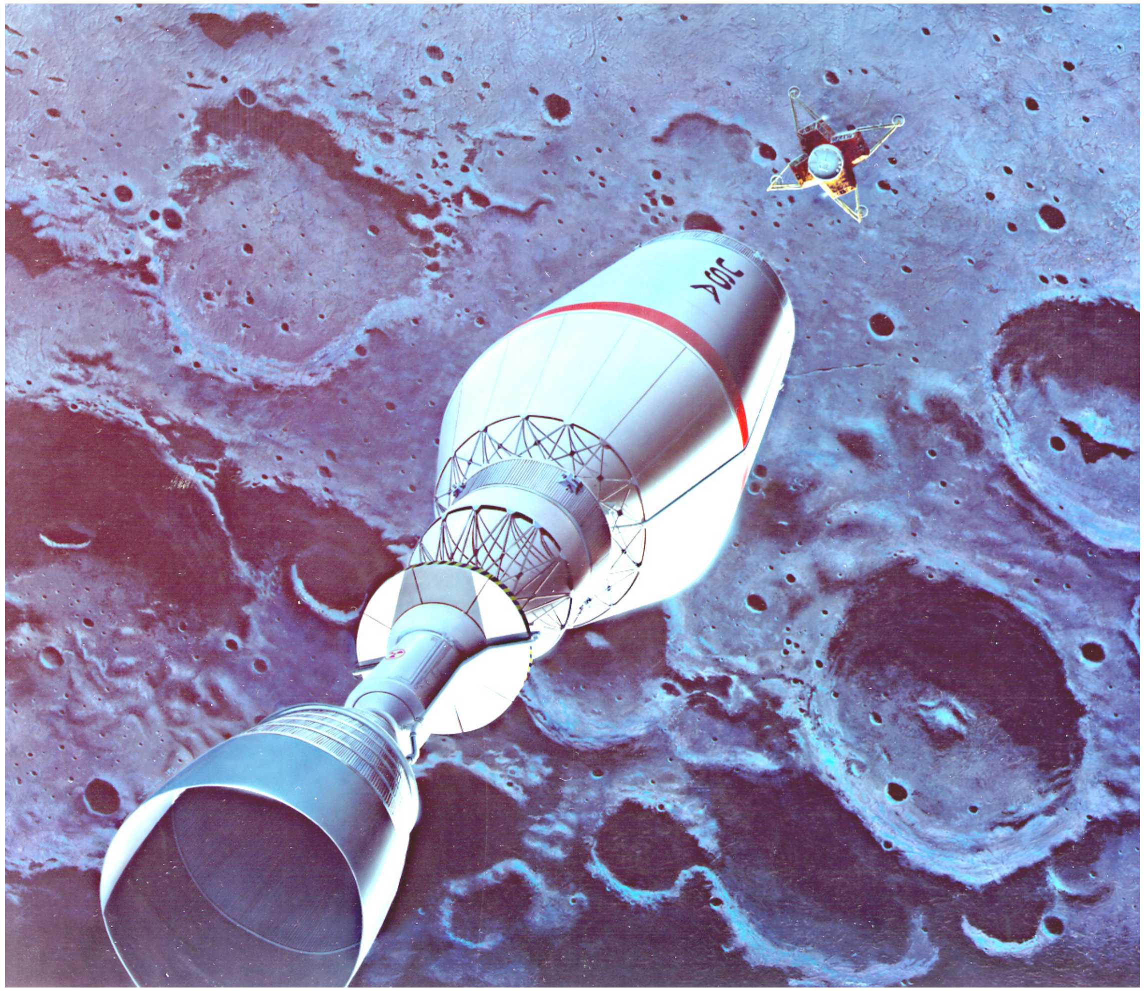

Ref: Borowski, NASA/TM 106739

Exploration Transportation

Robotic Science "Hybrid" BNTEP Vehicle

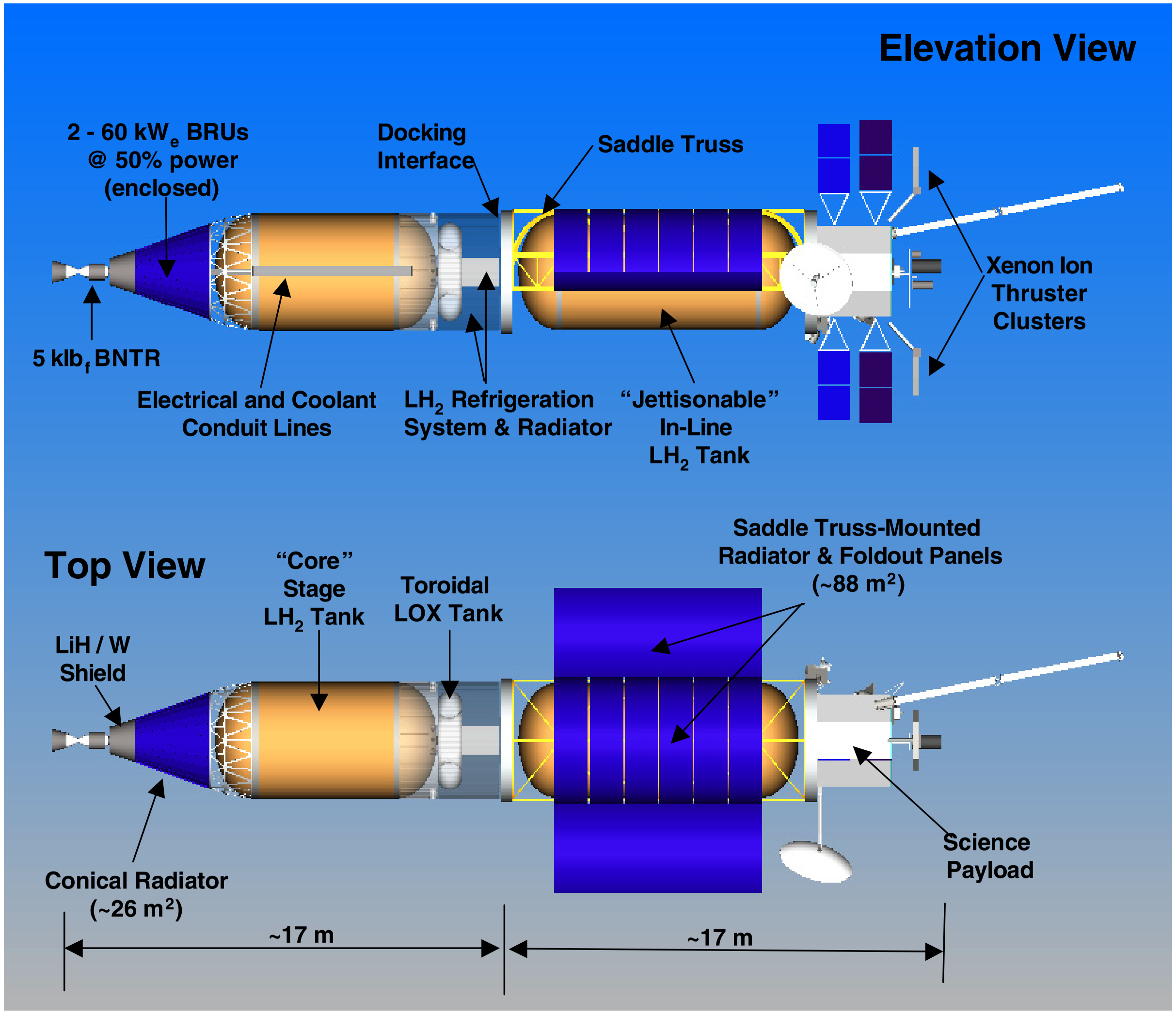

Space Transportation Project Office
Glenn Research Center

Significant Technology Development is Underway To Support Design Definition for Future “Bimodal” NTR Human Exploration Missions

“Propelling Us to New Worlds”

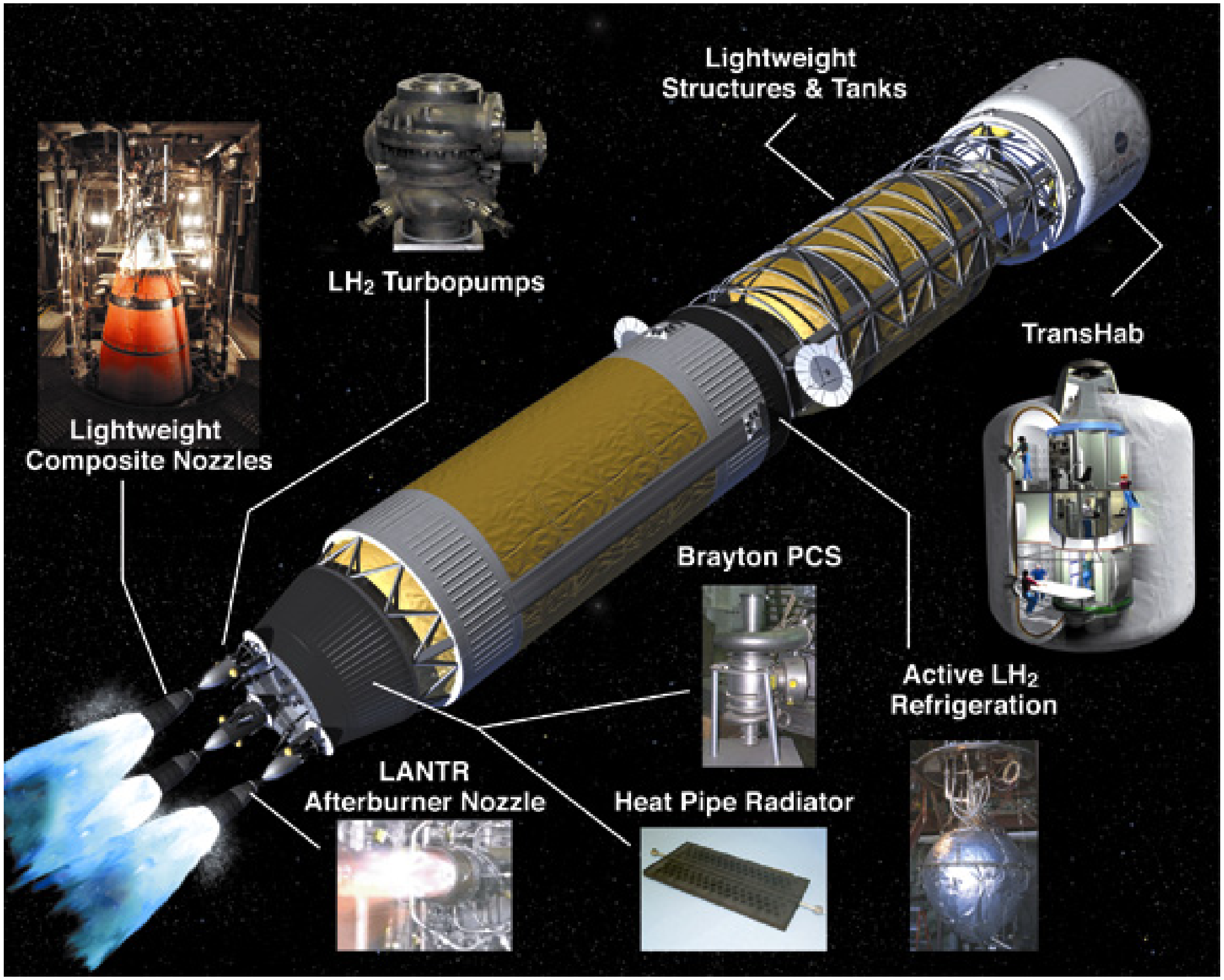

Exploration Transportation

HIGH TEMPERATURE PROPULSION SYSTEM STRUCTURAL SEALS
FOR FUTURE SPACE LAUNCH VEHICLES

Patrick H. Dunlap, Jr. and Bruce M. Steinetz
National Aeronautics and Space Administration
Glenn Research Center
Cleveland, Ohio

Jeffrey J. DeMange
University of Toledo
Toledo, Ohio

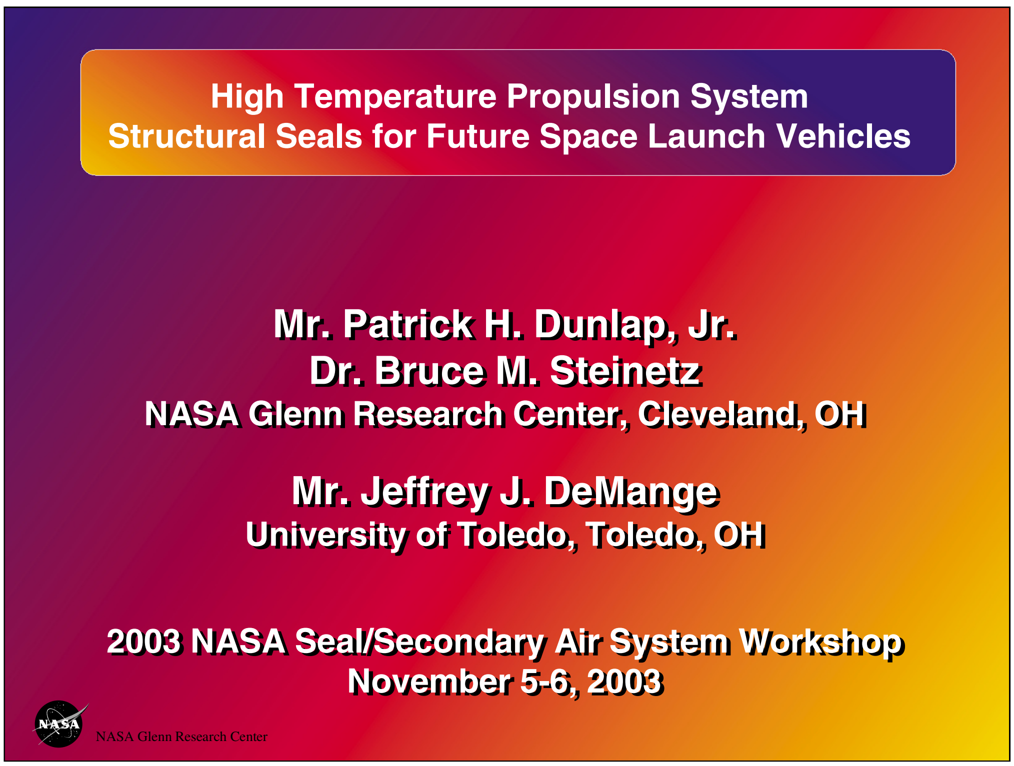

Introduction & Background

- High temperature (up to 2500 °F), dynamic seals required in advanced hypersonic engines to seal the perimeters of movable engine ramps
- NASA GRC has developed high temperature structural seals since National Aerospace Plane (NASP) program
  - Led NASP airframe and propulsion system seal development (1986-1992)
  - Seals met many requirements but fell short of leakage, durability, and resiliency goals
  - Seal development stopped due to program termination
- To overcome shortfalls, GRC currently developing advanced seals and seal preloading devices under NASA's Next Generation Launch Technology (NGLT) program

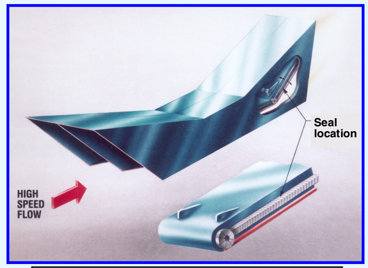

NASP Propulsion System Seals

NASA Glenn Research Center

High temperature, dynamic structural seals are required in advanced hypersonic engines to seal the perimeters of movable engine ramps for efficient, safe operation in high heat flux environments at temperatures from 2000 to 2500 °F. NASA GRC became involved in the development of high temperature structural seals in the late 1980's and early 1990's during the National Aerospace Plane (NASP) program. Researchers at GRC carried out an in-house program to develop seals for the NASP hypersonic engine and oversaw industry efforts for airframe and propulsion system seal development for this vehicle. The figure shows one of the seal locations in the NASP engine. Seals were needed along the edges of movable panels in the engine to seal gaps between the panels and adjacent engine sidewalls.

Seals developed during the NASP program met many requirements but fell short of leakage, durability, and resiliency goals. Due to program termination the seals could not be adequately matured. To overcome these shortfalls, GRC is currently developing advanced seals and seal preloading devices for the hypersonic engines of future space vehicles as part of NASA's Next Generation Launch Technology (NGLT) program.

Seal Challenges & Design Requirements

- Design requirements are demanding:
  - Withstand temperatures up to 2500 °F and high heat fluxes with minimal cooling (cooling equipment adds weight)
  - Limit leakage of hot gases and unburned propellant into backside cavities
  - Survive in chemically hostile environment (e.g., oxidation, steam, hydrogen)
  - Seal distorted sidewalls and remain resilient for multiple heating and loading cycles
  - Survive hot scrubbing with acceptable change in flow rates

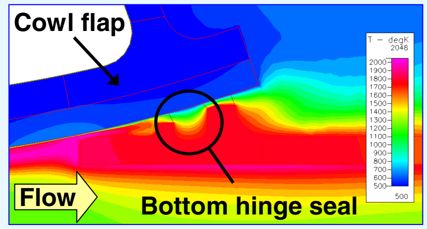

Temperatures predicted for ISTAR hinge line seal with flap closed and 0.030 in. seal gap (in K)

- Large technology gap exists: no seals have been demonstrated to meet these requirements.

Goal: Develop robust, reusable, resilient seals and preloading devices that operate at 2000 to 2500 °F for multiple missions and demonstrate performance in relevant environments

NASA Glenn Research Center

Hypersonic engine seals have a demanding set of design requirements. As engine systems are developed for future vehicles, seal temperatures are expected to increase to as much as 2000 to 2500 °F. To meet engine performance, safety, and life goals, the seals must withstand these extreme temperatures with minimal active cooling to limit the need for complex, heavy seal purge cooling systems. Engine seals must limit the leakage of hot, pressurized (~100 psi) gases and unburned propellant into backside cavities to prevent explosive mixtures from forming there. The seals must operate in an oxidizing/steam environment and resist hydrogen embrittlement if hydrogen is used as a propellant. Structural and thermal loads on the engine sidewalls can cause distortions that the seals must accommodate. To stay in contact with the walls, the seals must remain resilient and flexible for multiple heating cycles. The seals will also be rubbed over these distorted, rough walls as the engine panels holding the seals are actuated. The seals must survive the hot scrubbing without incurring increases in leakage due to wear.

A large technology gap exists because no seals have been demonstrated to meet these challenging requirements. It is GRC’s goal to develop robust, reusable resilient seals and preloading devices that meet these requirements for multiple missions and demonstrate their performance in relevant environments.

Seal Specimens

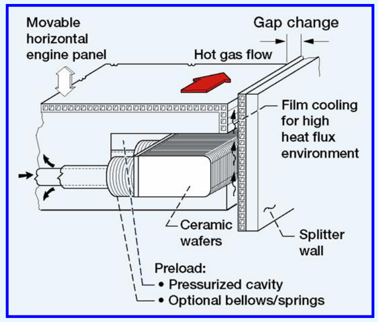

- Ceramic wafer seals originally developed during NASP program
  - Preloading device behind wafers maintains contact with sealing surface
  - Evaluated several wafer materials: aluminum oxide, silicon carbide, silicon nitride
- Current design:
  - Material: monolithic silicon nitride (Honeywell AS800)
  - Size: 0.5 in. wide x 0.92 in. long x 0.125 in. thick

NASA Glenn Research Center

Ceramic wafer seals were originally developed during the NASP program. They are composed of a series of thin ceramic wafers installed in a channel in a movable panel and preloaded from behind to keep them in contact with the opposing sealing surface. Materials that were evaluated for the wafer seals during the NASP program included a cold-pressed and sintered aluminum oxide, a sintered alpha-phase silicon carbide, a hot-isostatically-pressed silicon nitride, and a cold-pressed and sintered silicon nitride. A detailed analytical comparison of all the materials that were considered ranked the advanced silicon nitride ceramics as the most promising material for future consideration.

Given that these tests were performed in the late 1980’s, considerable improvements have been made since then to produce stronger and tougher ceramic materials. Because of these improvements and the high ranking of silicon nitride as a candidate wafer seal material, GRC selected silicon nitride as the best candidate for these seals. The wafers tested in the current study were made of monolithic silicon nitride (Honeywell AS800) and were 0.5-in. wide, 0.92-in. tall, and 0.125 in. thick. They had corner radii of 0.050 in.

Seal Preloading Device Requirements

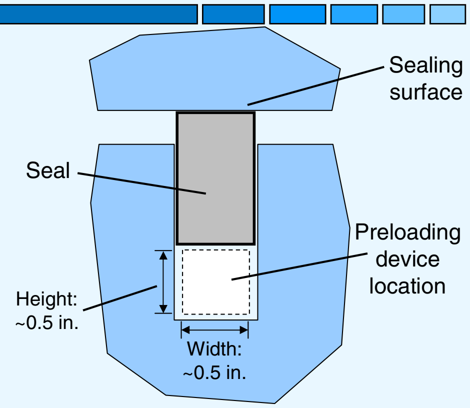

- Goal: Develop resilient device that keeps seal in contact with sealing surface
- Requirements are also demanding:
  - Operate in hot, oxidizing environment (2000+ °F)
  - Provide ~0.1 in. stroke with minimal permanent set for multiple load and heating cycles
  - Fit in small area behind seals (~0.5 in. x 0.5 in.)

NASA Glenn Research Center

The high temperature seal preloading devices that are being developed and evaluated would be installed behind the seals to ensure sealing contact with the opposing sealing surfaces. The requirements for these devices are also quite challenging. They must operate in the same environment and temperature as the seals while providing the required stroke (nominally 0.1 in.) with a permanent set of less than 20 percent of that stroke for multiple loading and heating cycles. Complicating this effort further is the limited amount of space available for the preloader behind the seals. The cross sectional area of the device must fit in a space that would be about 0.5 in. wide by about 0.5 in. high. Ideally the device would be about as long as the seal and able to be installed around corners. The device must be stiff enough to support the seal and keep it pressed against the sealing surface but soft enough that it does not apply excessive loads to that surface.

Seal Preloading Device Designs

- Canted coil springs
  - Unique load vs. displacement curve provides nearly constant force over large range
  - Long, linear springs
  - Cross section: 0.450 in. high x 0.508 in. wide
  - Tested stainless steel (302 SS) springs to investigate feasibility as preloading device
- Silicon nitride compression springs
  - Potential for high temperature use (2000+ °F)
  - Evaluated 2 designs:
    - Standard design
      - 0.815 in. high x 0.520 in. diam.
      - Max deflection: 0.098 in.
    - Modified design
      - 0.694 in. high x. 0.435 in. diam.
      - Max deflection: 0.043 in.

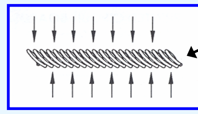

Canted coil spring

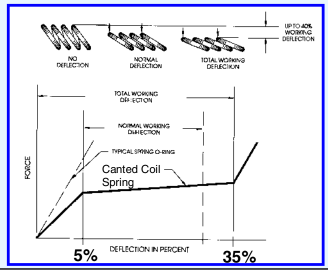

Large working deflection of canted coil spring

Silicon nitride compression springs

NASA Glenn Research Center

Two types of seal preloading devices were evaluated in this study. The first was a canted coil spring produced by Bal Seal Engineering Company, Inc. These springs have several unique features that could make them very good seal preloading devices. Unlike typical compression springs that generate increasing amounts of force as they are compressed, the force produced by canted coil springs remains nearly constant over a large deflection range. This is an appealing feature for a seal preloading device because it could provide a large amount of stroke and resiliency to a seal without applying excessive loads to the seal or the opposing sealing surfaces. Another advantageous feature of canted coil springs is that they are produced in long, linear lengths that would allow them to be installed in a groove directly behind a seal and potentially around corners. The baseline canted coil springs evaluated in this study were Bal Seal part number 109MB-(84)L-2 and were made of 302 stainless steel. Stainless steel springs were used to investigate the feasibility of this seal preloader concept.

Another concept that was evaluated as a potential seal preloading device was a silicon nitride compression spring produced by NHK Spring Co., Ltd. Two different designs were tested: a standard spring and a modified design. Because they are made of silicon nitride, these springs have the potential to be used as high temperature (2000+ °F) seal preloading devices.

Hot Compression and Scrub Test Rig

- System components
  - Servohydraulic load frame (MTS)
    - Actuator: 3300 lb, 6 in. stroke
    - Load cells: 500 lb, 3300 lb
    - Dual servovalves: 1 gpm, 15 gpm
  - Custom box air furnace (ATS)
    - Temperatures up to 3000°F (14.5 kW)
    - Large working volume (9” W x 14” D x 18” H)
    - Front and back loading doors & top port
  - Laser extensometer (Beta LaserMike)
    - Non-contact Class II laser extensometer
    - 0 to 2 in. measurement range
    - ±0.25 mil accuracy

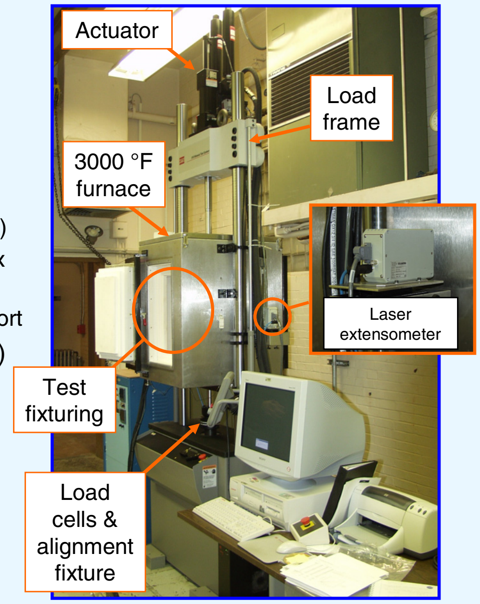

NASA Glenn Research Center

Compression tests and scrub tests were performed on the preloading devices and seals using a new state-of-the-art test rig at GRC. This test rig is capable of performing either high temperature seal compression tests or scrub tests at temperatures of up to 3000 °F using different combinations of test fixtures made of monolithic silicon carbide (Hexoloy α-SiC). The main components of this test rig are a servohydraulic load frame, an air furnace, and a non-contact laser extensometer. The load frame has a top-mounted actuator capable of generating a load of 3300 lb over a 6 in. stroke at rates from 0.001 to 8 in./sec. The box furnace has a working volume that is 9 in. wide by 14 in. deep by 18 in. high. Test fixtures are configured inside the furnace so that the stationary base for each test setup sits on top of a loading rod on a load cell below the furnace. Two different load cell ranges are available, 500 lb or 3300 lb, depending on the seal that is being tested and the loads that are expected during a test. The 500 lb load cell has an accuracy of ± 0.15 lb (± 0.03% of full scale), and the accuracy of the 3300 lb load cell is ± 2.64 lb (± 0.08% of full scale). The load cells are used to measure compressive loads applied to the seals during a compression test or frictional loads on the seals during scrub testing. The laser extensometer was used to measure the amount of compression during testing. The laser system has a measurement range of up to 2 in. and an accuracy of ± 0.00025 in.

Hot Compression Test Fixture

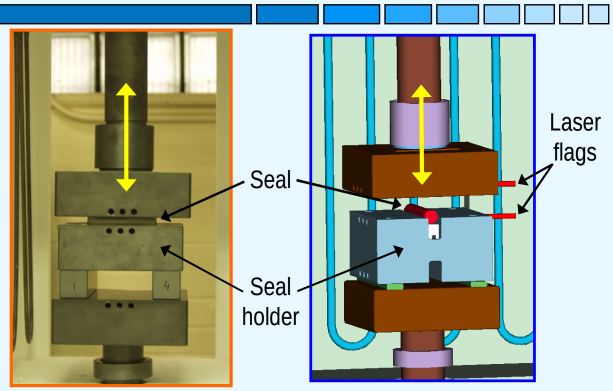

- Test fixtures made of silicon carbide for use at up to 3000 °F
- Measure load vs. linear compression, resiliency, and stiffness of seals and preloading devices
- Tested springs alone and wafer seals on top of springs
- Cyclic load tests in displacement control with 30-60 sec. hold at max compression
- Specimen lengths = 4 in.; groove width = 0.5 in.
- Tests performed at room temperature, 1600 °F, and 2000 °F

NASA Glenn Research Center

Compression tests were performed inside the furnace using this test set up. These tests were performed to determine the resiliency and stiffness of the preloading devices and to generate load versus displacement (i.e., linear compression) data. Test specimens were installed into a holder that rested on the stationary base described above. A movable platen attached to the actuator was translated up and down to load and unload the test specimens.

Compression tests were conducted at room temperature on the canted coil spring by itself and with a set of 31 wafer seals on top of a canted coil spring to see how the seals and spring performed together. Tests were conducted on individual silicon nitride compression springs at both room temperature and at 2000 °F. Tests were also performed with 31 wafer seals on top of a set of silicon nitride springs (modified spring design) to see how they performed together. These tests were performed at 1600 °F. Four springs were placed below the wafers on 1.15-in. centers. A thin load transfer element (0.02-in.-thick silicon carbide) was placed between the springs and the wafers to distribute the load from the four springs to the wafers.

Test specimens were typically loaded and unloaded for a total of 20 cycles for each test. The silicon nitride compression springs, however, were tested for 10 cycles. Each load cycle consisted of loading a test specimen at a rate of 0.001 in/sec to the specified amount of compression, holding at that compression level for 30 to 60 sec., and then unloading at 0.001 in/sec to the starting point. There was no hold time after the specimen was unloaded between load cycles.

Compression Test Results: Canted Coil Springs

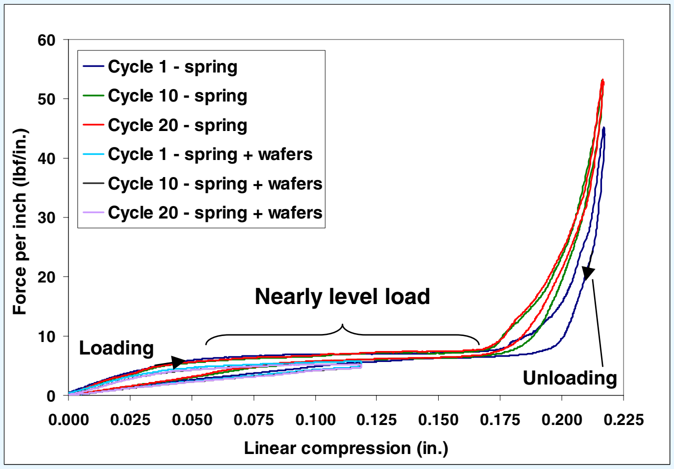

- Large deflection range (0.110 in.) with nearly constant load of 6 to 7 lbf/in. for springs alone
- Curves for wafer seals on top of springs similar to those for springs by themselves
- Little hysteresis for loading and unloading curves and ~100% resiliency with load cycling
- Initial feasibility of canted coil spring as preloading device demonstrated with stainless steel; high temperature materials required for use at 2000+ °F

NASA Glenn Research Center

This is a representative plot of the compression test results for cycles 1, 10, and 20 of tests on a canted coil spring by itself and for a set of wafer seals on top of a spring. The initial portion of the loading curves for the spring by itself showed a gradual increase in force vs. linear compression up to a deflection of about 0.060 in. where the load leveled off at about 6 lbf/in. At this point, the curves flattened out and the force remained nearly constant until the spring deflection reached about 0.170 in. (38% of free height) and the coils began contacting each other. Over this 0.110 in. deflection range, the load slowly rose from 6 to 7 lbf/in. The force on the spring rose sharply beyond deflections of 0.170 in. This unique force vs. deflection curve is typical of a canted coil spring. The large deflection range in which the load remained nearly constant makes canted coil springs appealing as seal preloading devices because they could provide a large amount of stroke and resiliency to a seal without applying excessive loads to the seal or the opposing sealing surfaces.

Results for a room temperature compression test performed using a set of 31 wafer seals on top of a canted coil spring show that the loading and unloading curves for this test were very similar to those for the spring by itself, and there was little hysteresis in the curves. The results of this test also showed no permanent set or loss of resiliency as load cycles 1 and 20 were almost identical.

This series of tests on stainless steel canted coil springs demonstrated the initial feasibility of using this type of spring as a seal preloading device. The authors recognize that the springs would have to be made out of a different material for applications at 2000+ °F.

Compression Test Results: Silicon Nitride Compression Springs

*Note: 4 springs tested under wafer seals; 1 spring used for other tests

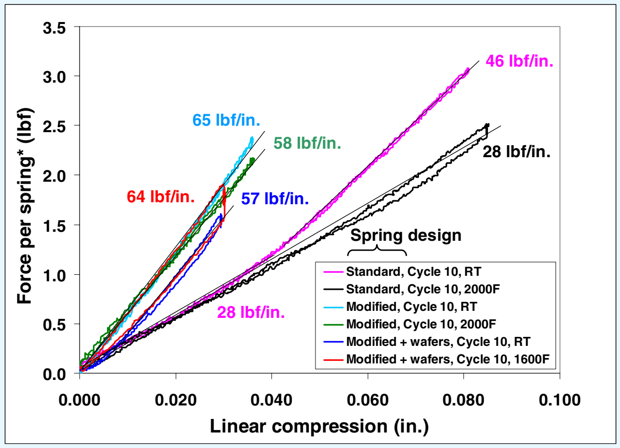

- **No permanent set at room temperature, 1600 °F, or 2000°F for any test**
- **Little hysteresis for tests of springs alone**
- **Some hysteresis for wafer seals on top of springs; possibly due to friction between wafers and groove side walls**
- **2000°F testing had more effect on standard springs than on modified design**
- **Springs show promise for use as high temperature seal preloading devices**

NASA Glenn Research Center

This figure shows the results of the compression tests performed on the silicon nitride compression springs with and without wafer seals installed on top of them. In all of these tests there was no permanent set or relaxation observed after 10 load cycles at room temperature, 1600 °F, or 2000 °F. For clarity, the figure only shows the curves for cycle 10 of each test because they were almost identical to the curves for all other load cycles. For all of the tests performed on the silicon nitride springs by themselves, there was very little hysteresis in their load vs. linear compression data. For the tests performed with seals on top of the springs, there was virtually no hysteresis for the room temperature tests but a small amount for the tests at 1600 °F. It is possible that during the high temperature test, there was some small amount of friction between the wafers and the side walls of the seal groove that caused this hysteresis as the wafers and springs were unloaded during each load cycle.

Spring constants for each test case are also shown. The modified spring design had a spring constant of 65 lbf/in. at room temperature and 58 lbf/in. at 2000 °F, indicating that the springs were slightly less stiff at high temperatures. The elastic modulus of silicon nitride at 2000 °F is about 5% lower than it is at room temperature which helps explain this behavior. The standard spring design showed a different type of loading behavior, though. Its load versus linear compression curve at room temperature had two different regions. In the linear compression range up to about 0.040 in., the standard spring had a spring constant of about 28 lbf/in. From 0.040 in. to 0.083 in., the spring became stiffer with a spring constant of 46 lbf/in. This type of behavior did not occur during the test at 2000 °F, though, as the spring constant remained at 28 lbf/in throughout the test.

Overall, these results show that the silicon nitride springs show promise for use as high temperature seal preloading devices.

Hot Scrub Test Fixture

- Measure seal frictional loads and wear rates
- Test parameters:
  - Tests performed at room temperature
  - Tested 32 wafers on top of 4 silicon nitride compression springs in both 4-in. seal grooves
  - Spring compression of 0.030 in. provides preload of ~2 lb/in.
  - Seal gap size = 0.125 in.
  - Surface roughness of rub surfaces was 5.8 µin in scrubbing direction before test
  - Stroke = 1 in. in each direction (2 in. per cycle)
  - Stroke rate = 2 in./sec
  - 1000 scrub cycles; 2000 in. of scrubbing

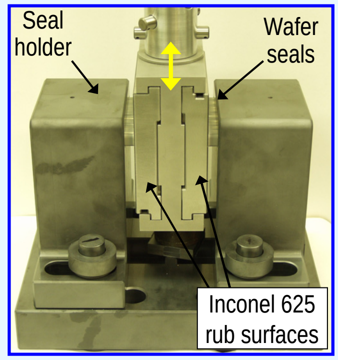

NASA Glenn Research Center

The main test rig that was used for the compression tests was also used to perform scrub tests on the seals using this set of test fixtures. Tests were performed at room temperature to evaluate seal wear rates and frictional loads as the seals were scrubbed against Inconel 625 rub surfaces. The rub surfaces had an average surface roughness before testing of about 6 µin in the scrubbing direction and 3 µin in the transverse direction. The seals were installed in grooves in two stationary seal holders on either side of a pair of movable rub surfaces. The rub surfaces were assembled in a holder that was connected through the upper load train to the actuator. The gaps between the rub surfaces and the seals were set by spacer shims in front of and behind the seal holders. A gap size of 0.125 in. was used for these tests.

Four silicon nitride compression springs (modified spring design) were installed in the bottom of each seal groove to keep the wafer seals preloaded against both rub surfaces. A load transfer element was placed on top of the springs to support the wafers and distribute the load from the springs. Thirty two wafers were installed into each seal holder to fill the 4-in.-long seal grooves. The amount of compression on the seals and springs (0.030 in.) was set through an interference fit between the seals and the rub surfaces resulting in a preload of about 2 lb per inch of seal.

During these tests, the seals were held in place in the holders while the rub surfaces were scrubbed up and down against them. For each load cycle a triangle wave was used with a stroke length of 1 in. in each direction and a stroke rate of 2 in./sec. There was no hold time between scrub direction changes. The seals were subjected to 1000 scrub cycles at 1 Hz for a total scrub length of 2000 in. for each test. Frictional loads were measured by the load cell under the furnace below the test fixture base. Seal wear rates were determined by examining the condition of the seals before and after each test and by measuring seal weight changes and changes in flow rates.

Scrub Test Results

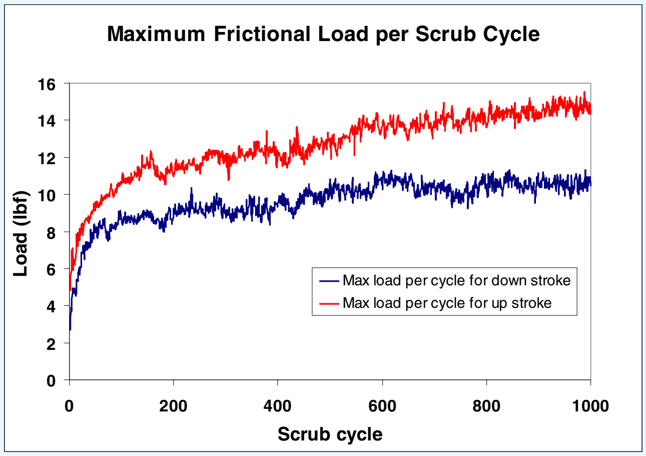

- Frictional forces rose steadily with cycling to peak load of ~15.5 lb
- Friction coefficient increased with cycling as Inconel 625 rub surface became rougher:
  - Beginning of test: friction coeff. was 0.38 with surface roughness of ~6 µin
  - By end of test: friction coeff. was 0.94 with surface roughness of 6-43 µin

NASA Glenn Research Center

Peak frictional loads during the up and down strokes of each scrub cycle are presented in this figure for the room temperature scrub test. During this test, the frictional loads started around 6 lbf at the beginning of the test and gradually rose as the test proceeded until they reached about 15.5 lbf by the end of the test. The seals were installed so that the springs behind them provided a load against the Inconel 625 rub surfaces of about 2 lbf/in. over both 4-in. seal lengths. This resulted in a normal load of 16 lbf during testing. Based on this normal load, the friction coefficient from about 0.4 to almost 1.0 by the end of the test. Before this scrub test, the average surface roughness of the rub surfaces was about 6 µin in the scrubbing direction and 3 µin in the transverse direction. After testing, the surface roughness had risen to a range of 6 to 43 µin in both directions. This increase in surface roughness during testing likely contributed to the increase in frictional forces as the test proceeded.

Scrub Test Results

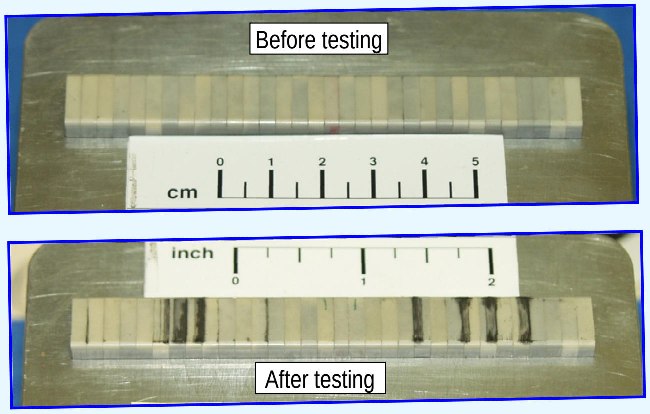

- Silicon carbide wafer seals developed during NASP program chipped during flow testing
- Little if any damage to new silicon nitride wafer design during scrub testing
  - No chips in wafers
  - Weight of wafer stacks almost identical before and after testing

NASA Glenn Research Center

After the scrub test was completed, the seals and rub surfaces were inspected for signs of damage. These figures show what the seals looked like before and after scrubbing. The seals showed little if any damage after testing. Wear debris from the rub surface can be seen on some of the wafers in locations that correspond to areas on the rub surface that were worn during the test. None of the wafers were chipped or broken during testing, and the total weight of both wafer sets before and after testing was almost identical. Silicon carbide wafer seals tested during the NASP program were much more damage-prone and chipped during static flow testing even without scrubbing. The silicon nitride wafers tested in the current study appear to be much more robust and damage-resistant.

Flow Test Results

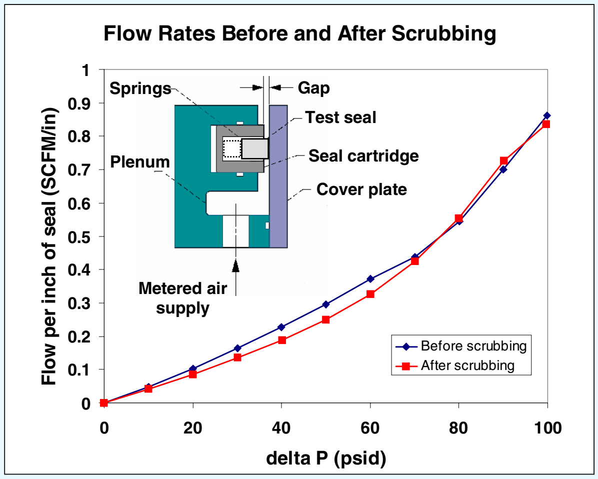

- Performed flow tests on wafers before and after scrub test with silicon nitride compression springs behind seals; gap size = 0.135 in.
- No change in flow rates after room temperature scrub testing

NASA Glenn Research Center

Flow test results for the wafer seals before and after scrub testing are presented here for a gap size of 0.135 in. These tests were performed with four silicon nitride springs installed behind the wafers to keep them preloaded against the cover plate. Flow rates for the wafers before and after scrubbing were almost identical in both cases. This is consistent with the observation that the wafers were not damaged during the scrub test. These results are encouraging because they show that the seals are still effective at blocking flow even after 1000 scrub cycles at room temperature.

Development of High Temperature Seal Preloading Devices

- Goal: Develop preloading devices that are resilient above 2000 °F
- Contracted with Refractory Composites, Inc. for design, analysis, and fabrication of devices (contract NAS3-03114)
- Concepts being considered:
  - CMC wave spring
  - Canted coil spring made of coated refractory metal
- Completed initial modeling and analyses of devices
- Performing materials characterization tests
- Additional details in presentation by T. Paquette and J. Palko

Wave Spring

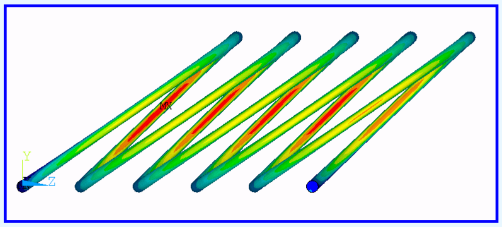

Sample stress results for modeling of canted coil spring

NASA Glenn Research Center

In this study, tests were performed on canted coil springs made of stainless steel to evaluate their performance at room temperature and assess the feasibility of using this type of spring as a seal preloading device. While the results of these tests were promising, higher temperature seal preloaders are required for future applications in which the temperature of the seals and preloading devices will reach 2000 to 2500 °F. Researchers at GRC have contracted with Refractory Composites, Inc. for the design, analysis, and fabrication of such devices. Two concepts are currently being considered: a ceramic matrix composite (CMC) wave spring and a canted coil spring made of a refractory metal with an oxidation coating. RCI and their subcontractor Connecticut Reserve Technologies, Inc. have completed the initial modeling and analyses for these devices and are currently performing materials characterization tests on candidate materials. Additional details on this effort will be shown later in the presentation by Ted Paquette and Joe Palko.

Summary

- **Initial feasibility of canted coil spring as seal preloading device demonstrated at room temperature**
  - **Met stroke requirement**
  - **Modest unit loads would minimize potential seal and sidewall damage**
  - **Need to use different material for 2000+ °F (in development)**
- **Silicon nitride compression springs also showed promise as high temperature seal preloading devices**
- **Wafer seals performed well in room temperature scrub test**
  - **No chips in wafers or any other signs of damage**
  - **No change in flow rates after scrub test**
- **Future work:**
  - **Investigate seal + preloading device combinations that meet resiliency goals at high temperature**
  - **Perform high temperature scrub tests on wafer seals**

NASA Glenn Research Center

Based on the results of these tests, the following conclusions were made:

1. Canted coil springs are promising seal preloading devices. Room temperature compression tests performed with wafer seals on top of a spring showed that the spring met the stroke requirement with no permanent set or loss of resiliency for 20 load cycles. The modest unit loads produced by this type of spring would minimize potential damage to the seals and adjacent sealing surfaces. These feasibility tests were performed on springs made of stainless steel. High temperature materials will need to be used for applications at 2000+ °F.

2. Silicon nitride compression springs also show promise as high temperature seal preloading devices. After repeated loading at temperatures up to 2000 °F the springs showed little hysteresis and excellent resiliency.

3. Silicon nitride wafer seals performed very well in the room temperature scrub test. There were no signs of damage after the wafers were scrubbed against Inconel 625 rub surfaces at room temperature for 2000 in. of scrubbing (1000 cycles). None of the wafers were chipped or broken, and the total weight of each wafer set before and after testing was almost identical. Flow rates for the wafers before and after scrubbing were also almost identical.

More work needs to be done to investigate seal and preloading device combinations that ultimately satisfy all of the seal requirements. The authors plan to investigate other wafer shapes and sizes to see if those changes affect seal durability and frictional forces. Longer scrub tests will also be performed at high temperatures to examine seal durability for more than 1000 scrub cycles.

ADVANCED CONTROL SURFACE SEAL DEVELOPMENT FOR FUTURE SPACE VEHICLES

Jeffrey J. DeMange
University of Toledo
Toledo, Ohio

Patrick H. Dunlap, Jr. and Bruce M. Steinetz
National Aeronautics and Space Administration
Glenn Research Center
Cleveland, Ohio

Advanced Control Surface Seal Development for Future Space Vehicles

Mr. Jeffrey J. DeMange
University of Toledo
Toledo, OH

Mr. Patrick H. Dunlap, Jr. &
Dr. Bruce M. Steinetz
NASA Glenn Research Center
Cleveland, OH

2003 NASA Seal/Secondary Air System Workshop
November 5th- 6th, 2003

Control Surface Seal Challenges and Design Requirements

- Limit hot gas flow and heat transfer to underlying low-temperature structures
- Withstand temperatures of:
  - 2100 °F for tile-based TPS
  - 2600 °F for CMC control surfaces
- Stay resilient for multiple load/heating cycles
- Limit loads against sealing surfaces
- Resist scrubbing damage

X-37

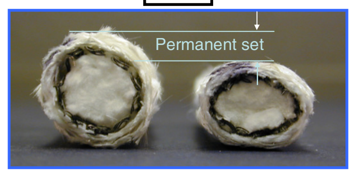

Baseline Seal

Goal: Develop long life, high temperature control surface seals and demonstrate performance in relevant environments

NASA Glenn Research Center

THE UNIVERSITY OF TOLEDO

High temperature control surface seals have been identified as a critical technology in the development of future space vehicles. These seals must withstand temperatures of up to 2600 °F and protect underlying temperature-sensitive structures (such as actuators and airframe components) from high heat fluxes. In addition, the seals must maintain their sealing capability by remaining resilient during flight conditions. The current baseline seal, used on the Shuttle orbiters and the X-38 vehicle, consists of a Nextel 312 sheath, an internal Inconel X-750 knitted spring tube, and hand-stuffed Saffil batting. Unfortunately at high temperatures (> 1500 °F), the seal resiliency significantly degrades due to yielding and creep of the spring tube element. The permanent set in the seals can result in flow passing over the seals and subsequent damage to temperature sensitive components downstream of the seals. Another shortcoming of the baseline seal is that instances have been reported on Shuttle flights where some of the hand-stuffed Saffil batting insulation has been extracted, thus potentially compromising the seal. In vehicles where the thermal protection systems are delicate (such as with Shuttle tiles), the control surface seals must also limit the amount of force applied to the opposing surfaces. Additionally, in many applications the seals are subjected to scrubbing as control surfaces are actuated. The seals must be able to withstand any damage resulting from this high temperature scrubbing and retain their heat/flow blocking abilities.

Control Surface Seal
Advanced Design Approaches

Improvements to…

- **Resiliency**
  - Spring Tube
    - Materials – ODS superalloys (MA 754, PM 2000)
    - Architecture – Wire diam., knit pattern, etc.
  - Preloaders
    - Type – Canted coil, compression, wave springs
    - Materials – Refractory alloys, ceramic, CMC
  - Core structure/architecture
- **Flow blockage**
  - Core structure/architecture
- **Core integrity**
  - Core structure/architecture
- **Wear resistance**
  - Materials – Oxidation resist. metals (Haynes 214, PM 2000, Kanthal A1)
  - Architecture

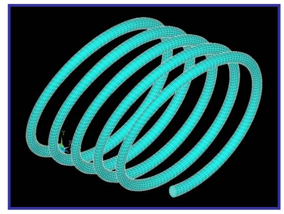

Canted Coil Spring

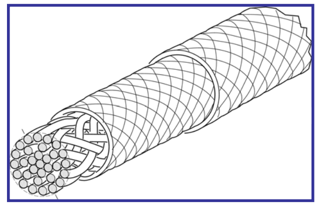

Braided Core Design

NASA Glenn Research Center

THE UNIVERSITY OF TOLEDO

Currently, the Seals Team at NASA GRC has ongoing efforts in several areas to improve the baseline seal design. These include developing improved spring tube elements with higher temperature capabilities to impart enhanced resiliency to the seals. Another promising approach to improving resiliency involves the use of high temperature preloaders (such as compression springs, canted coil springs, etc.) placed behind the seals. Investigations into engineering the core structure to optimize resiliency and flow blocking characteristics are also being conducted. An optimized core structure would improve core integrity and prevent extraction of the insulating material. Finally, improvements to the wear resistance of the seals are being pursued through material substitutions and architectural changes to the seal outer layers.

Resiliency: Baseline Spring Tube Study

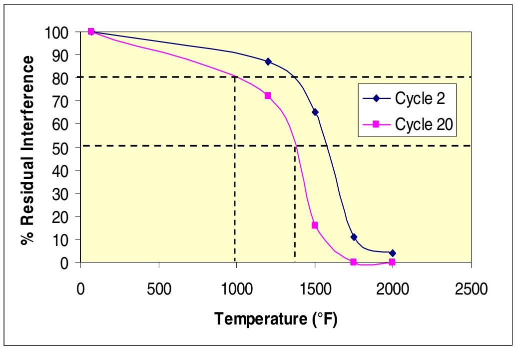

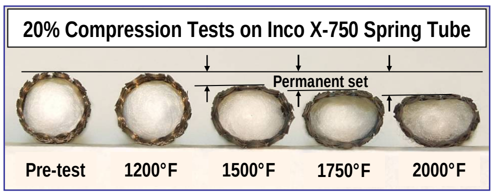

- **High Temp. Compression Tests**
  - Inco X-750 Spring Tube for X-38 / Shuttle seal
    (Boeing Spec MB160-047, ST5)
  - Tested at RT, 1200 °F, 1500 °F, 1750 °F, 2000 °F
    - Compressed 20%
    - 20 cycles
- **Results**
  - Significant drop in resiliency >1200 °F
  - After 20 cycles
    - 80% Resiliency – 1000 °F
    - 50% Resiliency – 1400 °F

NASA Glenn Research Center

In order to better understand the performance envelop of the Inconel X-750 spring tube element in the baseline seal, NASA GRC conducted a series of high temperature compression tests. Results from the tests demonstrated a substantial decrease in resiliency of the spring tube above 1200 °F. Not surprisingly, this behavior mirrors the temperature dependent yield strength behavior of the alloy. These results also provide some rough design guidelines for use temperatures of seals with this spring tube element. For example, in order to retain 50% resiliency, the maximum use temperature is approximately 1400 °F. This temperature is still well below anticipated temperature in many of the X-vehicles.

The Materials Challenge

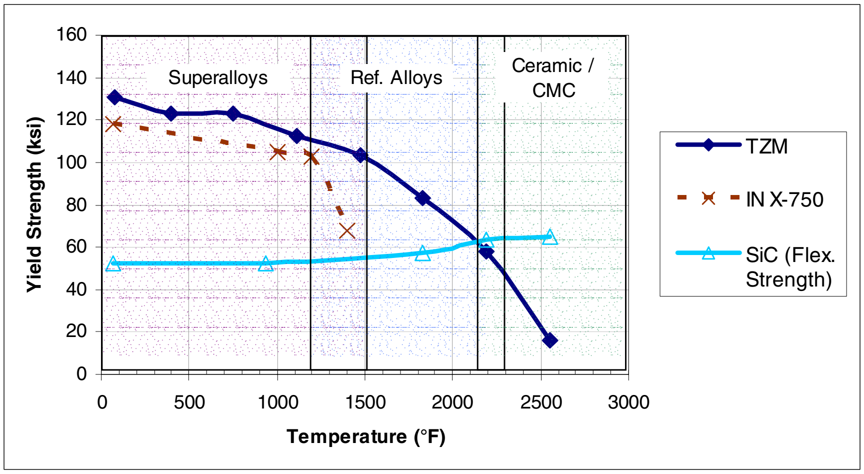

- ***Superalloys*** – Limited strength/creep beyond 1500 °F – 1800 °F
- ***Refractory Alloys*** – Good strength/creep to ~2300 °F, poor oxidation resistance
- ***Ceramic/CMC*** – Good strength/creep >2300 °F, limited elasticity

NASA Glenn Research Center

The aggressive high temperature environments these seals are used in result in significant challenges regarding the fabrication of these seals. As previously noted, the superalloy systems (such as Inconel X-750) cannot adequately endure the high temperatures anticipated in these next generation space vehicles. A moderate improvement in the performance of the seals can likely be realized by substitution with the newer oxide dispersion strengthened (ODS) alloys, such as Inconel MA754 and Plansee PM 2000. However, in order to increase the use temperature of these seals near the anticipated application temperatures, different material systems such as refractory alloys or ceramic/CMC must be considered. While these materials exhibit improved high temperature strength and creep properties when compared to the superalloy systems, they also posses some severe limitations. For example the refractory alloys generally demonstrate poor oxidation resistance and require protective coatings. The ceramic and CMC materials have limited elasticity making it difficult to fabricate seals or preloaders into complex shapes. The reduced elasticity also limits the “stroke” of these devices to accommodate large changes in gap size. However, despite these challenges, ceramic-based preloader have been fabricated for GRC and have shown promise in high temperature testing.

Preloaders:
A Potential Solution to Resiliency Issue

The use of separate preloaders behind the seals offers several potential benefits:

1. Better ***resiliency*** – preloader is insulated by thermal barrier seal
2. Better ***control of force*** applied to opposing surfaces (can be “dialed” in)
3. Improved ***flow/heat blocking*** ability when used with “dense” seals

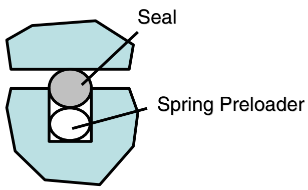

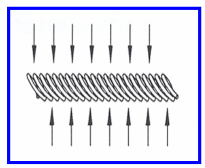

Canted Coil Spring

Si_3N_4 Comp. Springs

NASA Glenn Research Center

NASA GRC is vigorously pursuing development of high temperature preloading devices to improve the resiliency of high temperature sealing systems. These preloaders would generally be installed behind a thermal barrier seal to maintain positive sealing capabilities. The preloading devices offer several potential benefits over current SOA seals, including better resiliency, the ability to better “dial in” stiffness properties, and the capacity to use highly effective flow-blocking seals that may be too stiff otherwise. Several variants of these preloaders are under investigation, such as high temperature canted coil springs and ceramic compression springs.

Test Specimens

- **Baseline Shuttle/X-38 design**
  - 2x N312 / IN X-750 / Saffil batting
- **Engineered core designs**
  - AC1
    - 2x N550 / N312 uniaxial fibers
  - BC1 (Albany Techniweave)
    - 2x N440 / 3 layers braided N440 seals
  - TC1 (Albany Techniweave)
    - 4x N440 / alternating layers N440 seal wrap & N440 sheath / N440 uniaxial seals
- **Canted Coil Spring Preloader**
  - 302 SS MB109 Spring (Bal Seal)

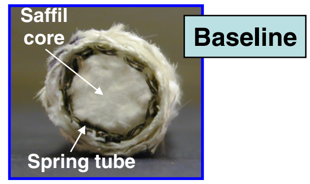

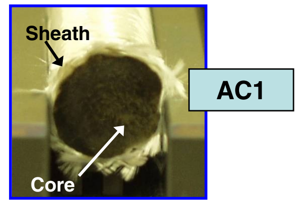

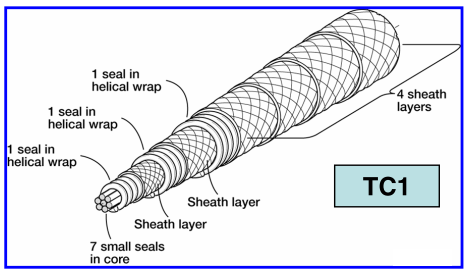

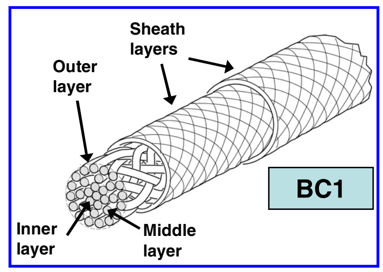

NASA Glenn Research Center

Several next-generation control surface seal prototypes and preloaders were evaluated for improved seal performance. The current control surface seal described earlier was used as a baseline for evaluations. Several seals with “engineered” cores were also fabricated and tested. While these seals do not possess internal spring elements, the construction of the core was designed to possibly enhance resiliency, flow blocking, and core integrity. Stainless steel canted coil spring (CCS) preloaders were also investigated.

Hot Compression Testing

- **System components**
  - Servohydraulic load frame (MTS)
  - Custom box air furnace (ATS)
  - Laser extensometer (Beta LaserMike)
- **Test Procedure**
  - 4 in. long specimens
  - Temperature – RT and 2000 °F
  - Preload to 1.0 lb
    (0.25 lb/in of seal)
  - 20 cycles
    - Load at 0.001 in/s to 20%
    - Dwell for 60 s
    - Fully unload at 0.001 in/s

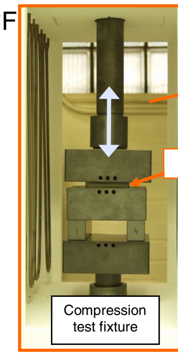

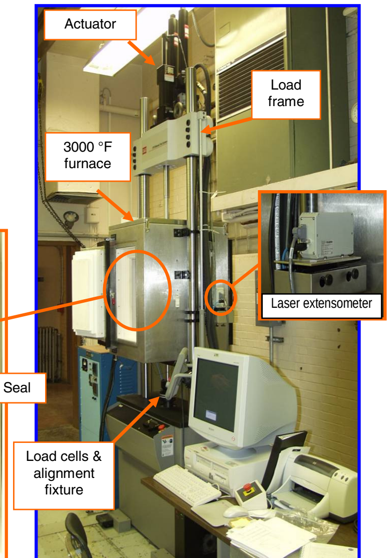

NASA Glenn Research Center

Room temperature and high temperature (2000 °F) compression testing of the seal specimens previously described was conducted using NASA's new high temperature compression rig. The rig consists of several main components including a servohydraulic load frame, a 3000°F air furnace, and laser extensometer to accurately measure compression levels. Four inch seal specimens were tested under low-rate cyclic loading.

Compression Test Comparison - Resiliency

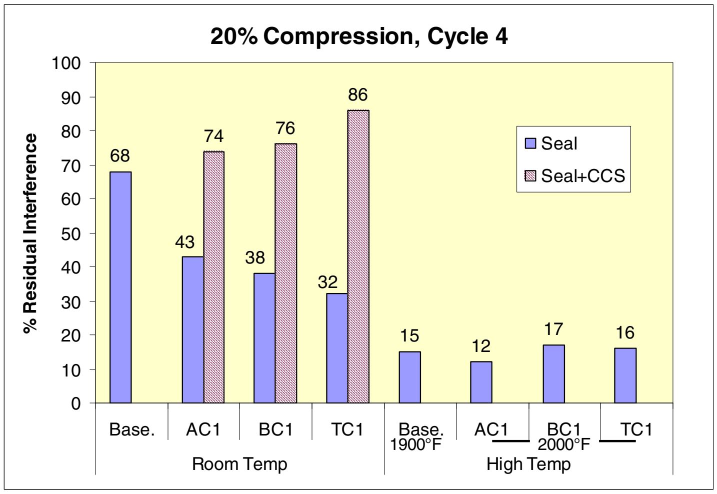

Note: Std. design tested in slightly different setup

- Significant drop in resiliency at high temperatures for all seals (Std. shows the most drop)
- Engineered core designs not significantly better than baseline design at room temp. or high temp.
- Substantial improvement in resiliency (up to 26%) by using canted coil spring vs. std. design

NASA Glenn Research Center

Results from the compression testing illustrated that the engineered core seals did not in-and- of-themselves improve resiliency vs. the baseline seal. However incorporation of the canted coil spring loader produced substantial improvements both in comparison to the engineered cores themselves (168% improvement) and to the baseline seal design (up to a 26% improvement). At high temperatures the baseline seal suffered a significant loss in resiliency which is not surprising based on the high temperature performance of the Inconel X-750 spring tube. At these temperatures, the engineered core alternatives demonstrated similar performance compared to the baseline spring tube seal.

Compression Test Comparison – Force vs. Displacement

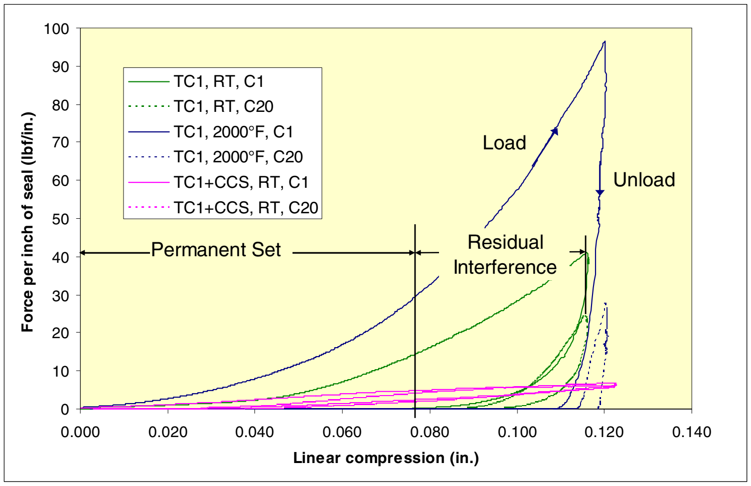

- TC1+CCS design showed significantly lower force (closer to std. design @ 2 lbf/in) and better load retention during cycling
- Substantial drop in load vs. cycling for RT (15%) and 2000 °F (72%)

NASA Glenn Research Center

A representative plot of seal load vs. linear compression for the TC1 seal design showed a significant drop in load capacity with this seal at both room temperature and high temperature. This indicates permanent set in the seals and a potential reduction in sealing abilities. By contrast, the room temperature test conducted on the seal with the CCS preloader demonstrated marked improvement in load retention, signifying sustained sealing capability. In addition, the compression curve for this seal+CCS showed fairly “flat” load vs. displacement performance, similar to the canted coil spring by itself. This behavior is beneficial in that the seal system can accommodate large strokes with minimal increases in force applied to opposing surfaces.

Compression Test Comparison – Resiliency Engineered Core Designs

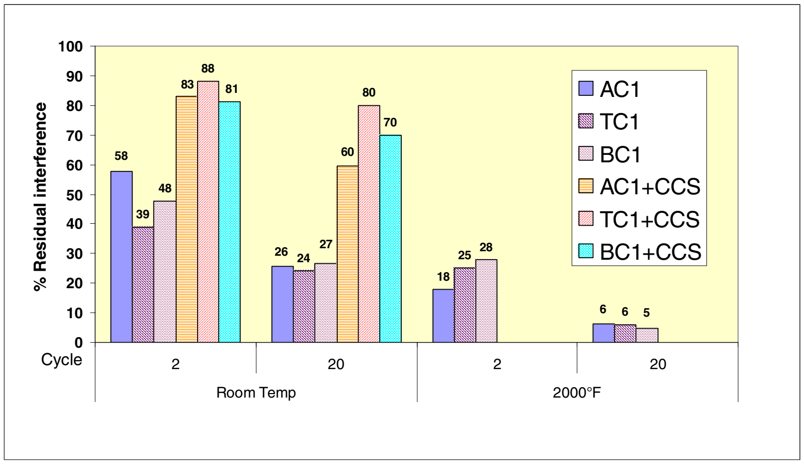

- Residual interference decreased with load cycling
- By 20th load cycle all seals had similar residual interference at room temperature and 2000 °F respectively (without springs)
- Canted coil springs behind seals improved residual interference by 2.3-3.3x by 20th load cycle (most sustained improvement is with TC1 design)

NASA Glenn Research Center

A closer examination of the resiliency for the engineered core alternatives showed that initially at room temperature the AC1 seal had the best performance. After load cycling, all seals demonstrated a reduction in residual interference due to compaction in the groove and exhibited similar resiliency values after 20 cycles. The canted coil spring yielded a substantial enhancement in resiliency for all the seals with the TC1 design showing the most sustained improvement as the candidates were load cycled. At high temperature, all the seal candidates demonstrated similar performance, especially after 20 cycles.

Compression Test Comparison – Peak Load
Engineered Core Designs

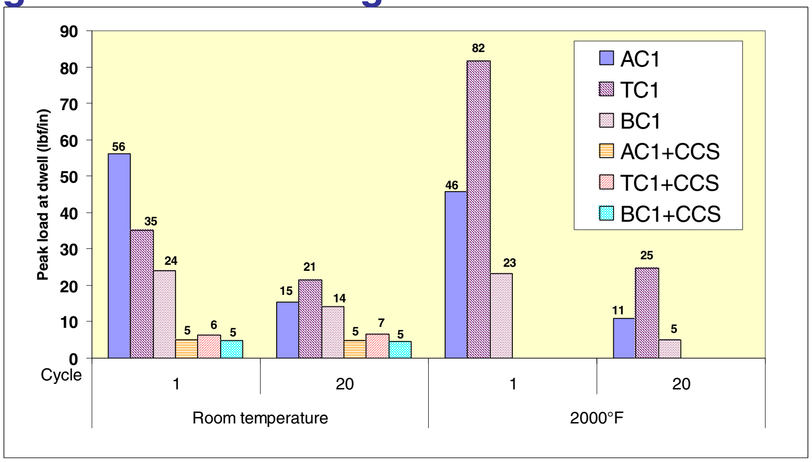

- AC1 was stiffer than TC1 and BC1 at room temp.
- TC1 showed significant increase in force at 2000°F, AC1 and BC1 showed drop in load
- After 20 cycles the room temp. and 2000 °F peak loads for the TC1 seal were similar, AC1 and BC1 were slightly higher at room temp.
- Seals on top of canted coil springs produced loads comparable to springs by themselves

NASA Glenn Research Center

THE UNIVERSITY OF TOLEDO

A comparison of the peak loads at room temperature showed that during the first cycle, the AC1 design had the greatest stiffness. After 20 cycles, the loads between the three seals were similar with the TC1 design exhibiting the smallest drop in load capacity. The seals on top of the canted coil springs yielded nearly identical loads for the three alternatives and demonstrated minimal effect of load cycling. At 2000 °F, the TC1 design had the highest load and appeared to become stiffer in contrast to the AC1 and BC1 seals. The reasons for this increase are unknown, but the phenomenon was repeatable. However, after 20 cycles, the peak loads for the TC1 seal at room temperature and high temperature were similar perhaps indicating this effect diminished with load cycling.

Flow Testing

- **System components**
  - Al flow fixture (4 in -12 in lengths)
  - 0-5 psid pressure transducer
  - 0-3000 SLPM flowmeters (100, 750, 1500, 3000 SLPM flowmeters)
- **Test Procedure**
  - 4 in long specimens
  - 0.25 gap (nominal)
  - 20% compression
  - 2 psid

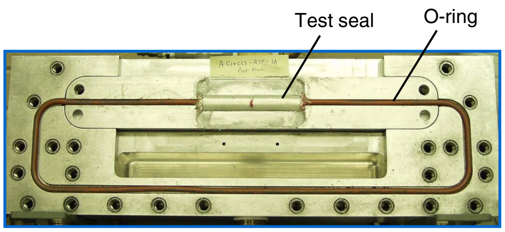

Test Setup for 4-in. Seal

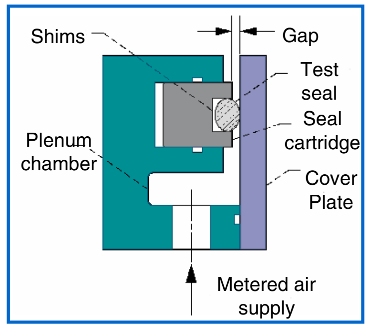

NASA Glenn Research Center

Low pressure (2 psid) flow testing was also conducted on the seal candidates using a modification to the linear flow fixture at GRC to accommodate shorter samples. The seals were tested under 20% compression using a nominal 0.250 gap.

Flow Test Comparison

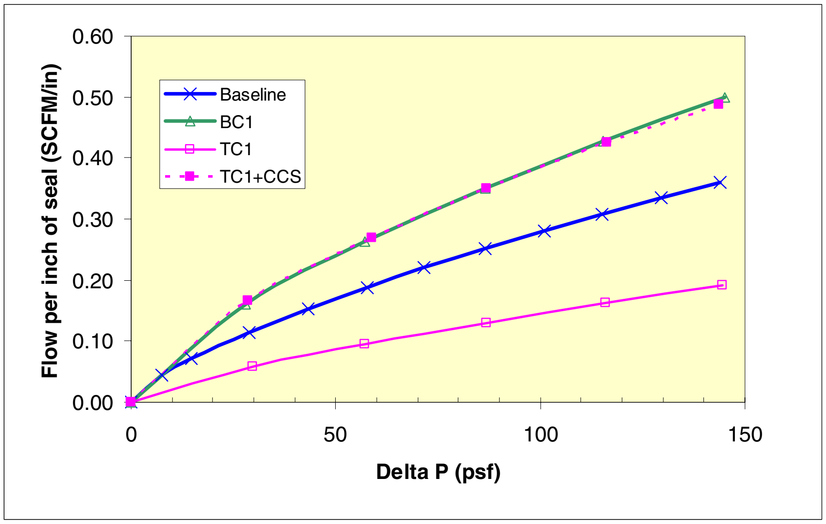

- The TC1 design showed improvement in flow vs. the baseline design
- TC1 had approx. ½ the flow of the baseline design at 144 psf (1.0 psi)
- When the CCS was used with the TC1 design, a notable increase in flow was observed

NASA Glenn Research Center

Flow tests with the engineered core designs showed mixed results relative to the baseline seal. The BC1 seal had worse leakage performance when compared to the baseline. This was probably the result of the seal being undersized by 0.060 in. relative to the groove. By contrast, the TC1 design demonstrated better flow-blocking performance. This seal was also slightly undersized (0.020 in. smaller than the groove width), but had a higher core density relative to both the baseline and BC1 designs. Despite this improvement, the TC1 seal would not be suitable in applications where force on opposing surfaces may be an issue (such as with Shuttle tile) due to its relatively high stiffness value. As discussed earlier, a preloader can reduce this force and was therefore tested. The combination of the TC1 seal and CCS demonstrated higher leakage rates than the baseline seal (up to 40% higher). The reason for this behavior is likely due to the slightly undersized seal (vs. groove width) that did not compress as much as the seal without a spring preloader and therefore did not adequately fill the groove. Careful sizing of the seal relative to the groove should help to alleviate this problem.

CMC Control Surface Compatibility Tests

- **Materials**
  - Nextel 440 and 720 fabrics - 3M and Albany Techniweave
  - Hexoloy SiC fixturing - Saint-Gobain
  - C/SiC CMC test panel – GE
  - C/C CMC test panel – SAIC
    - Coated with C-CAT SiC/TEOS/Type A Sealant on top and bottom surfaces
    - Coated with Ceraset (Dupont) on sides (after samples were cut)
- **Tests**
  - Samples heated to 2600 °F+ @ nominal 500°F/hr in air
  - Loaded with a 5 lb weight (7-8 psi)

NASA Glenn Research Center

THE UNIVERSITY OF TOLEDO

Testing was also conducted to assess the compatibility (i.e. bonding) of seal sheath materials against some of the new thermal protection system (TPS) ceramic matrix composite (CMC) materials at high temperatures. These TPS systems are anticipated to be used in many of the upcoming reusable space vehicles. The tests were conducted by vertically stacking the materials in an 2600 °F air furnace and subjecting the test stack to a 5 lb load.

CMC Compatibility Test Results

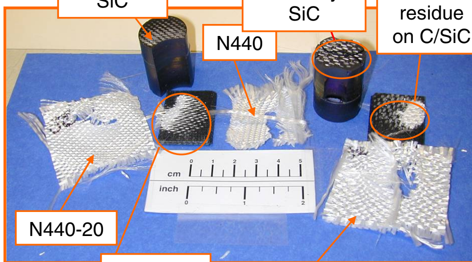

C/SiC

- All Nextel fabric samples showed some degree of sticking to the GE C/SiC test panels when exposed to 2600 °F+ in air
- There was minimal sticking between the Hexoloy SiC fixturing and the GE C/SiC
- N720 appeared to be a little more "brittle" than N440 after heat exposure at 2600 °F+ in air

C/C

- There was significant sticking of the C/C CMC to both Nextel 440 and Nextel 720 fabric
- There was significant sticking of the C/C CMC to the Hexoloy SiC fixturing
- N720 appeared to be a little more "brittle" than N440 after heat exposure at 2600 °F+ in air

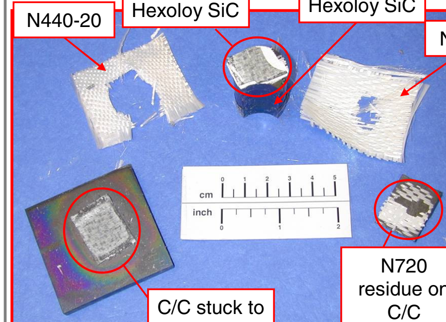

NASA Glenn Research Center

Results for the two CMC candidates showed varying degrees of sticking in all cases. In the worst instances, portions of Nextel fabric were ripped out as the stack was disassembled. During an actual flight, this type of damage could result in seal damage and/or control surface damage. Further work on optimizing the oxidation coatings for these CMC materials and their interaction with sheath fabrics will likely be needed to mitigate this issue.

Summary

- New seals with canted coil preloaders demonstrated promise for next generation control surface seals
  - Up to a 26% improvement in room temperature resiliency vs. baseline spring tube design
  - Load comparable to baseline design
  - Engineered cores eliminate core extraction observed with baseline design
- Twisted core design (TC1) showed best combination of resiliency and flow blocking ability
- CMC preliminary evaluations showed potential issues with sheath material candidates (Nextel fabric) sticking to C/SiC and C/C CMC
- Future work:
  - Advanced control surface seals
    - Optimize seal + preloading device combinations that meet resiliency and flow blocking goals at high temperature
    - Evaluate and optimize durability of engineered core seals
  - X37 control surface seal development
    - Conduct high temperature scrub and compression testing as well as RT flow testing on flaperon seal candidates against CMC test panels

NASA Glenn Research Center

Testing of several new control surface seal candidate systems at NASA GRC has indicated significant promise in improving upon the current baseline seal design. The use of preloaders along with improved seal designs have demonstrated substantial enhancements in resiliency as well as expanded operational envelopes (in terms of ability to accommodate large gap changes and block the flow of high temperature gases). Future work will need to be done to fully optimize these seal systems and asses their suitability in upcoming space vehicles, such as the X-37 spacecraft.

HIGH TEMPERATURE METALLIC SEAL DEVELOPMENT FOR AERO PROPULSION AND GAS TURBINE APPLICATIONS

Greg More
The Advanced Products Company
E. Greenwich, Connecticut

Amit Datta
Advanced Components & Materials, Inc.
North Haven, Connecticut

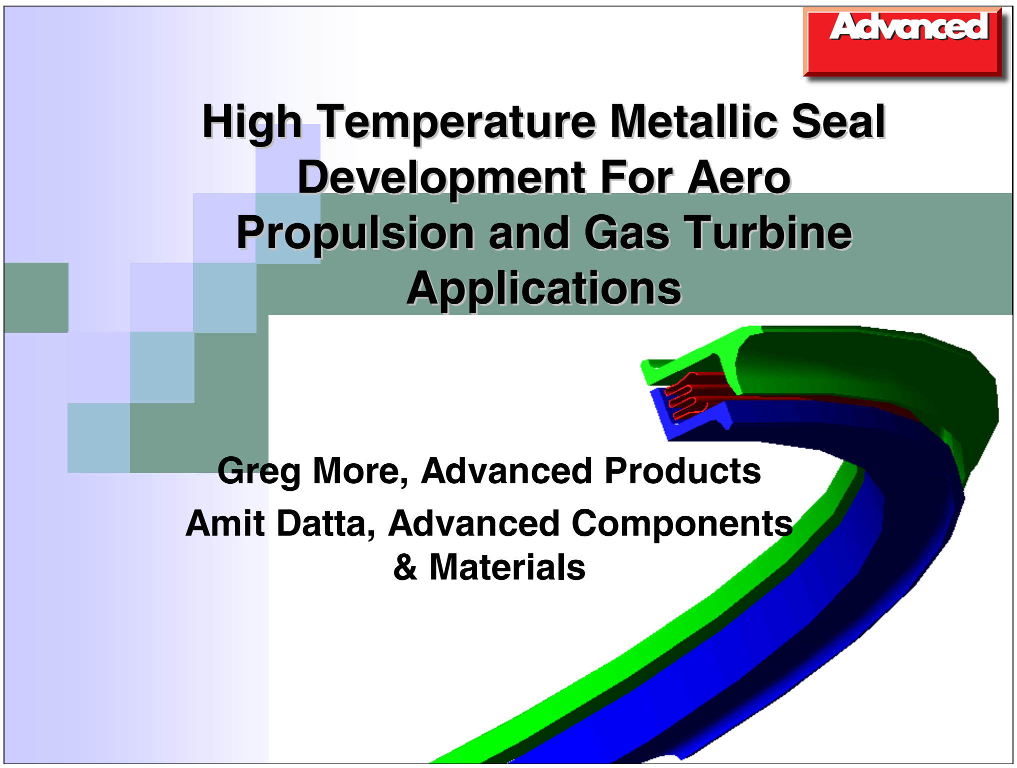

Advanced

Outline

- Background
- Enhanced designs based on cold formable alloys - René 41, PM1000
- New concepts
  - Designs incorporating a thermal barrier
  - Designs incorporating cast blade alloys
- Conclusions

Advanced

Background

Market needs for high temperature (1500 – 1800 ºF)

Seals:

- **Reduce cooling air and simplify seal cavity structure in current gas turbine engines**
- **Gas Turbine Combustor seal applications**
  - **Locations where metal sealing was previously not an option**
- **Seals for engine heat exchanger panels and back-up structures for future hypersonic engines.**

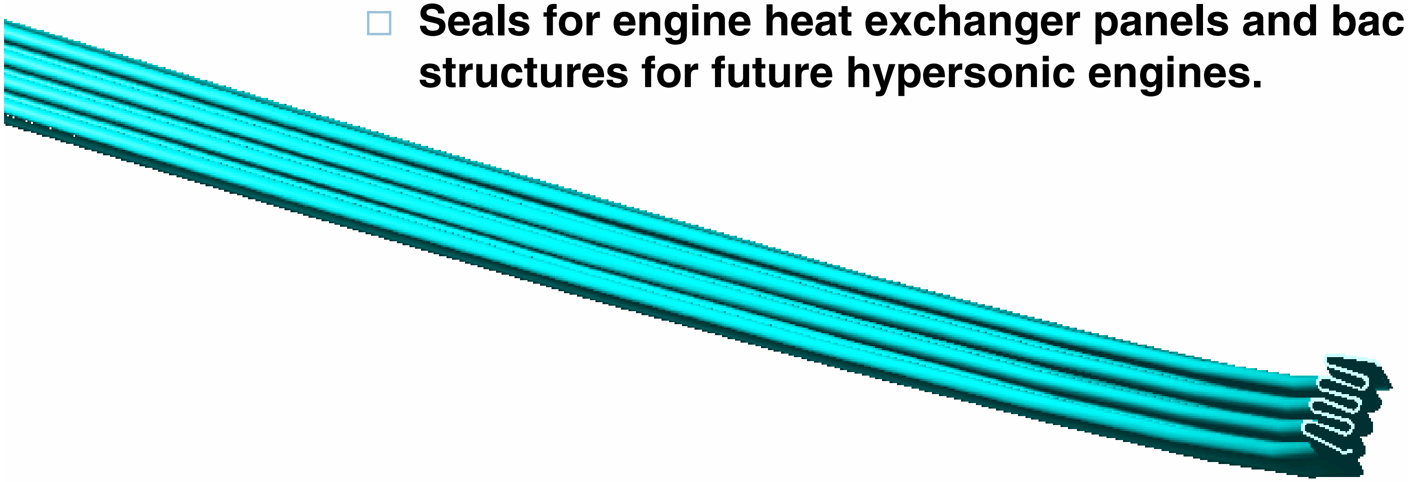

Advanced

Background

- Current seals are made from cold formable superalloy sheet metal alloys, such as 718, Waspaloy… *needs cooling air*
- Based on comprehensive stress relaxation studies, René 41 (a γ′ hardened superalloy) and PM1000 (an oxide dispersion hardened alloy) were identified as candidate alloys
- E type seals have been made and characterized
  - Seals have been high temperature performance tested
  - Demonstrated superior characteristics when compared with existing designs and materials

PM1000 E type seals

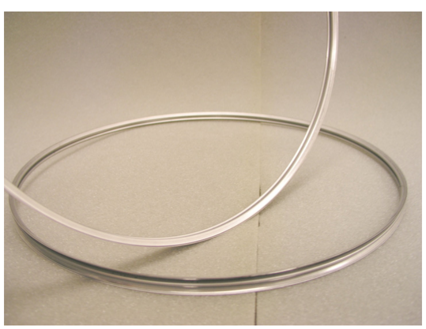

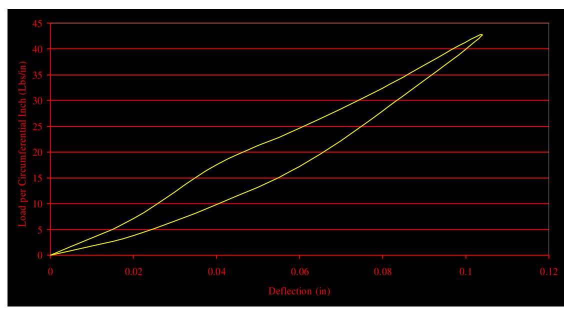

Room Temperature load vs. deflection for PM1000 E type seal

PM1000 E type seals

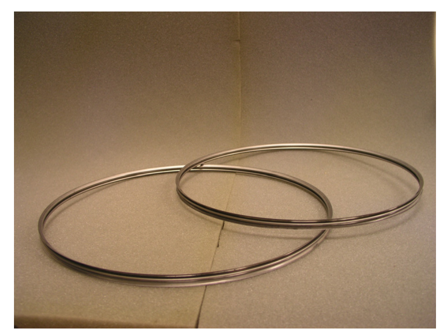

Advanced

Enhanced Designs Based on New Alloys

- Material Stress relaxation design concerns

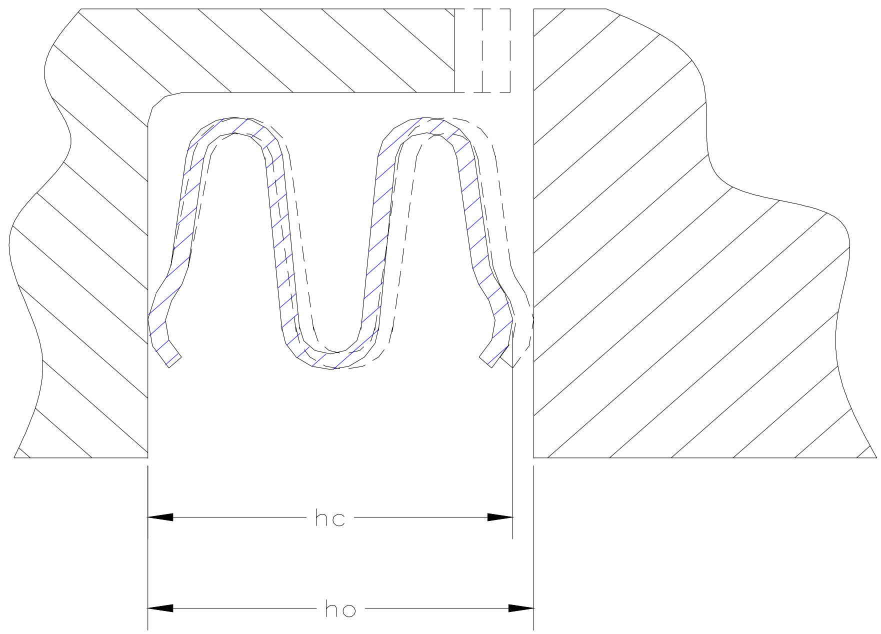

Seal gap created resulting from stress relaxation at elevated temperatures. The original height ho is reduced to hc creating a gap when the flange moves away from the compressed condition.

Advanced

Enhanced Designs Based on New Alloys

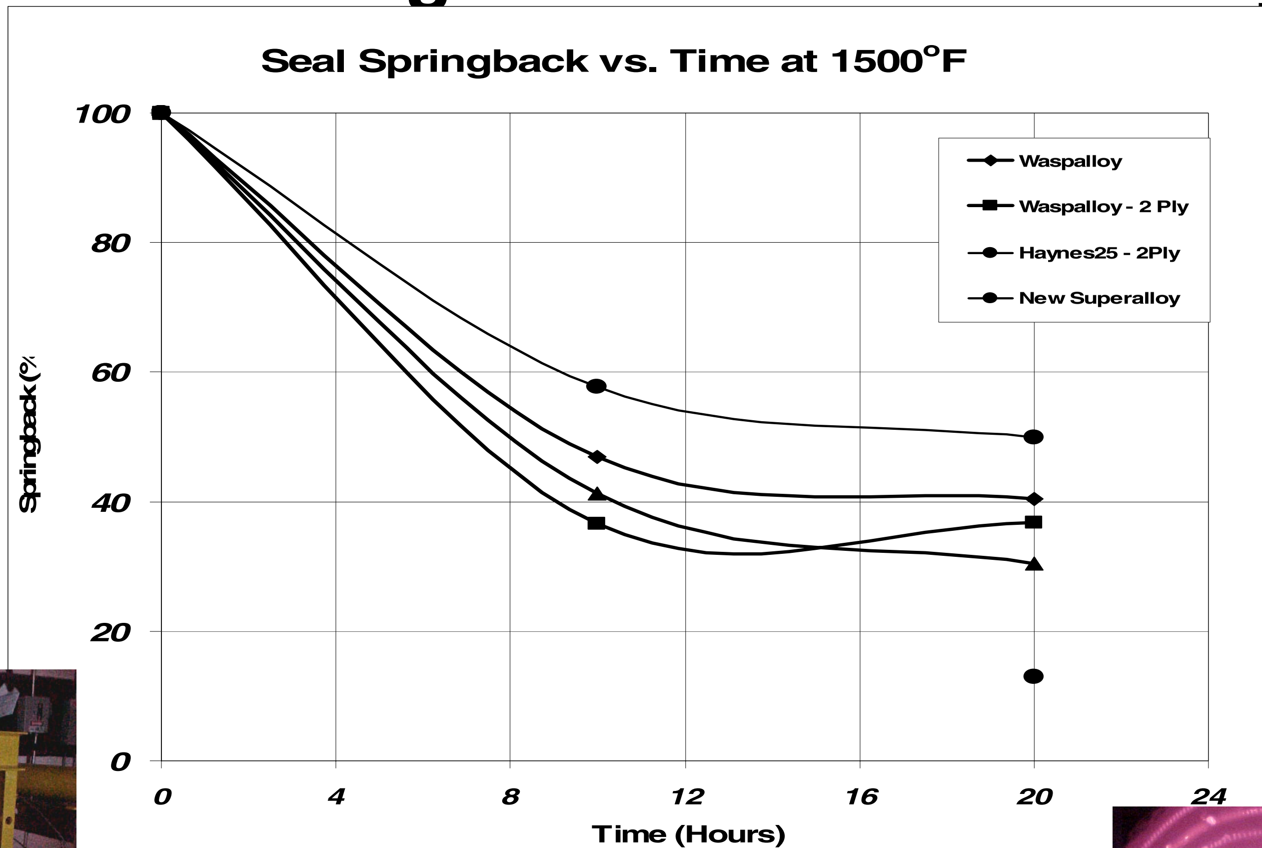

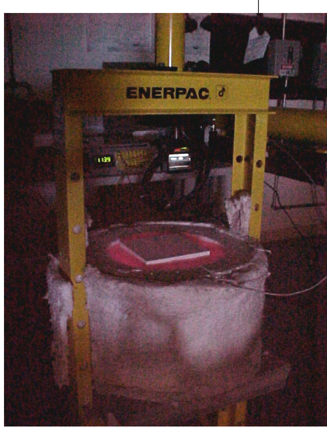

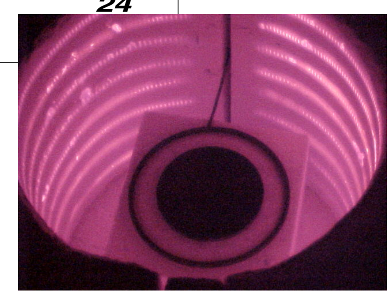

Residual spring back as % of total compression vs. exposure time at 1500 ºF

Advanced

New Seal Concepts

- **Seal design incorporating an integral thermal barrier**

  - *Integral thermal barrier insulates the spring element from high temperature*

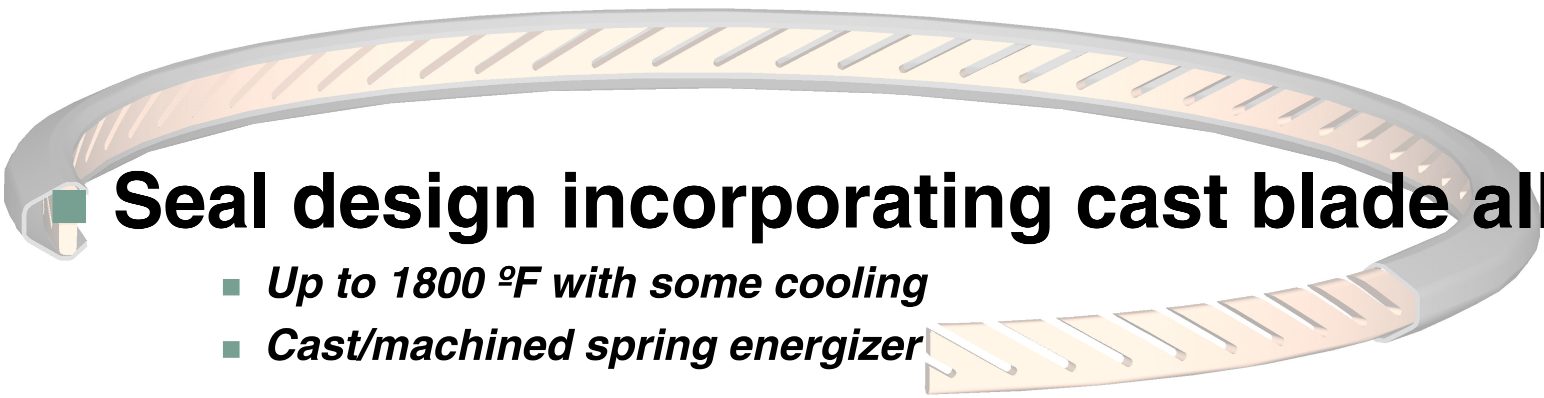

- **Seal design incorporating cast blade alloy**
  - *Up to 1800 ºF with some cooling*
  - *Cast/machined spring energizer*

Advanced

Designs Incorporating Integral Thermal Barrier

- Incorporating an insulating element into a metallic seal configuration can significantly lower spring element temperatures
- By lowering spring element temperatures, stress relaxation can be significantly reduced
- Multiple configurations are possible
- An insulated seal has been design, manufactured, and tested in conjunction with ALSTOM Power
- Seal consists of a compliant insulating cover and a much stiffer spring energizing element
- The insulating cover protects the inner spring energizer from high temperature exposure and permits the spring element to operate at a lower temperature
- The spring energizer maintains the sealing load

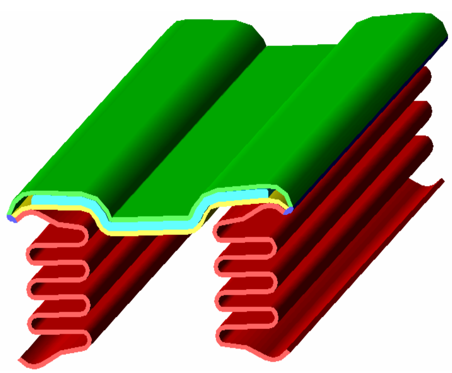

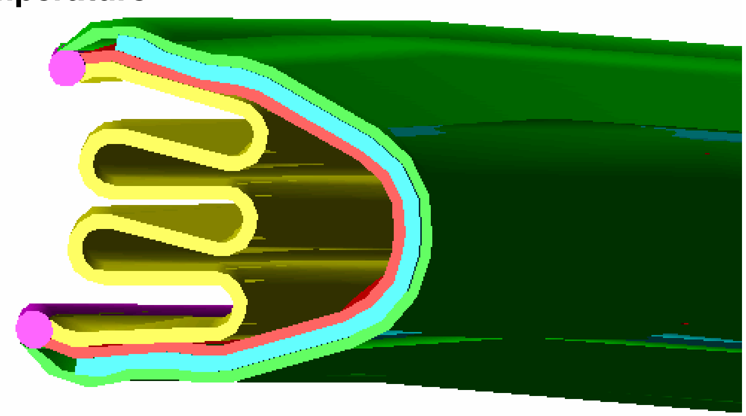

Combustor Liner Seal Incorporating Integral Thermal Barrier

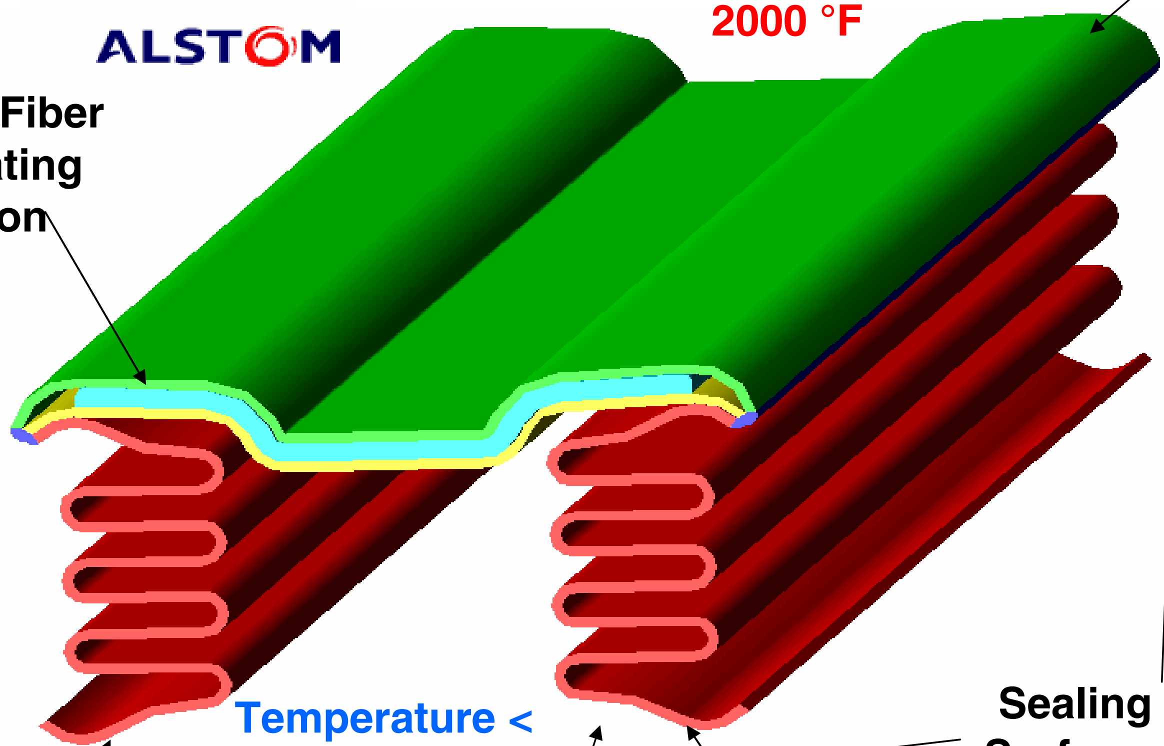

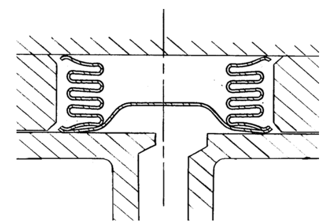

Seal configuration as installed

Patent Pending Design

Advanced

Thermal Paint Test Results

- Seals were coated with a Rolls Royce proprietary thermal paint to measure temperature drop across seal and effectiveness of thermal insulation
- Test set-up and evaluation was headed by ALSTOM Power and testing was performed in their full size test engine

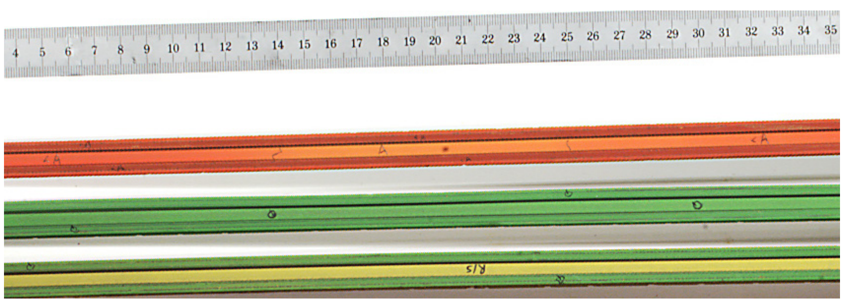

Thermal Gradients on Cold Side

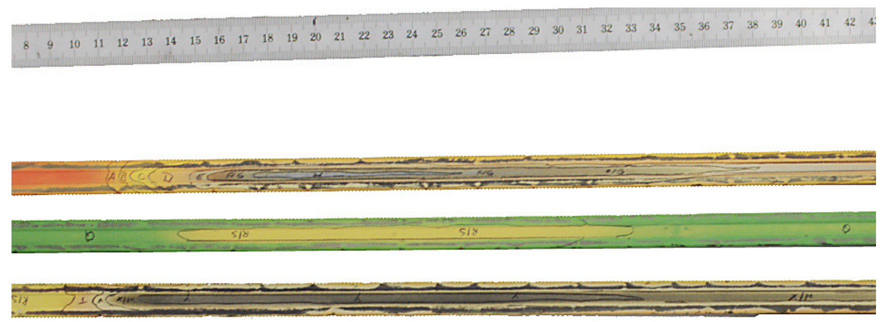

Thermal Gradients on Hot Side

- Testing has been performed and evaluations are complete:
  - Non-Insulated seal showed a temperature drop of < 200 °F
  - Insulated seals showed a temperature drop of > 1000 °F

Advanced

Designs Incorporating Cast Blade Alloys

- Blade alloys are strengthened by very stable γ′ phases, stable up to 1800 ºF
- Not suitable for cold/hot forming seal cross sections
- Sealing surface is provided by a cold formable oxidation resistant alloy jacket
- Seal is energized by a blade alloy spring

Advanced

Designs Incorporating Cast Blade Alloys

Characteristics of Candidate Metal Alloys for High Temperature Seals

Characteristics	MARM 247	PM 1000	PM 2000
Yield Strength at 1800 ºF	90 Ksi	26 Ksi	12 Ksi
1000 hr creep-rupture strength at 1900 ºF	25 Ksi	15 Ksi	6 Ksi
Cyclic oxidation resistance at 2200 ºF (wt. change in 1000 hr.)	1 mg/cm^2	0 mg/cm^2	0 mg/cm^2

Advanced

Designs Incorporating Cast Blade Alloys

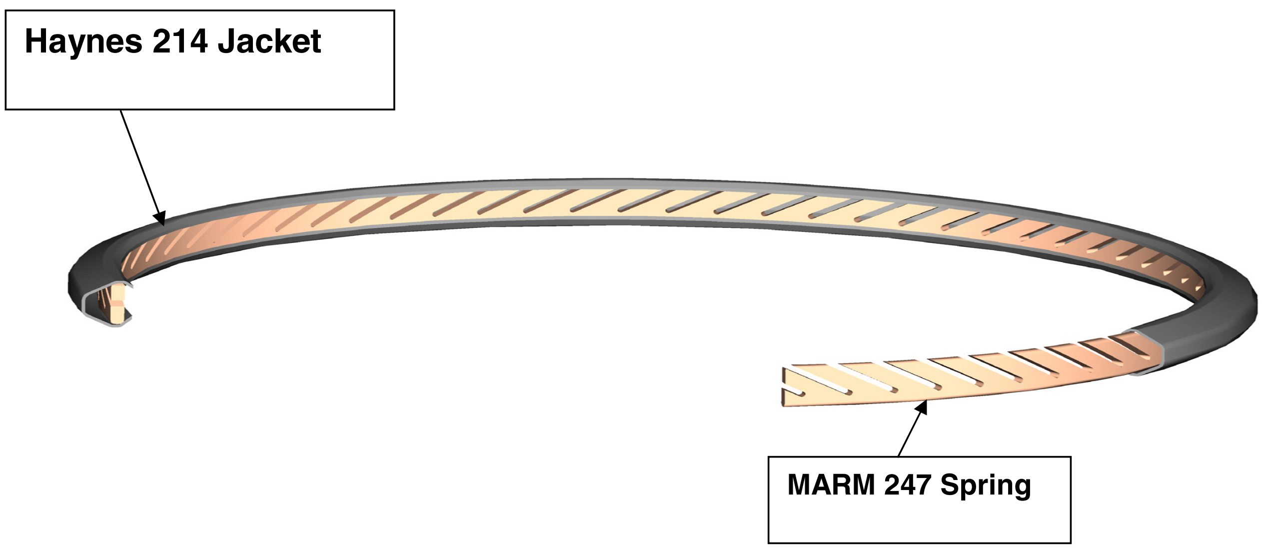

(Patent Pending)

Designs Incorporating Cast Blade Alloys

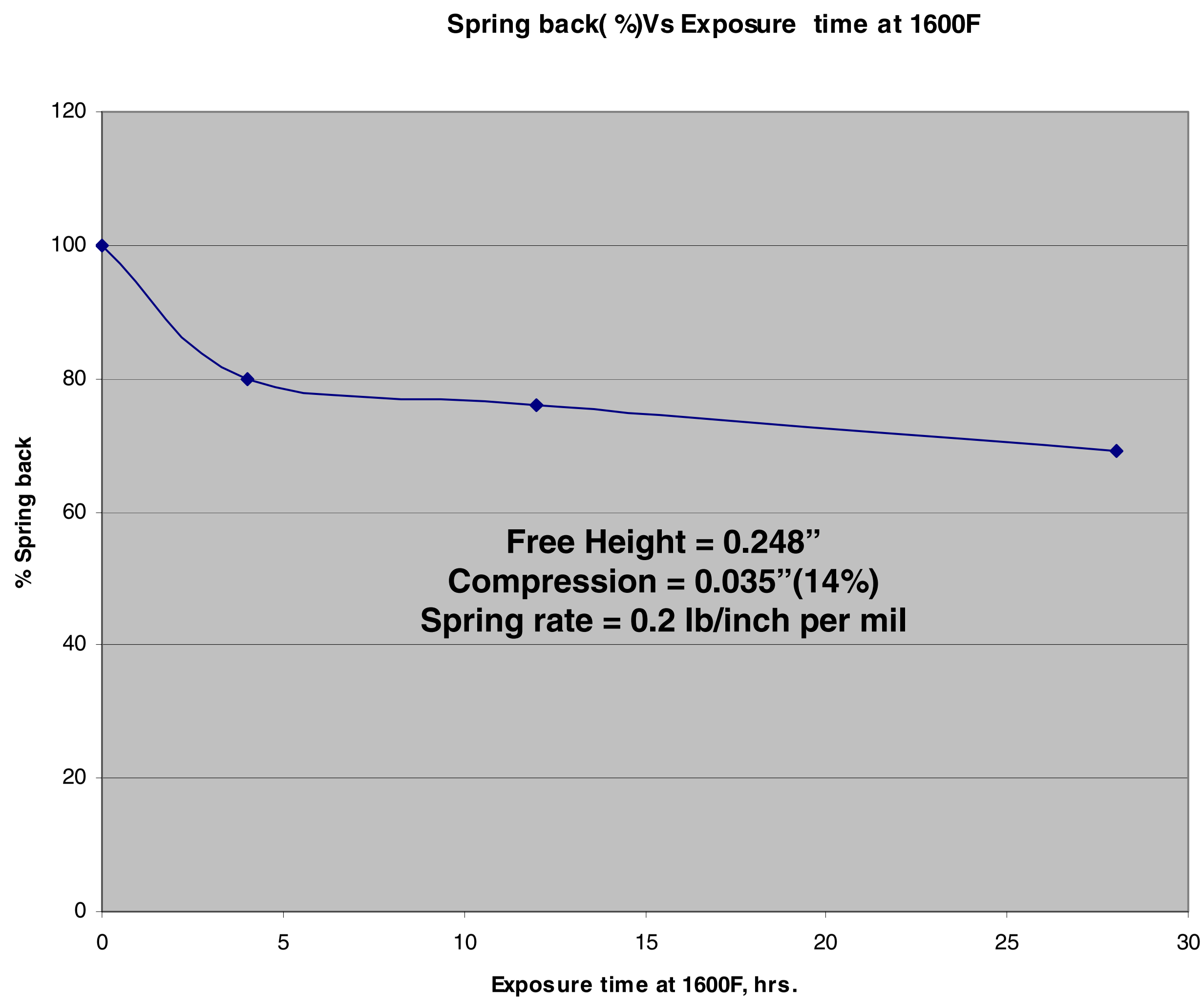

Advanced

Conclusions

- Improved seal performance has been demonstrated with new alloys, such as Rene'41 and PM1000
  - Further development is ongoing with the optimization of an ODS base material seal
- New concepts incorporating blade alloy springs and integral thermal barriers are being evaluated to raise the application envelope.

Advanced

Questions ?

BRAZEFOIL HONEYCOMB

Geosef Straza
AeroVision International
San Diego, California

NASA Seal/Secondary Air Delivery Workshop

Sponsored by
NASA Glenn Research Center
November 5 and 6, 2003

BrazeFoil Honeycomb

The evolution of brazing honeycomb:

First, there was braze powder, then braze tape, and now there is…

BrazeFoil Honeycomb!

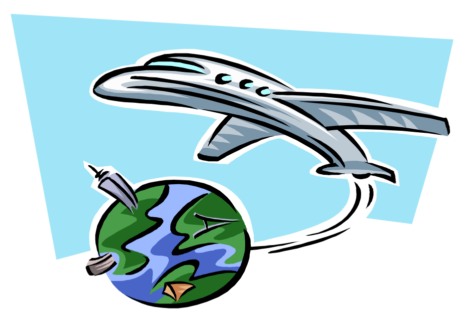

Close-up of BrazeFoil Honeycomb

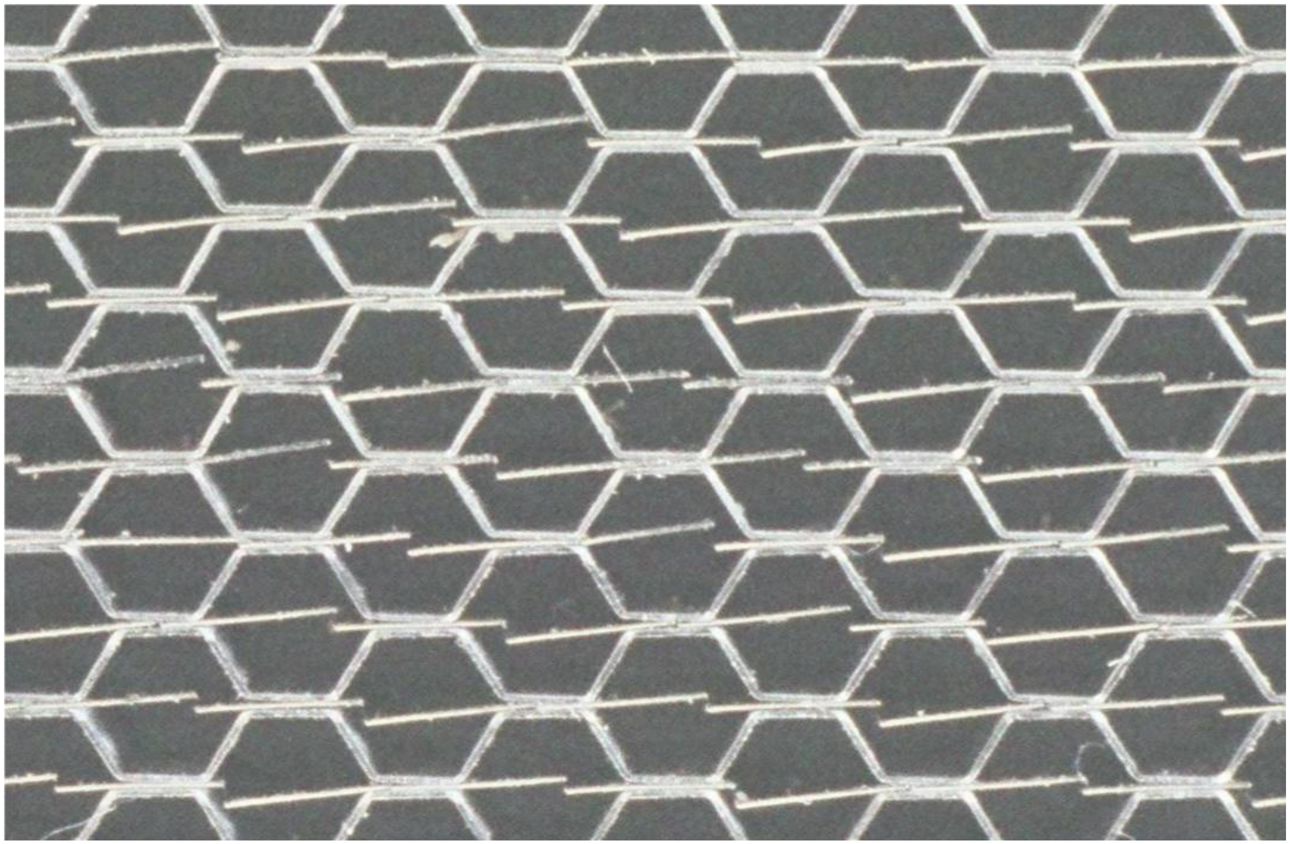

What is BrazeFoil Honeycomb?

- BrazeFoil Honeycomb is a patented process that incorporates the braze alloy into the honeycomb cell structure.
- The Braze foil is slit to create flexibility and reduce stress in the honeycomb.
- A ribbon of braze alloy passes through every cell.
- An amount of braze alloy is perfectly matched to each honeycomb node to form complete joints at the base of each honeycomb cell.

Turbine Seal Applications

- Seals
- Shrouds
- Stators
- Cases
- Vanes

Product Improvements

- Creates a superior quality part
- Accurate way to apply correct amount of braze alloy
- 100% Uniformity, eliminating inconsistencies
- Optimizes braze joint formation and performance
- Provides reliable melting and flow
- Assures better honeycomb to substrate contact
- Unlimited Shelf life
- Environmental, Health, and Safety (EH&S) benefits

Process Improvements

- Increases productivity and yield
- Reduces labor, rework, and rejects
- Eliminates powder or tape operation
- Eliminates filled cells
- Eliminates grinding operation (no braze splatter)
- Eliminates contaminant and residue (no organic binders)
- Eliminates process variability
- No out-gassing which saves furnace time
- Maintains a better, more breathable environment

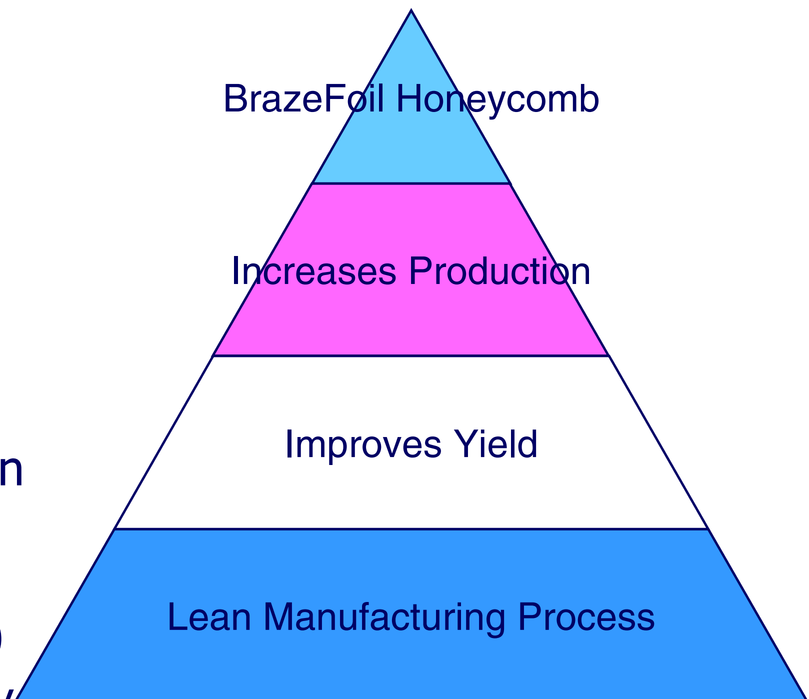

Benefits to Engine Manufacturers

- Weight savings
- Potential extended life to knife-edge seals (Advanced Turbine Seal Programs)
- Reduced machining at tear-down (subsequent repairs)

Process Advantages of Braze Foil H/C

Barnes Aerospace
Advanced Fabrications Division
BARNES® GROUP INC

Estimated **Weight Savings** by part number

Part No.	Engine	Savings/Engine
2083M10	CF6-80E	.359 lbs.
2083M11	CF6-80E	.503 lbs.
2083M12	CF6-80C	.361 lbs.
2083M13	CF6-80C	.506 lbs.
2083M14	CF6-80C	.529 lbs.
2083M15	CF6-80E	.449 lbs.
1474M80	CF6-80C	.453 lbs.
1862M61	CF6-80C	.365 lbs.
1862M62	LM6000	.359 lbs.
1862M63	LM6000	.503 lbs.
1862M64	LM6000	.526 lbs.
L47753	LM6000	.458 lbs.
L47754	LM6000	.596 lbs.
L47755	LM6000	.772 lbs.
9663M69	LM2500	.477 lbs.
9663M70	LM2500	.492 lbs.

Total Savings

Engine	*lbs.*
CF6-80E	*1.311*
CF6-80C	*2.214*
LM6000	*3.214*
LM2500	*.969*

Prepared by:
Gary Studt
10-29-03

Comparison

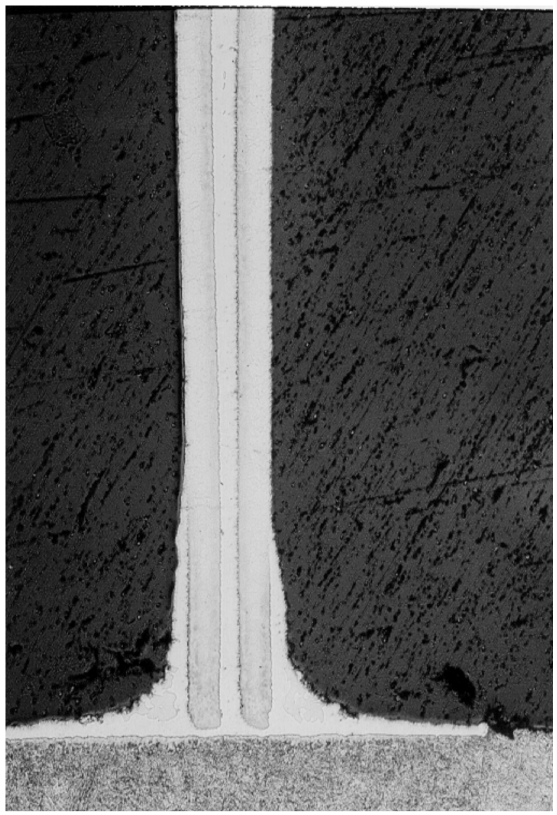

BrazeFoil Honeycomb

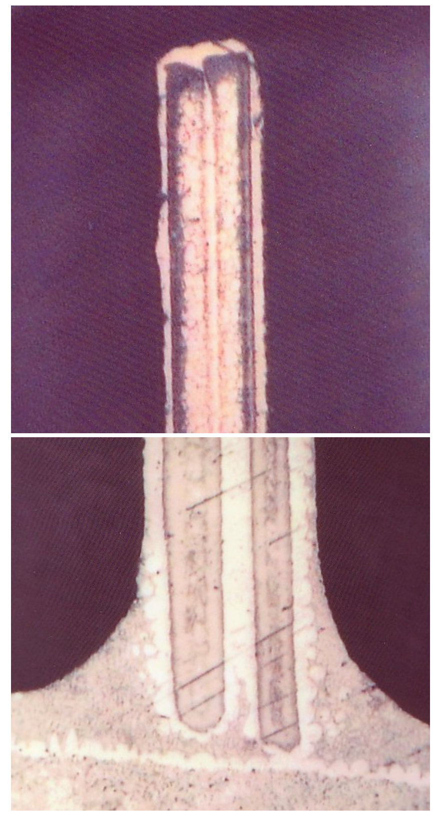

Standard Honeycomb brazed with powder

BrazeFoil Honeycomb Peel Test

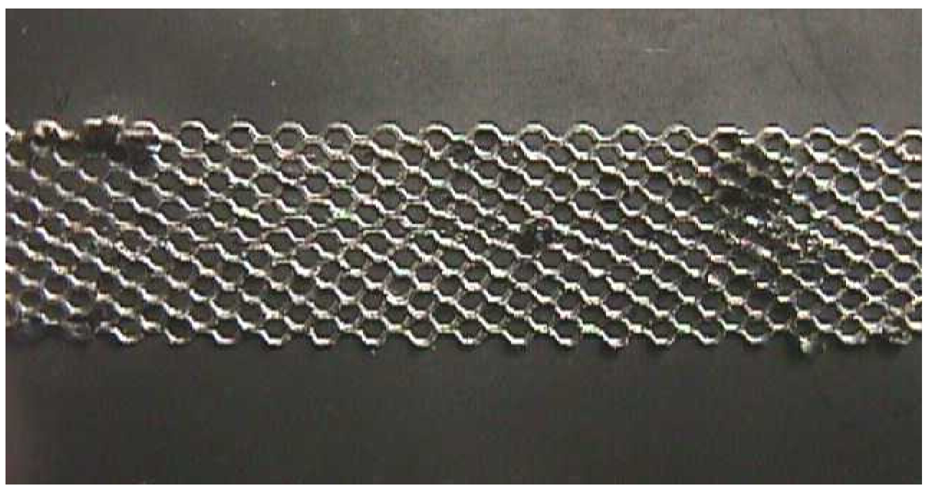

BrazeFoil Honeycomb Fillet

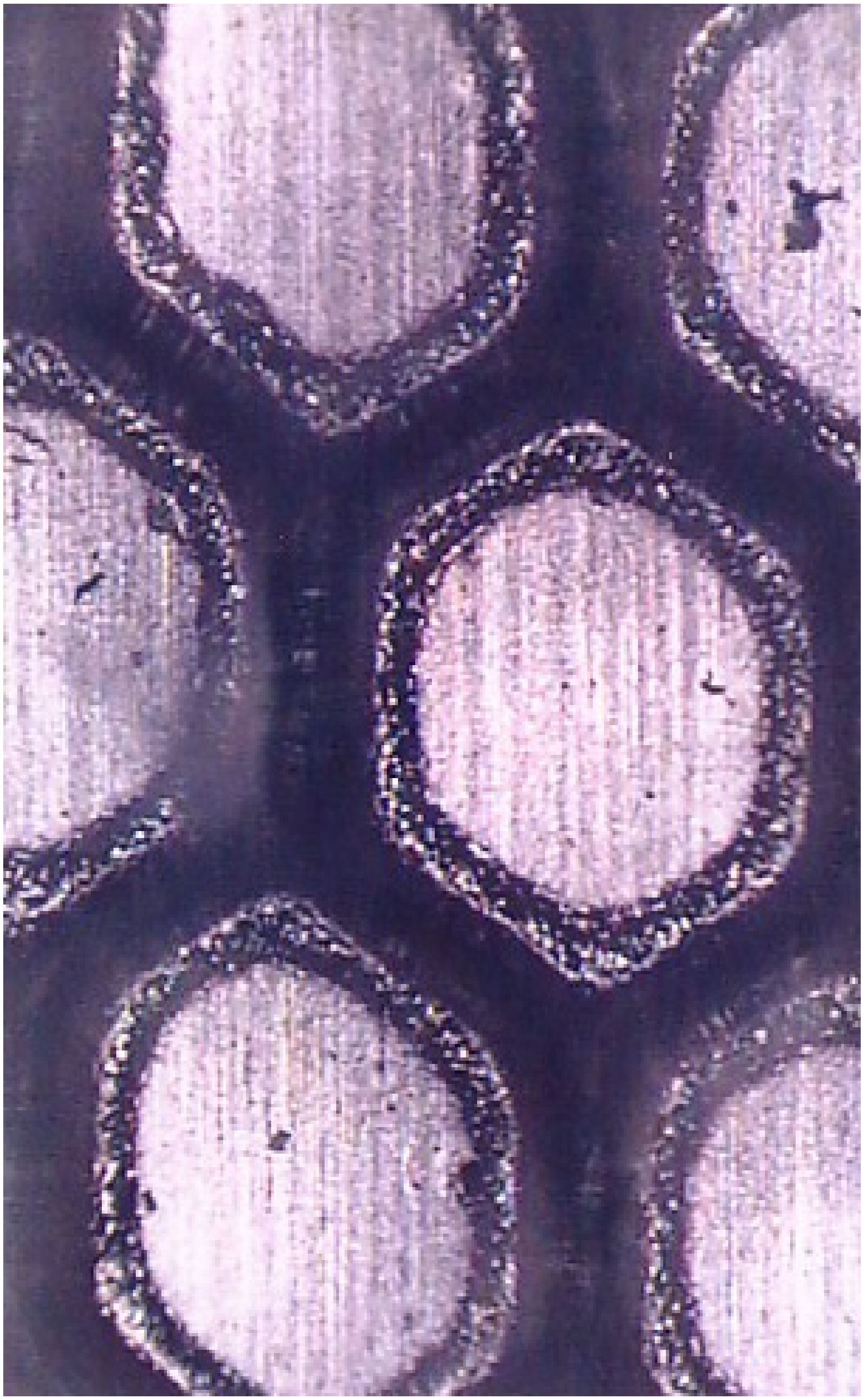

Knife-edge Seal Testing

- To be completed by:
  National Research Council Canada,
  Institute for Aerospace Research,
  Structures, Materials, and Propulsion Laboratory

BrazeFoil Honeycomb Micrograph

RR Micros of Aerovision Honeycomb Integral Braze Alloy

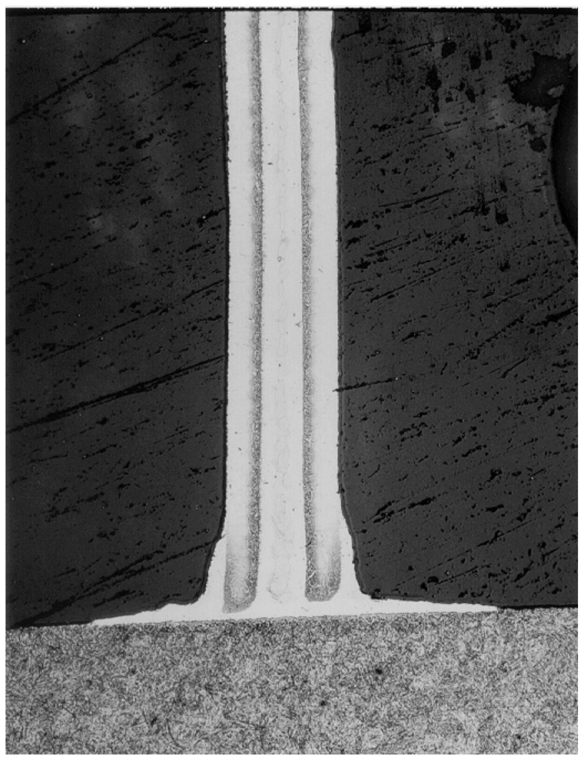

Integral Braze Foil Only

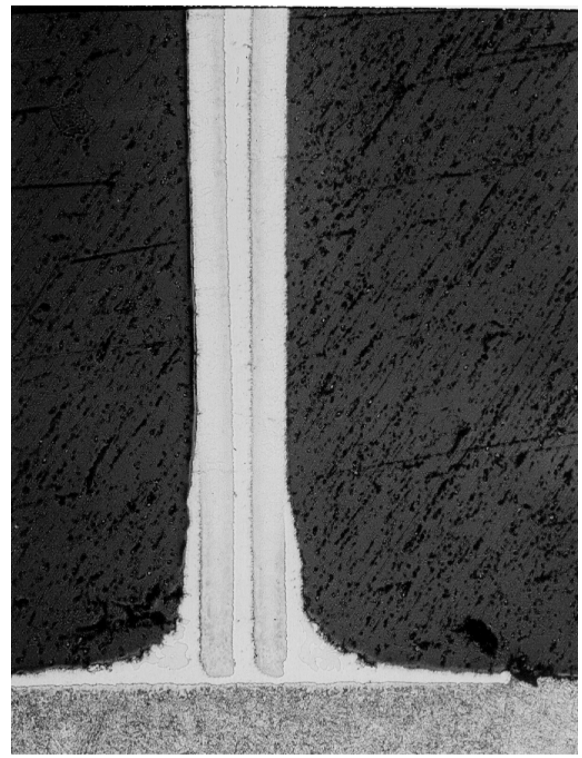

Integral Braze Foil with Face Feed

Rolls-Royce EIS 1270 Rev. D 11/20/01

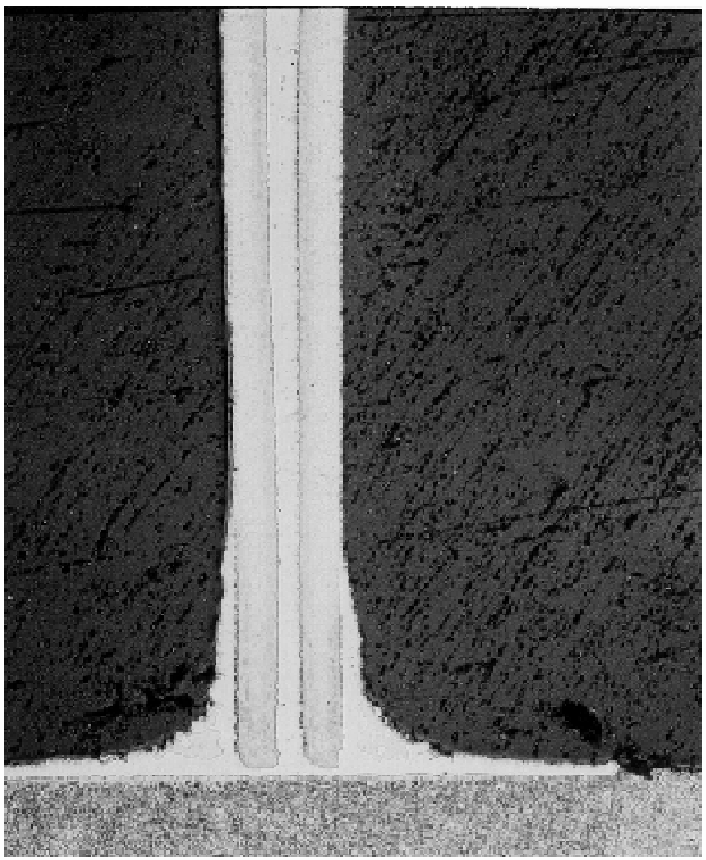

3.5.6 Excessive Bond Material: For honeycomb height taller than .060 inch, bonding material shall not exceed 25% of cell height. For honeycomb height less than .060 inch, bonding material shall not exceed a height of .015 inch. Bonding material may encroach on open cell walls above the maximum height, if the thickness of the encroaching material does not exceed .0005 inch.

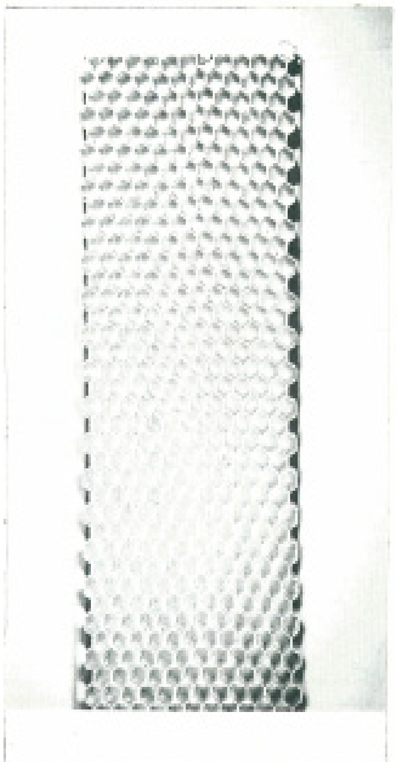

FIGURE 1
Brazed sample in as received condition
Show a clean brazed Joint

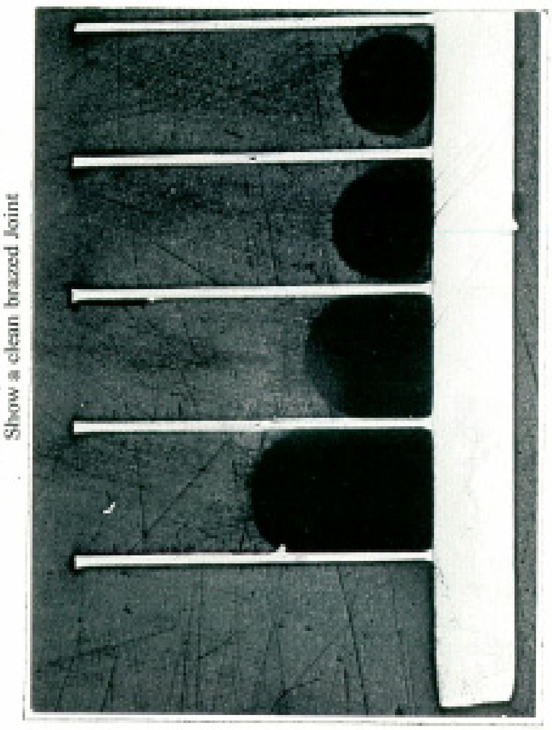

FIGURE 2
Cross-section of a honeycomb braze joint at 10X
Etchant: Kallings reagent

HONEYCOMB BRAZE EVALUATION

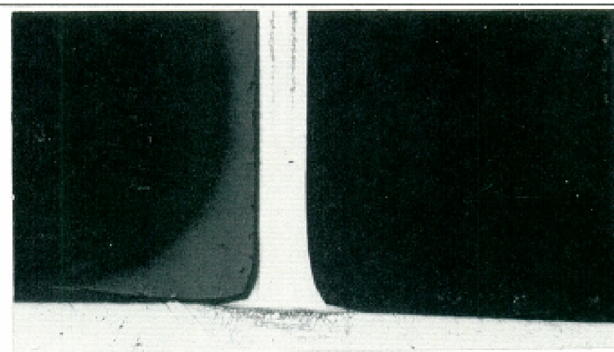

FIGURE 3
Honeycomb Brazed Post at 50X
Etchant: Kallings reagent

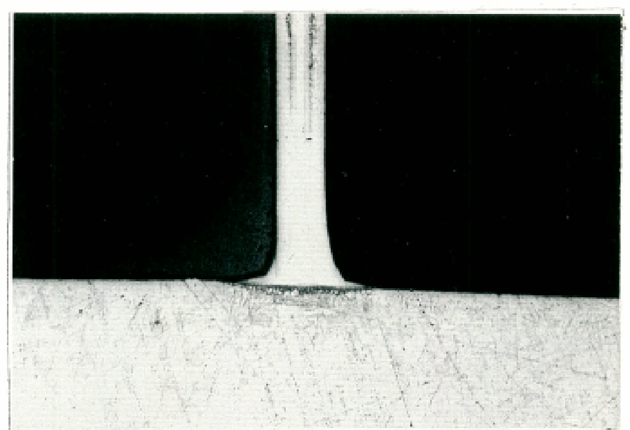

FIGURE 4
Honeycomb Brazed Post at 50X
Etchant: Kallings reagent

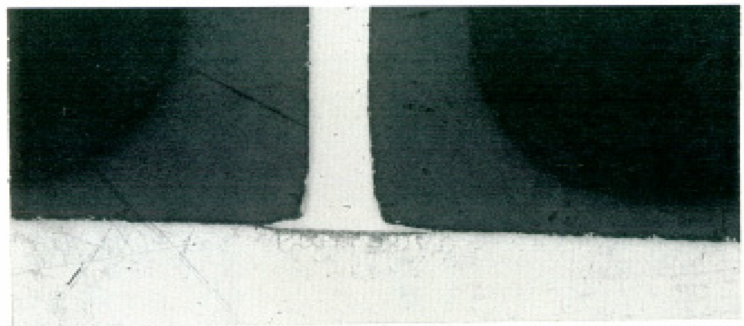

FIGURE 5
Honeycomb Brazed Post at 50X
Etchant: Kallings reagent

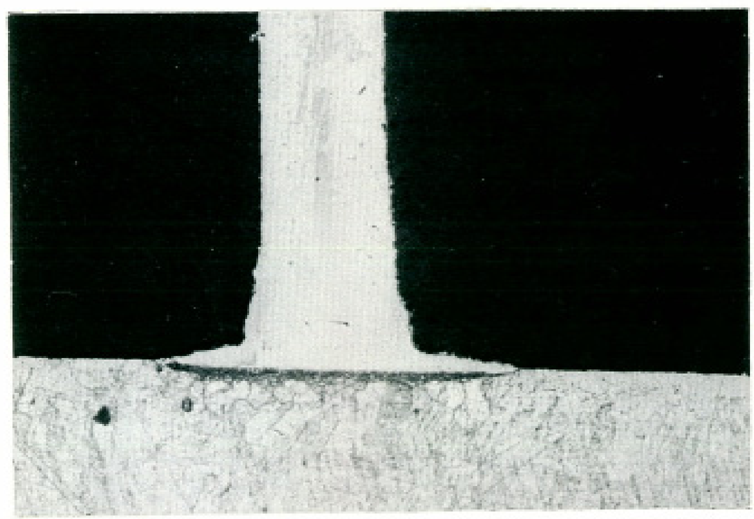

FIGURE 6
Honeycomb Brazed Post at 100X
Etchant: Kallings reagent

Approvals

- **Pratt & Whitney**
  - PWA 36123
- **Rolls-Royce**
  - EIS 1270

Structural Applications

- Hypersonic Flight Vehicles
- Marine Industry to include advanced ship hulls
- Commercial aircraft
- Oil Industry to include deep drilling applications
- Civil applications such as super-structures and bridges

Possible Structural Advantages

- Increased strength to weight / cost ratios
- Increased manufacturing efficiency
- More consistent sandwich so that stresses are more predictable

Sandwich Structure Micrograph

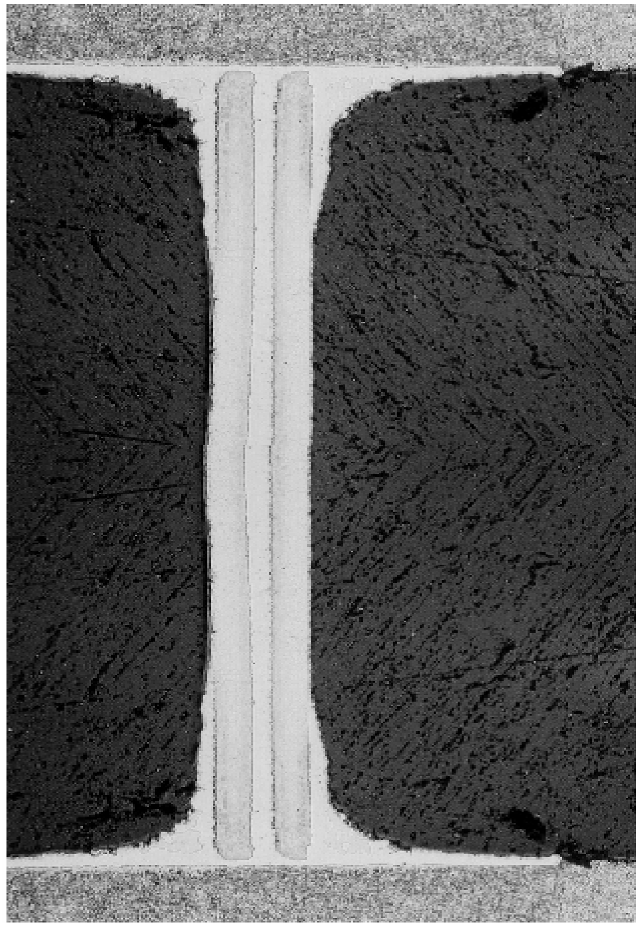

Estimated Stress Allowable Values for ISTAR Heat Exchanger Panel (Psi)

Material Property Test	Cell size @ thickness	3/16"@ 0.002" (47 lbs)	¼" @ 0.003" (46 lbs)	3/8" @ 0.005" (45 lbs)
Stabilized Compression		1900	1975	1950
Tension		1200	1250	1225
Ribbon Shear		700	725	750
Longitudinal Shear		1200	1250	1300

All combinations of panels estimated an average weight savings of approximately 13% over other types of brazed honeycombs.

Presented by:

- Geosef (Joey) Straza
  AeroVision International

- Dan Kay
  Kay & Associates

REPORT DOCUMENTATION PAGE

Form Approved
OMB No. 0704-0188

1. AGENCY USE ONLY (*Leave blank*)	2. REPORT DATE	3. REPORT TYPE AND DATES COVERED
	September 2004	Conference Publication

4. TITLE AND SUBTITLE

2003 NASA Seal/Secondary Air System Workshop

5. FUNDING NUMBERS

WBS–22–708–48–01

6. AUTHOR(S)

Bruce M. Steinetz and Robert C. Hendricks, editors

7. PERFORMING ORGANIZATION NAME(S) AND ADDRESS(ES)

National Aeronautics and Space Administration
John H. Glenn Research Center at Lewis Field
Cleveland, Ohio 44135–3191

8. PERFORMING ORGANIZATION REPORT NUMBER

E–14436–1

9. SPONSORING/MONITORING AGENCY NAME(S) AND ADDRESS(ES)

National Aeronautics and Space Administration
Washington, DC 20546–0001

10. SPONSORING/MONITORING AGENCY REPORT NUMBER

NASA CP—2004-212963–VOL1

11. SUPPLEMENTARY NOTES

Proceedings of a conference held at Ohio Aerospace Institute sponsored by NASA Glenn Research Center, Cleveland, Ohio, November 5–6, 2003. Responsible person, Bruce M. Steinetz, organization code 5950, 216–433–3302.

12a. DISTRIBUTION/AVAILABILITY STATEMENT

Unclassified - Unlimited
Subject Categories: 37, 16, and 99 Distribution: Nonstandard

Available electronically at http://gltrs.grc.nasa.gov

This publication is available from the NASA Center for AeroSpace Information, 301–621–0390.

12b. DISTRIBUTION CODE

13. ABSTRACT ***(Maximum 200 words)***

The 2003 NASA Seal/Secondary Air System Workshop covered the following topics: (i) Overview of NASA's perspective of aeronautics and space technology for the 21st century; (ii) Overview of the NASA-sponsored Low Emissions Alternative Power (LEAP), Ultra-Efficient Engine Technology (UEET), Turbine-Based Combined-Cycle (TBCC), and Revolutionary Turbine Accelator (RTA) programs; (iii) Overview of NASA Glenn's seal program aimed at developing advanced seals for NASA's turbomachinery, space propulsion, and reentry vehicle needs; (iv) Reviews of advanced sealing concepts, test results, experimental facilities, and numerical predictions; and (v) Reviews of material development programs relevant to advanced seals development. The NASA UEET and TBCC/RTA program overviews illustrated for the reader the importance of advanced technologies, including seals, in meeting future turbine engine system efficiency and emission goals. For example, the NASA UEET program goals include an 8- to 15-percent reduction in fuel burn, a 15-percent reduction in CO_2, a 70-percent reduction in NO_x, CO, and unburned hydrocarbons, and a 30-dB noise reduction relative to program baselines. The workshop also covered several programs NASA is funding to investigate advanced reusable space vehicle technologies and advanced space ram/scramjet propulsion systems. Seal challenges posed by these advanced systems include high-temperature operation, resiliency at the operating temperature to accommodate sidewall flexing, and durability to last many missions.

14. SUBJECT TERMS

Seals; Turbine; Abradable; Materials; Analyses; Experimental; Design

15. NUMBER OF PAGES

408

16. PRICE CODE

17. SECURITY CLASSIFICATION OF REPORT	18. SECURITY CLASSIFICATION OF THIS PAGE	19. SECURITY CLASSIFICATION OF ABSTRACT	20. LIMITATION OF ABSTRACT
Unclassified	Unclassified	Unclassified	